QUALITATIVE AND QUANTITATIVE ANALYSIS OF CYTOCHEMICAL MARKERS IN RAT PRIMARY SENSORY NEURONS

A Thesis Submitted to the
University of Manitoba

In Partial Fulfillment of the Requirements
for the Degree

Doctor of Philosophy
in
Physiology

by

Patrick A. Carr
5270588

April 28, 1992

ISBN 0-315-77743-5

QUALITATIVE AND QUANTITATIVE ANALYSIS OF CYTOCHEMICAL MARKERS IN RAT PRIMARY SENSORY NEURONS

BY

PATRICK A. CARR

A Thesis submitted to the Faculty of Graduate Studies of the University of Manitoba in partial fulfillment of the requirements for the degree of

DOCTOR OF PHILOSOPHY

CONTENTS

ACKNOWLEDGEMENTS

This may seem obvious, but many people have been directly or indirectly involved in the work presented in this thesis. Without sounding trite, I would like to acknowledge my indebtedness and send my sincere thanks to:

-Jim through whom I have been introduced to the world of academia and science. Thanks for showing me that if you work hard enough and your heart is in the right place then you can accomplish anything. I owe what I am scientifically, to you. I wait with baited breath for your dictionary!

-Sandi for her patience and understanding of the long hours and of my need to occasionally play in the ivory tower.

-Lyn Polson and Mike Sawchuk for their unhesitating assistance whenever it was needed.

-Toshi Yamamoto who has taught me more than he or I will ever know.

-Dave McCrea for the ear, enthusiasm and guidance.

-Brent Fedirchuk, Mike Angel and other work colleagues (Sohrab you know who you are) without whom these past years would have seemed like work. You have allowed me to maintain my perspective and prevented me from taking myself, or our occasional traumatic events, too seriously.

-my parents who encouraged and supported me and M.E. Green who shaped my priorities and will continue to influence me always.

ABSTRACT

Primary sensory neurons have been categorized according to modality responsiveness, somal size, cytology, and cytochemistry. A major aim in the study of primary afferents has been to determine relationships between dorsal root ganglia (DRG) neuronal physiology, anatomy and chemistry that underlie these classification schemes. Histochemical, immunohistochemical and image analysis techniques were used in the present investigation to determine the distribution and colocalizations of cytochrome oxidase (CO), carbonic anhydrase (CA), parvalbumin (PV), calbindin D28k (CaBP), calcitonin gene-related peptide (CGRP), fluoride-resistant acid phosphatase (FRAP) and AB893-IR in rat lumbar dorsal root ganglia. AB893-IR refers to structures immunoreactive [-IR] with an antibody #893 generated against rat liver gap junctions.

Quantitative histochemistry for CO activity in DRG neurons showed a full range of CO staining densities in each size class with many more large type A cells intensely stained than small type B cells. Immunohistochemistry for CO gave similar staining patterns. Most neurons displaying dense CO staining contained CA, PV and CaBP. The majority of neurons containing PV and CaBP were of the large A type. Cells containing CO, CA, PV and CaBP were rarely CGRP-IR. Thirty percent of all CGRP-IR cells displayed FRAP, while 50% of FRAP-positive cells were CGRP-IR. A large percentage (78%) of AB893-IR cells were CGRP-IR. Among small type B AB893-IR ganglion cells, 90% contained FRAP, while very few were substance P- or somatostatin-IR. In the dorsal horn of the spinal cord, AB893 labelled both individual fibers and rostrocaudally oriented, mediolaterally flattened sheets of fiber bundles. These observations suggest that one subpopulation of DRG neurons contains high levels of CO, CA, PV and CaBP while a separate population contains FRAP, CGRP and AB893-IR. This may have implications for the combinations of substances contained within neurons mediating specific modalities.

General Introduction

The hypothesis of this thesis is that there is a definable correspondence between the cytochemical profile displayed by subpopulations of primary sensory neurons and the sensory modalities they transmit. In certain nuclei of the brain, it is well established that specific neuronal markers or biochemical properties are reflective of the neurotransmitters released by cells in which they are found. However, in primary afferent neurons the relationship between cytochemistry and the neurotransmitters utilized by these cells is not as clear. Nevertheless, a large number of substances including many peptides, amino acids, purines or enzymes suggested to function as or represent markers of putative sensory neurotransmitters have been localized in dorsal root ganglia (DRG). In addition, many distinct subpopulations of DRG neurons have been demonstrated using cytochemical markers not thought to represent putative neurotransmitters. Therefore, a major question that has arisen from the study of primary afferents is, do substances found in particular subpopulations of sensory neurons reflect a processing or transmission of sensory information specific to only those cells? The results presented here address this issue and contribute to our understanding of both the breadth and complexity of this question. In order to present the scope of this issue and relevant aspects of the large body of literature in this field this introduction will: 1) briefly outline the many different categorization schema used for primary sensory neurons; 2) describe the information that each category provides about DRG cells; 3) discuss how the results gathered from these seemingly diverse studies relate to each other; and 4) provide some background on each of the cytochemical markers that were employed in the present studies.

Anatomy and cytology of dorsal root ganglion neurons

Primary sensory neurons, as conveyors of sensory information from peripheral tissues to the CNS and as effectors of various neurogenic efferent responses, have a conceptually

simple organization. They consist of somata located outside the CNS in sensory ganglia, peripheral axons ending in specialized receptor structures and central axons terminating in the CNS. Sensory ganglia are associated with both spinal and cranial sensory afferent nerves although for the purposes of this Introduction discussion will be restricted to spinal ganglia except where otherwise mentioned. Within a single DRG in mammalian species there may be tens of thousands of sensory neuron cell bodies ranging in size from 10 to 120 μm in diameter. Upon initial low power examination, a section of sensory ganglia may appear as a relatively homogeneous structure consisting largely of neuronal somata and axonal bundles. Closer inspection however, reveals that all neurons are not the same. The distribution of Nissl substance within sensory neuron cell bodies imparts a light appearance to some cells and a dark appearance to others (80,235). This intracellular organization is best visualized after the cells have been stained with methylene blue or by metallic impregnation (138). At the beginning of the century it was noted that the light cells tended to be larger in size than the dark cells. From this observation, two histological categories for sensory ganglia cell bodies were proposed; large light type A and small dark type B cells (80,131,132). These two classes of DRG neurons have been further subdivided based on the distribution and organization of intracellular organelles as observed at the subcellular level (64,98,136,190,220,224). Although many different ultrastructurally-based schema exist, most divide the DRG population into six unique subtypes with the large type A cells divided into three groups and the smaller type B cells divided into three or four groups.

Electrophysiological properties and modality responsiveness of sensory neurons

In addition to classification based on anatomical and ultrastructural attributes, primary sensory neurons have also been categorized electrophysiologically according to either the type of stimuli to which they are responsive or characteristics of their somatic action potentials. As outlined by Willis and Coggeshall (238) a variety of different

modalities are transmitted by sensory afferents including touch-pressure, flutter-vibration, tickle, warmth, cold, pain, itch, position sense and kinesthesia. Examples of specific functionally identified primary afferents include those transmitting sensory information from: 1. muscle spindle primary endings (group Ia afferents); 2. Golgi tendon organs (group Ib afferents); 3. muscle spindle secondary endings (group II afferents); 4. tylotrich hair follicle receptors; 5. guard hair follicle receptors; 6. Pacinian corpuscles; 7. Krause endings; 8. slowly adapting type I mechanoreceptors (possibly Merkel cells); 9. slow adapting type II mechanoreceptors (Ruffini endings); 10. down hair follicle receptors; 11. C-fiber low-threshold mechanoreceptors; 12. cool receptors; 13. A-delta high-threshold mechanoreceptors (HTM); 14. C-fiber HTM; 15. polymodal nociceptors; 16. thermal/mechanical nociceptors; and 17. possibly chemonociceptors (30-35,71,130,140,216,223,224,246). As is clear from this list, there are many classes of sensory neurons with distinct sensory modality responsiveness.

Electrophysiologically, primary sensory neurons are commonly categorized according to either their peripheral or central axon conduction velocity. The peripheral axon of rat A-alpha/beta neurons conducts between 30-100 m/s, A-delta neurons between 4-30 m/s and C-fibers less than 2.5 m/s (79). Numerous electrophysiological studies have also demonstrated that sensory neurons not only respond to particular stimuli (as imparted by the specificity of their associated receptor), but they appear to respond with a characteristic somatic action potential. Various electrophysiological parameters such as action potential rise time, action potential amplitude and duration, height of after-potential and duration, repolarization inflexion and time-dependent rectification may differ according to neuronal conduction velocity and/or the peripheral receptor innervated (15,37,79,120,202,253). To generalize, it appears that large myelinated fibers have shorter action potentials than small myelinated or unmyelinated fibers (except in rat where a subpopulation of A-beta neurons also have longer action potentials). The extended action potential duration is due to an inflexion on the repolarization phase

which is often attributed to a pronounced inward calcium current. DRG neurons as a population have been categorized according to these electrophysiological characteristics (253). F-neurons were described as large myelinated cells displaying a tetrodotoxin (TTX) sensitive sodium conductance; A-neurons were small unmyelinated cells with a TTX resistant sodium conductance and H-neurons were small myelinated and unmyelinated cells with a TTX resistant action potential mediated by both sodium and calcium. As mentioned above, it has become apparent that neurons responsive to different modalities display different action potential characteristics. This suggests that the peripheral receptor may somehow specify or be coupled with enzyme regulation or gene expression and thereby linked to either physical membrane composition or intrinsic properties governing ion channel responsiveness (202,238).

Dorsal root ganglia cytochemical markers

Following the advent of a number of practicable histochemical and immunohistochemical techniques, the distribution of a vast number of cytochemical or morphological markers (compounds that can be visualized microscopically in a subpopulation of DRG cells; Willis and Coggeshall [238]) has been examined in sensory ganglia. For the sake of clarity, these markers will be divided into three separate categories: 1) structural markers and cell-surface glycoconjugates; 2) markers and substances related to maintenance of cellular metabolic homeostasis; and 3) putative neurotransmitters and related substances.

Structural markers and cell-surface glycoconjugates. Structural markers localized in DRG cells include alpha-tubulin, actin and RT97 (a 200kd neurofilament protein subunit) (23,133,217). Of these markers, RT97 antibody is most commonly employed as it selectively labels the large light type A DRG cells (5,133). Membrane associated non-glycoconjugate markers that label subpopulations of DRG neurons include growth

associated protein (GAP)-43 and GAP-24, and neural cell adhesion molecule (N-CAM) (217,248). These particular markers are useful in developmental and regeneration studies where they may be used to recognize particular subpopulations of neurons expressing growth cones. Cell surface and intracellular carbohydrate glycoconjugates are a rapidly growing category of DRG neuronal markers (60-63,103,104,143). These compounds are labelled by either monoclonal antibodies or specific labelled plant lectins. To date more than twenty different antibodies and lectins have been employed as markers of a number of different carbohydrate/protein or carbohydrate/lipid residues (2,103,104,115,169,211). Of interest are the specific subpopulations of DRG neurons labelled by many of the lectins or monoclonal antibodies. Certain markers are localized only on small cells (lactoseries), some only on large cells (globoseries and the GM1 ganglioside-cholera toxin receptor) and yet others on cells of mixed sizes (69,201,211). The functional role of these glycoconjugates is unclear although it has been suggested that they may be important in development for cell-cell recognition, axon guidance or synapse formation.

Markers and substances related to maintenance of cellular metabolic homeostasis. Many of these markers such as cytochrome oxidase (CO), carbonic anhydrase (CA), parvalbumin (PV) and calbindin D28k (CaBP) will be discussed in detail in latter sections of the Introduction. Other markers have also been used as indicators of metabolic activity in DRG neurons. Succinic dehydrogenase, an oxidative enzyme in the citric acid cycle, is responsible for the conversion of succinate to fumarate (45,95,210,212,229,231). It is believed that the activity of this enzyme, as indicated by the density of its histochemical reaction product, is reflective of the metabolic activity level of the neuron as a whole. Similarly, glycogen phosphorylase, which breaks down glycogen to glucose-1-phosphate, has also been suggested to reflect the metabolic requirements or electrical activity of DRG neurons. In rat, peripheral electrical or noxious (mechanical, chemical or thermal) physiological stimuli were found to increase

glycogen phosphorylase histochemical reaction product density in a population of small DRG cells (245). This may indicate upregulation of some aspect of cellular metabolism after peripheral axon or sensory receptor stimulation. Unfortunately, glycogen phosphorylase histochemistry is only feasible in fresh unfixed tissue and therefore the results obtained using this technique have not been combined or compared with the distribution or density of other cytochemical markers which are visualized after tissue fixation.

Putative neurotransmitters and related enzymes. As mentioned earlier, a variety of substances including neuropeptides, biogenic amines, purines and excitatory amino acids have been implicated as putative primary afferent neurotransmitters, but none have been firmly established as such. Although critical analysis of the data upon which these substances are considered putative neurotransmitters is beyond the scope of this discussion, a list of various compounds localized within DRG neurons demonstrates the complexity of primary afferent neurotransmitter identification.

Most numerous in this list are the many different neuropeptides that have been localized within DRG neurons. These include substance P (SP), somatostatin (SOM), galanin (GAL), enkephalin, endorphin, dynorphin, bombesin (BOM), oxytocin, arginine-vasopressin, growth hormone releasing factor (GHRF) and corticotropin releasing factor (CRF) which are found in small type B cells (25,70,76,87,88,106,110,125,177,218,219,225,236). Some (calcitonin gene-related peptide [CGRP], cholecystokinin [CCK], vasoactive intestinal polypeptide [VIP] and histidine-isoleucine) however, are found in both small and medium/large cells (7,107,170,230,233). The prevalence of each peptide among DRG neurons varies substantially. CGRP, oxytocin and arginine-vasopressin are localized in almost 50% of DRG neurons (107,110) while CRF, GHRF, GAL, BOM and VIP may be found in less than 5% of the cells (70,106,107,218,219,233). The restricted localization and limited

occurrence of many of the DRG peptides, has led to considerable and ongoing analysis and continuing quantification of their complex distributions. Functionally, it is difficult to ascribe a single role to the peptides contained in primary afferents. At their central termination, it is suggested that many of the neuropeptides function as neurotransmitters or neuromodulators. As a generalization, it might be said that peptides, when applied iontophoretically onto dorsal horn neurons, produce a slow, long depolarization and excitation in contrast to the fast and short duration effects of, for example, excitatory amino acids (52,68,238). In addition, many intrathecally applied neuropeptides produce caudally directed scratching and biting, thought to be indicative of possible behavior-related situations under which they are released endogenously (52). Neuropeptides are also believed to have various actions in the periphery where their release from afferent terminals may regulate arterial smooth muscle tone, plasma extravasation, immune responses, wound healing, gastrointestinal and urogenital contractility, cardiac activity, gastric acid secretion and autonomic neuron excitation (91,96). The central and/or peripheral effects of the plethora of different neuropeptides have been intensely studied and the information thus gathered, together with their distribution in distinct subpopulations of DRG neurons, suggests that these substances do have neurotransmitter or effector roles in particular populations of sensory neurons.

A limited number of studies have reported the localization of substances which may be indicative of sensory neuron cholinergic or catecholaminergic transmission. Tyrosine hydroxylase, a catecholamine synthesizing enzyme, has been found in a small number of cells in lumbar, sacral, nodose and petrosal ganglia (111,112,188). The lack of dopamine beta-hydroxylase in these same cells suggests that they may use dopamine as a possible neurotransmitter. Serotonin has also been reported to be present in cells of nodose and dorsal root ganglia but this finding remains controversial (59,74,109,137). The localization of acetylcholinesterase in 10-15% of DRG small cells suggests that some cells may be cholinergic, although this is not supported by other work demonstrating the

lack of choline acetyltransferase in these cells (13,75). The existence of purinergic DRG neurons has been proposed based on the demonstrated effects of ATP and adenosine agonists or antagonists following iontophoretic application onto dorsal horn cells and intrathecal injection, respectively (55,72,186,207). Adenosine has also been shown to elicit vasodilation in peripheral tissues, possibly mimicking the actions of endogenously released adenosine from afferent neurons (185). It has been suggested that adenosine deaminase and 5′-nucleotidase (and possibly fluoride-resistant acid phosphatase [FRAP]) are markers of purinergic neurons although this has yet to be definitively demonstrated (52,167,206).

In addition to the neuropeptides, the most commonly suggested primary afferent neurotransmitter candidates are the excitatory amino acids (68). Immunohistochemical results have shown that up to 70% of all DRG neurons display both glutamate- and glutaminase-immunoreactivity (14,40,54). These cells are of small size, as are those which preferentially accumulate glutamine (220). However, primary afferents fibers originating from large type A cells may also utilize excitatory amino acids as transmitters (146). Pharmacological and electrophysiological data support the probability of at least some contribution of amino acids to primary afferent neurotransmission (68).

Coexistence of cytochemical markers

When the number and prevalence of individual primary sensory neuron cytochemical markers is considered it appears likely that there may be complex coexistence relationships between markers. Calcitonin gene-related peptide, which is present in a large percentage of DRG cells, is found to coexist with a number of other markers including SP, SOM, dynorphin, CCK, BOM, and GAL (38,76,107). These other markers, however, are not necessarily colocalized with each other and therefore may represent distinct subpopulations of the CGRP-containing neuronal population. In other instances, some markers are characterized by their lack of coexistence with other

substances, as in the case of SP, SOM and FRAP which are found in three largely separate populations (50,89,165,189). Moreover, FRAP or SOM rarely coexists with any neuropeptides. Exceptions, however, have been described. A small degree of coexistence has been reported between FRAP and SP or SOM (50) and an extensive coexistence was found between SOM and adenosine deaminase (167) and between FRAP and arginine-vasopressin (AVP) and oxytocin (110) in rat DRG. The presence of AVP in sensory neurons, however, is in doubt as a recent *in situ* hybridization study failed to detect AVP mRNA in rat DRG (23). Although many markers are colocalized in small cells, coexisting markers in large DRG neurons are less common. For example, whereas CGRP is colocalized with many different substances in small cells, this peptide in large cells seldom coexists with common large cell markers such as GM1 ganglioside and CA (69,201). To date, only a relatively small number of the total possible colocalization relationships have been described using a precise, quantitative approach. Examination of the coexistence of substances found in these cells is essential in order to develop a more complete understanding of the distinct cytochemical identities of DRG neurons and to eventually relate this to the modality responsiveness of those with particular cytochemical profiles.

The coexistence relationships between markers has been the focus of attention in sensory neurons for various reasons, although the functional relevance of this may not be immediately evident and consequently documentation of such relationships may seem trivial or even futile. However, if a relationship between cytochemistry and sensory modality transmission exists, then before this can be established, quantitative determination of cytochemical colocalization relationships is required for two reasons. First, in the absence of bona fide markers for individual modalities or submodalities, it is necessary to determine if currently known markers could be used to reveal such relationships. Second, any modality/cytochemistry relationship will most likely be represented by combinations of neuropeptides or enzymes rather than individual markers.

Relationships between sensory neuron classification schemes

As mentioned above, individual sensory neurons can be categorized according to morphological, ultrastructural, cytochemical and electrophysiological criteria. However, it is not entirely clear how neurons classified according to one scheme correspond to those classified according to the others. Initial studies indicated that there may be a correlation between the ultrastructural characteristics and either modality or cytochemistry of sensory neurons. In mouse it was demonstrated that ultrastructural subclasses of A-beta and A-gamma DRG neurons contain CA, that subclasses B-alpha and B-beta neurons contain FRAP and that the subclass of B-gamma neurons contains SP (220). Similarly in rat, B_1, B_2 and C-type cells (as classified ultrastructurally) were shown to contain tachykinins, C-type cells contained somatostatin and B, C and some large A_2-type cells contained CGRP (152). In a separate study in guinea pig, it was shown that sensory neurons belonging to the ultrastructural subclass B1 were high threshold mechanoreceptors or mechanical-cold nociceptors, that B2 neurons were polymodal nociceptors and that B3 neurons were cold receptors (224). However, it must be noted that because these studies were carried out in different species and involved different ultrastructural categories, it may be inappropriate to combine the results of the studies in an attempt to develop correspondences between cytochemical and sensory modality classification schemes. In general, studies involving ultrastructural examination of DRG neurons in combination with either immunocytochemical and histochemical techniques or prior identification of modality responsiveness are technically difficult and laborious and therefore have been infrequently undertaken. This is also true of direct light microscope studies where the relationship between modality and neuropeptide content of sensory afferents is examined by immunohistochemical analysis of functionally identified neurons (134). The number of cells that have been examined by this method is small and the results must be considered inconclusive.

Development of additional strategies capable of efficiently yielding information on large numbers of neurons are therefore needed in order to investigate the function of different DRG neuronal subpopulations. Histochemical or immunohistochemical markers of activity may be utilized to indicate neurons activated by physiological stimuli and thereby the modality responsiveness of the stimulated cells. Such relatively simple approaches would be compatible with many other histochemical methods and may be used in double-labelling studies.

Modality/cytochemistry correlations

It is quite plausible that putative transmitters or possibly proteins associated with sensory transduction processes or structural features of peripheral sensory receptors may be unique to certain DRG cells and may be correlates of or confer upon them different modality specificities. While it is at present uncertain whether definitive markers of modality specificity have been identified, several lines of albeit circumstantial evidence suggest at least some degree of correlation between the cytochemistry of primary afferent neurons and the sensory modalities they transmit. As discussed below, this evidence may be classified under three separate topics, namely: the tissues innervated by cytochemically-identified neurons; the correspondence between the laminar organization of the central arborizations of afferents containing particular neuropeptides or enzymes and modality-specific areas of the dorsal horn; and the release and electrophysiological actions of primary afferent putative neurotransmitters in the dorsal horn.

Peripheral projections. There is evidence that primary afferents innervating various tissues are responsive to only certain stimuli. For example, cutaneous tissue is innervated by mechanoreceptive, thermoreceptive, nociceptive and chemoreceptive (130) but obviously not spindle or Golgi tendon organ afferents; joints by mechanoreceptive and nociceptive but not thermoreceptive or muscle spindle afferents; muscle tissue by Golgi

tendon organ, muscle spindle or Pacinian corpuscle and nociceptive but not cutaneous specific low-threshold mechanoreceptive or (rarely) thermoreceptive afferents; and visceral tissue by nociceptive and some mechanoreceptive but rarely thermoreceptive afferents (238). The stimulus modality to which the sensory receptors in various tissues are responsive may be correlated, to a certain extent, with tissue specific innervation by neurons containing particular substances. It has been demonstrated that FRAP-containing neurons project largely to visceral and cutaneous tissue (149,150,160,173), although there is one report of some projections to muscle (160). Somatostatin-containing neurons were found to project to cutaneous tissue and muscle (160,173), but not to viscera (160). In contrast, CGRP was found in sensory neurons innervating visceral tissues (160) as well as in the majority of muscle and joint afferents and a large proportion of cutaneous afferents (160,173). Substance P-containing neurons were found to project to cutaneous, muscular, joint and visceral tissue (150,160,173). However, SP levels in muscle afferents were reported to be appreciably lower than in neurons innervating other tissues (150). In addition, the peripheral projections of neurons containing combinations of neuropeptides has been investigated. It was found that: neurons containing a combination of SP, CGRP, CCK and DYN project mainly to the skin; neurons containing a combination of SP, CGRP and CCK project mainly to blood vessels in skeletal muscle; neurons containing a combination of SP, CGRP and DYN project mainly to visceral tissue; and neurons containing a combination of SP and CGRP project mainly to the heart and visceral or systemic blood vessels (76). Therefore, the cytochemical differences observed in neurons projecting to different tissues may be related to the different modalities conveyed from distinct tissues. For example, as mentioned above, certain markers may confer sensory neuronal properties such as effector functions, firing frequency and modulatory interactions that characterize some afferents and not others and these properties may distinguish the response and transmission capabilities of afferents from different tissues.

Dorsal horn neuron responsiveness. It has been found that neurons in discrete regions of the dorsal horn are responsive to particular peripherally-applied physiological stimuli and that these spinal cord regions correspond to the distribution of at least some primary afferent cytochemical markers. It therefore appears that there may be a correlation between the modality-responsiveness of dorsal horn neurons, the lamina specific terminations of functionally-identified primary afferent central arborizations, and the laminar organization of cytochemically identified afferents. Most lamina I neurons respond to noxious or thermal input, lamina II outer (IIo) neurons are excited by both nociceptive and non-nociceptive input, while many lamina II inner (IIi) neurons along with some lamina III cells may contribute to the processing of innocuous, low-threshold mechanoreception (16,139,187,196,247).

With respect to the central terminations of cytochemically homogeneous subpopulations of sensory neurons, afferents containing CGRP are distributed in lamina I, II and III, substance P-containing afferents innervate lamina IIo, SOM-containing afferents terminate in lamina IIi and FRAP-containing afferents are localized along the middle third of lamina II (165,168,197,214). This lamina specific distribution may be related to at least two other aspects of sensory neuron organization. First, coexistence of markers in DRG may be reflected by an overlap in their distribution in the dorsal horn. For example, SP and SOM in DRG are colocalized with CGRP (107). In the spinal cord dorsal horn this relationship is reflected by CGRP staining which encompasses that of SP and SOM. Second, the central terminations of cytochemically-identified afferents appear lamina-specific similar to the organization of the central terminations of certain functionally-identified afferents. This may suggest that cytochemically-identified afferents have a laminar specific dorsal horn distribution determined by the modality they transmit. An example of this possibility involves FRAP or SOM containing primary afferent terminals which are localized to similar dorsal horn regions as the central termination of functionally-identified unmyelinated low-threshold mechanoreceptors

(223). However, for other primary afferent peptides that have more widespread terminations in both lamina I and II as well as deeper layers, it is difficult, or at least not yet possible, to correlate their distribution with any particular modality.

Release and action of putative neurotransmitters. Evidence that peptides and amino acids contained within sensory neurons may function as neurotransmitters or neuromodulators includes functional and behavioral studies which have detailed the release of these putative primary afferent neurotransmitters (PAT) in the dorsal horn, the post-synaptic effects of iontophoretic or bath application of these substances, the blockage or potentiation of PAT effects by antagonists or agonists, respectively, and the ability of intrathecal application of PAT to elicit stereotypical behaviors. The release of neuropeptides in the dorsal horn of the spinal cord following peripheral nerve or modality-specific stimulation has been studied with antibody microprobe, push-pull cannula, spinal superfusion and microdialysis techniques (17,29,65,78,126,161-163). While each method detects an accumulation of substances in the extracellular space following afferent excitation, the common disadvantage of these techniques is that the source of the released PAT cannot be determined with certainty. Most neuropeptides present in afferent terminals are also present in descending pathways and intrinsic dorsal horn neurons which may contribute to the pool of detected substances (50,94,105,159,178,227,228). Thus, caution is required in the interpretation of such release studies. Nevertheless, this approach has generated some evidence to support the notion that particular modalities are transmitted by primary afferents containing particular neuropeptides. In brief, studies have shown that SOM release is increased following thermonociceptive stimulation (126,161,162), neurokinin A release is increased after both thermonociceptive and mechanonociceptive stimuli (65) and SP release is increased following electrical stimulation of unmyelinated fibers, capsaicin administration or thermonociceptive and mechanonociceptive stimuli (17,29,66,73,78).

One study reported an increase in extracellular CGRP levels following noxious thermal and noxious mechanical cutaneous stimuli (163). As primary sensory neurons are the only source of CGRP in the spinal cord dorsal horn (47; see however 49,153), a contribution from other sources with respect to this peptide, is unlikely.

The results from iontophoresis or bath application experiments have demonstrated that at least some neuropeptides, amino acids or purines can excite dorsal horn neurons, and that this excitation can be altered by pharmacological intervention. For example, it has been shown that: 1. iontophoretically or bath applied SP can prolong the excitation of, or depolarize, either physiologically-unidentified or nociceptive dorsal horn neurons (83,157,164,191) and these effects can be antagonized by SP antibodies or analogues (192,193); 2. iontophoretic or bath application of CGRP mediates a slow depolarization in some dorsal horn neurons (204,205) and excites low-threshold mechanoreceptive and wide dynamic range but not nociceptive-specific dorsal horn neurons (158) 3. iontophoretically applied vasoactive intestinal polypeptide excites nociceptive and non-nociceptive neurons (102,206); 4. glutamate and aspartate depolarize some dorsal horn neurons and importantly not others (209,254) and 5. iontophoretic application of ATP excites non-nociceptive and some wide dynamic range but not nociceptive-specific dorsal horn neurons (72,207). These results cannot be strictly taken to indicate that the actions of the individual putative neurotransmitters tested correspond to those produced by activation of sensory neurons in which the transmitters may be contained, or indeed that these substances are even released from primary afferent neurons. Nevertheless, some of the above studies do suggest a certain degree of signalling specificity of particular neuropeptides, amino acids and purines. Due to the large number of coexisting substances in DRG, it is likely that actual sensory signals are mediated by a chemical mosaic released from afferent central terminals. Therefore, it might be worthwhile to take into consideration coexistence relationships in sensory neurons and to formulate on this basis neurotransmitter "cocktails" consisting of combinations of putative

neurotransmitters which may then be tested for physiological effects on dorsal horn neurons.

All of the above information, taken *in toto* does suggest that there is a relationship between the cytochemistry of certain subpopulations of primary afferent neurons and their modality responsiveness. In this thesis, the distribution and coexistence relationships of CO, CA, PV, CaBP, CGRP, FRAP and AB893-IR (AB893-IR refers to structures that are immunoreactive [-IR] with an antibody designated #893 which was generated against rat liver gap junctions) were examined in rat DRG and, where appropriate, functional (ie. possible relationships to modality) relevance is discussed. Specific details concerning the cytochemical markers utilized or subjects investigated are provided below.

Parvalbumin/ Calbindin D28k

The high affinity calcium binding proteins PV and CaBP are widely distributed throughout the central and peripheral nervous systems (43). In the CNS, PV and CaBP have a mostly complementary distribution, although they do coexist in Purkinje cells of the cerebellum, in the basolateral nucleus of the amygdala, in the olfactory tubercles and in neurons of the medial trapezoid nucleus (43). In general, CaBP is widely distributed within the limbic system and the hypothalamus. It is also found in thalamic projection neurons, striato-nigral cells, neurons of the nucleus basalis of Meynert and in retinal, cochlear and vestibular ganglion cells (43). Conversely, PV is localized within many interneurons in the cerebral cortex, hippocampus, cerebellum and spinal cord. It is also found in projection neurons of the thalamic reticular nucleus, globus pallidus, substantia nigra pars reticulata and in retinal, cochlear and vestibular ganglion cells (43). Early indications suggested that throughout the CNS PV was colocalized with GABA in neurons characterized by high electrical activity (41,42,44). This now appears to have been an inappropriate generalization, although some PV-containing cells in the cerebral

cortex do contain GABA and these and other PV-IR cells may have high activity levels (43,113). In any case, the role of these calcium binding proteins in neurons has not been firmly established. It has been suggested that PV and CaBP may act as intracellular calcium transporters or buffers to restrict, reestablish or partition calcium concentrations in either fast-firing neurons or neurons that produce calcium spikes (9,43,82). The strong correlation between the localization of PV and high levels of both CO and 2-deoxyglucose in the zebra finch suggests that PV may be present in neuronal systems that can reach high levels of metabolic and electrical activity (26,27).

Several reports have described the distribution of PV and CaBP in DRG neurons (6,81,183). These neurons have been suggested to be muscle afferents on the basis of their size, response to specific trophic factors in culture and peripheral projections (11,12,24,43,182,184). Parvalbumin-IR axons have been localized around intrafusal muscle fibers and may be seen to contact muscle spindles (43). In extensor digitorum longus, axons innervating bag fibers were found to be PV-IR while sensory afferents to both bag and chain fibers were CaBP-IR (43). Neither PV or CaBP staining is found in ventral roots. Although the function of these calcium binding proteins in the PNS is unknown, their distribution may be related to other inherent properties of DRG neurons. In rat DRG, most or all cells with unmyelinated axons and some A-beta neurons are reported to have a substantial slow inward calcium current characterized by an inflexion on the repolarization phase of the action potential (79). As both PV and CaBP are localized in large cells, it is possible that these proteins are present in the subpopulation of A-beta neurons with the inward calcium current. This would be consistent with reports describing the development of substantial calcium dependent spikes in muscle afferents and myenteric neurons (86,99), both of which have been suggested to contain PV or CaBP (36,43,182). If correct, the above suggests that in DRG these calcium binding proteins may function to buffer greater loads of intracellular calcium (19). Recently it was reported that intracellular injection of PV into cultured DRG neurons at

concentrations found in neurons *in vivo* can elevate the intracellular calcium buffering capacity of the injected cells (46), suggesting that PV can contribute significantly to intracellular calcium buffering in DRG neurons *in vivo*. A reduction in available calcium may result in a decrease in the calcium dependent outflow of potassium which would result in attenuated afterhyperpolarization and accommodation. This, in turn, may allow increased firing rates in these neurons. A similar shortened refractory period is seen when the calcium chelator EGTA (which has a calcium binding affinity comparable to PV and CaBP) is injected into neurons (43,122,151). In Parts I, III and V of this thesis results are presented on the distribution of PV and CaBP in rat DRG, the CO density levels in PV- and CaBP-containing cells and the CA and CGRP content of PV or CaBP-containing cells.

Cytochrome oxidase

Cytochrome oxidase is the terminal enzyme in the electron transport chain and therefore its activity is believed to be directly related to the oxygen consumption of cells. The maintenance of ion balance is thought to constitute the bulk of energy expenditure in neurons with protein synthesis and neurotransmitter metabolism requiring relatively small amounts of energy from the oxidative pathway (241). Histochemistry for CO has been used extensively as a marker of neuronal activity in the CNS (241). Its utility as an indicator of activity is supported by numerous studies showing a correlation between histochemically determined CO levels and neuronal activity (108,147,241-244).

In normal tissue, nuclei that have a high basal electrical or synaptic activity such as ocular dominance columns, whisker barrel fields, auditory relay nuclei, the CA3 region of the hippocampus, basal ganglia, certain thalamic or brainstem nuclei and Clarke's or intermediolateral nuclei in the spinal cord are characterized by dense CO staining (241). At the cellular level, it has been demonstrated that neither the size nor type of neuron governs CO activity as both small or large neurons may be CO light or dense as may

individual similar sized cells in, for example, a motor neuron pool (241,244). Similarly, basal CO levels are not thought to be associated with, or related to, the type of putative neurotransmitter utilized by a cell (241). With respect to other morphological markers, high levels of CO activity are thought to correspond best with the distribution of either succinic dehydrogenase, Na^+/ K^+-ATPase or parvalbumin (26,27,241).

Additional evidence supporting a relationship between CO levels and neuronal electrical activity has been gathered from work demonstrating CO activity changes in response to an alteration in the functional activity of a tissue or individual neuron. A reduction in activity in auditory, visual, somatosensory or olfactory afferents have all resulted in a decrease in CO levels in nuclei associated with these systems (241). It has also been demonstrated that CO levels may be increased in certain neurons following either electrical or pharmacological stimulation (147,232,242) or after the development of synaptic transmission (148). Although CO is often employed as a marker of electrical activity in nervous tissue, these studies usually describe CO staining levels in specific areas or nuclei rather than reaction product densities in individual neurons. This is because in the CNS CO is visualized largely in neuropil, therefore making it very difficult to determine neuronal perikaryal CO densities as distinct from surrounding tissue. In DRG sections however, the lack of neuropil allows an unobstructed view of most neuronal cell bodies. As such, CO staining densities are easily quantified in these cells. Incidentally, our development of specific CO immunohistochemical techniques has allowed visualization of CO levels in neuronal cell bodies of the CNS without concomitant labelling of neuropil. This technique, therefore, may be used to examine the relative levels of CO enzyme in individual neurons of the brain and spinal cord.

In monkey DRG, CO was shown to have a heterogeneous distribution among neurons with no apparent correlation between somal size and the density of CO reaction product (244). In parts II, III and V qualitative and quantitative results are presented on: 1) the level of both histochemical and immunohistochemical CO staining in rat primary sensory

neurons; and 2) the level of CO reaction product in CA-, PV- and CaBP-containing primary afferent neurons.

Carbonic anhydrase

Carbonic anhydrase, or more specifically the CAII isozyme, is another histochemical marker that is presumed to reflect the activity of DRG neurons. In the CNS this enzyme has been found only in glia cells (39) but its presence in brain synaptosomes (252) and possibly in the mesencephalic nucleus of the trigeminal nerve (1; see however, 240) suggests that it is likely present in neurons as well. In sensory ganglia it is localized in a population of medium and large size neurons as well as in satellite cells (180,181,220,239,240). Carbonic anhydrase is thought to be a marker of tonic activity based on its role in the regulation of intraneuronal carbon dioxide levels through catalysis of CO_2 hydration and the facilitation of CO_2 diffusion (56,180,181,199). In addition, it may also be involved in the maintenance of cellular pH and certain ion concentrations (208) through bicarbonate-chloride or sodium-hydrogen ion exchange mechanisms. As a cell becomes more active carbon dioxide is quickly removed from the cellular milieu to prevent suppression of oxidative metabolism. This is accomplished by CA which promotes the hydrolysis of CO_2 to HCO_3^- and H^+. These ions are then removed in exchange for Cl^- and Na^+ which serves to maintain pH and ionic balance (208). In most neurons, intracellular chloride concentrations are maintained at levels far below that of the extracellular milieu. In some sensory neurons however, it has been demonstrated that intracellular chloride may be elevated above extracellular levels (3,172). Chloride would thus tend to flow outward if the appropriate channels were opened during transmitter action. This chloride efflux would result in significant depolarization in sensory neuron central terminals as may occur during primary afferent depolarization (PAD) (53). Although higher intracellular than extracellular chloride levels have not been demonstrated in rat primary sensory neurons, we suggest that one of the functions of CA

may be to maintain elevated cytoplasmic chloride levels in neurons that have the capability of PAD.

In spite of the fact that the peripheral projection sites of CA-containing afferents have not been studied in detail, they do appear to exhibit some degree of tissue specific innervation. On the basis of retrograde tracing studies and observations of CA reaction product in annulospiral afferent nerve terminals around intrafusal muscle, it was proposed that a large portion of CA-containing neurons innervate muscle with only a minor contribution (4-6%) to cutaneous tissue (179-181,198-200,222,240). It has been further suggested that, although all primary afferents may contain some level of CA, particularly large amounts of CA are localized in tonically active (therefore generating relatively large amounts of carbon dioxide) muscle afferents mediating the monosynaptic stretch reflex (180,181,240). This notion is based on the previous demonstrations of the extreme sensitivity of the excitability of monosynaptic reflexes to carbon dioxide levels (114) and the depression of monosynaptic responses by increased systemic carbon dioxide or acetazolamide (a potent CA inhibitor) application (67). Studies examining the relationship between CA content and either CO staining densities, PV-IR or CaBP-IR in rat primary sensory neurons are presented in Parts II and II.

Fluoride-resistant acid phosphatase

A variety of different acid phosphatases have been localized in DRG neurons. Most however, do not label a specific subpopulation of cells (238). In the late 1960's and early 70's it was found that a certain non-lysosomal fluoride resistant enzyme labelled a subpopulation of small type B sensory neurons in DRG and a sublayer of the substantia gelatinosa in the spinal cord of rats (116,117). This enzyme, named fluoride-resistant acid phosphatase (FRAP), is found in approximately 50-60% of all DRG neurons and in the middle third of lamina II in the spinal cord dorsal horn (60,62,119,165,197). Dorsal root ganglia neurons containing FRAP have rarely been found to contain other enzyme or

peptide markers (51,110). In addition to its demonstration in DRG neurons and central axons this enzyme is also found in peripheral axons following obstruction of axoplasmic flow (116,149,150). Ligation of either peripheral or central axons results in the accumulation of FRAP on the ganglia side of the ligature suggesting that this enzyme is transported out from the cell body (116). Similarly, dorsal rhizotomy or root ligation ablates labelling in that area of the dorsal horn innervated by the manipulated root (48,116,118). Centrally, FRAP is localized in terminals and preterminal axons and can occasionally be observed in dorsal roots. At the ultrastructural level, FRAP is localized in unmyelinated axons at small dark sinuous primary afferent C_1 terminals of type 1-synaptic glomeruli (48,116,117,197). Within the terminals the enzymatic reaction product is often localized on or between synaptic vesicles or at the axon surface membrane of the terminal.

The function of FRAP in primary afferent neurons remains obscure. It has been suggested that this enzyme may play a role in central synaptic or secretory function based on its distribution in a restricted population of DRG cells, its precise localization in substantia gelatinosa, its central disappearance following dorsal root or peripheral nerve cut or crush and its concentration in axon terminals. A similar enzyme has been localized in prostate, adrenal medulla and various endocrine tissues (8,60,62,234). In these tissues its intimate association with secretory granules (60,62,234) suggests it may play a role in secretory processes. To postulate a function for FRAP in sensory neurons at this juncture would be highly speculative. FRAP histochemistry (and the very similar thiamine monophosphatase histochemistry) is most often used as a pure morphological marker without implication of a specific function associated with the labelling unlike labelling for neuropeptides and other putative neurotransmitters. Interestingly however, it appears that FRAP-containing neurons do have a specific peripheral projection. It has been demonstrated in a number of studies that there are less FRAP afferents in muscle as compared to skin or visceral nerves (149,150,160). In Part IV of this thesis results from

our investigation of the peptidergic content of FRAP-containing primary afferent neurons will be presented. It was previously proposed by Hunt and Rossi (93) that "peptide and nonpeptide-containing afferents represent two distinct C-fiber pathways innervating similar peripheral structures and conveying similar information, but to different areas within the dorsal horn". This hypothesis, to our knowledge, has not been directly tested and therefore we examined this issue using FRAP (a nonpeptide) and CGRP (a peptide) as morphological markers.

Calcitonin gene-related peptide

Calcitonin gene-related peptide is a 37 amino acid neuroactive peptide derived from the alternate processing of RNA from the calcitonin gene (4,203). High levels of CGRP have been found in both trigeminal and spinal ganglia and dense immunoreactive fiber plexi are observed in the dorsal horn of the spinal cord (77,129,237). CGRP is found in approximately 50% of all spinal sensory neurons of small, medium and large sizes making it one of the most widely distributed peptides in DRG (98,107,123,171). Due to its extensive distribution in DRG, CGRP has been found to coexist with many different peptides including SP, SOM, CCK, VIP, GAL, BOM, dynorphin and enkephalin (38,76,107,153). In some instances CGRP may coexist with more than one peptide. Peripherally CGRP-IR axons innervate viscera, special sense organs, skin, deep tissues, bone and blood vessels (96). Within skin, CGRP-IR nerve fibers innervate blood vessels, sweat glands, hair follicles and terminate near, but do not innervate, Meissner corpuscles and Merkel's discs (97,124). It appears that most peripheral CGRP-IR fibers are unmyelinated and many end in what resemble free-nerve endings (97,124). It has been postulated that in the periphery CGRP is released non-synaptically from terminals to diffuse and have a paracrine-like influence on an immediate area (97). In this manner, CGRP may function as a potent vasodilator to control cutaneous blood flow or act to regulate smooth muscle tone, secretion of gastric juices or insulin, constriction of airways

or wound healing (96). In the dorsal horn of the rat spinal cord, it has been suggested that primary sensory neurons are the only source of CGRP (47; see however 49). In horse however, CGRP-IR dorsal horn neurons have been observed (153). Centrally, CGRP may have a role in the transmission or modification of nociceptive input. CGRP has been shown to: 1) produce slow and prolonged excitation of dorsal horn neurons (158,204,205); 2) potentiate substance P release in the dorsal horn (175); 3) produce prolonged caudally directed biting, licking and scratching when applied intrathecally in conjunction with substance P (237); 4) be released in the dorsal horn following peripheral noxious stimuli (163); 5) increase in DRG in response to development of peripheral arthritis (128); and 6) inhibit substance P endopeptidase (135). In addition, intrathecal application of antibodies to CGRP was shown to produce an analgesic effect (127). This evidence therefore suggests that CGRP may be involved in at least some peripheral or central aspect of primary afferent function. Studies examining the coexistence relationship of CGRP with PV, CaBP and FRAP and the contribution of unmyelinated afferent fibers to the CGRP-IR observed in the dorsal horn of the rat spinal cord are presented in Part I and IV.

Electrical coupling of primary afferent neurons

In addition to work on the distribution of various morphological markers in DRG we also investigated other aspects of sensory neuron physiology. Part VI of this thesis describes our attempt to determine immunohistochemically whether the gap junction protein connexin32 is expressed in afferent neurons. The antibody employed in this study (antibody #893, hereafter referred to as AB893) was generated against rat liver gap junctions and was previously found to recognize both neuronal and glial gap junctions in rat and fish CNS (166,215,250,251). The expected presence of connexin32 (which at the time of this study was the only known gap junction protein) in DRG neurons was based on the many indications of electrical interactions and/or possible gap junction coupling

involving primary sensory neurons. It has been suggested that electrical coupling between peripheral axons may contribute to cutaneous axon reflex mechanisms (130,226). In addition, in normal tissue morphological or electrophysiological correlates of coupling have been described between DRG cell bodies during development (176), between primary afferent fiber terminals and Deiters cells in the lateral vestibular nucleus (121,221,249), between primary afferent cell bodies in the trigeminal nerve mesencephalic nucleus (10,84,85,90) and between primary afferent axons in dental pulp and in peripheral nerve or skin (28,142,144,145,154-156). There has also been much speculation about the possible occurrence of electrical communication between damaged primary afferent neurons (28,20-22,57,92,141,142,156,194,195,213). It has been suggested that injury to peripheral nerves may result in ephaptic or other forms of electrical coupling between neurons. Indeed, ultrastructural examination of abnormal nerves containing electrically coupled fibers has revealed close appositions between adjacent axonal membranes (18,21,57,58,100,101,174,194,195) although whether this is the anatomical basis for post-traumatic neuronal electrical communication remains uncertain. Therefore, it appears that the definitive morphological correlates of electrical interactions have not been found. This may prove difficult however, as the localization of gap junctions using conventional EM techniques is a formidable task even in areas where they are known to be present.

In an attempt to examine whether connexin32 is present in normal primary sensory neurons, an immunohistochemical study using AB893 was undertaken in rat trigeminal, cervical, thoracic, lumbar and sacral ganglia, dorsal spinal cord and spinal trigeminal nuclei (Part VI). Although the antibody #893 was generated against liver gap junctions, we are uncertain whether it recognizes a gap junction protein (connexin32) in DRG. However, it does label a unique and possibly anatomically important subpopulation of primary sensory neurons in sensory ganglia and their fibers in the spinal cord. In light of these results we make no claim that AB893 recognizes connexin32 in this tissue. Rather

it is utilized to study the distribution, coexistence relationships and central afferent fiber organization of a subpopulation of primary afferent neurons.

REFERENCES

1. Aldskogius, H.; Arvidsson, J. and Hansson, P. (1988) Carbonic anhydrase enzyme histochemistry of cranial nerve primary sensory afferent neurons in the rat. Histochem. **88**, 151-154.

2. Alvarez, F.J.; Rodrigo, J.; Jessell, T.M.; Dodd, J. and Priestley, J.V. (1989) Morphology and distribution of primary afferent fibers expressing alpha-galactose extended oligosaccharides in the spinal cord and brainstem of the rat. Light microscopy. J. Neurocytol. **18**, 611-629.

3. Alvarez-Leefmans, J.F.; Gamino, F.J.; Giraldez, S.M. and Nogueron, I. (1988) Intracellular chloride regulation in amphibian dorsal root ganglion neurones studied with ion-selective microelectrodes. J. Physiol. **406**, 225-246.

4. Amara, S.G.; Arriza, J.L.; Leff, S.E.; Swanson, L.W.; Evans, R.M. and Rosenfeld, M.G. (1985) Expression in brain of a messenger RNA coding a novel neuropeptide homologous to calcitonin gene-related peptide. Science **229**, 1094-1097.

5. Anderton, B.; Coakham, H.B.; Garson, J.A.; Harper, A.A.; Harper, E.I. and Lawson, S.N. (1982) A monclonal antibody against neurofilament protein specifically labels the large light cell population in rat dorsa root ganglia. J. Physiol. **334**, 97-98P.

6. Antal, M.; Freund, T.F. and Polgár, E. (1990) Calcium-binding proteins, parvalbumin- and calbindin D 28k-immunoreactive neurons in the rat spinal cord and dorsal

root ganglia: a light and electron microscopic study. J. Comp. Neurol. **295**, 467-484.

7. Baber, N.S.; Dourish, C.T. and Hill, D.R. (1989) The role of CCK, caerulein, and CCK antagonists in nociception. Pain **39**, 307-328.

8. Bahsoon, J.D.; Hyde, S. and Keen, P. (1984) Analysis of the acid phosphatases of rat sensory ganglia by isoelectric focusing on polyacrylamide gels. J. Neurochem. **42**, 482-486.

9. Baimbridge, K.G.; Miller, J.J. and Parkes, C.O. (1982) Calcium-binding protein distribution in the rat brain. Brain Res. **239**, 519-525.

10. Baker, R. and Llinas, R. (1971) Electrotonic coupling between neurons in the rat mesencephalic nucleus. J. Physiol. **212**, 45-63.

11. Barakat, I. and Droz, B. (1989) Inducing effect of skeletal muscle extracts on the appearance of calbindin-immunoreactive dorsal root ganglion cells in culture. Neuroscience **28**, 39-47.

12. Barakat, I. and Droz, B. (1989) Calbindin-immunoreactive sensory neurons in dissociated dorsal root ganglion cell cultures of chick embryo: role of culture conditions. Dev. Brain Res. **50**, 205-216.

13. Barber, R.P.; Phelps, P.E.; Houser, C.R.; Crawford, G.D.; Salvaterra, P.M. and Vaughn, J.E. (1984) The morphology and distribution of neurons containing choline acetlytransferase in the adult rat spinal cord: an immunocytochemical

study. J. Comp. Neurol. **229**, 329-346.

14. Battaglia, G. and Rustioni, A. (1988) Coexistence of glutamate and substance P in dorsal root ganglion neurons of the rat and monkey. J. Comp. Neurol. **277**, 302-312.

15. Belmonte, C. and Gallego, R. (1983) Membrane properties of cat sensory neurons with chemoreceptor and baroreceptor endings. J. Physiol. **342**, 603-614.

16. Bennett, G.J.; Abdelmoumene, M.; Hayashi, H. and Dubner, R. (1980) Physiology and morphology of substantia gelatinosa neurons intracellularly stained with horseradish peroxidase. J. Comp. Neurol. **194**, 809-827.

17. Bergstrom, L.; Hammond, D.L.; Go, V.L.W. and Yaksh, T.L. (1983) Concurrent measurement of substance P and serotonin in spinal superfusates: failure of capsaicin and p-chloroamphetamine to co-release. Brain Res. **270**, 181-184.

18. Bernstein, J.J. and Pagnanelli, D. (1982) Long-term axonal apposition in rat sciatic nerve neuroma. J. Neurosurg. **57**, 682-684.

19. Blaustein, M.P. (1988) Calcium transport and buffering in neurons. Trends Neurosci. **11**, 438-443.

20. Blumberg, H. and Janig, W. (1982) Activation of fibers via experimentally produced stump neuromas of skin nerves: ephaptic transmission or retrograde sprouting? Exp. Neurol. **76**, 468-482.

21. Blumberg, H. and Janig, W. (1981) Neurophysiological analysis of efferent sympathetic and afferent fibers in skin nerves with experimentally produced neuromata. In: Siegfried, J.; Zimmerman, M., eds. Phantom and Stump Pain. Berlin: Springer; 15-31.

22. Blumberg, H. and Janig, W. (1984) Discharge pattern of afferent fibers from a neuroma. Pain **20**, 335-353.

23. Boehmer, C.G.; Norman, J.; Catton, M.; Fine, L.G. and Mantyh, P.W. (1989) High levels of mRNA coding for substance P, somatostatin and alpha-tubulin are expressed by rat and rabbit dorsal root ganglia neurons. Peptides **10**, 1179-1194.

24. Bossart, E.; Barakat, I. and Droz, B. (1988) Expression of calbindin immunoreactivity by subpopulations of primary sensory neurons in chick embryo dorsal root ganglion cells grown in coculture or conditioned medium. Dev. Neurosci. **10**, 81-90.

25. Botticelli, L.J.; Cox, B.M. and Goldstein, A. (1981) Immunoreactive dynorphin in mammalian spinal cord and dorsal root ganglia. Proc. Natl. Acad. Sci. **78**, 7783-7786.

26. Braun, K.; Scheich, H.; Schachner, M. and Heizmann, C.W. (1985) Distribution of parvalbumin, cytochrome oxidase acitivity and 14C-2-deoxyglucose uptake in the brain of the zebra finch. I. Auditory and vocal motor systems. Cell Tissue Res. **240**, 101-115.

27. Braun, K.; Scheich, H.; Schachner, M. and Heizmann, C.W. (1985) Distribution of parvalbumin, cytochrome oxidase acitivity and 14C-2-deoxyglucose uptake in the brain of the zebra finch. II. Visual system. Cell Tissue Res. **240**, 117-127.

28. Brenan, A. and Matthews, B. (1983) Coupling between nerve fibres supplying normal and injured skin in the cat. J. Physiol. **334**, 70-71p.

29. Brodin, E.; Linderoth, B.; Gazelius, B. and Ungerstedt, U. (1987) *In vivo* release of substance P in cat dorsal horn studied with microdialysis. Neurosci. Lett. **76**, 357-362.

30. Brown, A.G. and Fyffe, R.E.W. (1978) The morphology of group Ia afferent fibre collaterals in the spinal cord of the cat. J. Physiol. (Lond) **274**, 111-127.

31. Brown, A.G. and Fyffe, R.E.W. (1979) The morphology of group Ib afferent fibre collaterals in the spinal cord of the cat. J. Physiol. (Lond) **296**, 215-228.

32. Brown, A.G.; Fyffe, R.E.W. and Noble, R. (1980) Projections from Pacinian corpuscles and rapidly adapting mechanoreceptors of glabrous skin to the cat's spinal cord. J. Physiol. (Lond) **307**, 385-400.

33. Brown, A.G.; Fyffe, R.E.W.; Rose, P.K. and Snow, P.J. (1981) Spinal cord collaterals from axons of type II slowly adapting units in the cat. J. Physiol. (Lond) **316**, 469-480.

34. Brown, A.G.; Rose, P.K. and Snow, P.J. (1977) The morphology of hair follicle afferent fiber collaterals in the spinal cord of the cat. J. Physiol. (Lond) **272**,

779-797.

35. Brown, A.G.; Rose, P.K. and Snow, P.J. (1978) Morphology and organization of axon collaterals from afferent fibers of slowly adapting type I units in cat spinal cord. J. Physiol. (Lond) **277**, 15-27.

36. Buchan, A.M.J. and Baimbridge, K.G. (1988) Distribution and co-localization of calbindin D28k with VIP and neuropeptide Y but not somatostatin, galanin and substance P in the enteric nervous system of rat. Peptides **9**, 333-338.

37. Cameron, A.A.; Leah, J.D. and Snow, P.J. (1986) The electrophysiological and morphological characteristics of feline dorsal root ganglion cells. Brain Res. **362**, 1-6.

38. Cameron, A.A.; Leah, J.D. and Snow, P.J. (1988) The coexistence of neuropeptides in feline sensory neurons. Neuroscience **27**, 969-979.

39. Cammer, W. and Tansey, F.A. (1988) The astrocyte as a locus of carbonic anhydrase in the brains of normal and dysmyelinating mutant mice. J. Comp. Neurol. **275**, 65-75.

40. Cangro, C.B.; Sweetnam, P.M.; Wrathall, J.R.; Haser, W.B.; Curthoys, N.P. and Neale, J.H. (1985) Localization of elevated glutaminase immunoreactivity in small DRG neurons. Brain Res. **336**, 158-161.

41. Celio, M.R. (1984) Parvalbumin as a marker for fast firing neurons. Neurosci. Lett. Suppl. **18**, S332.

42. Celio, M.R. (1986) GABA neurons contain the calcium binding protein parvalbumin. Science **232**, 995-997.

43. Celio, M.R. (1990) Calbindin D-28k and parvalbumin in the rat nervous system. Neuroscience **35**, 375-475.

44. Celio, M.R. and Heizmann, C.W. (1981) Calcium-binding protein parvalbumin as a neuronal marker. Nature **293**, 300-302.

45. Chalmers, G.R. and Edgerton, V.R. (1989) Marked and variable inhibition by chemical fixation of cytochrome oxidase and succinate dehydrogenase in single motoneurons. J. Histochem. Cytochem. **37**, 899-901.

46. Chard, P.S.; Bleakman, D. and Miller, R.J. (1991) Parvalbumin is an intracellular neuronal calcium buffering protein. Soc. Neurosci. Abstr. **17**, 343.

47. Chung, K.; Lee, W.T.; and Carlton, S.M. (1988) The effects of dorsal rhizotomy and spinal cord isolation on calcitonin gene-related peptide containing terminals in the rat lumbar dorsal horn. Neurosci. Lett. **90**, 27-32.

48. Coimbra, A.; Sodre-Borges, B.P. and Magalhães, M.M. (1974) The substantia gelatinosa Rolandi of the rat. Fine structure, cytochemistry (acid phosphatase) and changes after dorsal root section. J. Neurocytol. **3**, 199-217.

49. Conrath, M.; Taquert, H.; Pohl, M. and Carayon, A. (1989) Immunocytochemical evidence for calcitonin gene-related peptide-like neurons in the dorsal horn and

lateral spinal nucleus of the rat cervical spinal cord. J. Chem. Neuroanat. **2**, 335-347.

50. Dalsgaard, C.-J.; Hökfelt, T.; Johansson, O. and Elde, R. (1981) Somatostatin immunoreactive cell bodies in the dorsal horn and the parasympathetic intermediolateral nucleus of the rat spinal cord. Neurosci. Lett. **27**, 335-339.

51. Dalsgaard, C.-J.; Ygge, J.; Vincent, S.R.; Ohrling, M.; Dockray, G.J. and Elde, R. (1984) Peripheral projections and neuropeptide coexistence in a subpopulation of fluoride-resistant acid phosphatase reactive spinal primary sensory neurons. Neurosci. Lett. **51**, 139-144.

52. Dalsgaard, C.-J. (1988) The sensory system. In: Bjorklund, A.; Hökfelt, T.; Owman, C., eds. Handbook of chemical neuroanatomy, the peripheral nervous system, vol. 6. Amsterdam: Elsevier, 599-636.

53. Davidoff, R.A. and Hackman, J.C. (1984) Spinal Inhibition. In: Davidoff, R.A. ed. Handbook of the spinal cord, vols 2 and 3, anatomy and physiology. New York: Marcel Dekker, 385-459.

54. De Biasi, S. and Rustioni, A. (1988) Glutamate and substance P coexist in primary afferent terminals in the superficial laminae of spinal cord. Proc. Natl. Acad. Sci. **85**, 7820-7824.

55. Delander, G.E. and Hopkins, C.J. (1986) Spinal adenosine modulates descending antinociceptive pathways stimulated by morphine. J. Pharmacol. Exp. Ther. **239**, 88-93.

56. Deutsch, H.F. (1987) Carbonic anhydrases. Int. J. Biochem. **19**, 101-113.

57. Devor, M. and Bernstein, J.J. (1982) Abnormal impulse generation in neuromas: electrophysiology and ultrastructure. In: Culp, W.J.; Ochoa, J., eds. Abnormal nerves and muscles as impulse generators. New York: Oxford University Press, 363-380.

58. Devor, M. (1984) The pathophysiology and anatomy of damaged nerve. In: Wall, P.D.; Melzack, R., eds. Textbook of pain. Edinburgh: Churchill Livingston Press, 34-48.

59. Di Carlo, V. (1983) Serotoninergic fibers in dorsal roots of the spinal cord. Neurosci. Lett. **43**, 119-125.

60. Dodd, J.; Jahr, C.E.; Hamilton, P.N.; Heath, M.J.S.; Matthew, W.D. and Jessell, T.M. (1983) Cytochemical and physiological properties of sensory and dorsal horn neurons that transmit cutaneous sensation. Cold Spring Harbour Symp. Quant. Biol. **48**, 685-695.

61. Dodd, J.; Solter, D. and Jessell, T.M. (1984) Monoclonal antibodies against carbohydrate differentiation antigens identify subsets of primary afferent neurones. Nature **311**, 469-472

62. Dodd, J.; Jahr, C.E. and Jessell, T.M. (1984) Neurotransmitters and neuronal markers at sensory synapses in the dorsal horn. In Kruger, L. and Liebeskind, J.C., eds. Advances in Pain Research and Therapy, vol. 6. Raven Press, New York; p.

105-122.

63. Dodd, J. and Jessel, T.M. (1985) Lactoseries carbohydrates specify subsets of dorsal root ganglion neurons projecting to the superficial dorsal horn of rat spinal cord. J. Neurosci. **12**, 3278-3294.

64. Duce, I.R. and Keen, P. (1977) An ultrastructural calssification of the neuronal cell bodies of rat dorsal root ganglion using zinc iodine-osmium impregnation. Cell Tissue Res. **185**, 263-277.

65. Duggan, A.W.; Hope, P.J.; Jarrott, B.; Schaible, H.-G.; Fleetwood-Walker, S.M. (1990) Release, spread and persistence of immunoreactive neurokinin A in the dorsal horn of the cat following noxious cutaneous stimulation. Studies with antibody microprobes. Neuroscience **35**, 195-202.

66. Duggan, A.W.; Hendry, I.A.; Morton, C.R.; Hutchison, W.D. and Zhao, Z.Q. (1988) Cutaneous stimuli releasing immunoreactive substance P in the dorsal horn of the cat. Brain Res. **451**, 261-273.

67. Esplin, D.W. and Rosenstein, R. (1963) Analysis of spinal depressant actions of carbon dioxide and acetazolamide. Acta. Int. Pharmacodyn. **143**, 498-513.

68. Evans, R.H. (1989) The pharmacology of segmental transmission in the spinal cord. Prog. in Neurobiol. **33**, 255-279.

69. Fried, K.; Arvidsson, J.; Robertson, B.; Brodin, E. and Theodorsson, E. (1989) Combined retrograde tracing and enzyme/immunohistochemistry of trigeminal

ganglion cell bodies innervating tooth pulps in the rat. Neuroscience **33**, 101-109.

70. Fuxe, K.; Agnati, L.F.; McDonald, T.; Locatelli, V.; Hökfelt, T.; Dalsgaard, C.-J.; Battistini, N.; Yanaihara, N.; Mutt, V. and Cuello, A.C. (1983) Immunohistochemical indications of gastrin releasing peptide-bombesin-like immunoreactivity in the nervous system of the rat. Codistribution with substance P-like immunoreactive nerve terminal systems and coexistence with substance P-like immunoreactivity in dorsal root ganglion cell bodies. Neurosci. Lett. **37**, 17-22.

71. Fyffe, R.E.W. (1984) Afferent fibers. In: Davidoff, R.A., ed. Handbook of the spinal cord, anatomy and physiology, vols. 2 and 3. New York: Marcel Dekker; 79-136.

72. Fyffe, R.E.W. and Perl, E.R. (1984) Is ATP a central synaptic mediator for certain primary afferent fibers from mammalian skin? Proc. Natl. Acad. Sci. **81**, 6890-6893.

73. Gamse, R.; Molnar, A. and Lembeck, F. (1979) Substance P release from spinal cord slices by capsaicin. Life Sci. **25**, 629-636.

74. Gaudin-Chazal, G.; Portalier, P.; Barrit, M.C. and Puizillout, J.J. (1985) Serotonin-like immunoreactivity in paraffin-sections of the nodose ganglia of the cat. Neurosci. Lett. **33**, 169-172.

75. Giacobini, E. (1959) Quantitative determination of cholinesterase in individual spinal

ganglion cells. Acta. Physiol. Scand. **45**, 238-254.

76. Gibbins, I.L.; Furness, J.B. and Costa, M. (1987) Pathway-specific patterns of the co-existence of substance P, calcitonin gene-related peptide, cholecystokinin and dynorphin in neurons of the dorsal root ganglia of the guinea-pig. Cell Tissue Res. **248**, 417-437.

77. Gibson, S.J.; Polak, J.M.; Bloom, S.R.; Sabate, I.M.; Mulderrry, P.M.; Ghatei, M.A.; McGregor, G.P.; Morrison, J.F.B.; Kelly, J.S.; Evans, R.H. and Rosenfeld, M.G. (1984) Calcitonin gene-related peptide immunoreactivity in the spinal cord of man and of eight other species. J. Neurosci. **4**, 3101-3111.

78. Go, V.L.W. and Yaksh, T.L. (1987) Release of substance P from the cat spinal cord. J. Physiol. **391**, 141-167.

79. Harper, A.A. and Lawson, S.N. (1985) Electrical properties of rat dorsal root ganglion neurones with different peripheral nerve conduction velocities. J. Physiol. **359**, 47-63.

80. Hatai, S. (1902) Number and size of the spinal ganglion cells and dorsal root fibers in the white rat at different ages. J. Comp. Neurol. **12**, 107-124.

81. Heizmann, C.W. (1984) Parvalbumin, an intracellular calcium-binding protein; distribution, properties and possible roles in mammalian cells. Experentia **40**, 910-921.

82. Heizmann, C.W. and Berchtold, M.W. (1987) Expression of parvalbumin and other

calcium binding proteins in normal and tumor cells: a topical review. Cell Calcium **8**, 1-41.

83. Henry, J.L. (1976) Effects of substance P on functionally identified units in cat spinal cord. Brain Res. **114**, 439-451.

84. Hinrichsen, C.F.L. (1970) Coupling between cells of the trigeminal nucleus. J. Dent. Res. **49**, 1369-1373.

85. Hinrichsen, C.F.L. and Larramendi, L.M.H. (1970) The trigeminal mesencephalic nucleus. II Electron microscopy. Am. J. Anat. **127**, 303-320.

86. Hirst, G.D.S. and Spence, I. (1973) Calcium action potentials in mammalian peripheral neurones. Nature (New Biol.) **243**, 54-56.

87. Hökfelt, T.; Kellerth, J.O.; Nilsson, G. and Pernow, B. (1975) Substance P: Localization in the central nervous system and in some primary sensory neurons. Science **190**, 889-890.

88. Hökfelt, T.; Elde, R.; Johansson, O.; Luft, R. and Arimura, A. (1975) Immunohistochemical evidence for the presence of somatostatin, a powerful inhibitory peptide, in some primary sensory neurons. Neurosci. Lett. **1**, 231-235.

89. Hökfelt, T.; Elde, R.; Johansson, T.; Luft, T.; Nilsson, G. and Arimura, A. (1976) Immunohistochemical evidence for separate populations of somatostatin-containing and substance P-containing primary afferent neurons in the rat.

Neuroscience **1**, 131-136.

90. Holland, G.R. (1987) The effects of nerve section on the incidence and distribution of gap junctions in the odontoblast layer of the cat. Anat. Rec. **218**, 458-465.

91. Holzer, P. (1988) Local effector functions of capsaicin-sensitive sensory nerve endings: involvement of tachykinins, calcitonin gene-related peptide and other neuropeptides. Neuroscience **24**, 739-768.

92. Huizar, P.; Kuno, M. and Miyata, Y. (1975) Electrophysiological properties of spinal motoneurons of normal and dystrophic mice. J. Physiol. **248**, 231-246.

93. Hunt, S.P. and Rossi, J. (1985) Peptide- and non-peptide-containing unmyelinated primary afferents: the parallel processing of nociceptive information. Phil. Trans. R. Soc. Lond. **B308**, 283-289.

94. Hunt, S.P.; Kelly, J.S.; Emson, P.C.; Kimmel, J.R.; Miller, R.J. and Wu, J.-Y. (1981) An immunohistochemical study of neuronal populations containing neuropeptides or gamma-aminobutyrate within the superficial layers of the rat dorsal horn. Neuroscience **6**, 1883-1898.

95. Hyden, H.; Lovtrup, S. and Pigon, A. (1958) Cytochrome oxidase and succinoxidase acitivities in spinal ganglion cells and in glial capsule cells. J. Neurochem. **2**, 304-311.

96. Ishida-Yamamoto, A. and Tohyama, M. (1989) Calcitonin gene-related peptide in the nervous tissue. Prog. Neurobiol. **33**, 335-386.

97. Ishida-Yamamoto, A.; Senba, E. and Tohyama, M. (1989) Distribution and fine structure of calcitonin gene-related peptide-like immunoreactive nerve fibers in the rat skin. Brain Res. **491**, 93-101.

98. Ishida-Yamamoto, A. and Senba, E. (1990) Cell types and axonal sizes of calcitonin gene-related peptide-containing primary sensory neurons of the rat. Brain Res. Bull. **24**, 759-764.

99. Ito, F. and Komatsu, Y. (1979) Calcium-dependent regenerative responses in the afferent nerve terminal of the frog muscle spindle. Brain Res. **175**, 160-164.

100. Janig, W. (1985) Causalgia and reflex sympathetic dystrophy: In which way is the sympathetic nervous system involved? Trends Neurosci. **8**, 471-477.

101. Janig, W. (1988) Pathophysiology of nerve following mechanical injury. In: Dubner, R.; Gebhart, G.F. and Bond, M.R., eds. Pain Research and Clinical Management, vol. 3. Amsterdam: Elsevier; 89-108.

102. Jeftinija, S.; Murase, K.; Nedeljikov, V. and Randic, M. (1982) Vasoactive intestinal polypeptide excites mammalian dorsal horn neurons both *in vivo* and *in vitro*. Brain Res. **243**, 158-164.

103. Jessell, T.M. and Dodd, J. (1990) Carbohydrates and carbohydrate-binding proteins in the nervous system. Ann. Rev. Neurosci. **13**, 227-255.

104. Jessell, T.M. and Dodd, J. (1989) Functional chemistry of primary afferent neurons.

In: Wall, P.D.; Melzak, R., eds. Textbook of pain. Edinburgh: Churchill Livingston Press; 82-99.

105. Johansson, O.; Hökfelt, T.; Pernow, B.; Jeffcoate, S.L.; White, N.; Steinbusch, H.W.M.; Verhofstad, A.A.J.; Emson, P.C. and Spindel, E. (1981) Immunohistochemical support for three putative transmitters in one neuron: coexistence of 5-hydroxytryptamine, substance P- and thyrotropin releasing hormone-like immunoreactivity in medullary neurons projecting to the spinal cord. Neuroscience **6**, 1857-1881.

106. Jozsa, R.; Korf, H.-W. and Merchenthaler, I. (1987) Growth hormone-releasing factor (GRF)-like immunoreactivity in sensory ganglia of the rat. Cell Tissue Res. **247**, 441-444.

107. Ju, G.; Hökfelt, T.; Brodin, E.; Fahrenbrug, J.; Fischer, J.A.; Frey, P.; Elde, R. and Brown, J.C. (1987) Primary sensory neurons of the rat showing calcitonin gene-related peptide immunoreactivity and their relations to substance P-, somatostatin-, galanin-, vasoactive intestinal polypeptide- and cholecystokinin-immunoreactive ganglion cells. Cell Tissue Res. **247**, 417-431.

108. Kageyama, G.H. and Wong-Riley, M.T.T. (1982) Histochemical localization of cytochrome oxidase in the hippocampus: correlation with specific neuronal types and afferent pathways. Neuroscience **7**, 2337-2361.

109. Kai-Kai, M.A. and Keen, P.A. (1985) Localization of 5-hydroxytryptamine to neurons and endoneurial mast cells in rat sensory ganglia. J. Neurocytol. **14**, 63-78.

110. Kai-Kai, M.A.; Anderton, B.H. and Keen, P.A (1986) Quantitative analysis of the interrelationships between subpopulations of rat sensory neurons containing arginine vasopressin or oxytocin and those containing substance P, fluoride-resistant acid phosphatase or neurofilament protein. Neuroscience **18**, 475-486.

111. Katz, D.M.; Markey, K.A.; Goldstein, M. and Black, I.B. (1983) Expression of catecholaminergic characteristics by primary sensory neurons in the normal adult rat *in vivo*. Proc. Natl. Acad. Sci. **80**, 3526-3530.

112. Katz, D.M. and Black, I.B. (1986) Expression and regulation of catecholaminergic traits in primary sensory neurons: Relationship to target innervation *in vivo*. J. Neurosci. **6**, 983-989.

113. Kawaguchi, Y.; Katsumaru, H.; Kosaka, T.; Heizmann, C.W. and Hama, K. (1987) Fast spiking cells in rat hippocampus (CAl region) contain the calcium-binding protein parvalbumin. Brain Res. **416**, 369-374.

114. King, C.E.; Garrey, W.E. and Bryan, W.R. (1932) The effect of carbon dioxide, hyperventilation, and anoxemia on the knee jerk. Am. J. Physiol. **102**, 305-318.

115. Kirchgessner, A.L.; Dodd, J. and Gershon, M.D. (1988) Markers shared between dorsal root and enteric ganglia. J. Comp. Neurol. **276**, 607-621.

116. Knyihar, E. (1971) Fluoride-resistant acid phosphatase system of nociceptive dorsal root afferents. Experientia **27**, 1205-1207.

117. Knyihar, E. and Gerebtzoff, M.A. (1973) Extra-lysosomal localization of acid phosphatase in the spinal cord of the rat. Exp. Brain Res. **18**, 383-395.

118. Knyihar, E.; Laszlo, I. and Tornyos, S. (1974) Fine structure and fluoride-resistant acid phosphatase activity of electron dense sinusoid terminals in the substantia gelatinosa Rolandi of the rat after dorsal root transection. Exp. Brain Res. **19**, 529-544.

119. Knyihar-Csillik, E. and Torok, A. (1989) Cytochemical restoration in the upper dorsal horn after transganglionic degenerative atrophy: Temporospatial and fine structural correlates. Neuroscience **33**, 75-91.

120. Koerber, H.R.; Druzinsky, E. and Mendell, L.M. (1988) Properties of somata of spinal dorsal root ganglion cells differ according to peripheral receptor innervated. J. Neurophysiol. **60**, 1584-1596.

121. Korn, H.; Sotelo, C. and Crepel, F. (1973) Electrotonic coupling between neurons in the rat lateral vestibular nucleus. Exp. Brain Res. **16**, 255-275.

122. Krnjevic, K.; Puil, E. and Werman, R. (1975) Evidence for Ca^{2+}-activated K^{+} conductance in cat spinal motoneurons from intracellular EGTA injections. Can. J. Physiol. Pharm. **53**, 1214-1218.

123. Kruger, L.; Sternini, C.; Brecha, N.C. and Mantyh, P.W. (1988) Distribution of calcitonin gene-related peptide immunoreactivity in relation to the rat central somatosensory projection. J. Comp. Neurol. **273**, 149-162.

124. Kruger, L.; Silverman, J.D.; Mantyh, P.W.; Sternini, C. and Brecha, N.C. (1989) Peripheral patterns of calcitonin gene-related peptide general somatic innervation: Cutaneous and deep terminations. J. Comp. Neurol. **280**, 291-302.

125. Kummer, W. and Heym, C. (1986) Correlation of neuronal size and peptide immunoreactivity in the guinea pig trigeminal ganglia. Cell Tissue Res. **245**, 657-665.

126. Kuraishi, Y.; Hirota, N.; Hino, Y.; Satoh, M. and Takagi, H. (1985) Evidence that substance P and somatostatin transmit separate information related to pain in the spinal dorsal horn. Brain Res. **325**, 294-298.

127. Kuraishi, Y. Nakayama, Y.; Ohno, H.; Minami, M. and Sato, M. (1988) Antinociception induced in rats by intrathecal administration of antiserum against calcitonin gene-related peptide. Neurosci. Lett. **92**, 325-329.

128. Kuraishi, Y. Nakayama, Y.; Ohno, H.; Fujii, N.; Otaka, A.; Yajima, H. and Sato, M. (1989) Calcitonin gene-related peptide increases in the dorsal root ganglion of adjuvant arthritic rat. Peptides **10**, 447-452.

129. Kuwayama, Y. and Stone, R.A. (1986) Neuropeptide immunoreactivity of pericellualr baskets in the guinea pig trigeminal ganglion. Neurosci. Lett. **64**, 169-172.

130. La Motte, R.H.; Simone, D.A.; Bauman, T.K.; Shain, C.N. and Alreja, M. (1988) Hypothesis for novel classes of chemoreceptors mediating chemogenic pain and itch. In: Dubner, R.; Gebhart, G.F.; Bond, M.R. eds. Pain research and clinical

management, vol. 3. Amsterdam: Elsevier; 529-535.

131. Lawson, S.N.; Caddy, K.W.T. and Biscoe, T.J. (1974) Development of rat dorsal root ganglion neurones. Cell Tissue Res. **153**, 399-413.

132. Lawson, S.N. (1979) The postnatal development of large light and small dark neurons in mouse dorsal root ganglia: a statistical analysis of cell number and size. J. Neurocytol. **8**, 275-294.

133. Lawson, S.N.; Harper, A.A.; Harper, E.I.; Garson, J.A. and Anderton, B.H. (1984) A monoclonal antibody against neurofilament protein specifically labels a subpopulation of rat sensory neurones. J. Comp. Neurol. **228**, 263-272.

134. Leah, J.D.; Cameron, A.A. and Snow, P.J. (1985) Neuropeptides in physiologically identified mammalian sensory neurones. Neurosci. Lett. **56**, 257-263.

135. LeGreves, P.; Nyberg, F.; Terenius, L. and Hokfelt, T. (1985) Calcitonin gene-related peptide is a potent inhibitor of substance P degradation. Eur. J. Pharmacol. **115**, 309-311.

136. Lehtosalo, J.I.; Uusitalo, H.; Stjernschantz and Palkama, A. (1984) Substance P-like immunoreactivity in the trigeminal ganglion. Histochem. **80**, 421-427.

137. Lehtosalo, J.I.; Uusitalo, H.; Laakso, J.; Palkama, A. and Härkönen, M. (1984) Biochemical and immunohistochemical determination of 5-hydroxytryptamine located in mast cells in the trigeminal ganglion of the rat and guinea pig. Histochem. **80**, 219-223.

138. Lieberman, A.R. (1976) Sensory ganglia. In: Landon, D.N. ed. The peripheral nerve. London: Chapman and Hall; 188-278.

139. Light, A.R.; Trevino. D.L. and Perl, E.R. (1979) Morphological features of functionally defined neurons in the marginal zones and substantia gelatinosa of the spinal dorsal horn. J. Comp. Neurol. **186**, 151-172.

140. Light, A.R. and Perl, E.R. (1979) Spinal termination of functionally identified primary afferent neurons with slowly conducting myelinated fibers. J. Comp. Neurol. **186**, 133-150.

141. Lisney, S.J.W. and Devor, M. (1987) After discharge and interactions among fibers in damaged peripheral nerve in the rat. Brain Res. **415**, 122-136.

142. Lisney, S.J.W. and Pover, C.M. (1983) Coupling between fibres involved in sensory nerve neuromata in cats. J. Neurol. Sci. **59**, 255-264.

143. Marusich, M.F.; Pourmehr, K. and Weston, J.A. (1986) A monoclonal antibody (SN1) identifies a subpopulation of avian sensory neurons whose distribution is correlated with axial level. Develop. Biol. **118**, 494-504.

144. Matthews, B. (1976) Coupling between cutaneous nerves. J. Physiol. **254**, 37P-38P.

145. Matthews, B. and Holland, G.R. (1975) Coupling between nerves in teeth. Brain Res. **98**, 354-358.

146. Maxwell, D.J.; Christie, W.M.; Otterson, O.P. and Storm-Mathisen, J. (1990) Terminals of group Ia primary afferent fibers in Clarke's column are enriched with L-glutamate-like immunoreactivity. Brain Res. **510**, 346-350.

147. Mawe, G.M. and Gershon, M.D. (1986) Functional heterogeneity in the myenteric plexus: demonstration using cytochrome oxidase as a verified cytochemical probe of the activity of individual enteric neurons. J. Comp. Neurol. **249**, 381-391.

148. Mawe, G.M.; Gardette, R.; D'Agostaro, L. and Role, L.W. (1990) Development of synaptic transmission at autonomic synapses *in vitro* revealed by cytochrome oxidase histochemistry. J. Neurobiol. **21**, 578-591.

149. McMahon, S.B. (1986) The localisation of fluoride-resistant acid phosphatase (FRAP) in the pelvic nerves and sacral spinal cord of rats. Neurosci. Lett. **64**, 305-310.

150. McMahon, S.B.; Sykova, E.; Wall, P.D.; Woolf, C.J. and Gibson, S. (1984) Neurogenic extravasation and substance P levels are low in muscle as compared to skin, in the rat hindlimb. Neurosci. Lett. **52**, 235-240.

151. Meech, R.W. (1978) Calcium-dependent potassium activation in nervous tissue. Ann. Rev. Biophys. Bioeng. **7**, 1-18.

152. Merighi, A.; Polak, J.M.; Gibson, S.J.; Gulbenkian, S.; Valentino, K.L. and Peirone, S.M. (1988) Ultrastructural studies on calcitonin gene-related peptide-, tachkinins- and somatostatin-immunoreactive neurones in rat dorsal root

ganglia: Evidence for the colocalization of different peptides in single secretory granules. Cell Tissue Res. **254**, 101-109.

153. Merighi, A.; Kar, S.; Gibson, S.J.; Ghidella, S.; Gobetto, A.; Peirone, S.M. and Polak, J.M. (1990) The immunocytochemical distribution of seven peptides in the spinal cord and dorsal root ganglia of horse and pig. Anat. Embryol. **181**, 271-280.

154. Meyer, R.A. and Campbell, J.N. (1987) Coupling between unmyelinated peripheral nerve fibers does not involve sympathetic efferent fibers. Brain Res. **437**, 191-182.

155. Meyer, R.A. and Campbell, J.N. (1988) A novel electrophysiological technique for locating cutaneous nociceptive and chemospecific receptors. Brain Res. **441**, 81-86.

156. Meyer, R.A.; Raja, S.N. and Campbell, J.N. (1985) Coupling of action potential activity between unmyelinated fibers in the peripheral nerve of monkey. Science **227**, 184-187.

157. Miletic, V. and Randic, M. (1982) Neonatal rat spinal cord slice preparation: postsynaptic effects of neuropeptides on dorsal horn neurons. Dev. Brain Res. **2**, 432-438.

158. Miletic, V. and Tan, H. (1988) Iontophoretic application of calcitonin gene-related peptide produces a slow and prolonged excitation of neurons in the cat lumbar dorsal horn. Brain Res. **446**, 169-172.

159. Millhorn, D.E.; Seroogy, K.; Hökfelt, T.; Schmued, L.C.; Terenius, L.; Buchan, A. and Brown, J.C. (1987) Neurons of the ventral medulla oblongata that contain both somatostatin and enkephalin immunoreactivities project to nucleus tractus solitarii and spinal cord. Brain Res. **424**, 99-108.

160. Molander, C.; Ygge, J. and Dalsgaard, C.-J. (1987) Substance P-, somatostatin- and calcitonin gene-related peptide-like immunoreactivity and fluoride-resistant acid phosphatase-activity in relation to retrogradely labelled cutaneous, muscular and visceral primary sensory neurons in the rat. Neurosci. Lett. **74**, 37-42.

161. Morton, C.R., Hutchison, W.E. and Hendry, I.A. (1988) Release of immunoreactive somatostatin in the spinal dorsal horn of the cat. Neuropeptides **12**, 189-197.

162. Morton, C.R.; Hutchison, W.D.; Hendry, I.A. and Duggan, A.W. (1989) Somatostatin: evidence for a role in thermal nociception. Brain Res. **488**, 89-96.

163. Morton, C.R. and Hutchison, W.D. (1989) Release of sensory neuropeptides in the spinal cord: studies with calcitonin gene-related peptide and galanin. Neuroscience **31**, 807-815.

164. Murase, K.; Ryu, P.D. and Randic, M. (1986) Substance P augments a persistent slow inward calcium-sensitive current in voltage-clamped spinal dorsal horn neurons of the rat. Brain Res. **365**, 369-376.

165. Nagy, J.I. and Hunt, S.P. (1982) Fluoride-resistant acid phosphatase-containing

neurons in dorsal root ganglia are separate from those containing substance P or somatostatin. Neuroscience **7**, 89-97.

166. Nagy, J.I.; Yamamoto, T.; Shiosaka, S.; Dewar, K.M.; Whittaker, M.E. and Hertzberg, E.L. (1988) Immunohistochemical localization of gap junction protein in rat CNS: a preliminary account. In: Hertzberg, E.L.; Johnson, R., eds. Gap junctions. New York: Alan R. Liss, Inc.; 375-389.

167. Nagy, J.I. and Daddona, P.E. (1985) Anatomical and cytochemical relationships of adenosine deaminase-containing primary afferent neurons in the rat. Neuroscience **15**, 799-813.

168. Nagy, J.I.; Hunt, S.P.; Iversen, L.L. and Emson, P.C. (1981) Biochemical and anatomical observations on the degeneration of peptide-containing primary afferent neurons after neonatal capsaicin. Neuroscience **10**, 1923-1934.

169. Nakagawa, F.; Schuffe, B.A. and Spicer, S.S. (1986) Lectin cytochemical evaluation of somatosensory neurons and their peripheral and central processes in rat and man. Cell Tissue Res. **245**, 579-589.

170. Noguchi, K.; Senba, E.; Morita, Y.; Sato, M. and Tohyama, M. (1989) Prepro-VIP and preprotachykinin mRNAs in the rat dorsal root ganglion cells following peripheral axotomy. Mol. Brain Res. **6**, 327-330.

171. Noguchi, K.; Senba, E.; Morita, Y.; Sato, M. and Tohyama, M. (1990) Co-expression of alpha-CGRP and beta-CGRP mRNAs in the rat dorsal root ganglion cells. Neurosci. Lett. **108**, 1-5.

172. Obata, K. (1976) Excitatory effects of GABA. In: Roberts, E.; Chase, T.N.; Tower, D.B., eds. GABA in nervous system function. New York: Raven Press; 283-286.

173. O'Brien, C.; Woolf, C.J.; Fitzgerald, M.; Lindsay, R.M. and Molander, C. (1989) Differences in the chemical expression of rat primary afferent neurons which innervate skin, muscle or joint. Neuroscience **32**, 493-502.

174. Ochoa, J. and Noordenbos, W. (1979) Pathology and disordered sensation in local nerve lesions: An attempt at correlation. In: Bonica, J.J.; Leibeskind, J.C. and Albe-Fessard, P.G., eds. Advances in Pain Research and Therapy, vol. 3. New York, Raven Press; 67-90.

175. Oku, R.; Satoh, M.; Fujii, N.; Otaka, A.; Yajima, H. and Takagi, H. (1987) Calcitonin gene-related peptide promotes mechanical nociception by potentiating release of substance P from the spinal dorsal horn in rats. Brain Res. **403**, 350-354.

176. Pannese, E.; Luciano, L.; Iurato, S. and Reale, E. (1977) Intercellular junctions and other membrane specializations in developing spinal ganglia: A freeze fracture study. J. Ultrastruc. Res. **60**, 169-180.

177. Panula, P.; Hadjiconstantinou, M.; Yang, H.-Y.T. and Costa, E. (1983) Immunohistochemical localization of bombesin/gastrin-releasing peptide and substance P in primary sensory neurons. J. Neurosci. **3**, 2021-2029.

178. Pernow, B. Substance P. Pharmacol. Rev. 35: 85-141; 1983.

179. Perry, M.J.; Lawson, S.N. and Wood, J. (1991) Immunocytochemical properties of rat dorsal root ganglion (DRG) neurones innervating muscle, skin or viscera. Soc. Neurosci. Abstr. **17**, 105.

180. Peyronnard, J.M.; Charron, L.; Messier, J.P. and Lavoie, J. (1988) Differential effects of distal and proximal nerve lesions on carbonic anhydrase activity in rat primary sensory neurons, ventral and dorsal root axons. Exp. Brain Res. **70**, 550-560.

181. Peyronnard, J.M.; Charron, L.; Lavoie, J.; Messier, J.P. and Dubreuil, M. (1988) Carbonic anhydrase and horseradish peroxidase: double labelling of rat dorsal root ganglion neurons innervating motor and sensory peripheral nerves. Anat. Embryol. **177**, 353-359.

182. Philippe, E. and Droz, B. (1986) Effect of skeletal muscle on the expression of a calcium-binding protein (calbindin) in dorsal root ganglion of the chick embryo. Soc. Neurosci. Abstr. **12**, 1125.

183. Philippe, E. and Droz, B. (1988) Calbindin D-28k-immunoreactive neurons in chick dorsal root ganglion: ontogenesis and cytological characteristics of the immunoreactive sensory neurons. Neuroscience **26**, 215-224.

184. Philippe, E.; Garosi, M. and Droz, B. (1988) Influence of peripheral and central targets on subpopulations of sensory neurons expressing calbindin immunoreactivity in the dorsal root ganglion of the chick embryo. Neuroscience

26, 225-232.

185. Phillis, J.W. and Wu, P.H. (1981) The role of adenosine and its nucleotides in central synaptic transmission. Prog. Neurobiol. **16**, 187-239.

186. Post, C. (1984) Antinociceptive effects in mice after intrathecal injection of 5′-N-ethylcarboxamide adenosine. Neurosci. Lett. **51**, 325-330.

187. Price, D.D.; Hayashi, H.; Dubner, R. and Ruda, M.A. (1979) Functional relationships between neurons of marginal and substantia gelatinosa layers of primate dorsal horn. J. Neurophysiol. **42**, 1590-1608.

188. Price, J. and Mudge, A.W. (1983) A subpopulation of rat dorsal root ganglion neurones is catecholaminergic. Nature **301**, 241-243.

189. Price, J. (1985) An immunohistochemical and quantitative examination of dorsal root ganglion neuronal subpopulations. J. Neurosci. **5**, 2051-2059.

190. Rambourg, A.; Clermont, Y. and Beaudet, A. (1983) Ultrastructural features of six types of neurons in rat dorsal root ganglia. J. Neurocytol. **12**, 47-66.

191. Randic, M. and Miletic, V. (1977) Effect of substance P in cat dorsal horn neurones activated by noxious stimuli. Brain Res. **128**, 164-169.

192. Randic, M.; Ryu, P.D. and Urban, L. (1986) Effects of polyclonal and monoclonal antibodies to substance P on slow excitatory transmission in rat spinal dorsal horn. Brain Res. **383**, 15-27.

193. Randic, M.; Jeftinija, S.; Urban, L.; Raspantini, C. and Folkers, K. (1988) Effects of substance P analogues on spinal dorsal horn neurons. Peptides **9**, 651-660.

194. Rasminsky, M. (1980) Ephaptic transmission between single nerve fibers in the spinal nerve roots of dystrophic mice. J. Physiol. (Lond.) **305**, 151-169.

195. Rasminsky, M. (1978) Ectopic generation of impulses and cross-talk in spinal nerve roots of "Dystrophic" mice. Ann. Neurol. **3**, 351-357.

196. Rethelyi, M.; Light, A.R. and Perl, E.R. (1989) Synaptic ultrastructure of functionally and morphologically characterized neurons of the superficial spinal dorsal horn of cat. J. Neurosci. **9**, 1846-1863.

197. Ribeiro-da-Silva, A.; Castro-Lopes, J.M. and Coimbra, A. (1986) Distribution of glomeruli with fluoride-resistant acid phosphatase (FRAP)-containing terminals in the substantia gelatinosa of the rat. Brain Res. **377**, 323-329.

198. Riley, D.A.; Ellis, S. and Bain, J. (1982) Carbonic anhydrase activity in skeletal muscle fiber types, axons, spindles, and capillaries of rat soleus and extensor digitorum longus muscles. J. Histochem. Cytochem. **30**, 1275-1288.

199. Riley, D.A.; Sanger, J.R.; Matloub, H.S.; Yousif, N.J.; Bain, J.L.W. and Moore, G.H. (1988) Identifying motor and sensory myelinated axons in rabbit peripheral nerves by histochemical staining for carbonic anhydrase and cholinesterase activities. Brain Res. **453**, 79-88.

200. Riley, D.A.; Ellis, S. and Bain, J.L.W. (1984) Ultrastructural cytochemical localization of carbonic anhydrase activity in rat peripheral sensory and motor nerves, dorsal root ganglia and dorsal column nuclei. Neuroscience **13**, 189-206.

201. Robertson, B. and Grant, G. (1989) Immunocytochemical evidence for the localization of the GM1 ganglioside in carbonic anhydrase-containing and RT-97 immunoreactive rat primary sensory neurons. J. Neurocytol. **18**, 77-86.

202. Rose, R.D.; Koerber, H.R.; Sedivec, M.J. and Mendell, L.M. (1986) Somal action potential duration differs in identified primary afferents. Neurosci. Lett. **63**, 259-264.

203. Rosenfeld, M.G.; Mermod, J.J.; Amara, S.G.; Swanson, L.W.; Sawchenko, P.E.; Rivier, J.; Vale, W.W. and Evans, R.M. (1983) Production of a novel neuropeptide encoded by the calcitonin gene via tissue-specific RNA prodessing. Nature **304**, 129-135.

204. Ryu, P.D.; Gerber, G.; Murase, K. and Randic, M. (1988) Actions of calcitonin gene-related peptide on rat spinal dorsal horn neurons. Brain Res. **441**, 357-361.

205. Ryu, P.D.; Gerber, G.; Murase, K. and Randic, M. (1988) Calcitonin gene-related peptide enhances calcium current of rat dorsal root ganglion neurons and spinal excitatory synaptic transmission. Neurosci. Lett. **89**, 305-312.

206. Salt, T.E. and Hill, R.G. (1983) Neurotransmitter candidates of somatosensory primary afferent fibres. Neuroscience **10**, 1083-1103.

207. Salter, M.W. and Henry, J.L. (1985) Effects of adenosine 5′-monophosphate and adenosine 5′-triphosphate on functionally identified units on the cat spinal dorsal horn. Evidence for a differential effect of adenosine 5′-triphosphate on nociceptive vs non-nociceptive units. Neuroscience **15**, 815-825.

208. Sapirstein, V.S.; Strocchi, P. and Gilbert, J. M. (1984) Properties and function of brain carbonic anhydrase. In: Tshian, R.E.; Hewett-Emmett, D., eds. Biology and chemistry of the carbonic anhydrases, vol. 429. New York: Annals of the New York Academy of Sciences; 481-493.

209. Schneider, S.P. and Perl, E.R. (1988) Comparison of primary afferent and glutamate excitation of neurons in the mammalian spinal dorsal horn. J. Neurosci. **8**, 2062-2073.

210. Schoene, J.; Van Hees, J.; Gybels, J.; de Catro Costa, M. and Vanderhaeghen, J.J. (1985) Histochemical changes of substance P, FRAP, serotonin and succinic dehydrogenase in the spinal cords of rats with adjuvant arthritis. Life Sciences **36**, 1247-1254.

211. Scott, S.A.; Patel, N. and Levine, J.M. (1990) Lectin binding identifies a subpopulation of neurons in chick dorsal root ganglia. J. Neurosci. **10**, 336-345.

212. Seligman, A.M.; Karnovsky, M.J.; Wasserkrug, H.L. and Hanker, J.S. (1968) Nondroplet ultrastructural demonstration of cytochrome oxidase activity with a polymerizing osmiophilic reagent, diaminobenzidine (DAB). J. Cell Biol. **38**, 1-14.

213. Seltzer, Z. and Devor, M. (1979) Ephaptic transmission in chronically damaged peripheral nerves. Neurology **29**, 1061-1064.

214. Seybold, V. and Elde, R. (1980) Immunohistochemical studies of peptidergic neurons in the dorsal horn of the spinal cord. J. Histochem. Cytochem. **28**, 367-370.

215. Shiosaka, S.; Yamamoto, T.; Hertzberg, E.L. and Nagy, J.I. (1989) Gap junction protein in rat hippocampus: Correlative light and electron microscope immunohistochemical localization. J. Comp. Neurol. **281**, 282-297.

216. Shortland, P.; Woolf, C.J. and Fitzgerald, M. (1989) Morphology and somatotopic organization of the central terminals of hindlimb hair follicle afferents in the rat lumbar spinal cord. J. Comp. Neurol. **289**, 416-433.

217. Skene, J.H.P. (1989) Axonal growth-associated proteins. Ann. Rev. Neurosci. **12**, 127-156.

218. Skofitsch, G.; Zamir, N.; Helke, C.J.; Savitt, J.M. and Jacobowitz, D.M. (1985) Corticotropin releasing factor-like immunoreactivity in sensory ganglia and capsaicin sensitive neurons of the rat central nervous system: colocalization with other neuropeptides. Peptides **6**, 307-318.

219. Skofitsch, G. and Jacobowitz, D.M. (1985) Galanin-like immunoreactivity in capsaicin sensitive sensory neurons and ganglia. Brain Res. Bull. **15**, 191-195.

220. Sommer, E.W.; Kazimierczak, J. and Droz, B. (1985) Neuronal subpopulations in the dorsal root ganglion of the mouse as characterized by combination of ultrastructural and cytochemical features. Brain Res. **346,** 310-326.

221. Sotelo, C. and Palay, S.L. (1970) The fine structure of the lateral vestibular nucleus in the rat. II Synaptic organization. Brain Res. **18,** 93-115.

222. Sugimoto, T.; Takemura, M.; Ichikawa, H. and Akai, M. (1989) Carbonic anhydrase activity in the trigeminal primary afferent neuronal cell bodies with peripheral axons innervating the mandibular molar tooth pulps of the rat. Brain Res. **505,** 354-357.

223. Sugiura, Y.; Lee, C.L. and Perl, E.R. (1986) Central projections of identified, unmyelinated (C) afferent fibers innervating mammalian skin. Science **234,** 358-361.

224. Sugiura, Y.; Hosoya, Y.; Ito, R. and Kohno, K. (1988) Ultrastructural features of functionally identified primary afferent neurons with C (unmyelinated) fibers of the guinea pig: classification of dorsal root ganglion cell type with reference to sensory modality. J. Comp. Neurol. **276,** 265-278.

225. Sweetnam, P.M.; Wrathall, J.R. and Neale, J.H. (1986) Localization of dynorphin gene product-immunoreactivity in neurons from spinal cord and dorsal root ganglia. Neuroscience **18,** 947-955.

226. Szolcsanyi, J. (1988) Antidromic vasodilation and neurogenic inflammation. Agents and Actions **23,** 4-11.

227. Tessler, A.; Glazer, E.; Artymyshyn, R.; Murray, M. and Goldberger, M.E. (1980) Recovery of substance P in the cat spinal cord after unilateral lumbosacral deafferentation. Brain Res. **191**, 459-470.

228. Tessler, A.; Himes, B.T.; Artymyshyn, R.; Murray, M. and Goldberger, M.E. (1981) Spinal neurons mediate return of substance P following deafferentation of cat spinal cord. Brain Res. **230**, 263-281.

229. Tewari, H.B. and Borne, G.H. (1962) Histochemical evidence of metabolic cycles in spinal ganglion cells of rat. J. Histochem. Cytochem. **10**, 42-64.

230. Tuchscherer, M.M. and Seybold, V.S. (1985) Immunohistochemical studies of substance P, cholecystokinin-octapeptide and somatostatin in dorsal root ganglia of the rat. Neuroscience **14**, 593-605.

231. van Raamsdonk, W.; Smit-Onel, M.; Donselaar, Y. and Diegenbach, P. (1987) Quantitative cytochemical analysis of cytochrome oxidase and succinate dehydrogenase activity in spinal neurons. Acta Histochem. **81**, 129-141.

232. Vaughn, T.; Behbehani, M.M.; Zemlan, F.P. and Shipley, M. (1984) Increased cytochrome oxidase staining in rat spinal cord subsequent to peripheral noxious stimulation. Soc. Neurosci. Abstr. **14**, 119.

233. Villar, M.F.; Corté s, R.; Theordorsson, E.; Wiesenfeld-Hallin, Z.; Schalling, M.; Fahrenkrug, J.; Emson, P.C. and Hökfelt, T. (1989) Neuropeptide expression in rat dorsal root ganglion cells and spinal cord after peripheral nerve injury with

special reference to galanin. Neuroscience **33**, 587-604.

234. Vincent, S.R.; Schultzberg, M. and Dalsgaard, C.-J. (1982) Fluoride-resistant acid phosphatase in the rat adrenal gland. Brain Res. **253**, 325-329.

235. Warrington, W.B. and Griffith, F. (1904) On the cells of the spinal ganglia and on the relationship of their histological structure to the axonal distribution. Brain **27**, 297-326.

236. Weihe, E.; Hartschuh, W. and Weber, E. (1985) Prodynorphin opioid peptides in small somatosensory primary afferents of guinea pig. Neurosci. Lett. **58**, 347-352.

237. Wiesenfeld-Hallin, Z.; Hökfelt, T.; Lundberg, J.M.; Firssman, W.G.; Reuneche, M.; Tschopp, F.A. and Fischer, J.A. (1984) Immunoreactive calcitonin gene-related peptide and substance P coexist in sensory neurons to the spinal cord and interact in spinal behavioral responses of the rat. Neurosci. Lett. **52**, 199-204.

238. Willis, W.D. and Coggeshall, R.E. (1991) Sensory mechanisms of the spinal cord, second edition. New York: Plenum Press.

239. Wong, V.; Barrett, C.P.; Donati, E.J.; Eng, L.F. and Guth, L. (1983) Carbonic anhydrase activity in first-order sensory neurons of the rat. J. Histochem. Cytochem. **31**, 293-300.

240. Wong, V.; Barrett, C.P.; Donati, E.J. and Guth, L. (1987) Distribution of carbonic anhydrase activity in neurons of the rat. J. Comp. Neurol. **257**, 122-129.

241. Wong-Riley, M.T.T. (1989) Cytochrome oxidase: an endogenous metabolic marker for neuronal activity. Trends Neurosci. **12**, 94-101.

242. Wong-Riley, M.T.T.; Walsh, S.M.; Leake-Jones, P.A. and Merzenich, M.M. (1981) Maintenance of neuronal activity by electrical stimulation of unilaterally deafened cats demonstrable with cytochrome oxidase technique. Ann. Otol. Rhinol. Lar. **90 (Suppl. 82)**, 30-32.

243. Wong-Riley, M.T.T. and Carroll, E.W. (1984) The effect of impulse blockage on cytochrome oxidase activity in the monkey visual system. Nature **307**, 262-264.

244. Wong-Riley, M.T.T. and Kageyama, G.H. (1986) Localization of cytochrome oxidase in the mammalian spinal cord and dorsal root ganglia, with quantitative analysis of ventral horn cells in monkeys. J. Comp. Neurol. **245**, 41-61.

245. Woolf, C.J.; Chong, M.S. and Rashdi, T.A. (1985) Mapping increased glycogen phosphorylase activity in dorsal root ganglia and in the spinal cord following peripheral stimuli. J. Comp. Neurol. **234**, 60-76.

246. Woolf, C.J. (1987) Central terminations of cutaneous mechanoreceptive afferents in the rat lumber spinal cord. J. Comp. Neurol. **261**, 105-119.

247. Woolf, C.J. and Fitzgerald, M. (1983) The properties of neurons recorded in the superficial dorsal horn of the rat spinal cord. J. Comp. Neurol. **221**, 313-328.

248. Woolf, C.J.; Reynolds, M.L.; Molander, C.; O'Brien, C.; Lindsay, R.M. and

Benowitz, L.I. (1990) The growth-associated protein GAP-43 appears in dorsal root ganglion cells and in the dorsal horn of the rat spinal cord following peripheral nerve injury. Neuroscience **34**, 465-478.

249. Wylie, R.M. (1973) Evidence of electrotonic transmission in the vestibular nuclei of the rat. Brain Res. **50**, 179-183.

250. Yamamoto, T.; Shiosaka, S.; Whittaker, M.E.; Hertzberg, E.L. and Nagy, J.I. (1989) Gap junction protein in rat hippocampus: Light microscope immunohistochemical localization. J. Comp. Neurol. **281**, 269-281.

251. Yamamoto, T.; Maler, L.; Hertzberg, E.L. and Nagy, J.I. (1989) Gap junction protein in weakly electric fish (Gymnotide): Immunohistochemical localization with emphasis on structures of the electrosensory system. J. Comp. Neurol. **289**, 509-536.

252. Yandrasitz, J.R.; Ernst, S.A. and Salganicoff, L. (1976) The subcellular distribution of carbonic anhydrase in homogenates of perfused rat brain. J. Neurochem. **27**, 707-715.

253. Yoshida, S. and Matsuda, Y. (1979) Studies on sensory neurons of the mouse with intracellular-recording and horseradish peroxidase-injection techniques. J. Neurophysiol. **42**, 1134-1145.

254. Yoshimura, M. and Jessell, T. (1990) Amino acid-mediated EPSPs at primary afferent synapses with substantia gelatinosa neurones in the rat spinal cord. J. Physiol. **430**, 315-335.

Part I

Parvalbumin is highly colocalized with calbindin D28k and rarely with calcitonin gene-related peptide in dorsal root ganglia neurons of rat

P.A. Carr, T. Yamamoto, G. Karmy, K.G. Baimbridge and J.I. Nagy

Brain Research (1989) 497; 163-170

Abstract--Sections of lumbar dorsal root ganglia from rat were analyzed by immunohistochemical techniques to determine the size distribution and numbers of cells containing parvalbumin and calbindin D28k and to establish their coexistence relationships with each other and with cells containing calcitonin gene-related peptide (CGRP). The proportion of ganglia cells containing parvalbumin and calbindin D28k was 14% and 22%, respectively. The majority of cells immunoreactive for these proteins were of the large A type. Parvalbumin was colocalized almost completely (> 99%) with calbindin D28k and minimally (< 1%) with CGRP. Only 9% of the calbindin D28k-positive cells were immunoreactive for CGRP.

Parvalbumin (PV) and calbindin D28k (CaBP) are calcium binding proteins whose distribution in the central nervous system and peripheral tissues has been extensively documented in various species at both the cellular and ultrastructural levels (1,10,11,12,22). In peripheral tissues CaBP has been demonstrated immunohistochemically in enteric neurons of rat (5) and dorsal root ganglia (DRG) of chick (17,18). Parvalbumin has been found in rat spinal ganglia and peripheral nerves (8). Within DRG these proteins have been reported to occur in distinct subpopulations of cells. Ganglion neurons containing PV in the rat were seen to be of large size, while those containing CaBP in chick were both large and small size. This restricted distribution of CaBP and PV within the DRG suggests that they may contribute to the disposition of calcium within certain subclasses of sensory neurons. Although the function(s) of PV and CaBP is(are) not known, roles in calcium buffering (1,14), modification of neuronal excitability to synaptic input (2) or mediation of calcium dependent events (3,20) has been postulated. The objective of our present study was to provide a quantitative analysis of CaBP and PV in DRG of rat, to establish whether they exhibit coexistence relationships with each other and to examine possible colocalization with calcitonin gene-related peptide (CGRP) which has been well characterized according to its distribution in an abundance of both large and small cells (13).

METHODS

Adult, male Sprague Dawley rats weighing 250-350 g were anesthetized with chloral hydrate and perfused transcardially with cold (4°C) saline solution followed by a 4% paraformaldehyde and 0.16% picric acid fixative as described elsewhere (6). The fourth lumbar dorsal root ganglia (DRG) were then immersed in cold fixative for 2 hr and stored for at least 2 days in 15% sucrose containing 0.001% sodium azide and 0.1 M sodium phosphate buffer (pH 7.4). Cryostat sections of DRG were cut at a thickness of 8 to 15 μm, collected on gelatin coated slides and processed for PV, CaBP or CGRP immunohistochemistry by peroxidase-antiperoxidase or immunofluorescence methods.

Antibodies against PV, CaBP and CGRP were used at dilutions of 1:400 to 1:2000 in PBS containing 0.3% Triton X-100 (PBS-T). Sections were incubated with primary antisera for 40-68 hr at 4°C followed by a 40 min wash with two changes of PBS-T at room temperature. Tissue processed by the PAP method was incubated for two hours in secondary media consisting of goat anti-rabbit IgG (Sternberger-Meyer) diluted 1:20 in PBS-T and 1% bovine serum albumin (BSA). They were then washed for 40 min in two changes of PBS-T, incubated for two hours at room temperature in rabbit PAP (1:100; Sternberger-Meyer) diluted in PBS-T and 1% BSA and again washed for 40 min. Peroxidase activity was then visualized by reacting the sections in 50mM Tris-HCl buffer containing 0.005% hydrogen peroxide and 0.02% diaminobenzidine for 5-10 min. The sections were then dried, dehydrated and coverslipped with Permount. For immunofluorescence, sections incubated with primary antibody were washed and then incubated for 40 min to one hour with fluorescein isothiocyanate-conjugated donkey anti-rabbit IgG (Amersham) at a dilution of 1:20 in PBS with 1% BSA. Sections were then washed for 30 min in PBS and coverslipped with anti-fade medium. All primary antibodies used were generated in rabbit and have been characterized as previously described (5,16) (CGRP, Peninsula). The recognition of PV or CaBP epitopes by these antibodies appears not to be dependent on the presence of calcium which was therefore not included at any stage of tissue processing. It should also be noted that although other antibodies against CaBP recognize CaBP-related proteins in rat brain (19) the present CaBP antiserum reacts only with a single protein corresponding to Calbindin D28k (16). Comparisons of cellular localization of PV and CaBP were undertaken using adjacent cryostat sections collected onto separate slides. Analysis of the colocalization of the two calcium binding proteins with CGRP was conducted using either adjacent or sequentially processed sections. Sections processed sequentially were reacted for CGRP by the immunoperoxidase method and then processed for PV or CaBP by immunofluorescence. Photomicrographs of peroxidase reaction product or immunofluorescence in

corresponding areas of adjacent or sequentially processed sections were examined for determinations of coexistence. Microscope counts of PV- and CaBP-immunopositive cells were undertaken on immunofluorescent sections counterstained with ethidium bromide to allow counts of cells displaying nucleoli. Quantification of cell sizes was undertaken using an image analysis system (Amersham RAS-1000) on immunoperoxidase reacted sections counterstained with toluidine blue to allow visualization of the nucleoli (7). Following cell size analysis, the data was categorized into small ($\leq$1000 μm^2), intermediate (>1000 μm^2 and $\leq$1800 μm^2) or large (>1800 μm^2) cell size classes according to Carr et al. (7).

RESULTS

Dorsal root ganglion cells displaying CaBP-immunofluorescence are shown in Figure 1 (A,C) with corresponding adjacent sections stained for PV by either immunoperoxidase (B) or by immunofluorescence (D) methods. Both CaBP- and PV-positive cells of various sizes exhibited nuclear and diffuse, cytoplasmic staining with varying degrees of intensity and could easily be distinguished from non-immunoreactive cells. Very light CaBP immunoreactivity associated with what appeared to be the Golgi apparatus was seen in a small number of cells which were not included in the analysis due to the variability and consistently low intensity of this type of staining. No reaction product was seen in satellite cells or blood vessels although some axons appeared immunoreactive. From counts of 680 cells, 22% were positive for CaBP and from counts of 768 cells, 13.9% were positive for PV.

PV-positive cells ranged in size from 558 μm^2 to 3489 μm^2 and accounted for 12.5% of all intermediate and large size cells (Figure 2). CaBP-immunoreactive (IR) cells ranged in size from 251 μm^2 to 3091 μm^2 and accounted for 16% of all intermediate and large cells. In cells of very large size, with areas greater than 2500 μm^2, the two calcium binding proteins are expressed in almost equivalent proportions of cells (CaBP, 4.2%;

PV, 4.6%). In smaller cells (less than 1000 μm^2), the percentage of CaBP-positive neurons (6%) was greater than PV-positive cells (1.3%). In fact, no PV-positive cells with areas less than 500 μm^2 were observed. Viewed as a whole, the population of CaBP-IR cells comprised a higher proportion of DRG neurons and were distributed in a slightly larger size range than cells containing PV. Within the PV- and CaBP-positive populations (Table 1), it was found that greater than 90% of cells containing PV are of intermediate to large size (greater than 1000 μm^2) while cells containing CaBP were distributed among all the size categories with about 75% of CaBP-positive cells belonging to the intermediate and large size category.

The relationship between PV- and CaBP-containing cells is demonstrated in Figure 1. From 346 PV-IR cells examined, greater than 99% were found to be positive for CaBP. A slightly lower percentage (97%) of 353 CaBP-positive cells examined were also positive for PV. These percentages apply to a population consisting of mostly large and intermediate cells and perhaps some small cells. Technical limitations inherent in the analysis of adjacent sections of the thicknesses employed here preclude an accurate analysis of small cells some of which may not appear in both of a pair of adjacent sections.

Examples of comparisons between CGRP-immunopositive neurons and CaBP- and PV-positive cell populations are shown in Figure 3 and Figure 4. The different cellular localizations of CGRP and the calcium binding proteins allowed sequential processing of sections using two primary antibodies from the same species, as previously described (21). Punctate CGRP-immunoreactivity associated with the Golgi apparatus was visualized first by immunoperoxidase followed by immunofluorescence visualization of diffuse, cytoplasmic PV and CaBP immunostaining (Fig. 3c,d; Fig. 4c,d). As confirmation of this procedure, additional PV-CGRP and CaBP-CGRP studies were

conducted using adjacent sections (Fig. 3a,b; Fig. 4a,b). Results with either adjacent and sequentially processed tissue were similar and indicated that colocalization of both calcium binding proteins with CGRP was minimal. From 906 CaBP-positive cells examined 9% also exhibited CGRP-immunoreactivity and from 286 PV-positive cells examined less than 1% were stained for CGRP.

DISCUSSION

It was previously reported that the PV-positive subpopulation of rat DRG consists entirely of what was classified as large cells (8). The CaBP-positive subpopulation of chick DRG was reported to comprise 20% of the total cell population and by ultrastructural categorization this population was shown to consist of 30% large cells and 70% small cells (18). These results differ somewhat from our findings, which may be due to the different cell measuring techniques, fixations, tissue processing procedures or species employed.

Our demonstration of the almost complete colocalization of PV with CaBP in DRG is remarkable insofar as such coexistence has not been widely described in the mature central nervous system where the distribution of PV is, for the most part, distinctly different from that of CaBP (10,11,12). It should be noted, however, that the amount of coexistence of PV with CaBP in small cells could not be determined accurately, but due to the greater number of CaBP-IR than PV-IR small cells, and the fact that almost all PV-IR cells are also CaBP-IR, it would appear that the small CaBP-positive cells do not contain PV. This would suggest that at least two subpopulations of CaBP-positive DRG neurons exist; those containing and those lacking PV. On the basis of their differential distribution in brain, their colocalization within certain populations of DRG neurons, and the absence of PV in some CaBP-containing DRG neurons, it might be speculated that PV and CaBP have somewhat different functions and that some ganglia cells have a functional requirement for both proteins.

In both the central nervous system (4) and DRG (6), PV has been colocalized in neurons displaying dense cytochrome oxidase reaction product, which implies that PV is expressed by cells which have a high level of activity. In numerous brain areas PV has also been demonstrated in rapidly firing cells containing gamma-aminobutyric acid (GABA) (9,14). However, neither GABA nor its synthetic enzyme marker, glutamic acid decarboxylase, have been demonstrated in DRG. Thus, primary sensory neurons represent a clear dissociation of the relationship between GABAergic transmission and the presence of PV in what may be considered highly active cells based on their cytochrome oxidase content.

CGRP-immunoreactivity has been demonstrated in a high proportion of small, intermediate and large size classes of DRG neurons (13,15). We have demonstrated that CGRP-positive cells rarely contain PV and only a small percentage contain CaBP in the rat lumbar DRG. Since it has been reported that 50% of DRG cells contain CGRP (13) together with our observation that 22% contain CaBP, it appears that approximately 70% of all DRG neurons can be accounted for as containing either CGRP or CaBP. Consideration of the functional implications of the minimal coexistence of PV and CaBP with CGRP must await detailed information regarding the peripheral tissue innervated by sensory afferents containing these markers. However, this minimal colocalization may be considered in light of other findings from peripheral nervous tissue. It has been reported that most galanin-, somatostatin-, and substance P-IR cells in rat lumbar DRG also contain CGRP (13) and that CaBP-IR enteric neurons in rat lack galanin, somatostatin or substance P (5). If substance P, somatostatin and galanin in the enteric nervous system have the same relationship to CGRP as they do in DRG, then on the basis of minimal CaBP colocalization with CGRP in ganglia, we would predict that these three peptides are rarely expressed by CaBP-IR DRG neurons.

REFERENCES

1. Baimbridge, K.G., Miller, J.J. and Parkes, C.O. (1982) Calcium-binding protein distribution in the rat brain. Brain Research **239,** 519-525.

2. Baimbridge, K.G., Mody, I. and Miller, J.J. (1985) Reduction of rat hippocampal calcium-binding protein following commissural, amygdala, septal, perforant path and olfactory bulb kindlings. Epilepsia **26,** 460-465.

3. Berchtold, M.W., Celio, M.R. and Heizmann, C.W. (1984) Parvalbumin in non-muscle tissues of the rat. J. Biol. Chem. **259,** 5189-5196.

4. Braun, K., Scheich, H., Schachner, M. and Heizmann, C.W. (1985) Distribution of parvalbumin, cytochrome oxidase activity and ^{14}C-2-deoxyglucose uptake in the brain of the zebra finch. I. Auditory and vocal motor system. Cell Tissue Res. **240,** 101-115.

5. Buchan, A.M.J. and Baimbridge, K.G. (1988) Distribution and colocalization of calbindin D28k with VIP and neuropeptide Y but not somatostatin, galanin and substance P in the enteric nervous system of the rat. Peptides **9,** 333-338.

6. Carr, P.A., Yamamoto, T., Karmy, G., Baimbridge, K.G. and Nagy, J.I, (1989) Analysis of parvalbumin and calbindin D28k-immunoreactive neurons in dorsal root ganglia of rat in relation to their cytochrome oxidase and carbonic anhydrase content. Neuroscience **33,** 363-371.

7. Carr, P.A., Yamamoto, T., Staines, W.A., Whittaker, M.E. and Nagy, J.I. (1989)

Quantitative histochemical analysis of cytochrome oxidase in rat dorsal root ganglia and colocalization with carbonic anhydrase. Neuroscience **33,** 351-362.

8. Celio, M.R. and Heizmann, C.W. (1981) Calcium-binding protein parvalbumin as a neuronal marker. Nature **293,** 300-302.

9. Celio, M.R. (1986) Parvalbumin in most gamma-amino-butyric acid-containing neurons of the rat cerebral cortex. Science **231,** 995-997.

10. Garcia-Segura, L.M., Baetens, D., Roth, J., Norman, A.W. and Orci, L. (1984) Immunohistochemical mapping of calcium-binding protein immunoreactivity in the rat central nervous system. Brain Research **296,** 75-86.

11. Gerfen, C.R., Baimbridge, K.G. and Miller, J.J. (1985) The neostriatal mosaic: compartmental distribution of calcium-binding protein and parvalbumin in the basal ganglia of the rat and monkey. Proc. Natl. Acad. Sci. **82,** 8780-8784.

12. Heizmann, C.W. (1984) Parvalbumin, an intracellular calcium-binding protein; distribution, properties and possible roles in mammalian cells. Experientia **40,** 910-921.

13. Ju, G., Hokfelt, T., Brodin, E., Fahrenkrug, J., Fischer, J.A., Frey, P., Elde, R. and Brown, J.C. (1987) Primary sensory neurons of the rat showing calcitonin gene-related peptide immunoreactivity and their relation to substance P-, somatostatin-, galanin-, vasoactive intestinal polypeptide- and cholecystokinin-immunoreactive ganglion cells. Cell Tissue Res. **247,** 417-431.

14. Kawaguchi, Y., Katsumaru, H., Kosaka, T., Heizmann, C.W. and Hama, K. (1987) Fast spiking cells in rat hippocampus (CA_1 region) contain the calcium-binding protein parvalbumin. Brain Research **416,** 369-374.

15. Kruger, L., Sternini, C., Brecha, N.C. and Mantyh, P.W. (1988) Distribution of calcitonin gene-related peptide immunoreactivity in relation to the rat central somatosensory projection. J. Comp. Neurol. **273,** 149-162.

16. Mithani, S., Atmadja, S., Baimbridge, K.G. and Fibiger, H.C. (1987) Neuroleptic-induced oral dyokinesias: effects of progabide and lack of correlation with regional changes in glutamic acid decarboxylase and choline acetyltransferase activities. Psychopharmacology **93,** 94-100.

17. Philippe, E. and Droz, B. (1986) Effect of skeletal muscle on the expression of a calcium-binding protein (calbindin) in dorsal root ganglion of the chick embryo. Soc. Neurosci., Abstr. **12,** 1125.

18. Philippe, E. and Droz, B. (1988) Calbindin D-28k-immunoreactive neurons in chick dorsal root ganglion: ontogenesis and cytological characteristics of the immunoreactive sensory neurons. Neuroscience **26,** 215-224.

19. Pochet, R., Parmentier, M., Lawson, D.E.M. and Pasteels, J.L. (1985) Rat brain synthesizes two vitamin D-dependent calcium-binding proteins. Brain Res. **345,** 251-256.

20. Sans, A., Etchecopar, B., Brehier, A. and Thomasset, M. (1986) Immunocytochemical detection of vitamin-D-dependent calcium binding protein

(CaBP-28k) in vestibular sensory hair cells and vestibular ganglion neurons of the cat. Brain Research **364,** 190-194.

21. Senba, E., Daddona, P.E., Watanabe, T., Wu, J.-Y. and Nagy, J.I. (1985) Coexistence of adenosine deaminase, histidine decarboxylase, and glutamate-decarboxylase in hypothalamic neurons of the rat. J. Neurosci. **5,** 3393-3402.

22. Stichel, C.C., Singer, W., Heizmann, C.W. and Norman, A.W. (1987) Immunohistochemical localization of calcium-binding proteins, parvalbumin and calbindin-D28k, in the adult and developing visual cortex of cats: a light and electron microscopic study. J. Comp. Neurol. **262,** 563-577.

FIGURE LEGENDS

Fig. 1. Photomicrographs of sections showing CaBP and PV in neurons of lumbar DRG. (A,B) Photomontage of adjacent sections stained for CaBP by immunofluorescence (A) and for PV by immunoperoxidase (B). (C,D) Adjacent sections in which CaBP (C) and PV (D) are demonstrated by immunofluorescence. Arrows indicate corresponding cells in each pair of micrographs. Note that large (L) and small (S) cells are both PV- and CaBP-IR. Very light immunofluorescence for CaBP associated with what appears to be Golgi apparatus is seen in a small proportion of cells (arrowheads). Bars = 100 μm.

Fig. 2. A bar graph showing the percent of all DRG neurons of various size categories displaying PV- or CaBP-immunoreactivity. The dotted line indicates the size frequency distribution of all DRG neurons with regard to the area categories (7), but is not to scale for the y-axis.

Fig. 3. Photomicrographs of sections of lumbar DRG showing CaBP- and CGRP-IR neurons. (A,B) Montage of serial sections stained for CaBP by immunofluorescence (A) and CGRP by immunoperoxidase (B). (C,D) The same section stained first for CGRP by immunoperoxidase (D) and then for CaBP by immunofluorescence (C). Arrowheads indicate examples of corresponding cells containing either CGRP or CaBP but not both. Arrows indicate cells containing both CaBP and CGRP. Bars = 100 μm.

Fig. 4. Photomicrographs of DRG sections showing PV- and CGRP-IR neurons. (A,B) Photomontage of adjacent sections showing PV-IR (A) and CGRP-IR cells (B) by

immunoperoxidase. (C,D) The same section stained first for CGRP by immunoperoxidase (D) and then for PV by immunofluorescence (C). Corresponding cells in pairs of photomicrographs are indicated by arrows. Neurons containing PV lack CGRP. Bars = 50 μm (A,B), 100 μm (C,D).

Table 1. Percentages of PV-IR and CaBP-IR DRG neurons within particular size categories. The distribution of all DRG neurons according to percentages within the size categories is also indicated.

	Cross Sectional Area (μm^2)			
Neuronal Population	≤500	Small* >500 to ≤1000	Intermediate >1000 to ≤1800	Large >1800
All DRG neurons	13.7	37.6	20.9	27.9
CaBP-IR neurons	9.0	18.0	41.0	32.0
PV-IR neurons	0	9.3	46.8	43.9

*Small cells are subdivided into two size categories.

Values for CaBP- and PV-positive DRG neurons indicate the percentage of positive cells in each size category of all CaBP-IR and PV-IR DRG neurons, respectively.

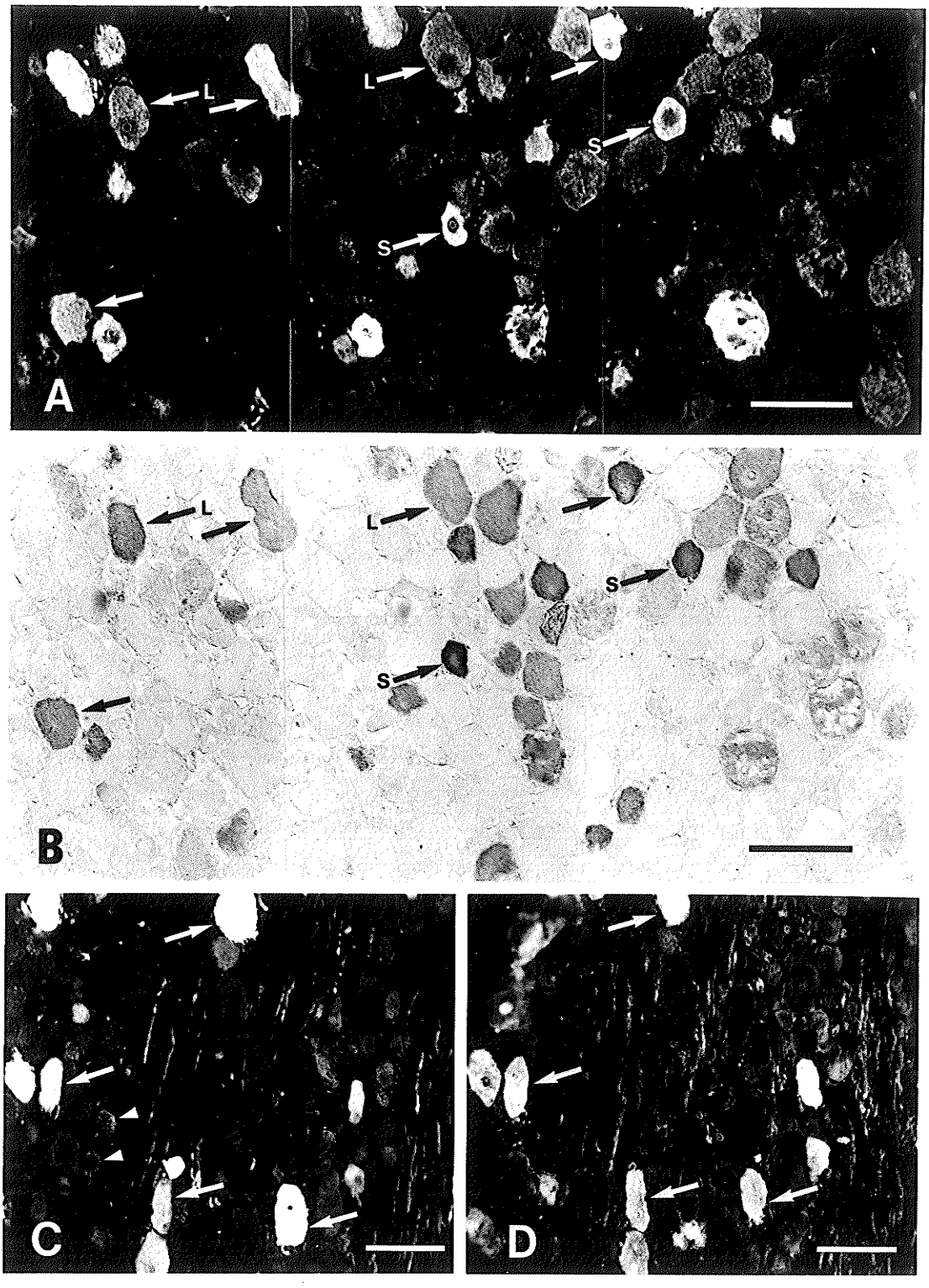

Fig. 1

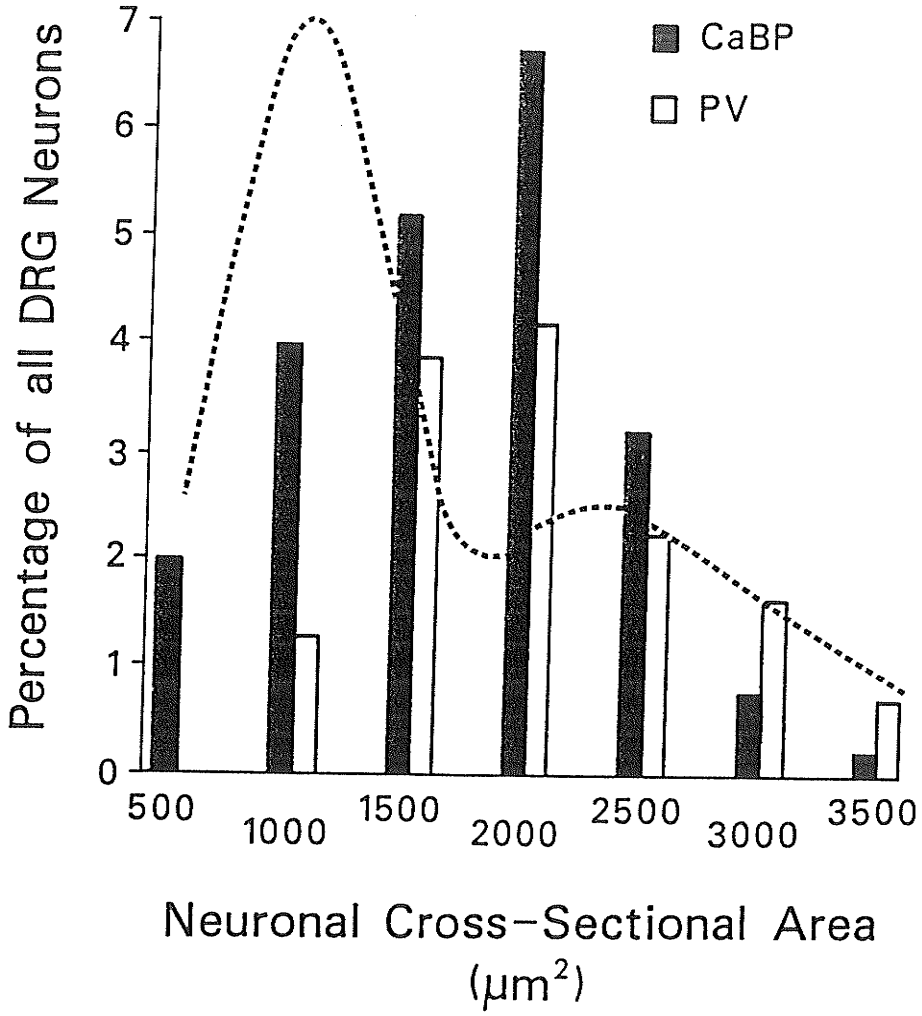
Percentage of all DRG Neurons
7
6
5
4
3
2
1
0
CaBP
PV
500
1000
1500
2000
2500
3000
3500
Neuronal Cross-Sectional Area
(μm²)

Figure 2

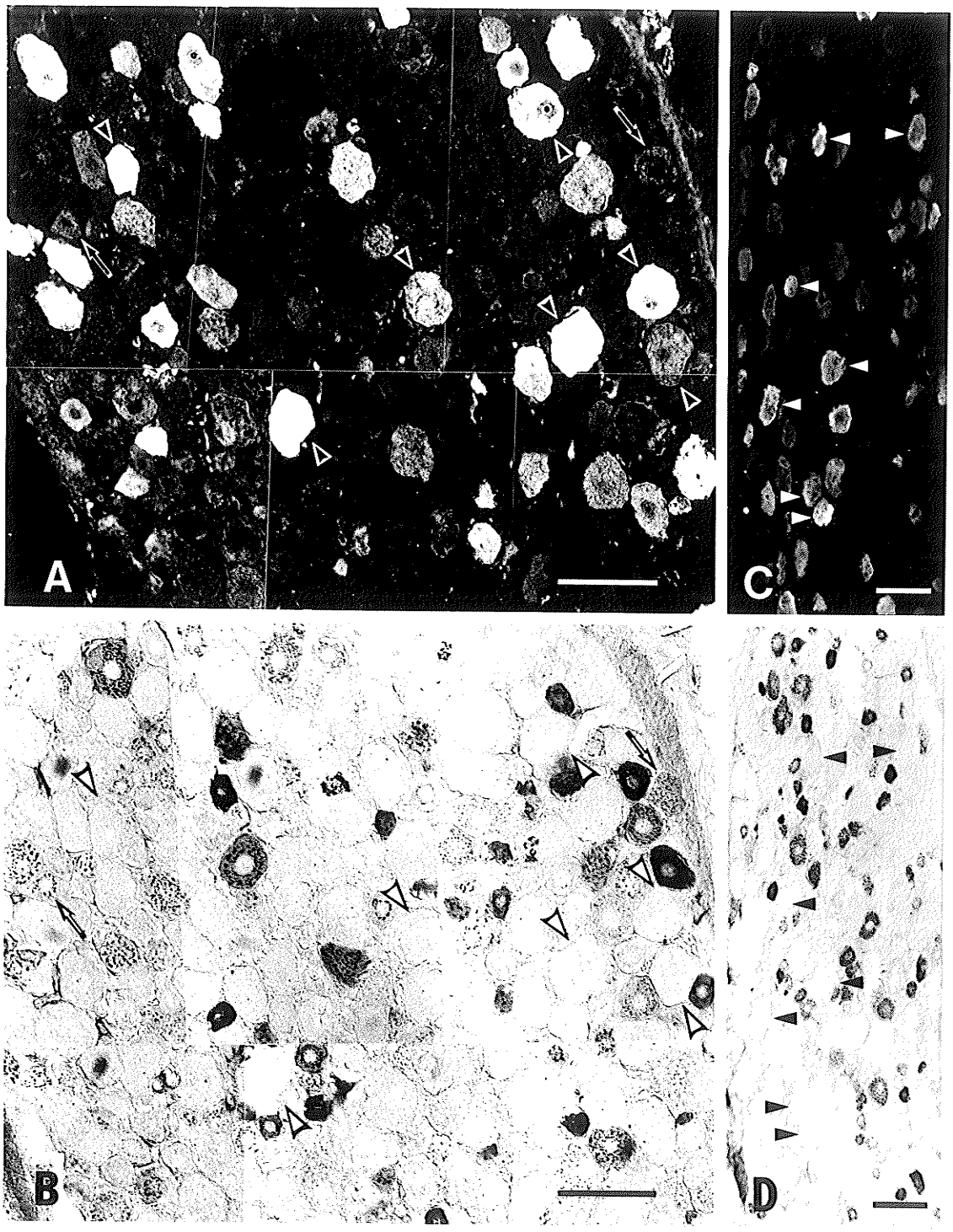

Fig. 3

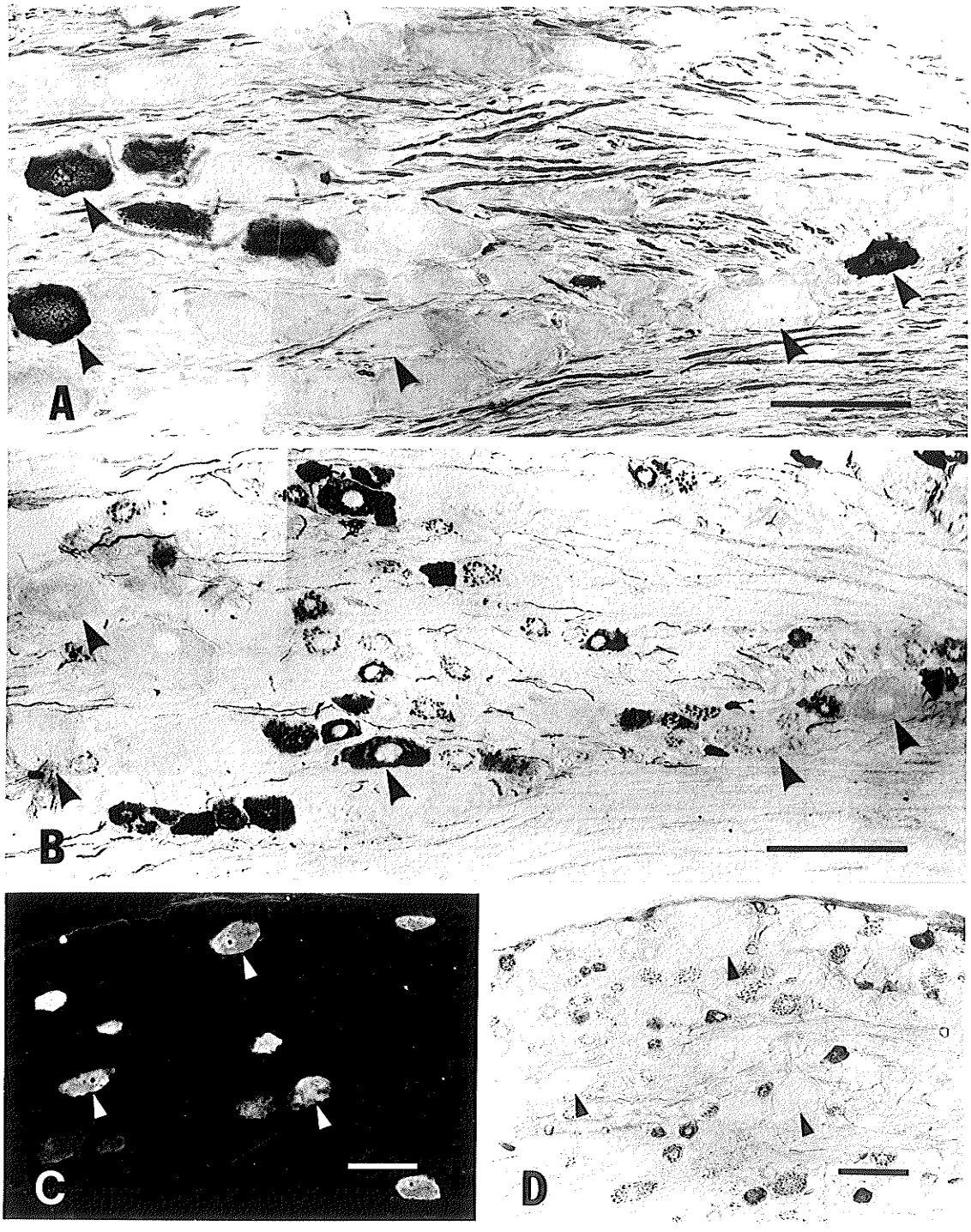

Fig. 4

Part II

Quantitative histochemical analysis of cytochrome oxidase in rat dorsal root ganglia and its colocalization with carbonic anhydrase

P.A. Carr, T. Yamamoto, W.A. Staines, M.E. Whittaker and J.I. Nagy

Neuroscience (1989) 33; 351-362

Abstract--A quantitative histochemical method was developed and standardized and then used to characterize the heterogeneity of cytochrome oxidase activity among primary afferent neuronal cell bodies in dorsal root ganglia of rat. In addition, the relationship between cytochrome oxidase and carbonic anhydrase activities in these neurons was determined. In tests of the procedure, the density of cytochrome oxidase reaction product evaluated repeatedly in individual neurons within sections of ganglia was found to increase linearly over incubation periods of up to 6 hours. The heterogeneity in cytochrome oxidase activity in ganglia was not simply a reflection of the heterogeneity in ganglion cell sizes. On the whole, each class of ganglion cell exhibited the full range of staining densities encountered but intense staining was observed in many more large type A cells than small type B cells. The latter, together with their termination fields within the substantia gelatinosa of the spinal cord, were lightly stained. A significant positive correlation was found between neuronal size and staining density ($r=0.43$). However, the large scatter in the plot of these two variables suggests that the expression of cytochrome oxidase in sensory neurons is governed to a considerable extent by properties of these neurons that are unrelated to their size. Analysis of cytochrome oxidase and carbonic anhydrase activities in the same ganglion cells revealed that all neurons with dense staining for the oxidase were anhydrase positive. Conversely, however, some intensely anhydrase-positive cells exhibited only light staining for cytochrome oxidase.

The heterogeneity of cytochrome oxidase activity among neurons in dorsal root ganglia may be related to the steady state electrophysiological activity of distinct populations of sensory neurons which in turn may be related to the specific sensory modalities these populations transmit. The observation that some neurons with the greatest abundance of carbonic anhydrase do not contain high or even moderate levels of cytochrome oxidase suggests some degree of dissociation between the functional requirement for carbonic anhydrase in sensory neurons and the rate of energy expenditure in these cells.

Neurons in dorsal root ganglia (DRG) are classically divided into two groups on the basis of cell size; large type A and small type B cells (2,16). Major goals regarding the neurochemical characterization of these cells have been to identify the transmitters and/or neuromodulators they utilize, to determine which transmitter substances might coexist in the same cells and to establish whether putative transmitter content is related to transmission of particular sensory modalities. Progress along these lines has led to the subdivision of type B cells based on certain of the cytochemical features they display. Subpopulations of these cells have been found to contain the peptides substance P (SP) or somatostatin (SOM), or the enzymes tyrosine hydroxylase (TH) or fluoride resistant acid phosphatase (FRAP) (10,22,26). These markers appear to represent four separate populations of cells with slightly different morphological characteristics (26). Various other neuroactive peptides and transmitter-related enzymes have been found within neurons encompassing one or more of these four populations such that different neurochemical markers may define the same or separate subpopulations of type B neurons. Investigations of the functions of these markers have not as yet allowed firm conclusions regarding relationships between their presence in DRG neurons and the sensory modalities these neurons transmit (7,15,18,38,39).

Recently, attention has been drawn to the classification of DRG neurons according to another class of cytochemical feature, namely histochemical demonstration of enzymes related to cellular metabolism. One of these, cytochrome C oxidase (CO), has in a number of systems allowed histochemical visualization of regional differences in normal metabolic activity and this metabolic parameter has been shown to change subsequent to experimental manipulations (42). The utility of CO histochemistry has been validated by evidence indicating that electrical activity and energy demands of neurons are closely coupled to the activity of this respiratory chain enzyme (11,12,32,42-44,47-49). The remarkably uneven distribution of CO activity observed in the CNS has also been found

among primary sensory neurons in DRG of various species (50). This heterogeneity was interpreted as reflecting the activity patterns of subclasses of ganglion cells that transmit different sensory modalities. Histochemical demonstrations of the metabolic enzyme carbonic anhydrase (CA) in a subpopulation of DRG neurons (14,30,34,40) has led to similar proposals wherein functional demands reflected by CA activity were related to the transmission of particular sensory modalities by sensory neurons that maintain relatively tonic patterns of activity (24,25,29).

With the ultimate aim of establishing whether CO histochemistry can be used to investigate relationships between the neurochemical features and the sensory modalities transmitted by DRG neuronal subpopulations, we report here the quantitative densitometric characterization of CO histochemical reaction product in DRG neurons of normal animals. In addition, the similarity of views regarding the involvement of CO and CA in energy metabolism in DRG neurons prompted us to compare the histochemical staining pattern produced by CO with that produced by CA.

METHODS

Tissue preparation

Adult, male Sprague Dawley rats (250-300g) were deeply anesthetized with chloral hydrate and perfused transcardially with cold (4°C) 0.9% saline containing 0.1% sodium nitrite and 100 units of heparin. For CO histochemistry this was followed by 200 to 300 ml of cold, freshly prepared 4% paraformaldehyde in 0.1 M phosphate buffer (pH 7.4) containing 0.16% picric acid (51). Some animals were perfused with this same fixative containing 0.2% glutaraldehyde. Lumbar sensory ganglia (L4 and L5) and spinal cords were removed and post-fixed for 2 or 16 hr in fixative without glutaraldehyde. The spinal cords were cryoprotected in 50 mM sodium phosphate buffer, pH 7.4, containing 25% sucrose and 10% glycerol for 24 hr. Transverse sections were cut on a sliding microtome at a thickness of 20 μm and collected in 0.1 M sodium phosphate buffer, pH 7.4, (PB) containing 0.9% saline (PBS). Dorsal root ganglia were stored for a minimum of 24 hr in PB containing 15% sucrose. Sections were cut on a cryostat (Leitz) at thicknesses of 5 to 15 μm, thaw mounted onto gelatin-coated slides, washed for 15 minutes in two changes of PB, and then processed for CO histochemistry. For CA histochemistry, animals were perfused with the 0.2% glutaraldehyde-containing fixative and ganglia were then post-fixed for 2 hr at 4°C in the same fixative without glutaraldehyde. Ganglia were then immersed in appropriate cryoprotectant solution for cryostat or sliding microtome sectioning.

Histochemistry for cytochrome oxidase

The method of Wong-Riley (42) or a slightly modified procedure was used to demonstrate CO activity. The standard reaction medium contained 0.03% cytochrome C

(Sigma, type III), 0.025 or 0.05% diaminobenzidine (DAB) and 4% sucrose in PB. Although in preliminary experiments, reaction times were varied from 0.5 to 6 hr, standard incubations were conducted at 37°C for 2 to 4 hr in the dark. Control incubations were run for equivalent times and consisted of four types. One utilized medium without cytochrome C. In others potassium cyanide, an inhibitor of CO activity (13) was added at concentrations of 0.01 or 1.0 mM. Finally, some sections were reacted in medium with 0.01 mM potassium cyanide but without cytochrome C. The reaction was terminated by rinsing the sections for 20 min in PB or in PB followed by a rinse in distilled water. Free-floating spinal cord sections were mounted from gelatin-ethanol or 50 mM Tris-HCl buffer. After drying, sections were either coverslipped with a 3:1 glycerol-water solution or dehydrated in alcohol, cleared in xylene and coverslipped with Permount.

Densitometric measurements

Quantitative determinations of CO reaction density were conducted with an Amersham RAS-1000 image analysis system linked by a video camera to a Nikon Optiphot microscope with a constant current power source. The microscope illumination and camera gain control were adjusted to encompass the optimal range of gray scales detected by the camera and a reference image was generated for a subtractive illumination correction to simulate even illumination. At the final working magnification, the system was then calibrated for optical density with a film of density standards and for dimensions with a stage graticule. The image of an area within a given DRG section containing many cells and largely free of fiber bundles was digitized and the image stored on 1.2 megabyte floppy disks. Typically, X40 objective magnification was used and the field in each digitized image contained up to 15 neurons. To avoid cell selection bias in ganglion sections, every eligible cell in a field was analyzed. The whole

of the substantia gelatinosa was sampled on each side of spinal cord sections. Following digitization, sections were counterstained with toluidine blue to facilitate the visualization of cells containing nucleoli. The images of CO-reacted cells in non-counterstained sections were later recalled for size and density measurements. Eligibility for inclusion in analysis was determined by comparing displays of the stored CO-reacted images with simultaneous displays of the live images of the same section after counterstaining. Only cells with nucleoli within the plane of the section were used for cell counts, cell area measurements and the determination of cellular optical density. Area was determined from the video display of stored images by cursoring around the perimeter of cells. Initial studies revealed less than 5% variation in values obtained from repeated area measurements of the same cell. The optical density of cells was obtained by sampling around the perimeter of a cell and then encircling the nucleus to exclude it from input.

Data analysis

Recorded and compiled data on optical density, cell number and cell size were analyzed with the aid of a Stata (The Computing Resource Center, California) statistics package. Analysis of size/density profiles was conducted on data from a single ganglia, or pooled from sections obtained from several L4 ganglia from the left and right sides of individual animals; data from separate animals were not pooled in the present study. Preliminary data on the frequency distribution of area and OD in the DRG of a number of rats revealed similar size and density distribution between individual animals, although there were some differences in the absolute range of densities. In order to avoid obscuring fine details in density distribution by variations between animals or technical factors, our indepth study thus focussed on the relationship of neuronal cross-sectional area and CO reaction density in a single L4 dorsal root ganglion from a

paraformaldehyde-picric acid fixed animal. The ganglion was sectioned at 15 μm and OD and areal analysis of 1271 CO-reacted cells displaying toluidine blue counterstained nucleoli was conducted.

For descriptive purposes, OD values were categorized into three bins and areal values into either three or four groups. These categories were intended to ease comparison of the data and are not functional classifications. Cells classified into four groups according to their neuronal cross-sectional area consisted of very small cells with areas less than 500 μm^2, small cells with areas between 500 and 1000 μm^2, intermediate or medium size cells with areas between 1000 and 1800 μm^2 and large cells with areas greater than 1800 μm^2. The small neurons ($\leq$1000 μm^2) were divided into two groups to determine if CO intensity was related to size category as has been previously seen for other neurochemical markers of these cells (26). For graphical presentation of the data, all cells with areas less than 1000 μm^2 were combined to form one bin of small cells. Since there appears to be some overlap between the large type A cells and small type B cells both in size and function (8,9,17,26,27), our selection of size categories was chosen to ensure confidence of designation of small cells as type B and large cells as type A cells. The intermediate cell size bin (1000-1800 μm^2) very likely includes both of these populations.

Optical density categories were generated by dividing the range of OD values into equal thirds over the full range of densities and designating the first category of cells with OD values less than 0.094 as lightly stained cells, the second category with OD values between 0.094 and 0.156 as moderately stained cells, and the third category with OD values greater than 0.156 as densely stained cells. Frequency distributions of both area and optical density were plotted after creating 15-20 bins for the abscissa. The results of optical density and area measurements of DRG neurons are presented as the percent of cells exhibiting light, moderate, or dense staining with respect to all the cells

within a size category and also with respect to all the cells analyzed.

CO reaction linearity with time

A different procedure was required for the determination of the CO reaction time course. This technique involved repeated density measurements of either individual DRG neurons or the substantia gelatinosa of the spinal cord. Sections, just prior to incubation in standard medium and every hour from 1 through 4, 6 and 8 hr, were removed from the incubation medium, coverslipped with PB containing 4% sucrose, and selected fields were then digitized and stored. This was usually accomplished within 10 min. The coverslips were then removed, and the sections returned to the medium to continue the reaction. Stage micrometer coordinates allowed the field of interest in each spinal cord and ganglion section to be approximately re-located for each consecutive reading. Precise correspondence of cells in DRG and fields in spinal cord was achieved by superimposing the live video image onto the simultaneously displayed stored image from the previous hour. Distortion of sections was minimal even after repeated coverslipping and any misalignment was made negligible by using the image from the immediately previous incubation period to re-align sections. This precise superimposition of sections allowed transposition of a computer generated map of identified cells from section to section. This map permitted the same cells or fields to be sampled for density and area measurements at all time points on the basis of those cursored on the image obtained at the last incubation time. An illumination correction was performed on a blank area of each slide at each time interval to control for possible non-specific deposition of DAB or inadvertent change in microscope adjustment. At the zero time point, a random field within the section was taken for measurement since the borders of individual cells in DRG or lamina in spinal cord in these very light sections could not be accurately identified.

Carbonic anhydrase histochemistry

Histochemistry for CA was conducted essentially as described by others (28,29,40). It should be noted that although fixatives containing high concentrations of glutaraldehyde are usually employed for CA histochemistry, the present studies utilized a weaker fixation compatible with procedures used for CO histochemistry. The incubation medium consisted of 1.75 mM $CoSO_4$, 11.7 mM KH_2PO_4, 157 mM $NaHCO_3$, and 53 mM H_2SO_4, pH 6.5 (40). As a control for histochemical specificity, some sections were processed in incubation medium containing 0.01 mM acetazolamide, an inhibitor of CA (6). This was found, in the present study, to eliminate all but a small amount of nuclear CA staining. Two approaches were used for the histochemical demonstration of CO and CA in the same cells. In the first, adjacent cryostat sections of lumbar ganglia (L4 or L5) were cut at a thickness of 5 μm and collected on separate gelatin-coated slides. One section was reacted for CO as described above and the adjacent section for CA. Slide mounted sections were washed in cold PB for 1 hr and then dipped into incubation medium for 5 sec followed by exposure to the atmosphere for 30 sec and this was repeated for 30 min. Sections were then dipped in an aqueous solution of 0.5% ammonium sulphate for 3 min, washed in PB for 5 min and coverslipped with a mixture of glycerol and 10 mM PB (3:1). In the second procedure, sections were processed sequentially, first for CO then for CA. Sections cut on a sliding microtome at a thickness of 20 μm, were processed free floating for CO histochemistry as described above, photographed and then gently immersed into CA incubation medium in a manner that would allow the sections to float on the surface of the medium. After 30 min the sections were collected onto glass slides, floated again on the surface of a 0.5% ammonium sulphate solution for 3 min, washed in PB for 5 min and finally mounted onto gelatin-coated slides and coverslipped with a mixture of glycerol and 10 mM PB (3:1).

RESULTS

General observations

Within the L4 and L5 DRG, CO reaction could be seen in both neuronal and non-neuronal elements. Neuronal cell populations exhibited very heterogeneous CO staining (Fig. 1A,C), while uniform densities of CO reaction product were observed within satellite cells populations (Fig. 1A). The subtle gradations in CO staining intensities among DRG neurons were more apparent in tissues fixed with paraformaldehyde and picric acid (Fig. 1A,C), than in tissue fixed with glutaraldehyde (Fig. 1B). As noted by others (32), glutaraldehyde fixation appeared to reduce CO activity and raise the histochemical detection threshold of this enzyme. In paraformaldehyde-picric fixed DRG sections, many neurons showing high CO activity were of medium to large size (>1200 μm^2) with relatively few small type B neurons exhibiting dense reaction product (Fig. 1C). However, cells of all sizes in the same section could be seen to exhibit light, moderate or dense CO staining (Fig. 1C). Heterogeneity in the patterns of intracellular CO reaction product deposition was also observed among DRG neurons. Homogeneous intracellular staining was the most common and consisted of evenly dispersed CO reaction product (Fig. 1C). Perinuclear staining was observed in a small number of cells and was characterized by more intense reaction product deposition near the nuclear envelope (Fig. 1F). Eccentric staining was also observed in a small number of cells and was characterized by dense CO product deposition in one region of the cytoplasm while the rest of the cell body was less intensely stained (Fig. 1B,C,D). These staining patterns and densities were found to be reproducible between animals and between sections through the same cells (compare Fig. 1D and E).

The pattern of CO staining within the dorsal horn of the L4 spinal cord segment is shown in Fig. 1G. Whereas the staining in most of the dorsal horn could be described in

relative terms as moderate, that in the substantia gelatinosa (SG) and marginal zone was noticeably less dense. A few cells intensely-stained for CO were occasionally seen within the marginal zone or outer SG. Generally these cells had diameters ranging from 10 to 15 μm, and although present throughout the L4 segment, were rare enough that they were not seen in every section. These neurons appear to be too small to be marginal cells, and from their size and position, are more likely to be members of the SG cell population termed limiting cells (3). Somewhat more numerous were small, very lightly stained neurons which were distributed throughout the SG. The differences in staining intensities between the SG and the rest of the dorsal horn was most evident in material post-fixed for 2 hr rather than for longer times.

In control incubations without cytochrome C, ganglion cells displayed a greatly attenuated reaction after incubation times of 2 and 5 hr but the general pattern of staining was the same as that seen with complete medium (Table 1). The persistence of staining in DRG neurons may be attributable to the presence of some functional endogenous cytochrome C. The intensity of CO staining in both DRG neurons and satellite cells showed concentration dependency for inhibition by cyanide. Reactivity in both types of cells was completely abolished with concentrations of 0.01 and 1.0 mM cyanide in the complete incubation medium but was still marginally apparent in the presence of 1 μM cyanide. The relatively low level of activity seen in the absence of cytochrome C was abolished with 10 μM cyanide (Table 1).

To allow the interpretation that the staining intensities seen reflected proportional differences in the activity of CO within different cells required that the rate of reaction product deposition be linear over the time periods at which comparisons were made. This should be reflected by the linear increase of optical density per time of incubation for all density ranges observed. In repeated density measurements of the same DRG neurons and spinal cord sections, this was found to be the case. The activity of CO was

very nearly linear for up to 4 hours in 110 of the DRG cells followed, for up to 6 hours in another 479 cells, and for up to 8 hours in 8 separate regions of the substantia gelatinosa in L4 spinal cord sections. Examples of time density curves for 5 individual ganglion neurons exhibiting a range of CO activities is shown in Fig. 2A. The extrapolated intersection of these lines at or near the origin is consistent with the negligible optical densities (<0.001) seen in unreacted sections, i.e. at the zero incubation time. As shown in Fig. 2B, a linear time/density behavior was also observed for the population as a whole.

Quantitative Analysis

Area and OD measurements of DRG neuronal cell bodies showed that values formed continuums across the entire range of area and CO reaction densities encountered. Optical density values for 99% of the cells ranged from 0.032 to 0.19 OD units and cell cross-sectional area ranged from 131 to 4738 μm^2. As shown in Tables 2 and 3, the population of cells comprising the very small and small size categories contained a relatively high percentage of light staining cells. The very small size group had no densely stained cells while the small size category had very few. The cells in these two size bins accounted for 50% of all cells analyzed and the frequency distribution of these cells (Fig. 3B) concurs with previous work (26) in that cells ranging in size from 200 μm^2 to 1000 μm^2 constitute the bulk of the small B-type cell population of the dorsal root ganglion. Cells greater than 1000 μm^2 were divided into two size bins (1000 to 1800 μm^2, medium size; >1800 μm^2, large size) for reasons given under Data Analysis in the Methods section. The medium size cell category represented 19% of all cells and contained an equal percentage of both lightly and moderately stained cells with a lesser, though not insignificant, number of densely stained cells. The large cell population had the lowest percentage of light cells and the highest percentage of both

moderately and densely stained cells of the three areal categories. The large size cells represented 31% of the analyzed cell population.

Area frequency distributions of absolute numbers for the three OD categories revealed that a relatively large number of lightly stained cells were of small size while moderately stained cells were found in similar numbers in both large and small size categories. Relatively few cells of any size exhibited dense CO reaction product (Fig. 3A). Examination of the OD frequency distribution for each of the three size categories revealed that many small cells contained little CO reaction product, while medium and large cells were fewer in number and displayed CO intensities covering a broader range of OD values. The large size category had the highest numbers of densely stained cells (Fig. 3C). The plots of the number of cells against OD units shown in Fig. 3C were generated using three cell size bins after it was determined that the two smallest size categories (less than 500 μm^2 and 500 to 1000 μm^2) were distributed similarly (Fig. 3D).

In a scatter plot of OD value against cross-sectional area of the 1271 neurons (Fig. 5), analysis of the linear regression demonstrated a line with a positive slope. The data, analyzed by Spearman's rank correlation, indicated a significant positive association ($r=0.43$) between OD and neuronal cross- sectional area ($p<.001$).

Colocalization of CA and CO

In contrast to CO, the CA reaction within DRG did not appear to vary discreetly across the range of product densities present; most cells were either densely stained or not reactive at all, although a very few did demonstrate moderate staining. Those which were positive were predominantly large cells, although some small cells were clearly stained as well (Fig. 5B,D,F). Positive CA staining was seen in some axons and in many

neuronal nuclei regardless of the intensity of the reaction product in the cell cytoplasm.

The levels of CO staining density in CA stained neurons as determined in both adjacent or sequentially processed sections is shown in Fig. 5A,B and Fig. 5C-F, respectively. Some individual DRG cells could be identified in adjacent sections as both densely stained for CO (Fig. 5A) and positive for CA (Fig. 5B). In serially processed tissue it can be seen that all neurons with dense CO staining (Fig. 5C) are consistently positive for CA (Fig. 5D). However, some CA-positive cells (Fig 5F) are seen with light staining for CO (Fig. 5D). This agrees with our visual estimates indicating a greater number of CA-positive cells per section compared with those densely stained for CO.

It is important to note that in black-and-white photomicrographs of sequentially processed sections, some cells showing a dense CO reaction are seen to be only marginally more densely stained after the CA reaction giving the impression that it may have been difficult to discern CA-staining in such cells. However, in the light microscope, brown reaction product in sections reacted first for CO was clearly distinguishable from black or gray reaction product subsequently generated in sections reacted for CA. Moreover, in control sections processed first for CO and then for CA in the presence of acetazolamide, no black or gray cytoplasmic staining was evident even in dense CO-reacted cells indicating that what was judged to be CA staining was not simply due to intensification of CO reaction product in these cells by the cobalt present in the CA incubation medium.

DISCUSSION

The present results confirm previous histochemical observations showing a heterogeneous distribution of CO activity in the primary afferent neuronal cell population in DRG of rat (50) and extend these observations to an analysis on a quantitative basis. Our results can be summarized as follows: 1.) The densitometric technique used to demonstrate CO heterogeneity was shown to be quantitative by the linear increase in CO reaction product deposition over time within individual neurons. Linear increases were seen within cells over a wide range of staining densities and this observation indicates that the proportional optical densities measured truly reflect proportional cellular activities of this enzyme; 2.) The staining intensity in most small type B cells (over 75%) fell within the most faintly reactive quadrant. The remaining 25% of the type B cells showed densities which matched the heterogeneity and range of staining intensities displayed by the rest of the population of DRG cells; 3.) Although there was a trend towards higher CO activity in larger cells, the data suggests that cell size is only a minor determinant of CO content; and 4.) The presence of high CO activity is invariably accompanied by positive staining for CA, but the presence of CA is not always accompanied by high CO activity.

Cytochrome oxidase

The feasibility of quantitative densitometric measurements of CO reaction product in individual cells and neurons has been demonstrated previously in a number of systems (21,36,50). Differences with regard to the present method and its characterization are, however, noteworthy. Repeated determination of CO product deposition in the same cells was undertaken as the most rigorous possible evaluation of linearity of the reaction over time. It allowed comparative characterization of the linearity in both light and dark-

staining neurons and provided data on the progression of staining in the selected cells. The neuronal nucleus was excluded from measurements since it is unstained and would therefore lower the average OD of small cells to a greater extent than it would large cells. The whole cytoplasm of the neuronal cell body was selected for density determination, thereby averaging out the non-homogeneous cytoplasmic staining observed in some cells. Finally, we used tissues which were fixed with paraformaldehyde-picric acid fixative. Under these conditions, the population of CO reacted cells presented a more heterogeneous staining pattern than with glutaraldehyde fixation and allowed analysis of cells falling into a greater number of discrete optical density categories. The data presented here argue for the validity of proportional measures of CO activity obtained following this fixation procedure. Moreover, unlike the stronger fixatives more generally used for CO, this fixation is compatible with histochemistry and immunohistochemistry for a wide range of substances that may be simultaneously examined in tissues prepared for CO histochemistry.

Our results are consistent with reports by others (45,46,50) that CO activity is also heterogeneously distributed within the dorsal horn of the spinal cord. It is likely that the light CO staining observed in the SG reflects relatively low activity in both intrinsic neuronal elements and primary afferent terminals within this area. The SG receives most of its primary afferent projections from type B cells, the majority of which displayed low levels of CO activity, whereas a higher proportion of large cells known to innervate mainly the more intensely staining deeper dorsal horn laminae, showed moderate or high levels of activity. It appears then from these examples that the CO-staining within the terminal fields of different classes of primary afferents correlates reasonably well with that of their cell bodies in DRG.

In view of the role of CO in cellular energy production, the large scatter observed in

the profile of CO density versus DRG cell size suggests that factors other than merely cell size must exert a more powerful influence on the energy demands of these neurons. Given demonstrated correlations between neuronal CO and the long-term functional activity of neurons (33), it is likely that CO levels reflect patterns of electrical activity in DRG neurons as has been previously suggested (50). Thus, cells with high CO activity may exhibit either frequent bouts of high firing rates or continuously maintained but more moderate rates of firing.

The present study focussed on the 4th lumbar (L4) ganglion containing the cell bodies of cutaneous and muscle afferent fibers carried within the sciatic nerve. Presumably the pattern of CO activity in this ganglion is a reflection of impulse traffic in L4 afferents and may not necessarily relate to any other ganglia. For instance, differences might be encountered due to divergent levels of activity seen in various muscle afferents (19). Thus, if CO staining densities in distinct DRG neuronal populations reflect largely the characteristic firing patterns required for the transmission of particular sensory modalities, then it would not be unreasonable to expect that cell number versus CO density profiles in other ganglia may be different from those observed here in L4 DRG. The present quantitative data may not necessarily be extrapolated to ganglia at other spinal levels.

It remains to be determined whether a particular level of CO intensity within DRG neurons reflects the electrophysiological activity of distinct subpopulations of DRG cells that have common neurochemical characteristics and transmit common sensory modalities. The histochemical procedures outlined for CO in this report allow investigation of the former issue since the procedures are readily compatible with simultaneous determination of other histochemical and immunohistochemical features of individual DRG cells. The issue concerning relationships between the neurochemical

features of DRG neurons and the sensory modalities they transmit may also be approached by an extension of the present methods to analyses of CO in experimental animals. For example, increases in CO staining intensity in neural structures have been reported to occur after relatively short periods of stimulation (19,35). Thus, quantitative examination of neuronal CO staining densities in ganglia of animals subjected to stimuli that selectively activate specific classes of sensory nerve fibers may reveal increased staining in distinct subpopulations of DRG neurons. These subpopulations may then be identified according to their neuropeptide or enzyme content.

Carbonic anhydrase

As shown by others (24,25,34,40,41), most CA positive DRG neurons were of the largest class. However, in contrast to previous reports, some small cells were also found to be CA-positive and we presume that this may be due to the different fixatives utilized. Since strong tissue fixation inactivates a fair proportion of CA activity (29,35), the weaker fixative used here may have led to greater CA activity. Indeed, our estimate of total CA-positive cells in the L4 DRG was 40%. Previous estimates of the proportion of all neurons containing CA in lumbar DRG have ranged from 20 to 38% (24,25,34,40,41) and that of all intermediate to large cells from 38 to 55% (24,25,41). It should be noted that accurate cell size measurements of CA reacted cells may need to take into account the uniformly and intensely CA-stained satellite cells surrounding CA-positive DRG neurons (34) which may give these neurons a larger appearance.

From the presence of CA in all cells showing high CO activity and given the participation of CA in promoting the transport of carbon dioxide in metabolically active cells, it may be reasonable to consider that it too is present in proportion to cellular energy requirements. However, this assumed relationship remains to be proven,

particularly given our observation that CA-containing DRG neurons outnumber those densely stained for CO. The proportions of CA-positive cells cited above were higher than the percentages of all cells, large cells or large plus medium size cells that were classified here as containing dense CO staining. Thus, not all cells with dense CA staining exhibit dense or even moderate CO staining. This is dramatically illustrated by the presence of CA-positive cells that in fact were clearly light for CO staining.

These results suggest that the role of CA may not be related entirely to energy metabolism within DRG neurons. This possibility has been noted and discussed by others (24,25,29,40) in relation to other known functions of CA (6). One role speculated on here concerns the reportedly high chloride ion levels in DRG neurons (23) and the relationship between CA and chloride transport that has been demonstrated in other cell types (4,31). Given the possibility that transmembrane movements of this ion in the central terminals of some sensory neurons may be responsible for generating presynaptic inhibition manifested as primary afferent depolarization (5), CA-positive DRG neurons may represent those subject to presynaptic inhibition by this ionic mechanism. Alternatively, CA may participate in maintaining appropriate chloride ion distributions across membranes at some peripheral sensory endings where transmembrane fluxes of this ion may be involved in the production of receptor potentials. The presence of CA in DRG neurons with light CO staining does not exclude the previously suggested possibility that CA is localized to a very large extent in muscle afferents (1,24,25,29,41), but does cast doubt on the suggestion that all CA-positive DRG neurons, be they muscle afferents or not, are tonically active.

REFERENCES

1. Aldskogius, H., Arvidsson, J. and Hansson, P. (1988) Carbonic anhydrase enzyme histochemistry of cranial nerve primary sensory afferent neurons in the rat. Histochemistry **88,** 151-154.

2. Andres, K.H. (1981) Untersuchungen uber den feinbau von spinal ganglien. Z. Zellforsch. Mikrosk. Anat. **55,** 1-48.

3. Cervero, F. and Iggo, A. (1980) The substantia gelatinosa of the spinal cord. A critical review. Brain **103,** 717-772.

4. Coulson, R.A. and Herbert, J.D. (1984) A role for carbonic anhydrase in intermediary metabolism. In: Biology and Chemistry of the Carbonic Anhydrases (eds Tashian, R.E. and Hewett-Emmett, D.), Vol. 429, pp. 505-515. Annals New York Academy Sciences, New York, N.Y.

5. Davidoff, R.A. and Hackman, J.C. (1984) Spinal inhibition: In Handbook of the Spinal Cord. Vol. 2 and 3: Anatomy and Physiology (ed Davidoff, R.A.), pp. 385-459. Marcel Dekker, New York.

6. Deutsch, H.F. (1987) Carbonic anhydrases. Int. J. Biochem. **19,** 101-113.

7. Duggan, A.W., Hendry, I.A., Morton, C.R., Hutchison, W.D. and Zhao, Z.Q. (1988) Cutaneous stimuli releasing immunoreactive substance P in the dorsal horn of the rat. Brain Res. **451,** 261-273.

8. Harper, A.A. and Lawson, S.N. (1985) Conduction velocity is related to morphological cell type in rat dorsal root ganglion neurones. J. Physiol. **359,** 31-46.

9. Hoheisel, U. and Mense, S. (1987) Observations on the morphology of axons and somata of slowly conducting dorsal root ganglion cells in the cat. Brain Res. **423,** 269-278.

10. Hokfelt, T., Elde, R., Johansson, Luft, R., Nilsson, G. and Arimura, A. (1976) Immunohistochemical evidence for separate populations of somatostatin-containing and substance P-containing primary afferent neurons in the rat. Neuroscience **1,** 131-136.

11. Horton, J.C. and Hubel, D.H. (1981) Regular patchy distribution of cytochrome oxidase staining in primary visual cortex of macaque monkey. Nature **292,** 762-764.

12. Horton, J.C. (1984) Cytochrome oxidase patches: a new cytoarchitectonic feature of monkey visual cortex. Philos. Trans. R. Soc. Lond. **304,** 199-253.

13. Jones, M.G., Bickar, D., Wilson, M.T., Brunori, M., Colosimo, A. and Sarti, P. (1984) A re-examination of the reactions of cyanide with cytochrome C oxidase. Biochem. J. **220,** 57-66.

14. Kazimierczak, J., Sommer, E.W., Philippe, E. and Droz, B. (1986) Carbonic anhydrase activity in primary sensory neurons. I. Requirements for the cytochemical localization in the dorsal root ganglion of chicken and mouse by light and electron microscopy. Cell Tissue Res. **245,** 487-495.

15. Kuraishi, Y., Hirato, N., Hino, Y., Satoh, M. and Takagi, H. (1985) Evidence that substance P and somatostatin transmit separate information related to pain in the spinal dorsal horn. Brain Res. **325,** 294-298.

16. Lawson, S.N. (1979) The postnatal development of large light and small dark neurons in mouse dorsal root ganglia: a statistical analysis of cell number and size. J. Neurocytol. **8,** 275-294.

17. Lawson, S.N, Harper, A.A., Harper, E.I., Garson, J.A. and Anderton, B.H. (1984) A monoclonal antibody against neurofilament protein specifically labels a subpopulation of rat sensory neurones. J. Comp. Neurol. **228,** 263-272.

18. Leah, J.D., Cameron, A.A. and Snow, P.J. (1985) Neuropeptides in physiologically identified mammalian sensory neurones. Neurosci. Lett. **56,** 257- 263.

19. Loeb, G.E. and Duysens (1979) Activity patterns in individual hindlimb primary and secondary muscle spindle afferents during normal movements in unrestrained cats. J. Neurophysiol. **42,** 420-440.

20. Mawe, G.M. and Gershon, M.D. (1985) Histochemical evaluation of the activity of single entric neurons: verification of the cytochrome oxidase technique. Soc. Neurosci. Abstr. 11 pp. 765.

21. Mawe, G.M. and Gershon, M.D. (1986) functional heterogeneity in the myenteric plexus: demonstration using cytochrome oxidase as a verified cytochemical probe of the activity of individual enteric neurons. J. Comp. Neurol. **249,** 381-391.

22. Nagy, J.I. and Hunt, S.P. (1982) Fluoride resistant acid phosphatase-containing neurons in dorsal root ganglia are separate from those containing substance P or somatostatin. Neuroscience **7,** 89-97.

23. Obata, K. (1976) Excitatory effects of GABA. In GABA in Nervous System Function (eds Roberts, E., Chase, T.N. and Tower, D.B.), pp.283-. Raven Press, New York.

24. Peyronnard, J.M., Charron, L., Lavoie, J., Messier, J.P. and Dubreuil, M. (1988) Carbonic anhydrase and horseradish peroxidase: double labelling of rat dorsal root ganglion neurons innervating motor and sensory peripheral nerves. Anat. Embryol. **177,** 353-359.

25. Peyronnard, J.M., Charron, L.F., Messier, J.P. and Lavoie (1988) Differential effects of distal and proximal nerve lesions on carbonic anhydrase activity in rat primary sensory neurons, ventral and dorsal root axons. Exp. Brain Res. **70,** 550-560.

26. Price, J. (1985) An immunohistochemical and quantitative examination of dorsal root ganglion neuronal subpopulations. J. Neurosci. **5,** 2051-2059.

27. Rambourg, A., Clermont, Y. and Beaudet, A. (1983) Ultrastructural features of six types of neurons in rat dorsal ganglia. J. Neurocytol. **12,** 47-66.

28. Riley, D.A., Ellis, S. and Bain, J. (1982) Carbonic anhydrase activity in skeletal muscle fiber types, axons, spindles, and capillaries of rat soleus and extensor digitorum longus muscles. J. Histochem. Cytochem. **30,** 1275-1288.

29. Riley, D.A., Ellis, S. and Bain, J.L.W. (1984) Ultrastructural cytochemical localization of carbonic anhydrase activity in rat peripheral sensory and motor nerves, dorsal root ganglia and dorsal column nuclei. Neuroscience **13,** 189-206.

30. Riley, D.A., Sanger, J.R., Matloub, H.S., Yousif, N.J., Bain, J.L.W. and Moore, G.H. (1988) Identifying motor and sensory myelinated axons in rabbit peripheral nerves by histochemical staining for carbonic anhydrase and cholinesterase activities. Brain Res. **453,** 79-88.

31. Sapirstein, V.S. (1984) Properties and function of brain carbonic anhydrase. In: Biology and Chemistry of the Carbonic Anhydrases (Tashian, R.E. and Hewett-Emmett, D. eds), Vol. 429, pp. 481-493. Annals New York Academy Sciences, New York, N.Y.

32. Silverman, M.S. and Tootell, R.B.H. (1987) Modified technique for cytochrome oxidase histochemistry: increased staining intensity and compatibility with 2-deoxyglucose autoradiography. J. Neurosci. Methods **19,** 1-10.

33. Sokoloff, L. (1977) Relation between physiological function and energy metabolism in the central nervous system. J. Neurochem. **29,** 13-26.

34. Sommer, E.W., Kazimierczak and Droz, B. (1985) Neuronal subpopulations in the dorsal root ganglion of the mouse as characterized by combination of ultrastructural and cytochemical features. Brain Res. **346,** 310-326.

35. Sugai, N. and Ito, S. (1980) Carbonic anhydrase, ultrastructural localization in the mouse gastric mucosa and improvements in the technique. J. Histochem. Cytochem.

28, 511-525.

36. Van Raamsdonk, W., Smit-Onel, M., Donselaar, Y. and Diegenbach, P. (1987) Quantitative cytochemical analysis of cytochrome oxidase and succinate dehydrogenase activity in spinal neurons. Acta Histochem. **81,** 129-141.

37. Vaughn, T., Behbehani, F.P., Zemlan, F.P. and Shipley, M. (1985) Increased cytochrome oxidase staining in rat spinal cord subsequent to peripheral noxious stimulation. Soc. Neurosci. Abstr. 10 pp. 119.

38. Wiesenfeld-Hallin, Z. (1986) Substance P and somatostatin modulate spinal cord excitability via physiologically different sensory pathways. Brain Res. **372,** 172-175.

39. Wiesenfeld-Hallin, Z., Villar, M.J. and Hokfelt, T. (1988) Intrathecal galanin at low doses increases spinal reflex excitability in rats more to thermal than mechanical stimuli. Exp. Brain Res. **71,** 663-666.

40. Wong, V., Barrett, C.P., Donati, E.J., Eng, L.F. and Guth, L. (1983) Carbonic anhydrase activity in first-order sensory neurons of the rat. J. Histochem. Cytochem. **31,** 293-300.

41. Wong, V., Barrett, C.P., Donati, E.J. and Guth, L. (1987) Distribution of carbonic anhydrase activity in neurons of the rat. J. Comp. Neurol. **257,** 122-129.

42. Wong-Riley, M. (1979) Changes in the visual system of monocularly sutured or enucleated cats demonstrable with cytochrome oxidase histochemistry. Brain Res. **171,** 11-28.

43. Wong-Riley, M. and Riley, D.A. (1983) The effects of impulse blockage on cytochrome oxidase activity in the cat visual system. Brain Res. **261,** 185-193.

44. Wong-Riley, M. and Carroll, E.W. (1984) The effect of impulse blockage on cytochrome oxidase activity in the monkey visual system. Nature **307,** 262-264.

45. Wong-Riley, M. and Kageyama, G. (1984) Histochemical localization of cytochrome oxidase in the spinal cord, dorsal root ganglion and skeletal muscle of normal rat, cat and monkey. Soc. Neurosci. Abstr. Vol. 10, Part 2, pp. 30.

46. Wong-Riley, M. and Hoppe, D.A. (1985) Cytochemical localization of cytochrome oxidase in the spinal cord and dorsal root ganglia, with quantitative analysis of ventral horn cells in the monkey. Soc. Neurosci. Abstr. 11 pp. 26.

47. Wong-Riley, M.T.T., Merzenich, M.M. and Leake, P.A. (1978) Changes in endogenous enzymatic reactivity to DAB induced by neuronal inactivity. Brain Res. **141,** 185-192.

48. Wong-Riley, M.T.T. and Welt, C. (1980) Histochemical changes in cytochrome oxidase of cortical barrels following vibrissal removal in neonatal and adult mice. Proc. Natl. Acads. Sci. U.S.A. **77,** 2333-2337.

49. Wong-Riley, M.T.T., Walsh, S.M., Leake-Jones, P.A. and Merzenich, M.M. (1981) Maintenance of neuronal activity by electrical stimulation of unilaterally deafened cats demonstrable with the cytochrome oxidase technique. Ann. Otol. Rhinol. Laryngol. **90 (Suppl. 82),** 30-32.

50. Wong-Riley, M.T.T. and Kageyama, G.H. (1986) Localization of cytochrome oxidase in the mammalian spinal cord and dorsal root ganglia, with quantitative analysis of ventral horn cells in monkeys. J. Comp. Neurol. **245,** 41-61.

51. Zamboni, L. and DeMartino, C. (1967) Buffered picric-acid formaldehyde: a new rapid fixative for electron microscopy. J. Cell Biol. **35,** 148A.

FIGURE LEGENDS

Fig. 1. Photomicrographs showing the histochemical localization of CO activity in sections of lumbar DRG and spinal cord. (A) A 5 μm section showing the heterogeneity of CO activity among DRG neurons. Non-neuronal CO staining is seen in satellite cells (arrows). (B) A section of DRG which was fixed in a glutaraldehyde-containing fixative. Note the reduced CO staining heterogeneity among neurons compared with A and C (C) Higher magnification of the section shown in (A) in which the three descriptive categories of CO staining intensity used in the text are indicated by L for light staining, M for moderate staining and D for dense staining. (D,E) Two adjacent sections showing the reproducibility of staining densities from section to section in corresponding neurons indicated by numbers. (F) Cells showing perinuclear deposition of CO reaction product (arrows). In B, C, and D note the eccentrically located region of dense staining in some neurons (arrowheads). (G) A spinal cord section showing much lighter staining in the substantia gelatinosa than the subjacent laminae. Note the mediolateral gradient in staining intensity which was a consistent observation. Very few neurons display a dense CO reaction (arrow). Magnifications: (A,C) X 140; (B) X 240; (D,E) X 430; (F) X 340; (G) X 125.

Fig. 2. (A) Time course of CO histochemical staining density in each of five individual neuronal cell bodies in sections of DRG. The five cells illustrate linearity of reaction product deposition at different staining densities. (B) Time course of CO histochemical staining density in populations of DRG neurons. The optical densities of the 479 cells reacted for 6 hours were divided into five bins of cells sharing common group densities and the average density in each bin was then plotted against time. The densities of cells in each group were averaged for each time point. Standard errors are encompassed by

the symbols at each data point. Fig. 3. Frequency distributions of CO reacted neurons in a dorsal root ganglion. (A) Frequency distribution of neuronal cross-sectional area for classes of cells designated as exhibiting light, moderate or dense CO reaction product. (B) Frequency distribution of the size of all analyzed cells expressed as percentage of total cell number. (C) Plot of number of cells against optical density of CO reaction product for three size categories of cells (small, medium and large). (D) Frequency distribution of CO reaction density in the two smallest size categories of cells expressed as percent of total cells in each size category. ($\leq$500 μm^2, circles; >500 to $\leq$1000 μm^2, squares)

Fig. 4. A scatter plot of neuronal cross-sectional area and CO reaction density for all analyzed cells including the plot of linear regression. Arrows on the right indicate densities at which cells were subdivided into the three CO staining categories light (L), moderate (M), or dense (D) depicted in Fig. 3A. Arrows above the plot indicate size limits for designation of cells as small, medium or large.

Fig. 5. Photomicrographs of DRG sections showing the relationship between CO and CA activity in neurons. (A,B) Adjacent sections reacted for CO (A) or for CA (B). Note that most cells with dense CO staining are also positive for CA (corresponding cells indicated by arrows). (C,D) Photomicrographs of the same section processed histochemically for CO (C), photographed, and then processed histochemically for CA (D). Virtually all cells designated as densely stained for CO (arrows) also exhibit CA reaction product (D, corresponding arrows). (E,F) Higher magnification of sections shown in (C,D). Note that some CA- positive cells (F, arrows) are lightly stained for CO (E, arrows). Magnifications: (A,B) X 145; (C,D) X 70; (E,F) X 140.

Table 1. Optical density measurements of CO reaction product in DRG neurons under standard and various control incubation conditions.

Treatment	Optical density: Reaction Time 2 hours	n	Optical density: Reaction Time 5 hours	n
normal medium (NM)	0.035 ± 0.001 (100)	99	0.08 ± 0.0019 (100)	120
NM + 10 μM KCN	0.005 ± 0.0006 (14)	13	0.023 ± 0.0008 (29)	85
NM + 1 mM KCN	0.001		0.001	
NM -cytochrome C	0.002 (5)		0.017 ± 0.0008 (21)	87
NM -cytochrome C + 10 μM KCN	0.001		0.001	

Values represent means ± S.E.M. of the indicated number (n) of cells analyzed for each condition. Values in parentheses indicate optical densities expressed as a percentage of those obtained in normal medium. For densities less than or equal to 0.002, the density in a single random field within a ganglion section is given since cell borders were not readily identifiable. KCN, potassium cyanide.

Table 2. Number of small, medium and large DRG neurons exhibiting light, moderate or dense CO reaction product as a percentage of all neurons within each size category.

	Cross Sectional Area (μm^2)			
	Small*		Medium	Large
Optical Density+	≤500	>500 to ≤1000	>1000 to ≤1800	>1800
Light	77.0	74.8	43.3	32.7
Moderate	23.0	23.2	43.3	51.8
Dense	0	1.9	13.4	15.5

* Small cells are subdivided into two size categories.

+ Quantitative optical density designations of light, moderate and dense CO reaction product are indicated in the text under Data Analysis in Methods section.
Values indicate the percentage of cells in each size category exhibiting a particular staining density.

Table 3. Number of small, medium and large DRG neurons exhibiting light, moderate or dense CO reaction product as a percentage of all neurons analyzed.

	Cross Sectional Area (μm^2)				
Optical Density+	Small* ≤500	>500 to ≤1000	Medium >1000 to ≤1800	Large >1800	Total% by optical density
Light	9.8	27.6	8.4	10.1	55.9
Moderate	2.9	8.6	8.4	16.0	36.0
Dense	0	0.7	2.6	4.8	8.1
Total % by size	12.7	36.9	19.4	30.9	

* Small cells are subdivided into two size categories.

+ Quantitative optical density designations of light, moderate and dense CO reaction product are indicated in the text.

Values indicate the number of DRG cells exhibiting a particular size and CO staining density as a percentage of all the cells analyzed. Total % by density indicates the percentage of all size categories exhibiting a particular staining density. Total % by size indicates the number of cells in each size category as a percentage of all the cells analyzed.

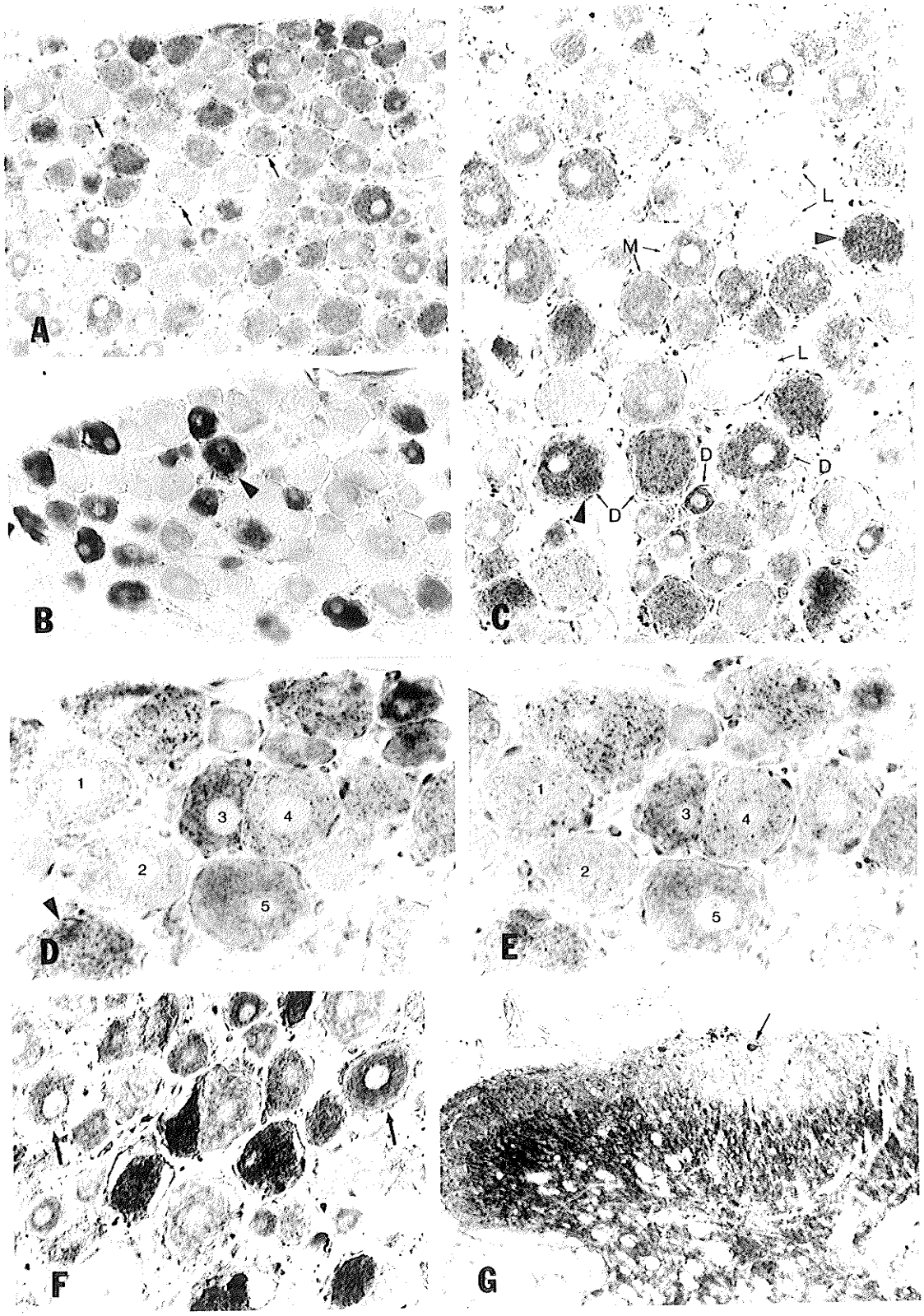

Fig. 1

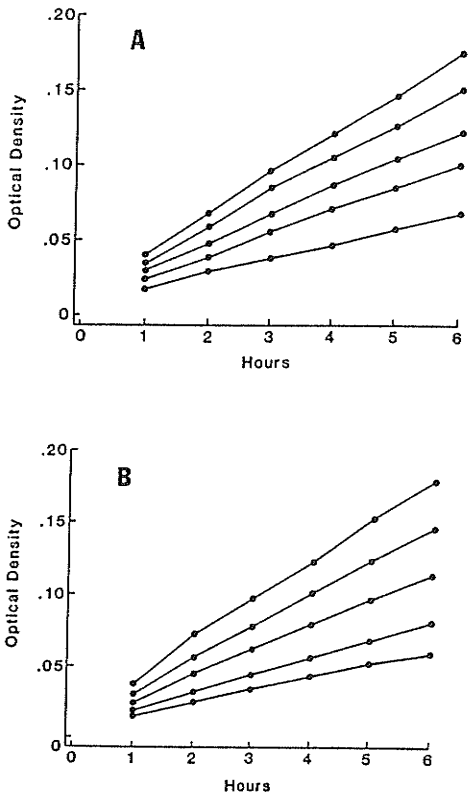
A
Optical Density
.20
.15
.10
.05
0
0
1
2
3
4
5
6
Hours
B
Optical Density
.20
.15
.10
.05
0
0
1
2
3
4
5
6
Hours

Figure 2

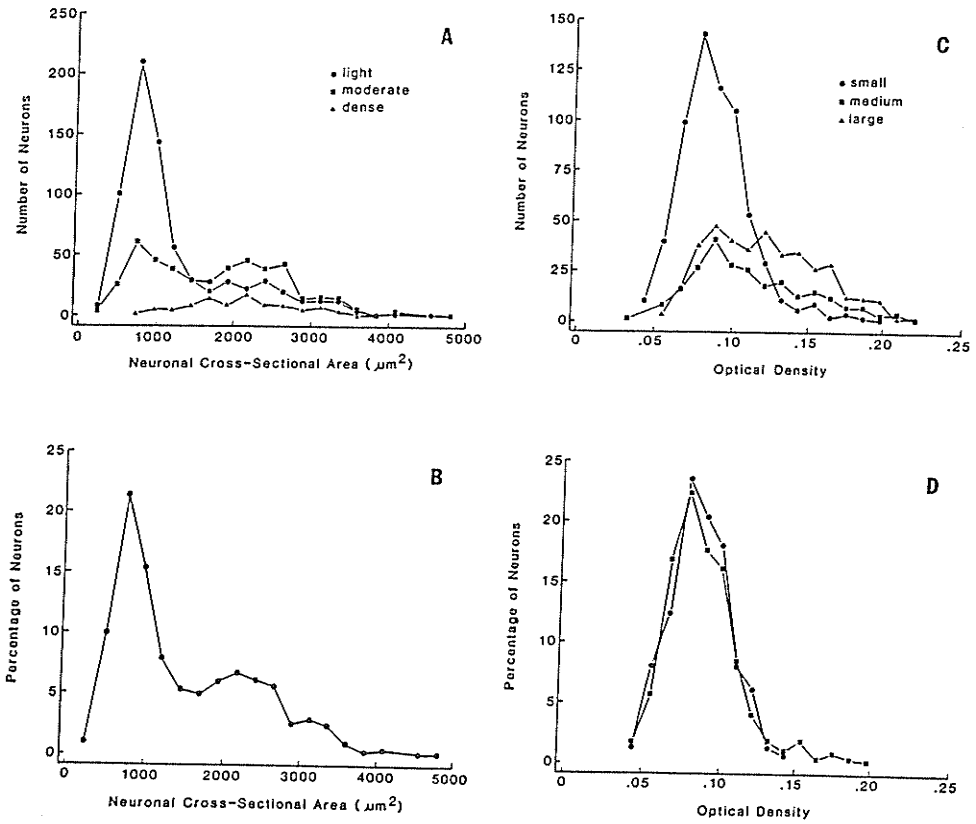
A
light
moderate
dense
Number of Neurons
Neuronal Cross-Sectional Area (μm²)
B
Percentage of Neurons
Neuronal Cross-Sectional Area (μm²)
C
small
medium
large
Number of Neurons
Optical Density
D
Percentage of Neurons
Optical Density

Figure 3

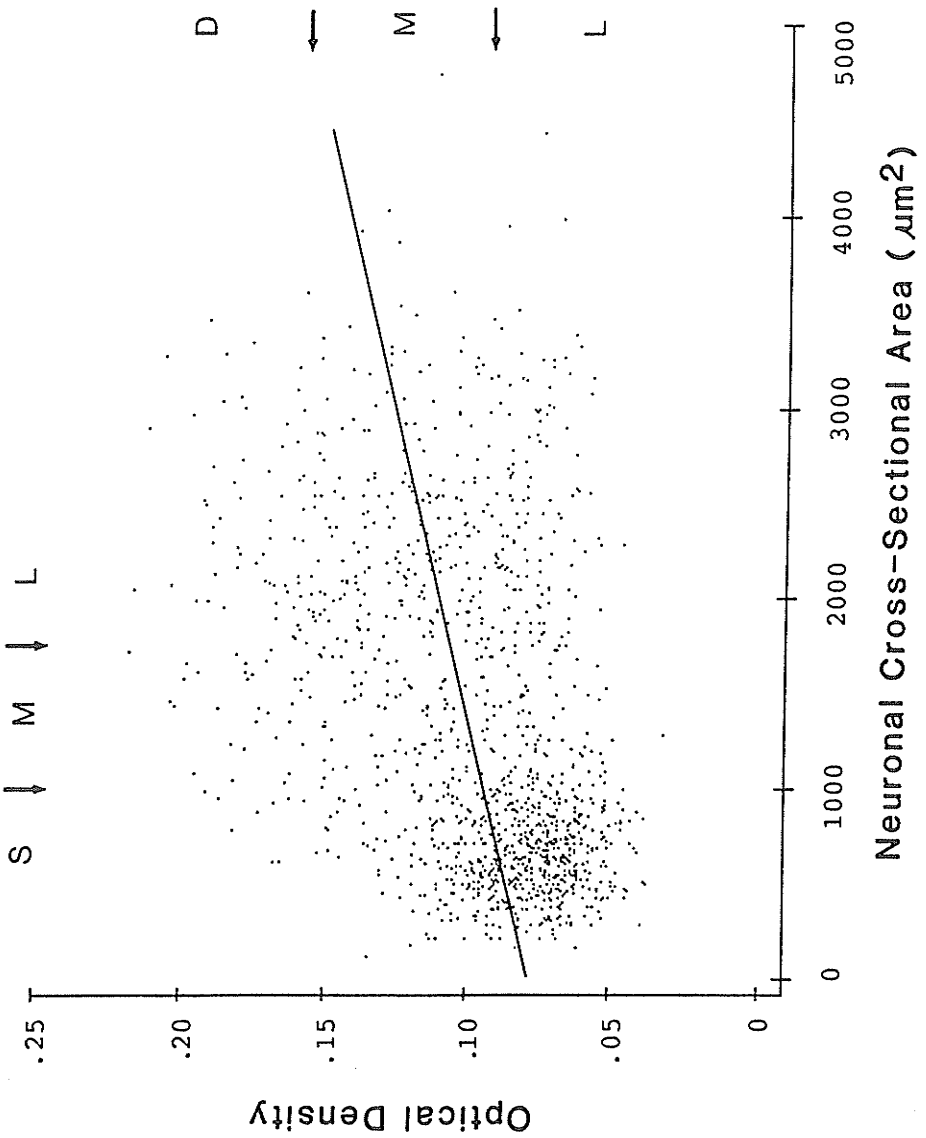
Optical Density
.25
.20
.15
.10
.05
0
0
1000
2000
3000
4000
5000
Neuronal Cross-Sectional Area (μm2)
S
M
L
D
M
L

Figure 4

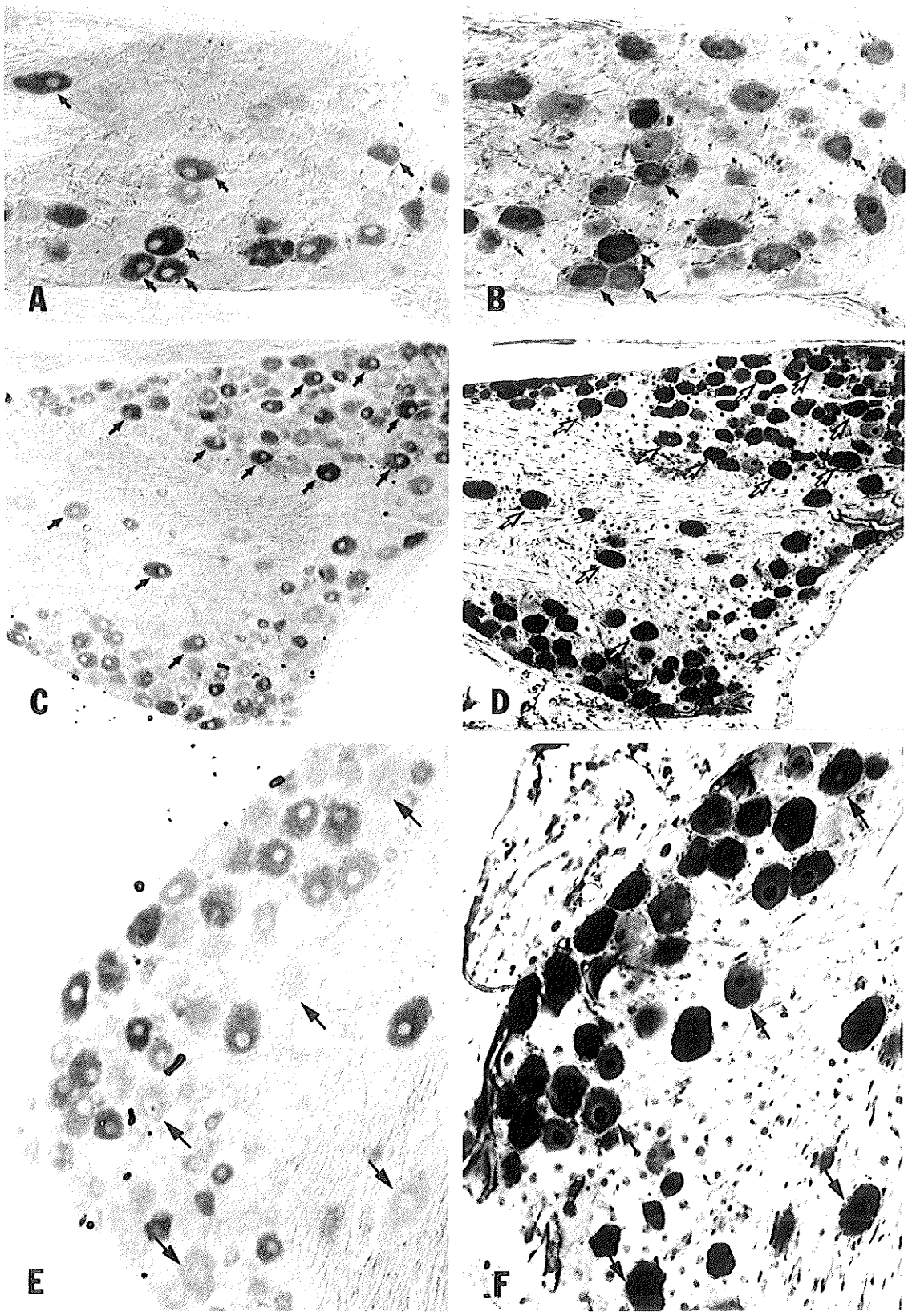

Fig. 5

Part III

Analysis of parvalbumin and calbindin D28k-immunoreactive neurons in dorsal root ganglia of rat in relation to their cytochrome oxidase and carbonic anhydrase content

P.A. Carr, T. Yamamoto, G. Karmy, K.G. Baimbridge and J.I. Nagy

Neuroscience (1989) 33; 363-371

Abstract--Histochemical and immunohistochemical techniques were used to determine relationships between the parvalbumin or calbindin D28k content and the cytochrome oxidase or carbonic anhydrase activity of neurons in lumbar dorsal root ganglia in rat. Subpopulations of dorsal root ganglion neurons that displayed parvalbumin- or calbindin D28k-immunoreactivity were classified as containing either light, moderate or dense histochemical reaction product for cytochrome oxidase and either a positive or negative reaction for carbonic anhydrase. It was found that approximately 90% of all parvalbumin and calbindin D28k-immunoreactive cells exhibited dense staining for cytochrome oxidase and that 87% of parvalbumin- and 76% of calbindin D28k-immunoreactive cells were positive for carbonic anhydrase. Conversely, 85% of all cells with a dense cytochrome oxidase reaction contained parvalbumin and calbindin D28k. Although not quantified, it appeared that many, but not all, carbonic anhydrase positive cells contained parvalbumin or calbindin D28k.

These results indicate the existence of a subpopulation of primary sensory neurons that contains parvalbumin and calbindin D28k and that expresses high levels of cytochrome oxidase and carbonic anhydrase activity. It is suggested that primary afferent neurons with this cytochemical profile transmit a sensory modality that requires them to discharge rapidly and/or frequently. The existence of a subpopulation of carbonic anhydrase-positive cells that lack immunoreactivity for parvalbumin or calbindin D28k suggests that the role of carbonic anhydrase in some sensory neurons is unrelated to functions requiring these calcium binding proteins.

The identification of an increasing number of calcium binding proteins that are selectively expressed in different cell types has allowed conceptualization of how calcium is able to serve as a second messenger for an immense range of intracellular events and how specificity of calcium actions are achieved. However, the proliferation of these proteins has generated the problem of deciphering the mechanism whereby each promotes or regulates the actions of calcium. Two such proteins that have recently received considerable attention are calbindin D28k (CaBP), originally referred to as vitamin D- dependent calcium binding protein (37), and parvalbumin (PV). Both PV and CaBP have been found in a wide variety of peripheral tissues (5,14,15,24) as well as in the central nervous system (CNS) where, although both PV and CaBP are again widely distributed, they occur only in discrete populations of neurons within any particular structure (1,2,8,9,13,16,18,33). The diverse distributions of PV and CaBP suggest their involvement in calcium-dependent processes that are common to functionally disparate types of cells and neurons. One possible role postulated for both proteins, partly on the basis of such commonality of cellular function, is that they serve to buffer or sequester calcium in cells that are highly metabolically or electrically active (2,9,15,18). Thus, in the CNS both PV and CaBP are often, though not always, found in neurons that are characterized by their high firing rates. It remains to be determined, however, whether the putative buffering capacity of either PV or CaBP is generally required in all neurons that maintain high levels of electrical activity or whether their presence is a reflection of more subtle requirements for calcium regulation in some very active neurons.

As in neurons elsewhere, calcium has a host of complex functions in primary sensory neurons within dorsal root ganglia (DRG) including mediation of transmitter or modulator release at central and peripheral sensory terminals, production of calcium spikes and regulation of intracellular energy metabolism (12,19,23,30,44). The presence of PV and CaBP in DRG neurons, as recently described (6,14,27), provides the

opportunity to correlate the suggested roles of these proteins in calcium regulation with emerging knowledge of the electrical, biochemical and neurochemical properties of various subpopulations of these neurons. Histochemical studies have shown that these properties include remarkably heterogenous levels of the enzymes cytochrome oxidase (CO) (7,43) and carbonic anhydrase (CA) (17,25,28,32,38,39) among DRG neurons. In most neural systems, histochemical staining density for CO is now a well established indicator of long-term patterns of neuronal electrical activity (43). In the case of CA, at least one of its many proposed roles is to facilitate removal of carbon dioxide generated in active cells (11). In view of evidence and speculations suggesting the preferential localization of PV and CaBP in neurons that are prone to relatively rapid or frequent discharge, we have investigated the relationships between the PV or CaBP content of DRG neurons and their levels of CO or CA.

METHODS

Tissue Preparation

Adult, male Sprague Dawley rats weighing 250-350 g were anesthetized with chloral hydrate and perfused transcardially with cold (4°C) 0.9% saline containing 0.1% sodium nitrite and 100 units of heparin. This was immediately followed by cold (4°C) freshly prepared fixative consisting of 4% paraformaldehyde and 0.16% picric acid in 0.1 M sodium phosphate buffer, pH 7.4, (para-picric fixative) (46) or 0.2% glutaraldehyde, 0.16% picric acid and 4% paraformaldehyde in 0.1 M phosphate buffer, pH 7.4 (para-picric-glu fixative). After perfusion, the L4 and L5 dorsal root ganglia (DRG) were removed and immersed in cold para-picric fixative for 2 hr. The ganglia were then stored in cryoprotectant solutions containing 15% sucrose and 0.001% sodium azide in 0.1 M phosphate buffer, pH 7.4, or 25% sucrose with 10% glycerol in 50 mM phosphate buffer, pH 7.4, for cryostat or freezing microtome sectioning, respectively. Dorsal root

ganglia sections were cut either on a cryostat (Leitz) at thickness of 5-15 μm and thaw-mounted onto gelatinized slides, or on a freezing microtome at a thickness of 20 μm and collected into cold 0.9% saline in 0.1 M sodium phosphate buffer, pH 7.4, (PBS).

Colocalization

Sections of DRG were processed immunohistochemically for PV or CaBP and histochemically for CO or CA. Determination of the relationship between the PV or CaBP content and the CO or CA content of DRG neurons was undertaken by analysis of adjacent or sequentially processed sections. Adjacent cryostat sections were cut from para-picric fixed tissue and collected on separate slides. Preliminary data was obtained from sections cut at a thickness of 5-8 μm; all data presented here were derived from sections cut at 7 μm. Pairs of slides were generated for the localization of PV- or CaBP-positive cells in sections on one slide and estimation of CO or CA reaction product in adjacent sections on another slide. All immunohistochemical processing of adjacent sections was carried out using the peroxidase-antiperoxidase (PAP) method for convenience of photography. Reacted sections were coverslipped with glycerol-water (3:1) and corresponding areas of adjacent sections were photographed to enable precise alignment of the same cells in photomicrographs.

Sections processed sequentially were reacted first for PV- or CaBP-immunofluorescence, coverslipped with anti-fade medium (36) and then photographed. The coverslips were then removed in either 0.1 M sodium phosphate buffer, pH 7.4, (PB) or PB containing 4% sucrose, and the tissue washed for 20 min in two changes of PB. Following the wash, the sections were reacted for CO or CA histochemistry. Immunofluorescence was used for all immunohistochemical procedures in sequentially processed tissue to allow subsequent visualization of CO or CA histochemical reaction

product. In photomicrographs of the same areas in either adjacent or sequentially processed sections, only corresponding cells identifiable in both photographic prints were included in the analysis.

Immunohistochemical techniques

All immunohistochemistry was conducted on slide-mounted sections except those taken for combination with free-floating carbonic anhydrase histochemistry as described below. Well characterized polyclonal antibodies against PV or CaBP were generated in rabbit (5,21) and used at dilutions of 1:400-1:2000 in PBS containing 0.3% Triton X-100 (PBS-T) for adjacent sections processed by immunoperoxidase and in PBS alone for sections sequentially processed by immunofluorescence. Sections were incubated with primary antisera for 40-68 hr at 4°C followed by a 40 min wash with two changes of PBS-T at room temperature. Triton X-100 was excluded from all washes of sequentially processed tissues. Sections processed by the PAP method were incubated for two hours in secondary media consisting of goat anti-rabbit IgG (Sternberger-Meyer) diluted 1:20 in PBS-T and 1% bovine serum albumin (BSA). They were then washed for 40 min in two changes of PBS-T and incubated for two hours at room temperature in rabbit PAP (1:100) (Sternberger-Meyer) diluted in PBS-T and 1% BSA. The sections were then washed in PBS-T for 20 min and washed for a further 20 min in 50 mM Tris-HCl buffer, pH 7.4. Peroxidase activity was then visualized by reacting the sections in 50 mM Tris-buffer containing 0.005% hydrogen peroxide and 0.02% diaminobenzidine for 5-10 min. The sections were then dried and coverslipped with glycerol-water (3:1). For immunofluorescence, sections incubated with primary antibody were washed and then incubated for 40 min to one hour with fluorescein isothiocyanate-conjugated donkey anti-rabbit IgG (Amersham) at a dilution of 1:20 in PBS with 1% BSA. Sections were then washed for 30 min in PBS and coverslipped with glycerol-water (3:1) or anti-fade

medium. The sections were then photographed, the coverslip removed, and the tissues prepared for sequential histochemical processing as described below.

Cytochrome Oxidase Histochemistry

Cytochrome oxidase histochemistry was conducted using a slight modification of the Wong-Riley method (40) in which the reaction medium contained one half the concentration of diaminobenzidine (0.025%) in PB with 4% sucrose and 0.03% cytochrome C (Sigma, type III). All incubations were conducted in the dark in a 37°C constant temperature water bath for 2-5 hr. Adjacent sections or sections which had previously been reacted for immunofluorescence were washed for 30 min in two changes of PB before immersion in the CO incubation medium. The reaction was terminated by two 15 min rinses of the sections in PB. The sections were then dried and coverslipped with glycerol-water (3:1).

Histochemistry of carbonic anhydrase

Histochemistry for CA was conducted essentially as described by others (28,38) except that weaker tissue fixatives (paraformaldehyde-picric acid) were used to allow compatibility with CaBP or PV immunohistochemistry. The incubation medium consisted of 1.75 mM $CoSO_4$, 11.7 mM KH_2PO_4, 157 mM $NaHCO_3$, and 53 mM H_2SO_4, pH 6.5, and was freshly made with each use (38). Some sections were processed in incubation medium containing 0.01 mM acetazolamide, an inhibitor of CA (11,20), which was found to eliminate cytoplasmic CA staining in the present studies. Two procedures were used for CA histochemistry in combination with PV or CaBP immunohistochemistry. In the first case, adjacent cryostat sections of lumbar ganglia (L4 or L5) were cut at a thickness of 5 μm and collected on separate gelatin-coated slides.

One section was reacted for CA and the adjacent section for CaBP or PV by the immunoperoxidase method as described above. Slide mounted sections were washed in cold PB for 1 hr and then immersed into incubation medium for 5 sec followed by exposure to the atmosphere for 30 sec. This immersion sequence was repeated for 30 min. Sections were then dipped in an aqueous solution of 0.5% ammonium sulphate for 3 min, washed in PB for 5 min, and coverslipped with a mixture of glycerol and 10 mM PB (3:1). In the second procedure, sections were processed sequentially first for PV or CaBP and then for CA. Sections were cut on a sliding microtome at a thickness of 20 μm, collected and washed for 1 hr in PB, and then processed free floating for PV or CaBP immunofluorescence as described above. The sections were then mounted onto slides (not gelatin-coated) from a 25% sucrose and 10% glycerol solution in 10 mM PB (pH 7.4), allowed to dry slightly, coverslipped with this same solution and photographed using a Dialux 20 microscope (Leitz) equipped with a L3 Phloemopak filter cube. The coverslips were then removed, the sections were carefully teased off the slides in PB, re-mounted onto slides, and dried for 30 sec. The slide was then gently immersed into the CA incubation medium in a manner that would allow the sections to float on the surface of the medium. After 30 min the sections were collected onto slides, floated again on the surface of 0.5% ammonium sulphate solution for 3 min, washed in PB for 5 min and finally mounted onto gelatin-coated slides and coverslipped with a mixture of glycerol and 10 mM PB (3:1).

RESULTS

General considerations

Dorsal root ganglion sections immunostained for PV or CaBP by either immunoperoxidase or immunofluorescence methods resulted in various intensities of nuclear and cytoplasmic staining in neuronal cell bodies. Nevertheless, cells were clearly

identifiable as being immunopositive or negative for these proteins. In comparisons of tissues fixed with or without glutaraldehyde, no readily discernible differences were evident in the distribution or intensity of PV- or CaBP-immunoreactivity in DRG neurons. As described in more detail elsewhere (6), most PV-immunoreactive (PV-IR) and CaBP-immunoreactive (CaBP-IR) neurons were large, presumably type A cells, but a small number of these were clearly small type B neurons. Thorough analysis of the CO and CA content of these small cells was not conducted in this study since they could not be identified with confidence and in sufficient numbers in adjacent sections which was deemed necessary to confirm results obtained from sections processed sequentially. In this regard, the similar results derived, at least for large cells, from adjacent and sequentially processed sections indicates that prior processing of sections for immunohistochemistry did not interfere with subsequent histochemical detection of CO or CA. In addition, it should be noted here that since PV appears to be contained almost entirely in a subpopulation of DRG neurons containing CaBP (6), observations with respect to PV can be considered to be, in part, confirmatory of those pertaining to CaBP.

Examples of CO staining density in PV-IR or CaBP-IR neurons are presented with both para-picric fixed and para-picric-glu fixed tissues. The para-picric-glu fix was preferred for sections processed sequentially since it more consistently maintained CO activity in sections previously processed for PV or CaBP immunofluorescence. However, while this fix preserved activity in cells heavily stained for CO, it substantially reduced CO reaction product in lightly or moderately stained cells, thus limiting comparisons of CO density in these cells with PV or CaBP content. Although quantitative documentation of CO density in PV- and CaBP-IR cells would have been feasible, this was not conducted since cells densely stained for CO with either fixative were easily distinguished and the results concerning the colocalization of PV and CaBP in these cells were sufficiently clear.

Correlation of PV-IR and CaBP-IR neurons with CO activity

Comparison of CaBP-IR cells with their CO staining density in adjacent sections obtained from para-picric fixed tissue is shown in Fig. 1A,B. In most cases where corresponding cells were confidently identified as such, CaBP-IR cells (Fig. 1A) were consistently the most densely stained for CO (Fig. 1B). Most cells considered to be moderately stained for CO were devoid of CaBP. Similar results were obtained in sections fixed with para-picric-glu and processed sequentially for CaBP (Fig. 1C) followed by CO (Fig. 1D). In this example, it can be seen that some small type B CaBP-IR neurons follow the CO staining pattern of their large cell counterparts. From a count of 532 CaBP-IR neurons compiled from both adjacent and sequentially processed sections, approximately 90% of the CaBP-IR cells exhibited the densest CO reaction seen among DRG neurons. The corresponding percentages obtained independently from adjacent or sequentially processed sections were 95% and 84%, respectively.

Demonstrations of CO reaction densities in PV-IR cells are shown in Fig. 2. In adjacent sections obtained from ganglia fixed with para-picric most large PV-IR neurons (Fig. 2A) contained dense CO reaction product (Fig. 2B). This is also shown in Fig. 2C,D for large cells and in addition illustrates relatively rare examples of adjacent sections through small DRG neurons which happened to be immunopositive for PV; these were also found to exhibit a dense CO reaction. In sequentially processed sections (Fig. 2E,F) from para-picric fixed tissue the correspondence between PV-IR cells and cells densely stained for CO is still evident but less striking due to loss of CO activity with the weaker fix. This illustrates the degree of CO activity loss that occurs when sections are sequentially processed for immunofluorescence followed by CO without at least a low concentration of glutaraldehyde in the perfusion fixative. For comparison,

sequentially processed sections of para-picric-glu fixed tissues are shown in Fig. 2G and H. From a count of 327 PV-IR neurons analyzed in sequentially processed and adjacent sections, 89% of these displayed robust staining for CO. The corresponding percentages obtained independently from adjacent or sequentially processed sections were 88% and 90%, respectively.

Correlation of PV-IR and CaBP-IR neurons with CA activity

Our results concerning the appearance and localization of CA reaction product in DRG were similar to those described by others (25,26,28,38,39). In tissue fixed with para-picric-glu, DRG neurons displayed more intense CA staining than those in tissue fixed with para-picric. In the present study, the deposition of uniform gray or black CA reaction product was considered to be indicative of those cells positive for CA. Comparisons of DRG neurons immunoreactive for PV or CaBP with those positive for CA are shown in Fig. 3. In adjacent sections of ganglia fixed with para-picric, most CaBP-IR cells (Fig. 3A) were found to be CA-reactive. Similar results were obtained in adjacent sections taken for comparison of PV with CA (not shown). In sections of ganglia fixed with para-picric-glu and taken for sequential processing for CaBP or PV by immunofluorescence followed by CA histochemistry, most CaBP-IR neurons (Fig. 3C) were CA-positive (Fig. 3D) and similarly most PV-IR cells (Fig. 3E) were CA-positive (Fig. 3F). From a count of 272 CaBP-IR neurons and 104 PV-IR neurons of all sizes, 76% and 87% of these, respectively, were found to be CA-positive. Quantification of the number of cells with CA reaction product but no immunoreaction for PV or CaBP was not undertaken in the present study. However, many, but not all, CA-positive cells contained PV or CaBP.

DISCUSSION

The main findings of the present report are that the majority of PV- and/or CaBP-IR neurons in lumbar DRG of rat contain CA and consistently exhibit dense staining for CO and that PV- and CaBP-positive neurons represent a subpopulation of cells containing CA. The similarities between PV-IR and CaBP-IR neurons with respect to their CO and CA content is consistent with our previous demonstrations of the colocalization of PV within a subpopulation of CaBP-positive DRG neurons and with the observation that nearly all DRG neurons that exhibit dense staining for CO also contain CA (6,7). These results taken together indicate the existence of a distinct subpopulation of DRG neurons that is distinguished by its parvalbumin [P], oxidase [O], calbindin D28k [C], and anhydrase [A] content. For convenience, these will be referred to henceforth as POCA-positive, POCA-containing or simply POCA neurons. In considering this nomenclature, we appreciate that the terms positive and containing imply presence or absence with respect to CO and CA, but recognize that all cells contain CO activity and that probably most DRG neurons and indeed most cell types express some level of CA (35) which is not visualized histochemically in fixed tissue (34). Nevertheless, it appears that some DRG neurons possess a far greater abundance of CO and CA compared with their neighbors and our proposed terminology is meant in reference to these relative differences.

The elevated rates of production of CO and CA in POCA neurons is assumed to have functional relevance. Four points that may be pertinent in this regard include: 1) correlations between the electrical activity of neurons and their CO content (40,41,42); 2) correlations between the high PV and CO content of some nuclei in brain (3,4); 3) observations that PV-IR and CaBP-IR neurons in the CNS are often those with the greatest firing rates (2,9,15,18); and 4) suggestions that some, though perhaps not all,

CA-containing neurons in DRG are likely to be tonically active (7,25,26,28). On the basis of these points and the present findings, we suggest that the subpopulation of DRG cells displaying POCA are among the most electrically active primary sensory neurons. Conversely, our observation that the vast majority (over 85%) of DRG neurons with dense staining for CO also contained PV and CaBP would support the suggestion that these calcium binding proteins may be required for their capacity to buffer heavy calcium loads in neurons that fire rapidly and/or exhibit calcium spikes (8,9,14,15). The requirement of these proteins in DRG neurons that produce calcium currents (12,23,45) remains uncertain since most POCA neurons were large type A cells whereas calcium currents in sensory neurons have been observed largely in somas with either unmyelinated fibers (45), which arise mostly from small type B cells, or with fibers ending in high threshold sensory receptors (29) which are unlikely to be tonically active. However, the possible requirement of PV and/or CaBP in such neurons is not excluded given the presence of these proteins in a subpopulation of small DRG neurons (6).

The occurrence of PV and CaBP in a very small proportion of DRG neurons that exhibited light or moderate CO activity (<10%) suggests either roles for these proteins additional to calcium buffering in active cells or, alternatively, their constitutive expression in POCA cells that have somewhat reduced CO activity during periods of electrical quiescence. In any case these cells and those densely stained for CO but apparently lacking PV or CaBP (15%) are exceptions that tend to negate our interpretations and suggest instead that POCA neurons represent a rather large, but distinct subpopulation of cells containing either high CO activity or these calcium binding proteins. However, several technical considerations need to be emphasized regarding these exceptions. First, it should be noted that histochemistry and immunohistochemistry are seldom totally reliable. Second, there is likely a small error associated with the identification of corresponding cells in adjacent sections. Third,

compared with the density of CO or CA staining in a cell represented in the full thickness of a section, the staining density in a cell only partially present in a section is likely to be lower and such cells would have been included in the present counts. Finally, based on densitometric analysis of CO staining in over 1000 DRG neurons (7), judgements of those presently designated as densely stained were considered to be conservative. Thus, our observation of about 90% colocalization of CaBP or PV in cells densely stained for CO and 76 to 87% colocalization of these proteins in cells positive for CA is probably an underestimate of the true correspondence. Indeed, in optimal material we found that the correspondence between neurons densely stained for CO and those positive for PV or CaBP approached 98%. The degree to which such a correspondence between high CO activity and CaBP or PV content exists among central neurons remains to be determined.

Carbonic anhydrase has a variety of complex functions related to cell metabolism and maintenance of ion homeostasis (10,11,22,31,35). Functions that may be most pertinent to its CO_2-hydrating activity in DRG neurons include facilitation of carbon dioxide transport in metabolically active cells and/or promotion of calcium sequestration within intracellular organelles. Given the relationship between CO activity and neuronal energy requirements, our observation, reported elsewhere (7), that very nearly all DRG neurons with dense CO histochemical staining also contain CA could be considered as evidence for these two possible roles of CA in at least some DRG neurons. This is now particularly reinforced by the proposed roles of PV and CaBP in electrically very active cells and the colocalization of these two proteins in CA-positive DRG neurons that also exhibit dense staining for CO. However, there appear to be significant numbers of CA-containing cells that exhibit very light CO reaction product which may indicate other functions for this enzyme (7). In this context, it has been previously suggested that CA is localized to a very large extent in, and may have some function related to, muscle afferents (25,26,28,39). Notwithstanding the possibility that POCA cells may represent a

subpopulation of such afferents, the peripheral projections of, and sensory information conveyed by, POCA neurons remains to be determined.

REFERENCES

1. Baimbridge, K.G. and Miller, J.J. (1982) Immunohistochemical localization of calcium-binding protein in the cerebellum, hippocampal formation and olfactory bulb of the rat. Brain Res. **245,** 223-229.

2. Baimbridge, K.G., Miller, J.J. and Parkes, C.O. (1982) Calcium-binding protein distribution in the rat brain. Brain Res. **239,** 519-525.

3. Braun, K., Scheich, H., Schachner, M. and Heizmann, C.W. (1985) Distribution of parvalbumin, cytochrome oxidase activity and ^{14}C-2- deoxyglucose uptake in the brain of the zebra finch. I. Auditory and vocal motor system. Cell Tissue Res. **240,** 101-115.

4. Braun, K., Scheich, H., Schachner, M. and Heizmann, C.W. (1985) Distribution of parvalbumin, cytochrome oxidase activity and ^{14}C-2- deoxyglucose uptake in the brain of the zebra finch. II. Visual system. Cell Tissue Res. **240,** 117-127.

5. Buchan, A.M.J. and Baimbridge, K.G. (1988) Distribution and co- localization of calbindin D_{28K} with VIP and neuropeptide Y but not somatostatin, galanin and substance P in the enteric nervous system of the rat. Peptides **9,** 333-338.

6. Carr, P.A., Yamamoto, T., Karmy, G., Baimbridge, K.G. and Nagy, J.I. (1989) Parvalbumin is highly colocalized with calbindin D28k and rarely with calcitonin-gene related peptide in dorsal root ganglia neurons of rat. Brain Res. **497,** 163-170.

7. Carr, P.A., Yamamoto, T., Staines, W.A., Whittaker, M.E. and Nagy, J.I. (1989)

Quantitative histochemical analysis of cytochrome oxidase in rat dorsal root ganglia and colocalization with carbonic anhydrase. Neuroscience **33,** 351-362.

8. Celio, M.R. and Heizmann, C.W. (1981) Calcium-binding protein parvalbumin as a neuronal marker. Nature **293,** 300-302.

9. Celio, M.R. (1986) Parvalbumin in most gamma-amino-butyric acid-containing neurons of the rat cerebral cortex. Science **231,** 995-997.

10. Coulson, R.A. and Herbert, J.D. (1984) A role for carbonic anhydrase in intermediary metabolism. In: Biology and Chemistry of the Carbonic Anhydrases, (R.E. Tashian and D. Hewett-Emmett eds.) Vol. 429, Annals New York Academy Sciences, New York, N.Y., pp. 505-515.

11. Deutsch, H.F. (1987) Carbonic anhydrases. Int. J. Biochem. **19,** 101-113.

12. Fedulova, S.A., Kostyuk, P.G. and Veselovsky, N.S. (1981) Calcium channels in the somatic membrane of the rat dorsal ganglion, effects of cAMP. Brain Res. **214,** 210-214.

13. Garcia-Segura, L.M., Baetens, D., Roth, J., Norman, A.W. and Orci, L. (1984) Immunohistochemical mapping of calcium-binding protein immunoreactivity in the rat central nervous system. Brain Res. **296,** 75-86.

14. Heizmann, C.W. (1984) Parvalbumin, an intracellular calcium-binding protein; distribution, properties and possible roles in mammalian cells. Experientia **40,** 910-921.

15. Heizmann, C.W. and Berchtold, M.W. (1987) Expression of parvalbumin and other CA^{2+}-binding proteins in normal and tumor cells: a topical review. Cell Calcium **8,** 1-41.

16. Jande, S.S., Maler, L. and Lawson, D.E.M. (1981) Immunohistochemical mapping of vitamin D-dependent calcium-binding protein in brain. Nature **294,** 765-767.

17. Kazimierczak, J., Sommer, E.W., Philippe, E. and Droz, B. (1986) Carbonic anhydrase activity in primary sensory neurons. I. Requirements for the cytochemical localization in the dorsal root ganglion of chicken and mouse by light and electron microscopy. Cell Tissue Res. **245,** 487-495.

18. Kosaka, T., Katsumaru, H., Hama, K., Wu, J.-Y. and Heizmann, C.W. (1987) GABAergic neurons containing the Ca^{2+}-binding protein parvalbumin in the rat hippocampus and dentate gyrus. Brain Res. **419,** 119-130.

19. Landowne, D. and Ritchie, J.M. (1971) On the control of glycogenolysis in mammalian nervous tissue by calcium. J. Physiol. (Lond.) **212,** 503-517.

20. Lonnerholm, G. (1984) Histochemical localization of carbonic anhydrase in mammalian tissue[a]. In: Biology and Chemistry of the Carbonic Anhydrases, (R.E. Tashian and D. Hewett-Emmett eds.) Vol. 429, Annals New York Academy Sciences, New York, N.Y., pp. 369-381.

21. Mithani, S., Atmadja, S., Baimbridge, K.G. and Fibiger, H.C. (1987) Neuroleptic-induced oral dyokinesias: effects of progabide and lack of correlation with regional

changes in glutamic acid decarboxylase and choline acetyltransferase activities. Psychopharmacology **93,** 94-100.

22. Moody, W. Jr. (1984) Effects of intracellular H^+ on the electrical properties of excitable cells. Ann. Rev. Neurosci. **7,** 257-78.

23. Neering, I.R. and McBurney, R.W. (1984) Role for microsomal calcium storage in mammalian neurones. Nature **309,** 158-160.

24. Parkes, C.O., Thomasset, M., Baimbridge, K.G. and Henin, E. (1984) Tissue distribution of human calcium-binding protein (28000 g mol^{-1}). Eur. J. Clin. Invest. **14,** 181-183.

25. Peyronnard, J.M., Charron, L., Lavoie, J., Messier, J.P. and Dubreuil, M. (1988a) Carbonic anhydrase and horseradish peroxidase: double labelling of rat dorsal root ganglion neurons innervating motor and sensory peripheral nerves. Anat. Embryol. **177,** 353-359.

26. Peyronnard, J.M., Charron, L.F., Messier, J.P. and Lavoie, J. (1988b) Differential effects of distal and proximal nerve lesions on carbonic anhydrase activity in rat primary sensory neurons, ventral and dorsal root axons. Exp. Brain Res. **70,** 550-560.

27. Philippe, E. and Droz, B. (1988) Calbindin D-28k-immunoreactive neurons in chick dorsal root ganglion: ontogenesis and cytological characteristics of the immunoreactive sensory neurons. Neuroscience **26,** 215-224.

28. Riley, D.A., Ellis, S. and Bain, J.L.W. (1984) Ultrastructural cytochemical

localization of carbonic anhydrase activity in rat peripheral sensory and motor nerves, dorsal root ganglia and dorsal column nuclei. Neuroscience **13,** 189-206.

29. Rose, R.D., Koerber, H.R., Sedivec, M.J. and Mendell, L.M. (1986) Somal action potential duration differs in identified primary afferents. Neurosci. Lett. **63,** 259-264.

30. Salt, T.E. and Hill, R.G. (1983) Neurotransmitter candidates of somatosensory primary afferent fibres. Neuroscience **10,** 1083-1103.

31. Sapirstein, V.S. (1984) Properties and function of brain carbonic anhydrase. In: Biology and Chemistry of the Carbonic Anhydrases (R.E. Tashian and D. Hewett-Emmett eds.) Vol. 429, Annals New York Academy Sciences, New York, N.Y., pp. 481-493.

32. Sommer, E.W., Kazimierczak, J. and Droz, B. (1985) Neuronal subpopulations in the dorsal root ganglion of the mouse as characterized by combination of ultrastructural and cytochemical features. Brain Res. **346,** 310-326.

33. Stichel, C.C., Singer, W. and Heizmann, C.W. (1988) Light and electron microscopic immunocytochemical localization of parvalbumin in the dorsal lateral geniculate nucleus of the cat: evidence for coexistence with GABA. J. Comp. Neurol. **268,** 29-37.

34. Sugai, N. and Ito, S. (1980) Carbonic anhydrase, ultrastructural localization in the mouse gastric mucosa and improvements in the technique. J. Histochem. Cytochem. **28,** 511-525.

35. Swenson, E.R. (1984) The respiratory aspects of carbonic anhydrase. In: Biology and Chemistry of the Carbonic Anhydrases (R.E. Tashian and D. Hewett-Emmett eds.) Vol. 429, Annals New York Academy Sciences, New York, N.Y., pp. 547-560.

36. Valnes, K. and Brandtzaeg, P. (1985) Retardation of immunofluorescence fading during microscopy. J. Histochem. Cytochem. **33,** 755-761.

37. Wasserman, R.H. (1985) Nomenclature of the vitamin D-induced calcium binding proteins. In: Vitamin D, (A.W. Norman et al. eds.) Berlin:DeGruyter, pp. 321-323.

38. Wong, V., Barrett, C.P., Donati, E.J., Eng, L.F. and Guth, L. (1983) Carbonic anhydrase activity in first-order sensory neurons of the rat. J. Histochem. Cytochem. **31,** 293-300.

39. Wong, V., Barrett, C.P., Donati, E.J. and Guth, L. (1987) Distribution of carbonic anhydrase activity in neurons of the rat. J. Comp. Neurol. **257,** 122-129.

40. Wong-Riley, M. (1979) Changes in the visual system of monocularly sutured or enucleated cats demonstrable with cytochrome oxidase histochemistry. Brain Res. **171,** 11-28.

41. Wong-Riley, M.T.T. and Welt, C. (1980) Histochemical changes in cytochrome oxidase of cortical barrels following vibrissal removal in neonatal and adult mice. Proc. Natl. Acads. Sci. U.S.A. **77,** 2333-2337.

42. Wong-Riley, M. and Riley, D.A. (1983) The effects of impulse blockage on cytochrome oxidase activity in the cat visual system. Brain Res. **261,** 185- 193.

43. Wong-Riley, M.T.T. and Kageyama, G.H. (1986) Localization of cytochrome oxidase in the mammalian spinal cord and dorsal root ganglia, with quantitative analysis of ventral horn cells in monkeys. J. Comp. Neurol. **245,** 41-61.

44. Yoshida, S., Matsuda, Y. and Samejima, A. (1978) Tetrodotoxin-resistant sodium and calcium components of action potentials in dorsal root ganglion cells of the adult mouse. J. Neurophysiol. **41,** 1096-1106.

45. Yoshida, S. and Matsuda, Y. (1979) Studies on sensory neurons of the mouse with intracellular-recording and horseradish peroxidase-injection techniques. J. Neurophysiol. **42,** 1134-1145.

46. Zamboni, L. and DeMartino, C. (1967) Buffered picric-acid formaldehyde: a new rapid fixative for electron microscopy. J. Cell Biol. **35,** 148A.

FIGURE LEGENDS

Figure 1. Photomicrographs of sections showing the relationship between the CaBP content and CO activity of neurons in lumbar DRG. (A,B) Adjacent sections stained immunohistochemically for CaBP by immunoperoxidase (A) or histochemically for CO (B). (C,D) Photomicrographs of the same section stained for CaBP by immunofluorescence (C), photographed, and then stained histochemically for CO (D). Arrows in each pair of micrographs indicate examples of corresponding cells. Note the CO staining density in CaBP-IR neurons. A and B depict sections from para-picric fixed tissue, and C,D depicts a section from para-picric-glu fixed tissue. Magnifications: (A,B) X 110; (B,C) X 150.

Figure 2. Photomicrographs of sections showing the relationship between the PV content and CO activity of neurons in lumbar DRG. (A,B,C,D) Adjacent sections stained immunohistochemically for PV by immunoperoxidase (A,C) or histochemically for CO (B,D). (A) corresponds to (B) and (C) with (D). Note the CO staining density in both large and small PV-IR neurons indicated by arrows in corresponding sections. (E,F) are the same section and (G,H) are the same section stained for PV by immunofluorescence (E,G), photographed, and stained histochemically for CO (F,H). (E,F) and (G,H) depict sections from para-picric or para-picric-glu fixed tissue, respectively. Note the CO staining density in PV-IR neurons indicated by arrows in corresponding sections. Magnifications: (A,B) X 120; (C,D) X 180; (E,F) X 145; (G,H) X 150.

Figure 3. Photomicrographs of sections showing the relationship between the PV or CaBP content and CA activity of neurons in lumbar DRG. (A,B) Adjacent sections stained immunohistochemically for CaBP by immunoperoxidase (A) or histochemically for CA (B). (C,D) are the same section and (E,F) are the same section stained for CaBP (C) or PV (E) by immunofluorescence, photographed and then stained histochemically for CA (D,F). Note that most, though not all, CaBP-IR and PV-IR neurons are CA-positive. Immunopositive and CA-positive cells are indicated by arrows in corresponding micrographs. Magnifications: (A,B) X 210; (C,D) X 90; (E,F) X 75.

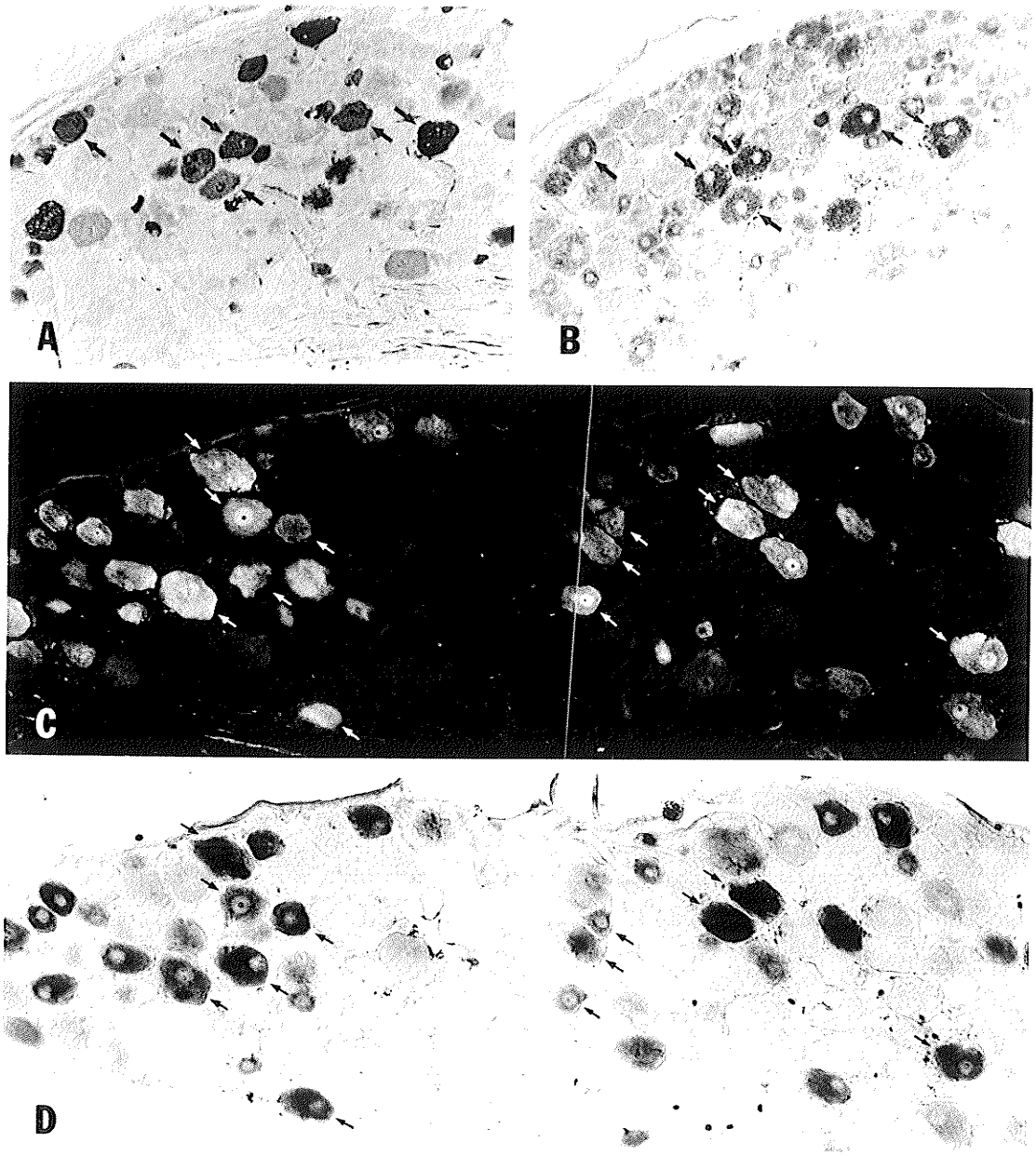

Fig. 1

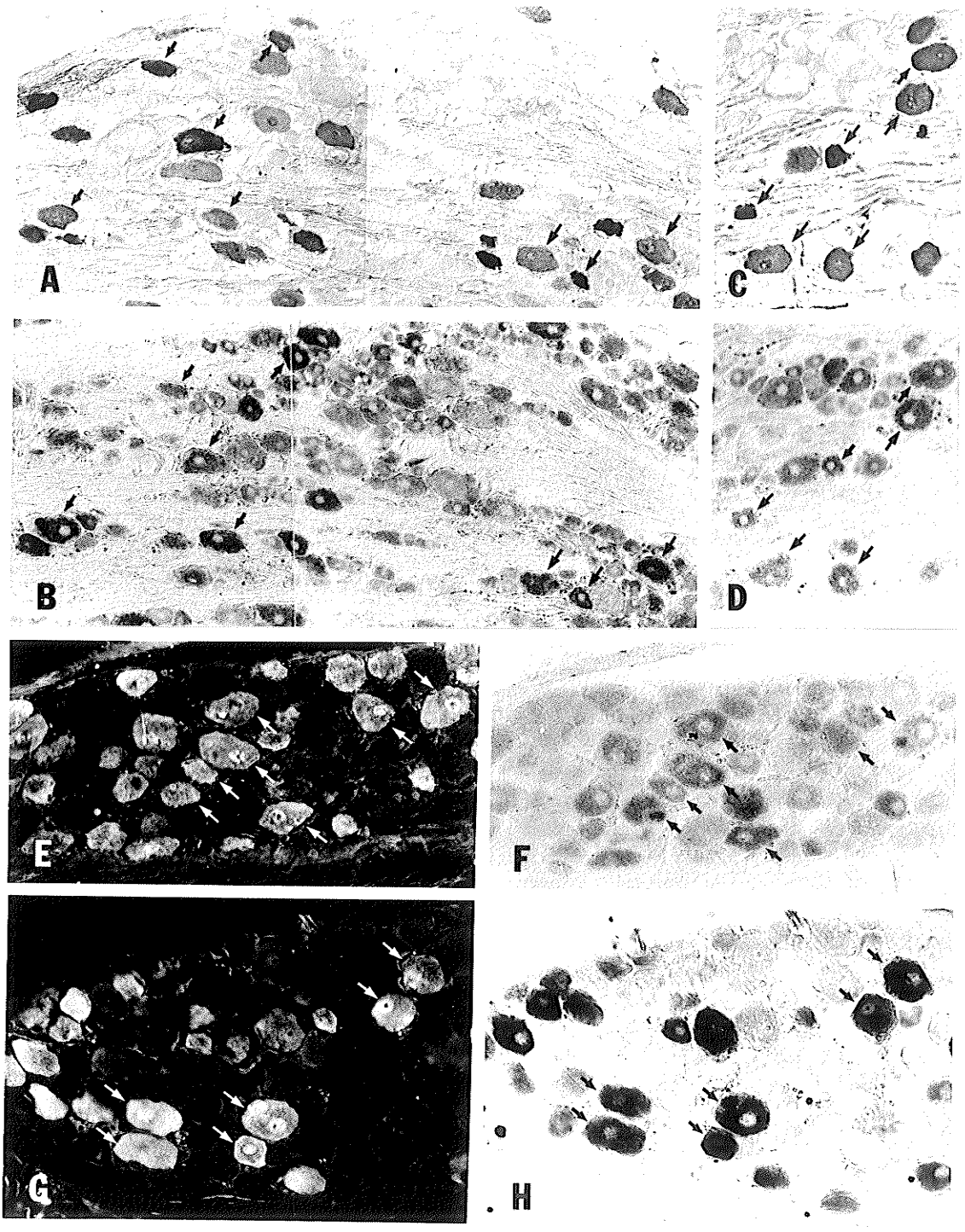

Fig. 2

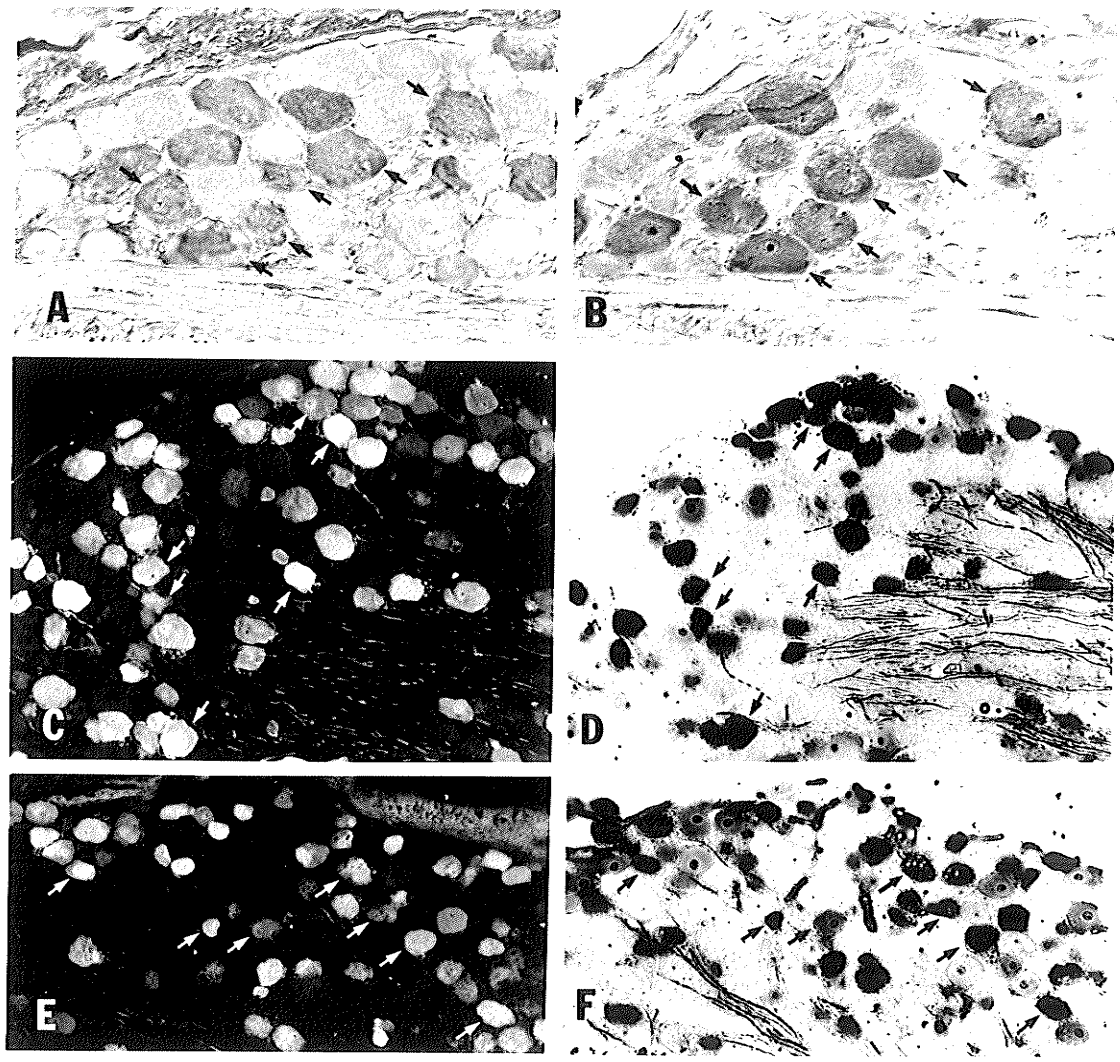

Fig. 3

Part IV

Calcitonin gene-related peptide in primary afferent neurons of rat: coexistence with fluoride-resistant acid phosphatase and depletion by neonatal capsaicin

P.A. Carr, T. Yamamoto and J.I. Nagy

Neuroscience (1990) 36; 751-760

Abstract--Immunohistochemical and histochemical techniques were used to re-examine the extent to which neonatal capsaicin treatment depletes calcitonin gene-related peptide in the dorsal horn of the spinal cord, to determine the localization of calcitonin gene-related peptide in relation to that of fluoride-resistant acid phosphatase in lumbar dorsal root ganglia, and to compare the distribution of these primary afferent markers in the dorsal horn.

A substantial depletion of calcitonin gene-related peptide was observed in the dorsal horn of adult animals treated neonatally with capsaicin suggesting that a large proportion of this peptide in the dorsal horn is contained within capsaicin-sensitive primary afferent fibers. In dorsal root ganglia 30% of all or 44% of small and medium sized calcitonin gene-related peptide-immunoreactive cells were positive for fluoride-resistant acid phosphatase. Conversely, 50% of cells positive for the phosphatase enzyme also displayed immunoreactivity for the peptide. In lamina II of the dorsal horn calcitonin gene-related peptide and fluoride-resistant acid phosphatase were found to have an overlapping distribution. The presence of fluoride-resistant acid phosphatase in a substantial proportion of neuropeptide-containing primary sensory neurons suggests a lack of segregation of sensory neuronal populations into peptide and non-peptide containing subgroups at least on the basis of non-peptide neurons defined as those containing fluoride-resistant acid phosphatase.

The distribution of calcitonin gene-related peptide (CGRP) in both the central and peripheral nervous system has been well documented (8,10,14,16,17,19,27,30,31) considering its recent description (27). The relationship of this peptide with other cytochemical markers has been particularly well defined in the sensory ganglia and spinal cord of a number of species (8,10,11,13,14,31,33). In sensory ganglia of rat, up to 50% of all neurons contain CGRP-immunoreactivity (10,14,19) and a large proportion of these also contains substance P, somatostatin, galanin and various other peptides (5,8,9,10,13,14,18,31). In the spinal cord, CGRP-immunoreactivity in fibers that are thought to be largely of primary afferent origin are found distributed within the superficial dorsal horn in lamina I and lamina II although there also appear to be a number of CGRP-immunoreactive (CGRP-IR) fibers extending into lamina III and deeper layers (1,2,10,29,31,32,33). Despite this wealth of documentation a number of points concerning primary afferent CGRP remain uncertain.

First, variable results have been obtained concerning the degree to which neonatal capsaicin treatment depletes CGRP-IR fibers in the spinal cord dorsal horn of rat. For example, CGRP immunoreactivity following this treatment has been reported to be either significantly reduced (31), slightly diminished (5), or even increased in certain areas of the dorsal horn (11). Second, it has been suggested that primary sensory C-fiber afferents may be divided into two subgroups consisting of peptide and non-peptide-containing neurons (12). Much of the support for this notion is derived from previous demonstrations that peptides such as substance P and somatostatin are not found (23) or only found rarely (4) within nonpeptide sensory neurons represented by those containing fluoride-resistant acid phosphatase (FRAP). Although a reasonable suggestion on the basis of available data, a large number of peptides have been described and new peptides continue to be found in primary sensory neurons. Thus, analyses of coexistence possibilities have not been exhausted. Third, the populations of peptide and non-peptide

containing primary sensory neurons are proposed to have somewhat different laminar distributions in the superficial dorsal horn. For example, the localization of substance P and somatostatin in this region has been described to be different than that of FRAP (12; see however, 23). However, the results of various studies that have mapped the distribution of FRAP or peptides such as CGRP (3,10,23,26,31,33) in the superficial dorsal horn of rat suggest that the ramifications of sensory fibers containing these markers may partially overlap, although a direct comparison of the distributions of FRAP and CGRP in this region has not been conducted.

In an attempt to clarify these issues, we examined the effect of neonatal capsaicin treatment on CGRP-IR fibers in the dorsal horn and compared the localization of CGRP and FRAP in both dorsal root ganglia (DRG) neurons and the superficial dorsal horn.

METHODS

Tissue preparation

Adult, male Sprague-Dawley rats weighing 240-380 g were anesthetized with chloral hydrate and perfused transcardially with cold (4°C) 0.9% saline containing 0.1% sodium nitrite and 100 units of heparin followed by cold (4°C) freshly prepared fixative consisting of 4% paraformaldehyde and 0.16% picric acid in 0.1 M sodium phosphate buffer, pH 7.4 (34). After perfusion, the spinal cord and lumbar dorsal root ganglia were immediately removed and post- fixed for 2 or 4 hr in cold fixative. The ganglia were then stored in cold 15% sucrose with 0.001% sodium azide in 0.1 M phosphate buffer (pH 7.4) and the spinal cords in a solution of 25% sucrose and 10% glycerol in 50 mM phosphate buffer (pH 7.4) for at least 2 days. Transverse and horizontal sections of the lumbar enlargement of the spinal cord were cut on a sliding microtome at a thickness of 20 μm and collected into cold 0.9% saline in 0.1 M phosphate buffer (pH 7.4) (PBS).

Sections of the fourth lumbar dorsal root ganglia were cut on a cryostat (Leitz) at a thickness of 15 μm and thaw-mounted onto gelatinized slides. Sections of spinal cord were also obtained from similarly prepared tissues of 12-13 week old adult rats that had been injected neonatally with either capsaicin or vehicle as described elsewhere (20,22). In brief, 48 hours after birth three male rats from the same litter received a single subcutaneous injection of capsaicin (50 mg/kg) in 10% ethanol, 10% Tween-80 and 0.9% sterile saline. Three control littermates received equal volumes of vehicle. The effectiveness of this treatment was confirmed in similarly treated littermates that showed a greater than 65% reduction in the number of FRAP-containing neurons in the DRG.

To determine the effect of neonatal capsaicin on the distribution of CGRP-IR fibers in the spinal cord, tissue from both capsaicin and vehicle-injected animals were processed by the peroxidase anti-peroxidase method. The relationship of CGRP to FRAP in both DRG and the spinal cord was examined using tissue processed sequentially first for CGRP-immunofluorescence and then for FRAP histochemistry. Following the immunofluorescence reaction, sequentially processed sections were coverslipped with 1-5% sucrose in 20 mM Tris-maleate buffer (pH 5.0). The tissue was then photographed, the coverslips removed, and the slides washed for 14-18 hr in cold (4°C) Tris-maleate buffer (pH 5.0). The sections were then reacted for FRAP histochemistry as described below, coverslipped with glycerol-water (3:1) and rephotographed. In some instances, CGRP-immunofluorescence as well as FRAP histochemical reaction product in spinal cord sections was photographed after completion of FRAP histochemistry.

Immunohistochemical techniques

All sections were incubated with rabbit antiserum to CGRP (Peninsula) at a dilution of either 1:1000 or 1:2000 in 0.1 M phosphate buffer containing 0.9% saline, 0.3%

Triton X-100 and 1% bovine serum albumin (PBS-T/BSA) for 40-68 hr at 4°C. The sections were then washed for 40 min in two changes of PBS, either with 0.3% Triton X-100 (PBS-T) for peroxidase reacted sections or without Triton X-100 for immunofluorescence reacted sections which were subsequently taken for FRAP histochemistry. Sections to be reacted by immunofluorescence were incubated with Texas Red conjugated donkey anti-rabbit IgG (Amersham) (1:50) in PBS for 1.5 hr at room temperature followed by two 45 min washes in PBS. The sections were then coverslipped, photographed and prepared for FRAP histochemistry as described above. Sections reacted by the peroxidase anti- peroxidase method were incubated in goat anti-rabbit IgG (Sternberger-Meyer) diluted 1:20 in PBS-T/BSA, washed for 40 min in two changes of PBS-T and then incubated in rabbit PAP (1:100) (Sternberger-Meyer) in PBS-T/BSA. The sections were then washed for 20 min in PBS-T and a further 20 min in 50 mM Tris-HCl buffer (pH 7.4) after which they were reacted for the visualization of peroxidase activity using 0.02% diaminobenzidine and 0.005% hydrogen peroxide in 50 mM Tris-HCl buffer. All peroxidase reacted tissue was mounted on slides, and then dehydrated in alcohol, cleared in xylene and coverslipped with Lipshaw mounting medium.

Fluoride-resistant acid phosphatase

Histochemical detection of FRAP was conducted according to a modification of methods previously described (20,23). Following an overnight wash in cold 20 mM Tris-maleate buffer (pH 5.0), the tissue was incubated for 14-18 hr at room temperature in 20 mM Tris-maleate buffer (pH 5.0) containing 12 mM sodium glycerophosphate, 1.5 mM lead nitrate and 0.5 mM sodium fluoride. Sections were then quickly rinsed in distilled water, incubated for 30 sec in 2% ammonium sulfide, again rinsed in water, and then coverslipped with glycerol-water (3:1) and photographed.

RESULTS

Capsaicin treatment

The appearance of CGRP immunohistochemical staining in spinal cord sections from vehicle- and capsaicin-injected animals is shown in Figures 1 and 2. In transverse sections of the lumbar spinal cord from control animals (Fig. 1A), CGRP-IR fibers were concentrated in Lissauer's tract and in lamina I and II of the dorsal horn with individual or conglomerates of several short stretches of fibers extending into the dorsal portion of lamina III. Fine CGRP-IR fibers were also observed throughout the remainder of the dorsal horn. More prominent in many but not all sections were CGRP-stained fiber bundles seen traversing lamina III, IV and V with some extending in a ventromedial orientation toward lamina X. Densely stained collections of fibers were occasionally observed in the dorsolateral funiculus while lightly stained fibers of a smaller calibre were often visible in the dorsolateral portion of the dorsal column adjacent to the dorsal horn. When seen individually most of the CGRP-IR elements in the dorsal horn were varicose, moderately stained fibers interspersed with an abundance of immunoreactive puncta. Some of the larger more densely stained fibers tended to exhibit a homogeneous non-varicose staining pattern. The appearance of CGRP-immunoreactivity in transverse sections from capsaicin-treated animals (Fig. 1B) is noticeably different from that seen in control tissue. There was a substantial reduction in the density of staining for CGRP throughout the dorsal horn with the greatest change occurring in the mid to ventral portion of lamina II and the whole of lamina III. A band of dense staining remained in lamina I and the most dorsal portion of lamina II although the number of fibers within, and staining density of, the band was considerably reduced. Immunoreactive fibers in the dorsolateral funiculus were almost totally depleted as were the majority of lightly stained fibers in the more ventral portions of the dorsal horn. The CGRP-IR fiber bundles traversing lamina III, IV and V were also absent in many, but not all sections; where present, their numbers were reduced.

The effect of neonatal capsaicin treatment on CGRP immunoreactivity is most evident in horizontal sections through superficial layers of the dorsal horn (Fig. 2). Just superficial to and possibly within lamina I in sections from control animals (Fig. 2A), an extensive and densely stained plexus of CGRP-IR fibers was observed traversing mediolaterally or rostrocaudally and in many cases appeared to be connected with rostrocaudally oriented fibers in Lissauer's tract and those in the superficial portion of lamina II. After capsaicin treatment, the largest of the CGRP-IR fiber plexi were no longer present and the number of rostrocaudally oriented fibers in Lissauer's tract was greatly decreased (Fig. 2B). The remaining CGRP-IR fibers were seen individually or in disorganized clusters displaying tortuous configurations. In horizontal sections through lamina II of control tissue (Fig. 2C), densely stained varicose fibers having largely a rostrocaudal orientation predominated. After capsaicin treatment these fibers were almost totally absent (Fig. 2D) leaving a disorganized arrangement of CGRP-IR fibers similar to that seen in lamina I of treated animals. The staining that persisted was localized to individual puncta or to varicose or non-varicose fibers.

CGRP-FRAP colocalization

The localization of CGRP in relation to that of FRAP in DRG neurons is shown in Figure 3. In sections stained for CGRP (Fig. 3A) large numbers of cells demonstrated either homogeneous cytoplasmic staining or punctate immunofluorescence which is generally considered to be associated with the Golgi apparatus. These staining patterns varied in intensity from light to very brilliant. From estimates of the size of the CGRP-positive cells based on visual comparisons with FRAP-containing neurons known to be of the small type B category, it was determined that approximately 68% of the CGRP-IR neurons were of approximately the same size as FRAP containing cells. This is in

agreement with previous findings that 70% of CGRP- and all FRAP-positive cells have sizes within the range of type B cells (14). However, in view of uncertainties regarding the classification of intermediate size cells as type A or type B, it can not be concluded that this percentage of CGRP-positive cells represents exclusively the type B cell population. Thus we refer to this population of CGRP-positive cells (68%) as small or medium size cells without implying cell type. In the same section subsequently processed for FRAP histochemistry, many small cells containing FRAP (Fig. 3B) exhibited a dense cytoplasmic reaction product while most unreacted cells displayed minimal background staining. In some cases variability in the quality of FRAP histochemistry was evident between sections and between animals. However, cell counts indicated that the intensity of staining, rather than the number of cells judged to be positive, was most affected by a poorer reaction. Analysis of pairs of micrographs of the same sections processed for CGRP and FRAP revealed that 50% of 1672 FRAP-positive cells counted were immunoreactive for CGRP. From a count of 2812 CGRP-positive cells, 30% contained FRAP reaction product. Using the proportion of small and medium CGRP cells that had been estimated to be approximately 68%, it was calculated that 44% of these were also stained for FRAP. When the results from four animals were examined separately it was found that the percentage of FRAP-positive cells displaying CGRP ranged from 36-71% and the percentage of CGRP-positive cells containing FRAP ranged from 26-33%. These variations between animals were likely due to the quality of CGRP- and FRAP-staining rather than differences inherent in the animals since in tissues exhibiting a high quality reaction the values obtained for the percentage of FRAP-positive cells containing CGRP (55%) correspond closely to the overall average (50%).

The distribution of CGRP and FRAP positive fibers in the superficial dorsal horn is shown in Figure 4. In figure 4A and 4B, CGRP immunofluorescence (Fig. 4A) was photographed before the section was reacted for FRAP histochemistry (Fig. 4B). Visual

inspection of these micrographs indicates that CGRP and FRAP staining overlap. This is better illustrated in Figure 4C and D where the same fields within these micrographs are closely opposed to allow comparison of localization. The higher magnification micrographs shown in Figure 4E to H are similar to those in Figure 4A to D except that the section was photographed after it had been stained for both CGRP and FRAP. In both these sets of micrographs it can be seen that the FRAP staining overlaps with the most ventrally located CGRP immunofluorescence. The density of CGRP-immunoreactivity in the region of overlap, however, was obviously lower than that seen dorsal to the layer of FRAP staining. From comparisons of micrographs where CGRP was photographed before or after completion of the FRAP reaction, we were unable to estimate the degree to which CGRP-immunofluorescence may have been obscured by the FRAP reaction product in the regions where they overlapped.

Technical points

Certain procedures were determined to be necessary to allow sequential processing of DRG and cord sections first for CGRP immunofluorescence and then for FRAP histochemistry. Following the immunofluorescent reaction it was found that coverslipping with anti-fade medium or glycerol substantially reduced the FRAP reaction. This difficulty was circumvented by coverslipping with 1-5% sucrose in 20 mM Tris-maleate buffer (pH 5.0). However, the absence of an anti-fade agent in the coverslipping medium necessitated the use of a second antibody conjugated fluorochrome that undergoes minimal quenching during photography. Texas Red was found to be suitable in this respect. Despite collection of ganglion sections on gelatinized slides, some sections coverslipped with the Tris-sucrose medium adhered and remained attached to the coverslip upon coverslip removal. This did not effect the FRAP reaction and it did not preclude photography of the same ganglion fields as were previously

photographed for CGRP immunofluorescence. An overnight wash in cold 20 mM Tris-maleate buffer (pH 5.0) after tissues had been processed for CGRP immunofluorescence was found to increase the intensity of the FRAP reaction compared with that seen in tissue washed for shorter times.

DISCUSSION

Widely disparate results regarding the effects of neonatal capsaicin on CGRP in the dorsal horn of the spinal cord as determined by immunohistochemical staining or radioimmunoassay (5,11,31) were obtained from rats injected with similar doses of capsaicin. The present qualitative study, which employed the same capsaicin dosage as used in these earlier reports, demonstrates that there is a substantially lower density of CGRP-IR elements in the dorsal horn of capsaicin-treated compared with control animals. In this regard, our data agrees with the report of Skofitsch and Jacobowitz (31). The reasons for the differences between our results and those of some others is not clear although strain of animals used and their age after capsaicin treatment may have been contributing factors in some cases. With respect to the CGRP-IR fibers remaining in the dorsal horn following neonatal capsaicin treatment, previous findings that the dosage of capsaicin treatment used here caused up to 90% depletion of unmyelinated primary afferent fibers in dorsal roots with a minimal effect on myelinated afferents (22,24) coupled with observations that virtually all CGRP in the dorsal horn of the spinal cord is of primary afferent origin (2,10) suggest that the remaining CGRP is localized to the central termination of myelinated primary afferent fibers. Such fibers appear to be concentrated in lamina I, the dorsal portion of lamina II, and in fiber bundles penetrating to deeper layers. However, we can only tentatively conclude that this represents the distribution of CGRP-positive myelinated afferents in normal animals since an anatomical rearrangement (21,25) or an altered production of CGRP in fibers surviving

neonatal capsaicin treatment cannot be excluded.

The occurrence of CGRP in DRG and its colocalization with various other peptides has been previously described in a number of species (8,10,13,14,18,31). In rabbit DRG, the localization of CGRP in relation to FRAP has also been examined and these have been determined to be present largely in separate neurons (28). Although a detailed study of the relationship between CGRP and FRAP has not been reported in rat, the lack of coexistence of FRAP with this widely occurring peptide in sensory neurons would strengthen the postulated classification of primary afferents into peptide and non-peptide subgroups as may be represented by CGRP and FRAP, respectively (12). This classification system was based largely on earlier observations that DRG neuronal populations containing FRAP are separate from those containing substance P or somatostatin (4,23) and that substance P- and FRAP-containing primary afferents have somewhat different distributions in the dorsal horn (23). However, FRAP has been observed to coexist almost entirely with another peptide found in DRG, namely, arginine vasopressin (15). In addition, there are some indications that there may be a very small degree of coexistence between FRAP and substance P (4,6). With regard to FRAP and CGRP, some possibility for their coexistence is provided by estimates that FRAP is contained within up to 70% of small DRG neurons (6,7,15,28) and CGRP within approximately 50% of all small cells (14). Moreover, it has been suggested that FRAP and CGRP may coexist in primary sensory fibers of the greater splanchnic nerve (19) and in both rabbit and rat lumbar DRG the occasional cell containing both FRAP and CGRP has been previously observed (28,29). Our results show that there is indeed a substantial population of primary afferent neurons that contain both a peptide (CGRP) and FRAP. Staining for FRAP was observed in 30% of CGRP positive neurons (44% of CGRP-positive small and medium size neurons) while 50% of the neurons containing FRAP displayed CGRP immunoreactivity. If the previous estimate that 50% of all small and

medium DRG cells contain CGRP (14) is applicable to our data, then 22% of all small and medium cells in lumbar DRG contain both CGRP and FRAP.

Our finding that CGRP and FRAP have an overlapping distribution in the dorsal horn is consistent with their colocalization in DRG particularly since both of these markers within the dorsal horn are thought to be contained entirely within primary afferents. Further support for the suggestion that FRAP staining is totally encompassed within the CGRP-IR layer in the dorsal horn is provided by observations that FRAP is present within the intermediate third of lamina II (3,23,26) and CGRP-immunoreactivity within lamina I, II (19,31,33) and the superficial portion of lamina III (10). Our results suggest that there are not two wholly separate subclasses of peptide and non-peptide primary afferent neurons at least on the basis of non-peptide neurons defined as those containing FRAP. Inasmuch as FRAP, SP and somatostatin are present within largely separate populations of DRG neurons (23) and SP has been found in many CGRP-positive DRG cells (8,10,14,18,31,33), our results further suggest the existence of three largely separate populations of primary sensory DRG neurons, namely, those which contain either CGRP plus FRAP, CGRP plus SP, or CGRP plus somatostatin. The relationship of these populations to the transmission of sensory modalities and the peripheral effector functions of sensory neurons remains to be determined.

REFERENCES

1. Carlton, S.M., McNeill, D.L., Chung, K. and Coggeshall, R.E. (1987) A light and electron microscopic level analysis of calcitonin gene-related peptide (CGRP) in the spinal cord of the primate: an immunohistochemical study. Neurosci. Lett. **82,** 145-150.

2. Chung, K., Lee, W.T. and Carlton, S.M. (1988) The effects of dorsal rhizotomy and spinal cord isolation on calcitonin gene-related peptide-labeled terminals in the rat lumbar dorsal horn. Neurosci. Lett. **90,** 27-32.

3. Coimbra, A., Sodre-Borges, B.P. and Magalhaes, M.M. (1974) The substantia gelatinosa Rolandi of the rat. Fine structure, cytochemistry (acid phosphatase), and changes after dorsal root section. J. Neurocytol. **3,** 199-217.

4. Dalsgaard, C.-J., Ygge, J., Vincent, S.R., Ohrling, M., Dockray, G.J. and Elde, R. (1984) Peripheral projections and neuropeptide coexistence in a subpopulation of fluoride-resistant acid phosphatase reactive spinal primary sensory neurons. Neurosci. Lett. **51,** 139-144.

5. Diez Guerra, F.J., Zaidi, M., Bevis, P., MacIntyre, I. and Emson, P.C. (1988) Evidence for release of calcitonin gene-related peptide and neurokinin A from sensory nerve endings in vivo. Neuroscience **25,** 839-846.

6. Dodd, J., Jahr, C.E., Hamilton, P.N., Heath, M.J.S., Matthew, W.D. and Jessell, T.M. (1983) Cytochemical and physiological properties of sensory and dorsal horn neurones that transmit cutaneous sensation. Cold Spring Harb. Symp. Quant. Biol.

48, 685-695.

7. Dodd, J., Jahr, C.E. and Jessell, T.M. (1984) Neurotransmitters and neuronal markers at sensory synapses in the dorsal horn. In Advances in Pain Research and Therapy, Vol. 6 (eds Kruger L. and Liebeskind J.C.), pp. 105-121. Raven Press, New York.

8. Franco-Cereceda, A., Henke, H., Lundberg, J.M., Petermann, J.B., Hokfelt, T. and Fischer, J.A. (1987) Calcitonin gene-related peptide (CGRP) in capsaicin-sensitive substance P-immunoreactive sensory neurons in animals and man: distribution and release by capsaicin. Peptides **8,** 399-410.

9. Gazelius, B., Edwall, B., Olgart, L., Lundberg, J.M., Hokfelt, T. and Fischer, J.A. (1987) Vasodilatory effects and coexistence of calcitonin gene-related peptide (CGRP) and substance P in sensory nerves of cat dental pulp. Acta Physiol. Scand. **130,** 33-40.

10. Gibson, S.J., Polak, J.M., Bloom, S.R., Sabate, I.M., Mulderry, P.M., Ghatei, M.A., McGregor, G.P., Morrison, J.F.B., Kelly, J.S., Evans, R.M. and Rosenfeld, M.G. (1984) Calcitonin gene-related peptide immunoreactivity in the spinal cord of man and of eight other species. J. Neurosci. **4,** 3101-3111.

11. Hammond, D.L. and Ruda, M.A. (1989) Developmental alterations in thermal nociceptive threshold and the distribution of immunoreactive calcitonin gene-related peptide and substance P after neonatal administration of capsaicin in the rat. Neurosci. Lett. **97,** 57-62.

12. Hunt, S.P. and Rossi, J. (1985) Peptide- and non-peptide-containing unmyelinated

primary afferents: the parallel processing of nociceptive information. Phil. Trans. R. Soc. Lond. **B308,** 283-289.

13. Ju, G., Hokfelt, T., Fischer, J.A., Frey, P., Rehfeld, J.F. and Dockray, G.J. (1986) Does cholecystokin-like immunoreactivity in rat primary sensory neurons represent calcitonin gene-related peptide? Neurosci. Lett. **68,** 305-310.

14. Ju, G., Hokfelt, T., Brodin, E., Fahrenkrug, J., Fischer, J.A., Frey, P., Elde, R. and Brown, J.C. (1987) Primary sensory neurons of the rat showing calcitonin gene-related peptide immunoreactivity and their relation to substance P-, somatostatin-, galanin-, vasoactive intestinal polypeptide- and cholecystokinin-immunoreactive ganglion cells. Cell Tissue Res. **247,** 417-431.

15. Kai-Kai, M.A., Anderton, B.H. and Keen, P. (1986) A quantitative analysis of the interrelationships between subpopulations of rat sensory neurons containing arginine vasopressin or oxytocin and those containing substance P, fluoride-resistant acid phosphatase or neurofilament protein. Neuroscience **18,** 475-486.

16. Kruger, L., Sternini, C., Brecha, N.C. and Mantyh, P.W. (1988) Distribution of calcitonin gene-related peptide immunoreactivity in relation to the rat central somatosensory projection. J. Comp. Neurol. **273,** 149-162.

17. Kruger, L., Silverman, J.D., Mantyh, P.W., Sternini, C. and Brecha, N.C. (1989) Peripheral patterns of calcitonin-gene-related peptide general somatic sensory innervation: cutaneous and deep terminations. J. Comp. Neurol. **280,** 291-302.

18. Lundberg, J.M., Franco-Cereceda, A., Hua, X., Hokfelt, T. and Fischer, J.A. (1985)

Co-existence of substance P and calcitonin gene-related peptide-like immunoreactivities in sensory nerves in relation to cardiovascular and bronchoconstrictor effects of capsaicin. European J. Pharmacol. **108,** 315-319.

19. Molander, C., Ygge, J. and Dalsgaard, C.-J. (1987) Substance P-, somatostatin- and calcitonin gene-related peptide-like immunoreactivity and fluoride resistant acid phosphatase-activity in relation to retrogradely labelled cutaneous, muscular and visceral primary sensory neurons in the rat. Neurosci. Lett. **74,** 37-42.

20. Nagy, J.I. and Daddona, P.E. (1985) Anatomical and cytochemical relationships of adenosine deaminase-containing primary afferent neurons in the rat. Neuroscience **15,** 799-813.

21. Nagy, J.I. and Hunt, S.P. (1983) The termination of primary afferents within the rat dorsal horn: Evidence for rearrangement following capsaicin treatment. J. Comp. Neurol. **218,** 145-158.

22. Nagy, J.I., Iversen, L.L., Goedert, M., Chapman, D. and Hunt, S.P. (1983) Dose-dependent effects of capsaicin on primary sensory neurons in the neonatal rat. J. Neurosci. **3,** 399-406.

23. Nagy, J.I. and Hunt, S.P. (1982) Fluoride resistant acid phosphatase-containing neurons in dorsal root ganglia are separate from those containing substance P or somatostatin. Neuroscience **7,** 89-97.

24. Nagy, J.I., Hunt, S.P., Iversen, L.L. and Emson, P.C. (1981) Biochemical and anatomical observations on the degeneration of peptide-containing primary afferent

neurons after neonatal capsaicin. Neuroscience **10,** 1923- 1934.

25. Rethelyi, M., Salim, M.Z. and Jancso, G. (1986) Altered distribution of dorsal root fibers in the rat following neonatal capsaicin treatment. Neuroscience **18,** 749-761.

26. Ribeiro-da-Silva, A., Castro-Lopes, J.M. and Coimbra, A. (1986) Distribution of glomeruli with fluoride-resistant acid phosphatase (FRAP)- containing terminals in the substantia gelatinosa of the rat. Brain Res. **377,** 323-329.

27. Rosenfeld, M.G., Mermord, J.-J., Amara, S.G., Swanson, L.W., Sawchenko, P.E., Rivier, J., Vale, W.W. and Evans, R.M. (1983) Production of a novel neuropeptide encoded by the calcitonin gene via tissue specific RNA processing. Nature **304,** 129-135.

28. Silverman, J.D. and Kruger, L. (1988a) Acid phosphatase as a selective marker for a class of small sensory ganglion cells in several mammals: spinal cord distribution, histochemical properties, and relation to fluoride-resistant acid phosphatase (FRAP) of rodents. Somatosens. Res. **5,** 219-246.

29. Silverman, J.D. and Kruger, L. (1988b) Lectin and neuropeptide labelling of separate populations of dorsal root ganglion neurons and associated "nociceptor" thin axons in rat testis and cornea whole-mount preparations. Somatosens. Res. **5,** 259-267.

30. Silverman, J.D. and Kruger, L. (1989) Calcitonin-gene-related-peptide-immunoreactive innervation of the rat head with emphasis on specialized sensory structures. J. Comp. Neurol. **280,** 303-330.

31. Skofitsch, G. and Jacobowitz, D.M. (1985) Calcitonin gene-related peptide coexists with substance P in capsaicin sensitive neurons and sensory ganglia of the rat. Peptides **6,** 747-754.

32. Takahashi, O., Traub, R.J. and Ruda, M.A. (1988) Demonstration of calcitonin gene-related peptide immunoreactive axons contacting dynorphin A (1-8) immunoreactive spinal neurons in a rat model of peripheral inflammation and hyperalgesia. Brain Res. **475,** 168-172.

33. Wiesenfeld-Hallin, Z., Hokfelt, T., Lundberg, J.M., Forssmann, W.G., Reinecke, M., Tschopp, F.A. and Fisher, J.A. (1984) Immunoreactive calcitonin gene-related peptide and substance P coexist in sensory neurons to the spinal cord and interact in spinal behavioral responses of the rat. Neurosci. Lett. **52,** 199-204.

34. Zamboni, L. and DeMartino, C. (1967) Buffered picric-acid formaldehyde: A new rapid fixative for electron microscopy. J. Cell Biol. **35,** 148A.

FIGURE LEGENDS

Figure 1. Photomicrographs showing CGRP-immunoreactivity in transverse sections of the lumbar dorsal horn from control (A) and capsaicin-treated rats (B). (A) In control material, intense staining is present within Lissauer's tract (arrowhead) and in lamina I, II and the dorsal portion of lamina III (small arrows). Bundles of fibers are seen extending ventromedially across lamina III, IV and V (large arrow) and in the dorsolateral funiculus. (B) Depletion of staining is seen throughout lamina II and the dorsolateral funiculus. Remaining superficial fibers are concentrated in a narrow band within lamina I and the outer portion of lamina II. The number of CGRP-IR fibers in the intermediate dorsal horn is also reduced. Magnifications: A,B, X 215.

Figure 2. Photomicrographs showing CGRP-IR fibers in horizontal sections through lamina I (A,B) and II (C,D) of the dorsal horn from control (A,C) and capsaicin-treated animals (B,D). Note the intensely stained fiber plexus (arrows) in lamina I of control material (A) and its absence after capsaicin treatment (B). In lamina II of the dorsal horn, the number and intensity of rostrocaudally oriented CGRP-IR fibers seen in controls (C) are largely eliminated after capsaicin treatment (D). Magnifications: A,B,C,D, X 230.

Figure 3. Photomicrographs showing CGRP-IR and FRAP-positive neurons in the same section of lumbar dorsal root ganglion. The section was stained for CGRP by immunofluorescence (A), photographed and then stained histochemically for FRAP (B). Arrows indicate examples of cells containing both CGRP and FRAP. Arrowheads indicate corresponding small cells containing either CGRP or FRAP but not both. Magnifications: A,B, X 130.

Figure 4. Photomicrographs of transverse sections through the dorsal horn of the spinal cord showing the comparative distribution of CGRP-immunoreactivity and FRAP reaction product. (A,B) The same section reacted first for CGRP by immunofluorescence (A), photographed and then stained histochemically for FRAP (B). (C,D) CGRP- and FRAP-staining in the same area of the dorsal horn indicated between the arrows in A and B. (E,F) The same section stained first for CGRP (D) and then for FRAP (E) followed by photography of both CGRP immunofluorescence and the FRAP reaction product. (G,H) CGRP- and FRAP-staining in the same area of the dorsal horn as indicated between the arrows in E and F. Note the overlap between the FRAP reaction product and the ventral portion of CGRP immunofluorescence. Magnifications: A,B,C,D, X 170; E,F,G,H, X 335.

Fig. 1

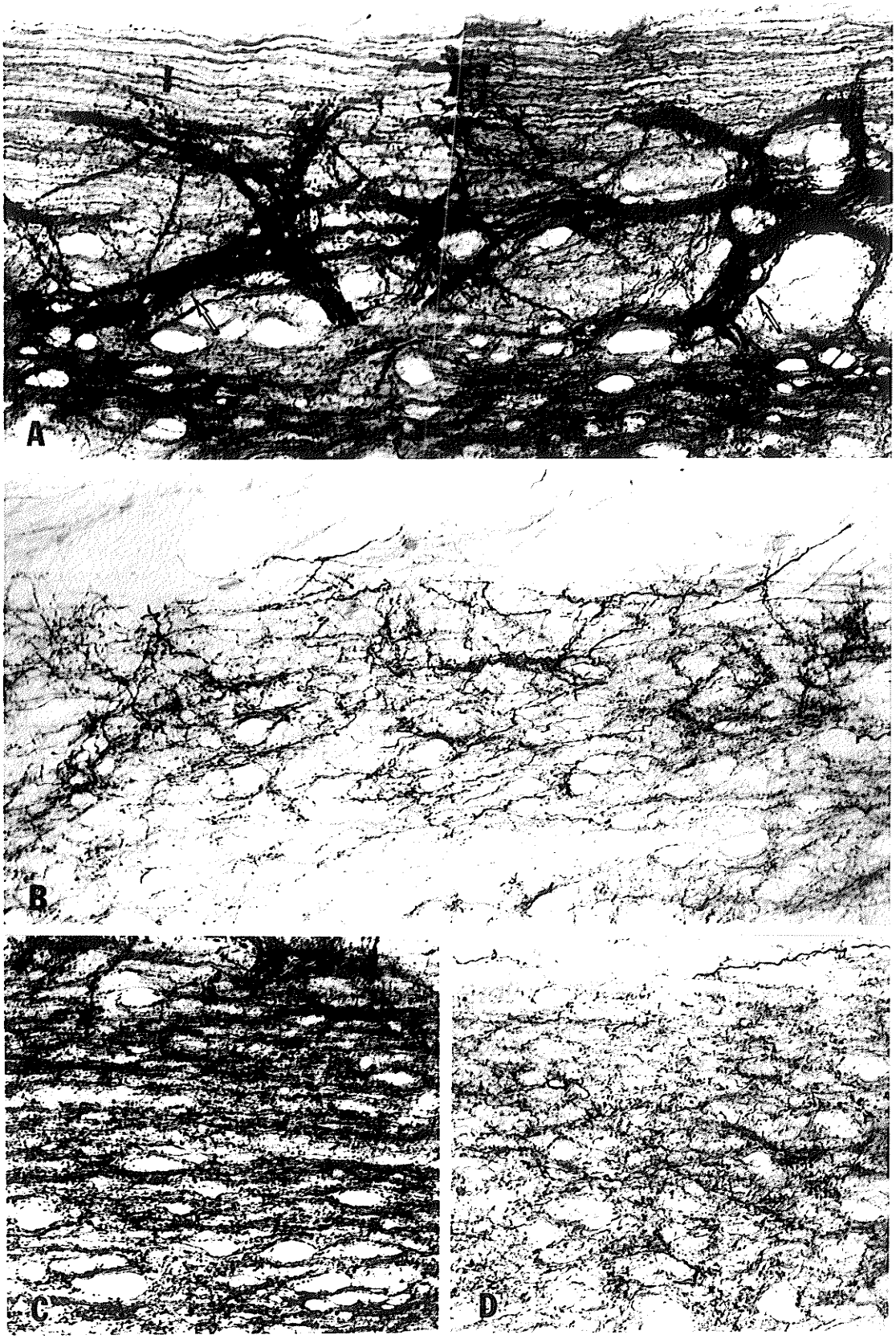

Fig. 2

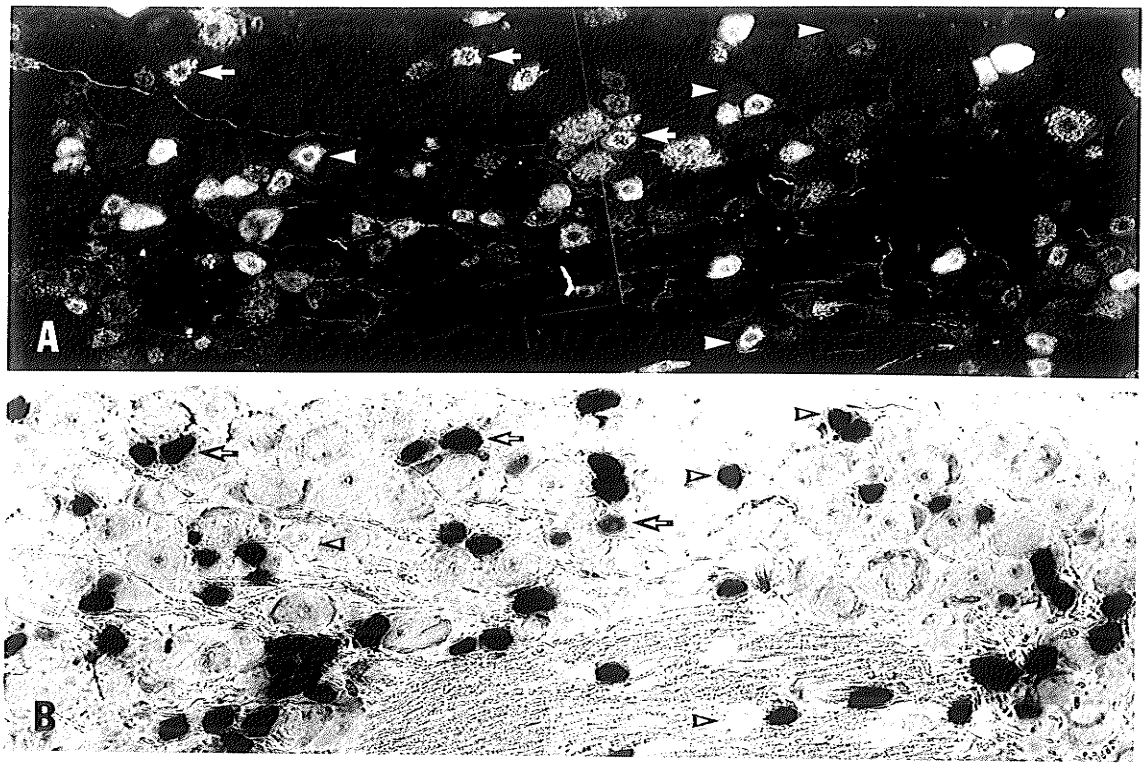

Fig. 3

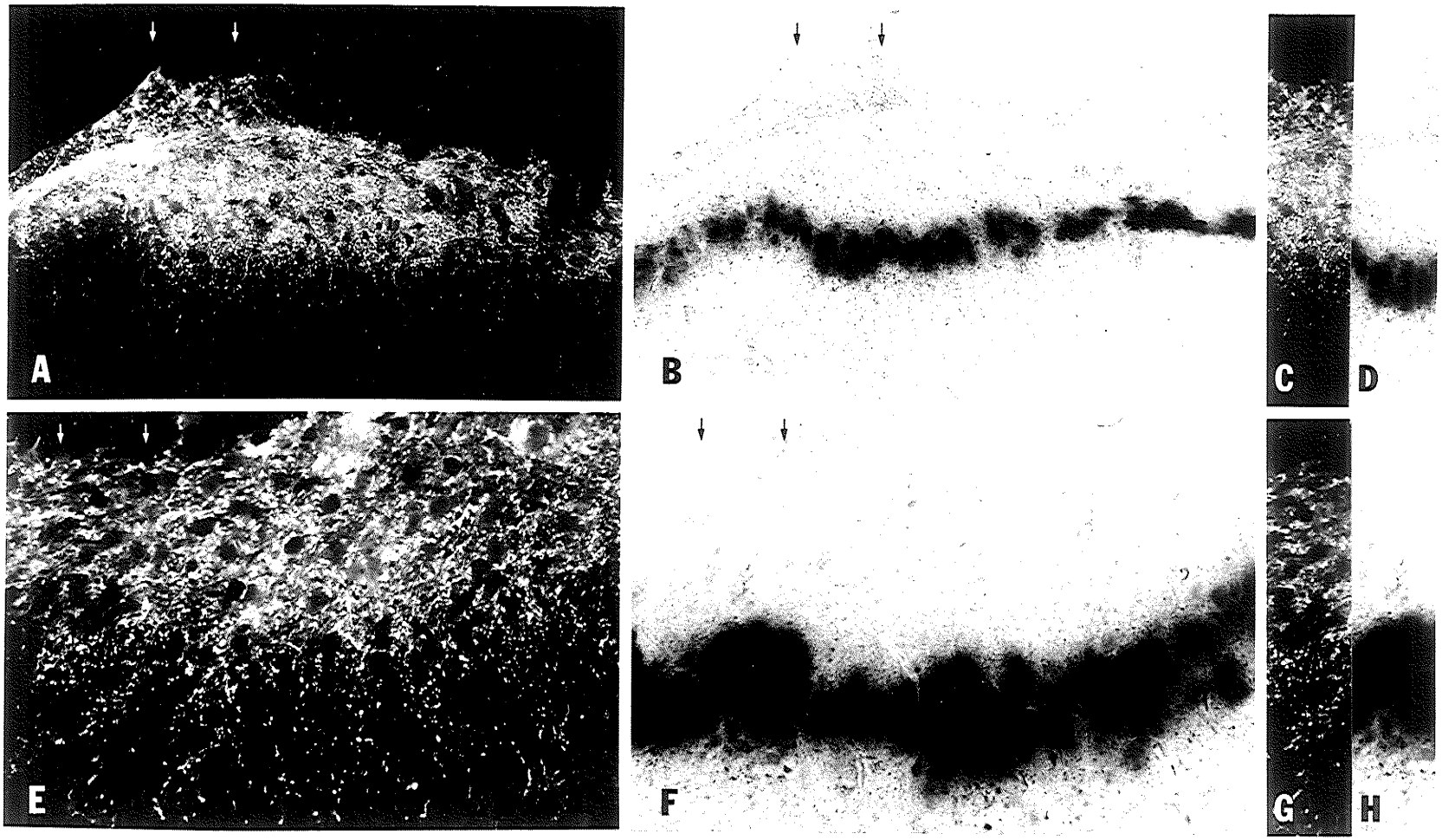

Fig. 4

Part V

Cytochrome oxidase immunohistochemistry in rat brain and dorsal root ganglia: visualization of enzyme in neuronal perikarya and in parvalbumin-positive neurons

G. Karmy, P.A. Carr, T. Yamamoto, S.H.P. Chan and J.I. Nagy

Neuroscience (1991) 40; 825-839

Abstract--Histochemical detection of cytochrome oxidase activity has been widely used to deduce patterns of neuronal electrical activity in the CNS. Here we investigated the utility of cytochrome oxidase localization by immunohistochemistry and compared immunostaining with histochemical staining patterns in dorsal root ganglia. In addition, a limited survey of cytochrome oxidase immunostaining density within what are thought to be highly active parvalbumin-immunoreactive neurons was conducted. The immunohistochemical approach produced granular cytoplasmic immunolabelling in neuronal cell bodies and allowed identification of individual labelled cells in all brain regions including those within dense immunoreactive networks of neuropil. Neuronal somata exhibited a wide range of staining densities which were particularly evident in the hippocampus and dorsal root ganglia. The distribution of neurons intensely immunoreactive for cytochrome oxidase within various structures was consistent with previous histochemical descriptions of enzyme activity. Densitometric measurements of immunohistochemical reaction product in individual neurons of hippocampus, substantia nigra, cerebellum and dorsal root ganglia showed that the rate of product deposition was linear with time under conditions chosen for comparisons of staining density. Quantitative analysis of cytochrome oxidase immunohistochemical and histochemical staining densities within the same cells in adjacent sections of dorsal root ganglion gave a correlation coefficient of $r=0.75$ ($p < 0.001$). In sections processed immunohistochemically for both cytochrome oxidase and parvalbumin, most but not all parvalbumin-containing cells displayed dense cytochrome oxidase immunolabelling. Conversely, many examples were found of neurons that were densely stained for cytochrome oxidase, but lacked parvalbumin.

Immunohistochemistry for cytochrome oxidase reveals the enzyme in neuronal cell bodies with a clarity not usually seen with the histochemical method. Combination of this immunohistochemical approach with simultaneous immunolabelling of other

neuronal markers, as shown here in the case of parvalbumin, is expected to assist the elucidation of patterns of activity in neurochemically identified cell types and anatomically defined neural systems.

A number of anatomical approaches have been developed to study normal or experimentally altered patterns of electrical activity in neurons. These include autoradiographic localization of radiolabelled 2′-deoxyglucose uptake (37) and immunohistochemical visualization of c-fos protooncogene induction (21,34) which detect short-term patterns of neuronal activity and histochemical determination of cytochrome oxidase (CO) activity which reveals long-term patterns of activity (49). The latter method is based on the premise that CO activity in the mitochondrial oxidative pathway parallels cellular energy demands for ATP and that maintenance of ionic gradients across plasma membranes represents a significant energy expenditure in neurons (29,36). Rather indirect support for the view that densities of histochemical staining for CO in neurons reflects their average level of electrical activity includes such considerations as the source, strength and placement of their synaptic input (13,25,42,48). Further support is provided by observations that the CO staining intensity of certain neuronal populations within structures such as the lateral geniculate nucleus, hippocampus, reticular thalamic nucleus and substantia nigra appears to correspond to their spontaneous firing rates (see 24,43,49). Stronger evidence for a close coupling between CO and neuronal activity originates from studies showing changes in CO histochemical staining densities in response to experimental manipulations which alter neuronal activity. For example, decreases in CO staining intensity have been observed in the lateral geniculate nucleus and visual cortex after intravitreal injection of tetrodotoxin or enucleation (45,47), and in the ventral cochlear nucleus, trapezoid body, inferior colliculus and several other auditory relay nuclei following blockade of auditory stimuli (44). Increases in staining density have been observed in myenteric ganglia after depolarization with veratridine (31) and in auditory relay nuclei after chronic electrical stimulation of the cochlear nerve (46).

Despite the ease, reliability and widespread use of CO histochemistry, this method has not been extensively applied to studies of CO activity in neurons identified according

to their morphological or transmitter characteristics. Such studies may have been impeded by the difficulty of visualizing CO reaction product in neurons embedded in regions of densely stained neuropil and, in some instances, by the incompatibility of technical conditions used for CO histochemistry and those used for immunohistochemical localization of other substances. Information regarding relative CO content of morphologically or chemically homogeneous neuronal populations could be of value in establishing relationships between their anatomical connections and overall level of activity. One widely distributed population of neurons suggested to be homogeneous with respect to properties that allow high frequencies of firing contains the calcium binding protein parvalbumin (PV). That the presence of PV is in fact one of these properties is suggested by the known role of calcium in regulating neuronal excitability (30,32), the proposed role of PV in buffering intracellular free calcium (9,19,39) and the expression of PV in neurons that are generally considered to be highly active or those that exhibit high frequency bursts of activity (3,4,9,27).

In order to extend the use of CO as an indicator of metabolic and electrical activity in neurons, the present study was undertaken to determine the utility of an immunohistochemical approach to enzyme localization and to investigate whether relative quantities of immunohistochemically detected CO protein correspond to the distribution of CO activity demonstrated by histochemistry. In addition, a general survey of CO immunostaining intensities in PV-containing neurons was conducted in sections simultaneously immunolabelled for both CO and PV.

METHODS

Tissue Preparation

Adult, male Sprague-Dawley rats weighing 250-360 g were anesthetized with chloral hydrate and perfused transcardially with cold (4°C) 0.9% saline containing 0.1% sodium nitrite and 100 units/100 ml of heparin followed by cold (4°C) freshly prepared fixative consisting of 4% paraformaldehyde in 0.1 M sodium phosphate buffer, pH 7.4. Some animals were perfused with fixative consisting of 4% paraformaldehyde and 0.16% picric acid in 0.1 M sodium phosphate buffer, pH 7.4. Brains and L5 dorsal root ganglia were removed and postfixed in cold fixative for 2-24 hr for brain tissue and overnight for ganglia. The tissue was then transferred into cryoprotectant solutions consisting of either 25% sucrose and 10% glycerol in 0.05 M sodium phosphate buffer (pH 7.4) or 15% sucrose in 0.1 M sodium phosphate buffer (pH 7.4) for sliding microtome or cryostat sectioning, respectively. All tissues were cut at thickness of 7-10 μm.

CO Immunohistochemistry

Sections were incubated for 40-72 hr with a previously characterized rabbit polyclonal antibody against whole CO (10,16,17), with the polyclonal antibody preadsorbed with purified beef heart CO, or with preimmune serum on immunoblots the polyclonal antibody was found to react with all of the subunits of rat brain and heart mitochondrial CO (unpublished observations). Antibody dilutions ranged from 1:500 to 1:4000 in 0.1 M sodium phosphate buffered 0.9% saline (PBS, pH 7.4) containing 1% BSA alone or 1% BSA with 0.3%, 0.6% or 1% Triton X-100. Optimum results were obtained with primary antibody dilutions of 1:500 in 0.3% Triton X-100. Following the primary incubation, sections were washed for 40 min in PBS containing 0.3% Triton X-100 (PBS-T), incubated for 2 hr in secondary incubation medium consisting of goat anti-

rabbit IgG (Sternberger-Meyer) diluted 1:20 in PBS-T with 1% BSA (PBS-T/BSA) and again washed for 40 min in PBS-T. The tissue was then incubated in rabbit PAP (Sternberger-Meyer) diluted 1:100 in PBS-T/BSA for 2 hr followed by a 20 min wash in PBS-T and a further 20 min wash in 50 mM Tris-HCl buffer, pH 7.4. The sections were then reacted in 50 mM Tris-buffer containing 0.005% hydrogen peroxide and 0.02% diaminobenzidine (DAB), washed in 50 mM Tris for 40 min, mounted onto slides from gelatin-alcohol, dehydrated and coverslipped with Permount.

CO Histochemistry

Cytochrome oxidase histochemistry was conducted as previously described (7) following a slight modification of the method of Wong-Riley (45). In brief, sections were incubated for 4-6 hr in the dark at 37°C in 0.1 M sodium phosphate buffer, pH 7.4, containing 0.03% cytochrome C (Sigma, type III), 0.025% diaminobenzidine (DAB) and 4% sucrose. Following the reaction, sections were washed for 20 min in 0.1 M sodium phosphate buffer, pH 7.4, and coverslipped with 3:1 glycerol/water.

Densitometric Measurements

Densitometric measurements of individual cells following both histochemical and immunohistochemical CO reactions were used to demonstrate the linearity of DAB reaction product deposition with time. This allowed a statistical correlation analysis between the densities obtained with the histochemical and immunocytochemical methods. Quantitation of reaction product densities within cells was undertaken with an Amersham RAS-1000 image analysis system linked by a video camera to a Nikon Optiphot microscope. Before each session of quantitation, the microscope illumination and camera gain control were adjusted to encompass the optimal range of gray scales

detected by the camera. Transient fluctuations in illumination intensity were corrected by digitizing a blank area of a slide adjacent to reacted tissue and subtracting its density from all subsequent measurements. Optical density scales and linear dimensions were calibrated at the objective magnifications routinely employed for tissue visualization. Digitized images were captured and stored on either 1.2 megabyte floppy disks or directly onto hard disk prior to selection and analysis of cells in the digitized fields. Optical densities and areas of individual cells were obtained by maneuvering a cursor around the perimeter of a cell. Nuclei were excluded from the density measurements of all cells taken for CO histochemical/immunohistochemical correlation analyses. Whole cell measurements including the nucleus were taken for tests of the linearity of reaction such that repeated digitization of the same cell gave a constant relative contribution of density within the nucleus and cytoplasm in each image. Small cells were selected for analysis from a magnified area of the digitized image to enable accurate determination of cellular boundaries.

Immunoreaction Linearity

Determination of CO immunohistochemical DAB reaction linearity with time was undertaken using sections that were processed up to the DAB reaction step as outlined above. The slides were then transferred to the microscope stage of the image analysis system and the sections were covered with 50 mM Tris-HCl buffer, pH 7.4. An area within the section containing many cells was then selected for an initial time zero density measurement. The Tris-buffer was then replaced with DAB solution and the progress of the reaction was monitored by digitization of the same area every 30 seconds for periods of up to 30 min. During this time the DAB solution was replenished every 4 min. An average of 15 cells per image, stored on floppy disks, were later randomly selected for analysis of optical density in each cell over the duration of the reaction.

CO immunohistochemistry-CO histochemistry correlation

Neurons in DRG were chosen for comparisons of the localization and density of CO immunohistochemical and histochemical reaction product for several reasons. First, DRG cell populations exhibit highly heterogeneous levels of histochemically detected CO thus allowing more stringent tests of correspondence with immunohistochemical detection. Second, the absence of neuropil permits unobstructed visualization of staining intensities within cell bodies and accurate quantitation of staining densities. And third, histochemical deposition of CO reaction product in DRG cells has been previously demonstrated to be linear under the conditions employed in the present study (7). Adjacent cryostat sections (7 μm) of DRG were collected on separate slides and one section of each pair was processed for CO immunohistochemistry and the other for CO histochemistry. Images of the same field within adjacent sections were recorded on computer and the optical densities of corresponding cells within these fields were determined. Photographs of adjacent sections were used to aid the identification of corresponding cells in each pair of sections. Cells which differed extensively in size or which appeared to have undergone processing damage were excluded from analysis. Statistical analysis of the correlation between densities obtained with histochemical and immunohistochemical methods was performed with the aid of a Stata (The Computing Resource Center, California) statistics package.

Simultaneous Immunohistochemistry for CO and PV

Sections of brain or DRG were processed first for CO immunohistochemistry as outlined above and then incubated for 40-72 hr at 4°C with a previously characterized rabbit polyclonal antibody against PV diluted 1:500 in PBS-T/BSA (33). Following the

primary incubation the sections were washed for 40 min in PBS solution containing 0.3% Triton X-100 and incubated for 2 hr at room temperature with fluorescein isothiocyanate-conjugated donkey anti-rabbit IgG (Amersham) diluted 1:20 in PBS-T/BSA. The sections were then coverslipped with anti-fade medium (40) and photographed. Although antisera against PV and CO were produced in the same species, cross-reactions between the various antibodies involved in the sequential double-labelling procedure was prevented by deposition of DAB precipitate and blockade of the series of antibodies used initially to visualize CO. While this precipitate also largely obscured visualization of PV-immunofluorescence in the cytoplasm, the presence of PV in the nucleus of PV-IR neurons and the absence of nuclear CO permitted visualization of PV in cells cut through the nucleus even when they contained dense cytoplasmic staining for CO. However, in order to aid visualization of PV-immunofluorescence, the concentration of anti-CO antisera was reduced to 1:1000; this together with glycerol coverslipping rather than dehydration of sections led to a less than optimal appearance of CO-immunostaining but produced relative density distributions similar to that seen under optimal conditions.

Given the availability of antisera from different species for CO and another substance to be localized, it would have been equally possible to react sections first for a substance by fluorescence, photograph the section and then process for CO by the PAP-method.

RESULTS

General observations

Under optimal conditions qualitative patterns of immunohistochemical staining for CO were found to be reproducible between animals. Under suboptimal conditions, reaction product in lightly stained cells approached background levels resulting in a loss of the overall heterogeneity of staining densities. The quality of staining was dependent

to various degrees on fixation and post-fixation conditions as well as on primary antibody and detergent concentrations in the antibody incubation media. Tissue fixed with 4% paraformaldehyde and post-fixed in this same fixative for 2-6 hr exhibited what was considered to be optimal staining of neuronal cell bodies. Tissue fixed with 4% paraformaldehyde containing 0.16% picric acid and post-fixed for 2-24 hr gave increased intensities of staining in areas of neuropil compared with that seen within cell bodies. An antibody dilution of 1:500 produced robust staining and as the antibody was stepwise diluted to 1:4000, only cell groups most intensely stained at 1:500 were visible. Sections incubated in medium containing 0.3% Triton X-100 displayed consistent staining patterns in all brain regions examined. Higher concentrations of Triton X-100 (0.6 and 1.0%) noticeably reduced staining density and omission of Triton X-100 gave remarkably low levels of staining. No immunohistochemical staining was obtained with antibody preadsorbed with purified CO and only light background staining was seen with preimmune serum at dilutions of 1:500.

Immuno-peroxidase Reaction Linearity

Tests of the linearity of immunoperoxidase reaction product deposition (Fig. 1) were conducted on CO-immunostained sections of DRG similar to those shown in Fig. 2A,C,E and in fields of hippocampal, nigral and cerebellar sections similar to those shown in Fig. 4. The progress of the reaction is shown for 5 cells in sections of DRG and 2 cells in each of the other areas. However, similar results were obtained from density measurements of a total of 105 cells in DRG, 30 cells in hippocampus, 30 cells in substantia nigra pars reticulata and 45 Purkinje cells in cerebellum. Repeated optical density measurements within individual cells in each of these regions indicated that the rate of DAB deposition in cells exhibiting different staining densities was linear with time for up to about 10 min after which it began to plateau. A standard reaction time of

8 min was chosen based on these results. The failure of linear portions of the curves to intersect the origin may be related to our use of Tris-buffer to set background levels and the replacement of this solution with the Tris-HCl buffer DAB-H_2O_2 mixture which may have exhibited some slight absorbance.

Dorsal Root Ganglia

Sections of DRG reacted by either histochemistry or immunohistochemistry for CO are shown in Fig. 2. Immunostained neurons exhibited a wide range of staining intensities and were classified as dense, moderate or light (Fig. 2A,C,E). Densely stained cells represented a minority of the neuronal population and included large type A and less often small type B cells. The majority of both type A and B cells displayed staining in the moderate to light range. Immunoreaction product had a granular appearance (Fig. 2C,E) and was uniformly distributed within the somal cytoplasm of most cells except on rare occasions where it tended to aggregate at one pole of the cell body (Fig. 2E). No reaction product was observed in the nucleus and very little was seen in fibers coursing through the section. In DRG sections processed by CO histochemistry (Fig. 2B,D,F), cells exhibited what appeared to be a narrower range of staining densities than seen immunohistochemically. Densely stained cells were mainly large type A neurons and the majority of the remaining cells were moderately or lightly stained. The appearance of staining within cell bodies was generally diffuse with some granularity and in most neurons was uniformly distributed throughout the cytoplasm (Fig. 2D,F). Accumulation of CO reaction product in subregions of the cytoplasm (Fig. 2D) was seen more often by histochemistry than by immunohistochemistry, but this may have been due to the greater staining density produced by the latter method and, consequently, failure to visualize such accumulation.

In visual comparisons of staining within the same cells in adjacent sections, the different range of densities given by the two procedures was such that in immunohistochemically processed sections maximally stained cells exhibited greater staining densities than their counterparts in the adjacent histochemically processed sections. With this consideration in mind, a correspondence of immunohistochemical and histochemical staining densities was found within many large type A neurons (Fig. 2). Comparison of densities within small neurons was more difficult due to the lower frequency with which the same neuron appeared in adjacent sections, but examples of correspondence were found (Fig. 2E,F). In order to facilitate reference to staining patterns for CO by the two methods, cells densely stained by immunohistochemistry and histochemistry will be referred to as CO-immunodense and CO-histodense, respectively. From counts of 190 neurons that exhibited dense staining by either method in adjacent sections, it was judged that 92% of CO-histodense neurons were also immunodense and 76% of the immunodense neurons were histodense. Counts were conducted of what were designated the densely stained populations as these could be readily distinguished from the more lightly stained populations.

Quantitative comparisons of CO immunohistochemical and histochemical staining densities in the same neurons in adjacent sections are shown in Fig. 3. Linear regression analysis of a total of 89 cells plotted in Fig. 3A revealed a correlation coefficient of $r=0.75$ ($p<0.001$). An attempt was made to exclude the possibility that some cells, particularly those of small sizes, may not span the full thickness of the 7 μm sections employed thereby giving erroneously low levels of staining density in corresponding cells. To this end, 25% of pairs of corresponding cells that had the greatest difference in cross sectional area in adjacent sections were eliminated from the correlation analysis (Fig. 3B). This maneuver made a negligible difference in the correlation obtained ($r=0.79$; $p<0.001$).

CO-immunolabelling in Brain

A detailed description of CO-immunolabelling patterns throughout the brain is beyond the scope of the present report, but a summary of our observations in various regions are as follows. The appearance of CO immunostaining within neurons in brain was similar to that described in DRG; the staining had a granular appearance and was localized in somal cytoplasm. In cerebral cortex (not shown), CO staining was heterogeneous among areas as well as between lamina. The most intense CO-immunoreactivity was seen in subpopulations of neurons in all layers of the cingulate cortex except layer 1. In other cortical areas immunodense neurons were observed in layers II to VI and those in layer V were most heavily labelled. In the hippocampus (Fig. 4A) immunodense neurons were scattered mainly in the stratum pyramidale and stratum oriens. Immunoreactive processes emerging from some somata in these layers could be followed for distances of up to 300 μm. The majority of neurons in the pyramidal cell layer exhibited moderate staining. In the dentate gyrus immunodense cell bodies were located predominantly in the hilus and less so in the granule cell layer. In the basal ganglia, the globus pallidus and substantia nigra pars reticulata (Fig. 4B) contained many large intensely stained neurons and some immunoreactive neuropil, and the striatum displayed a greater degree of neuropil staining than seen in most other brain regions and only a few moderately stained cells per section. In the cerebellum, moderate staining was seen in Purkinje cells and dense staining was seen in some interneurons (Fig. 4C). Examples of other regions containing intensely stained neurons included the red nucleus, ventral cochlear nucleus, nucleus of lateral lemniscus and the pontine nucleus.

CO-immunoreactivity in PV-positive Neurons

Relationships between CO-immunodense neurons and those immunoreactive for PV in DRG and some brain regions are shown in Figures 5, 6 and 7. Neurons were designated as CO-immunodense by comparing staining densities among cells within and/or between brain regions. Analyses were restricted to those neurons with a clearly visible nucleus that contained PV or displayed dense CO immunostaining. A small percentage of cells that may have been PV-positive, but exhibited very weak immunofluorescence were excluded from analyses. Figure 5 shows sections of DRG processed first by PAP for detection of CO and subsequently by immunofluorescence for visualization of PV. In PAP reacted sections (Fig. 5A) illuminated for fluorescence observations (Fig. 5B), the intensity of nuclear PV-immunofluorescence varied, but was sufficiently bright to permit unambiguous identification of PV-positive neurons. In control procedures where one of a pair of adjacent sections was processed for both CO and PV and the other for PV alone, all PV-IR cells identified in the latter section (Fig. 5E) displayed nuclear fluorescence in the former when cut through their nuclei (Fig. 5D) showing that the PAP procedure for CO (Fig. 5C) does not interfere with PV-immunofluorescence in the nucleus. In the cytoplasm of CO-immunodense cells (Fig. 5C), fluorescence was largely obscured (Fig. 5D) but could be observed between granules of DAB precipitate at higher magnification (Fig. 5F,G). In sections processed for both CO and PV but with omission of antibody against PV, no fluorescent staining was observed (not shown) indicating lack of crossreaction between the set of antibodies used to visualize PV and those used to visualize CO. As we have previously shown (5), about 14% of cells in DRG are PV-IR and the vast majority of these are large type A cells. A proportion of both large and small cell types appeared to be intensely immunostained for CO and visual inspection of 205 DRG cells showed that 93% of PV-IR neurons were CO-immunodense and 70% of immunodense neurons contained PV.

In brain CO-immunostaining density was assessed in certain populations of PV-IR neurons (Fig. 6,7) which overall were seen to be distributed in patterns similar to those previously described (8,12,14,18,20). From an inspection of 473 cells in cerebral cortex (Fig. 6A,B) it was found that 70% of PV-IR cells in layers II to IV were CO-immunodense and 83% of CO-immunodense neurons contained PV. In layers V and VI, 60% of PV-IR cells were CO-immunodense and 43% of CO-immunodense cells contained PV. From an analysis of 356 hippocampal neurons it was found that 80% of PV-IR cells in the CA3 region (Fig. 6C-F) were CO-immunodense and 30% of CO-immunodense neurons were PV-positive. In the CA1 region (Fig. 6G,H) 93% of the PV-IR neurons were CO-immunodense and 66% of CO- immunodense cells were immunoreactive for PV. In the dentate gyrus 90% of PV- IR cells were CO-immunodense and 10% of CO-immunodense cells contained PV. From counts of 133 cells in the substantia nigra pars reticulata (Fig. 7A,B), all PV-IR cells were CO-immunodense and 89% of CO-immunodense neurons contained PV. In globus pallidus all PV-containing cells were CO-immunodense (Fig. 7C,D) and virtually all CO-immunodense cells contained PV. In the striatum most PV-IR neurons exhibited relatively light CO-immunostaining (Fig. 7E,F). In the reticular thalamic nucleus all PV-IR cells exhibited dense staining for CO and in cerebellum PV-IR Purkinje cells were moderately immunostained.

DISCUSSION

The present results show the feasibility of an immunohistochemical approach to the detection of CO in neurons and demonstrate the application of this approach to investigations of relationships between the neurochemical characteristics of cells and their CO content. Our results are consistent with recent reports by Hevner and Wong-

Riley (20a) and Luo et al. (29a) who have also detected CO in the CNS by immmunohistochemistry and have shown a correspondence between immunohistochemical and histochemical staining patterns, although it was noted by these authors that neuronal cell bodies were sometimes more intensely labelled by the former than the latter method (20a). The overall higher level of neuropil immunolabelling obtained by Hevner and Wong-Riley (20a) than found here may be due to their use of a 4 to 6 hr immersion fixation of tissues which is consistent with our observation that weaker fixation produced heavier neuropil labelling.

In need of consideration are several technical factors related to the validity of qualitative or quantitative comparisons of CO immunohistochemical staining densities among cells as well as to the reliability with which immunolocalization of CO reflects either *in vivo* CO enzyme activity or that visualized histochemically. The first concerns the standard practice of insuring that staining density comparisons are made in tissue sections where the rate of reaction product deposition is linear with time over the full range of densities encountered (1). In the case of protocols involving deposition of DAB polymer, linearity is a particularly important issue in view of previous observations that accumulation of this reaction product at or near the site of its formation can potentially result in inactivation of the reaction process (38). This may lead to saturation of DAB deposition in cells with high levels of CO when, at similar reaction times, the deposition continues to proceed linearly in cells with low CO levels. We have previously shown that the conditions used here for histochemical localization of CO in individual cells of DRG led to a linear rate of product deposition with time (7), and now show that conditions can be chosen to produce similar linearity for CO detection by immunohistochemistry in individual cells of DRG and several brain regions, thus allowing assessment of the relative cellular content of the enzyme. It should be noted that the time period over which the peroxidase reaction is linear depends on the antibody

concentration in the primary incubation and therefore must be determined for each new antibody preparation.

A second concern is whether total enzyme content as reflected by immunostaining density necessarily parallels CO activity. This point warrants attention in view of evidence that CO activity may not only be regulated by enzyme production, but also by other equally important mechanisms involving activation of the enzyme (2,15,22). Moreover, since CO is a complex protein consisting of many subunits (11,23), results obtained by immunohistochemistry may be highly dependent on the relative representation of the specific subunits against which particular anti-CO antibody preparations are directed. Particular subunits may be present in a disassembled (41), but immunohistochemically detectable form either in the cytoplasm or within mitochondria. Finally, tissue preparation conditions may differentially affect the stability of portions of the enzyme necessary for catalytic activity and those that serve as antibody epitopes thus leading to possible discrepancies between staining densities produced by histochemical and immunohistochemical methods. Notwithstanding these potential sources of ambiguity, and despite variabilities inherent in extracting densitometric data from adjacent tissue sections processed by what sometimes can be capricious anatomical methods, we did obtain in individual cells of DRG a reasonably high correlation between the staining densities produced by histochemical and immunohistochemical detection of CO. Moreover, in various brain regions examined the densities of CO-immunoreactivity in neuronal cell bodies was qualitatively similar to previously reported CO staining patterns derived histochemically (13,24,43). This further suggests that immunostaining density is a valid indicator of at least perikaryal enzymatic activity; we have not yet completed a thorough analysis of tissues reacted optimally for demonstrating neuropil immunoreactivity. Some of the complications involving CO subunit structure may have been minimized by our use of a polyclonal antibody and its production against the

holoenzyme. However, it should be noted that despite the close correspondence between histochemical and immunohistochemical staining density, some small type B DRG cells appeared to display intense CO-immunoreactivity without correspondingly high histochemical enzyme activity. Since immunohistochemical staining density was generally much more robust, this discrepancy may be more apparent than real. On the other hand, positive identification of the same small cells in adjacent sections occurs less frequently than that of large cells and for this reason we cannot rule out the possibility that small cells were under-represented in our correlation analysis and consequently that a subpopulation of these cells contain some form of CO with low activity.

Two advantages offered by CO-immunohistochemistry over histochemistry are noteworthy. The first is that unlike the histochemical technique where label is found largely in neuropil, immunohistochemical fixation conditions can be chosen to produce immunolabelling predominantly of neuronal somata thus allowing identification of neurons which are normally obscured in histodense neuropil. Weak immunolabelling of neuropil after relatively strong tissue fixation is likely due to differential penetration rates of large molecular weight immunoreagents into cell soma compared with their processes, whereas the smaller histochemical reagents appear to penetrate into somata and processes equally well. The second is the compatibility of CO-immunohistochemistry with the inclusion of Triton X-100 in the incubation medium. Treatment with Triton X-100 may disrupt CO (35) and reduce histochemically detectable activity (6). From our experience this has been a considerable obstacle in colocalization studies of CO with other substances which require Triton X-100 for optimal immunohistochemical visualization.

Neuronal PV and CO Content

Parvalbumin is a calcium binding protein that, among other possible roles, has been proposed to contribute to calcium buffering in neurons which have characteristically high firing rates (for review see 9,19,20). This proposal is supported by several lines of evidence. In zebra finch the distribution of PV in auditory, visual and vocal motor systems was found to parallel that of dense histochemical staining for CO in these regions. In some of these systems neurons also exhibited high basal rates of 2-deoxyglucose uptake (3,4). In mammals evidence suggesting a relationship between neuronal expression of PV and firing capacity includes the presence of PV in many GABAergic systems that are highly electrically active (9,28,39) and the observation that kindling via stimulation of the Schaffer/commissural fiber system increases the number of PV-IR neurons in the hippocampus (26). More direct evidence has been obtained in rat hippocampus where intracellular recordings of PV-IR neurons demonstrated that they belong to the fast spiking class of hippocampal interneurons (27). Insofar as firing rates of PV-IR neurons may be indicated by their CO content, the present results are consistent with these findings in hippocampus and demonstrate that most PV-IR neurons are CO-immunodense in many regions of the brain including cortex, reticular thalamic nucleus, globus pallidus, and substantia nigra. Moreover, the finding that a high percentage of PV-containing neurons in DRG are CO-immunodense is consistent with our previous study in which histochemistry for CO was used to demonstrate high CO activity in PV-IR DRG neurons (6). Exceptions, however, were found as in the case of the cerebellum where PV-IR Purkinje cells were moderately CO-immunostained and the striatum where only a few PV-IR neurons were moderately stained and most had relatively light CO immunostaining. In addition, several structures contained some proportion of PV-IR neurons that were clearly not among those most densely stained for CO. The role of PV in Ca^{+2} buffering and its requirement in fast-spiking neurons remains uncertain, but has

been suggested to be related to prevention of activation of Ca^{+2} gated K+ channels thereby decreasing the duration or amplitude of afterhyperpolarization and the length of the refractory period (9). Our results indicate that while most PV-IR neurons have high levels of CO and therefore high electrical activity, it appears that high CO content is not a prerequisite for other electrical properties, such as fast-spiking capability, that may be endowed by PV.

Conclusions

Cytochrome oxidase immunohistochemistry, which combines the high resolution of immunolabelling methods with the previously demonstrated reliability of monitoring metabolic requirements by the histochemical method is a potentially powerful means of studying patterns of neuronal activity. The improved visualization of neuronal somata and the ability to colocalize CO with substances by double immunohistochemical labelling methods will enable determination of relative CO content in biochemically defined cell populations. Whether immunostaining patterns can be altered following the kind of experimental manipulations that have been shown to produce changes in histochemical staining patterns remains to be determined.

REFERENCES

1. Benno R.H., Tucker L.W., Joh T.H. and Reis D.J. (1982) Quantitative immunocytochemistry of tyrosine hydroxylase in rat brain. I. Development of a computer assisted method using the peroxidase-antiperoxidase technique. Brain Res. **246,** 225-236.

2. Bisson R., Schiavo G. and Montecucco C. (1987) ATP induces conformational changes in mitochondrial cytochrome c oxidase. Effect on the cytochrome c binding site. J. Biol. Chem. **262,** 5992-5998.

3. Braun K., Scheich H., Schachner M. and Heizmann C.W. (1985a) Distribution of parvalbumin, cytochrome oxidase activity and ^{14}C-2-deoxyglucose uptake in the brain of the zebra finch. I. Auditory and vocal motor system. Cell and Tissue Res. **240,** 101-115.

4. Braun K., Scheich, H., Schachner M. and Heizmann C.W. (1985b) Distribution of parvalbumin, cytochrome oxidase activity and ^{14}C-2-deoxyglucose uptake in the brain of the zebra finch. II. Visual system. Cell and Tissue Res. **240,** 117-127.

5. Carr P.A., Yamamoto T., Karmy G., Baimbridge K.G. and Nagy J.I. (1989) Parvalbumin is highly colocalized with calbindin D28k and rarely with calcitonin gene-related peptide in dorsal root ganglia neurons of rat. Brain Res. **497,** 163-170.

6. Carr P.A., Yamamoto T., Karmy G., Baimbridge K.G. and Nagy J.I. (1990) Analysis of parvalbumin and calbindin D28k-immunoreactive neurons in dorsal root ganglia of rat in relation to their cytochrome oxidase and carbonic anhydrase content.

Neuroscience **33,** 363-371.

7. Carr P.A., Yamamoto T., Staines W.A., Whittaker M.E. and Nagy J.I. (1990) Quantitative histochemical and morphometric analysis of cytochrome oxidase in rat dorsal root ganglia with carbonic anhydrase colocalization. Neuroscience **33,** 351-362

8. Celio M.R. and Heizmann C.W. (1981) Calcium-binding protein parvalbumin as a neuronal marker. Nature **293,** 300-302.

9. Celio M.R. (1986) Parvalbumin in most gamma-aminobutyric acid-containing neurons of the rat cerebral cortex. Science **231,** 995-997.

10. Chan S.H.P. and Tracy R.P. (1978) Immunological studies on cytochrome c oxidase. Arrangement of protein subunits in the solubilized and membrane-bound enzyme. Eur. J. Biochem. **89,** 595-605.

11. Denis M. (1986) Structure and function of cytochrome-c oxidase. Biochimie **68,** 459-470.

12. De Viragh P.A., Haglid K.G. and Celio M.R. (1989) Parvalbumin increases in the caudate putamen of rats with vitamin D hypervitaminosis. Proc. Natl. Acad. Sci. **86,** 3887-3890.

13. Difiglia M., Graveland G.A. and Schiff L. (1987) Cytochrome oxidase activity in the rat caudate nucleus: Light and electron microscope observations. J. Comp. Neurol. **255,** 137-145.

14. Endo T., Takazawa K., Kobayashi and Onaya T. (1986) Immunochemical and immunohistochemical localization of parvalbumin in rat nervous tissues. J. Neurochem. **46,** 892-898.

15. Ferguson-Miller S., Brautigan D.L. and Margoliash E. (1976) Correlation of the kinetics of electron transfer activity of various eukaryotic cytochromes c with binding to mitochondrial cytochrome c oxidase. J. Biol. Chem. **251,** 1104-1115.

16. Freedman J.A. and Chan S.H.P. (1983) Redox-dependent accessibility of subunit V of cytochrome oxidase: A novel use of ELISA as a probe of intact membranes. J. Biol. Chem. **258,** 5885-5892.

17. Freedman J.A., Leece B., Cooper C.E., Nicholls P. and Chan S.H.P. (1988) Effects of subunit V antibodies on the topology of the subunit and the activity of beef heart cytochrome-c oxidase. Biochem. Cell Biol. **66,** 1210- 1217.

18. Gerfen C.R., Baimbridge K.G. and Miller J.J. (1985) The neostriatal mosaic: compartmental distribution of calcium-binding protein and parvalbumin in the basal ganglia of the rat and monkey. Proc. Natl. Acad. Sci. **82,** 8780-8784.

19. Heizmann C.W. (1984) Parvalbumin, an intracellular calcium-binding protein; distribution, properties and possible roles in mammalian cells. Experientia **40,** 910-921.

20. Heizmann C.W. and Berchtold M.W. (1987) Expression of parvalbumin and other CA^{2+}-binding proteins in normal and tumor cells: a topical review. Cell Calcium **8,** 1-41.

20a. Hevner R.F. and Wong-Riley M.T.T. (1989) Brain cytochrome oxidase: Purification, antibody production, and immunohistochemical/histochemical correlations in the CNS. J. Neurosci. **9,** 3884-3898.

21. Hunt S.P., Pini A. and Evan G. (1987) Induction of c-fos-like protein in spinal cord neurons following sensory stimulation. Nature **328,** 632-634.

22. Kadenbach B. (1986) Regulation of respiration and ATP synthesis in higher organisms: hypothesis. J. Bioenerg. Biomemb. **18,** 39-54.

23. Kadenbach B., Kuhn-Nentwig L. and Buge U. (1987) Evolution of a regulatory enzyme: cytochrome-c oxidase (complex IV). In Current Topics in Bioenergetics (ed Lee C.P.), pp. 113-161. Academic Press, New York.

24. Kageyama G.H. and Wong-Riley M.T.T. (1982) Histochemical localization of cytochrome oxidase in the hippocampus: Correlation with specific neuronal types and afferent pathways. Neuroscience **7,** 2337-2361.

25. Kageyama G.H. and Wong-Riley M. (1986) Laminar and cellular localization of cytochrome oxidase in the cat striate cortex. J. Comp. Neurol. **245,** 137-159.

26. Kamphuis W., Huisman E., Wadman W.J., Heizmann C.W. and Lopes-da-Silva F.H. (1989) Kindling induced changes in parvalbumin immunoreactivity in rat hippocampus and its relation to long-term decrease in GABA- immunoreactivity. Brain Res. **479,** 23-34.

27. Kawaguchi Y., Katsumaru H., Kosaka T., Heizmann C.W. and Hama K. (1987) Fast spiking cells in rat hippocampus (CA1 region) contain the calcium-binding protein parvalbumin. Brain Res. **416,** 369-374.

28. Kosaka T., Katsumaru H., Hama K., Wu J.-Y. and Heizmann C.W. (1987) GABAergic neurons containing the Ca^{2+}-binding protein parvalbumin in the rat hippocampus and dentate gyrus. Brain Res. **419,** 119-130.

29. Lowry O.H. (1975) Energy metabolism in brain and its control. In Brain Work, Alfred Benzon Symposium VIII (eds Ingvar D.H. and Lassen N.A.), pp. 48-64. Academic Press, Copenhagen.

29a. Luo X.G., Hevner R.F. and Wong-Riley M.T.T. (1989) Double labeling of cytochrome oxidase and gamma-aminobutyric acid in central nervous system neurons of adult cats. J. Neurosci. Meth. **30,** 189-195.

30. Marty A. (1989) The physiological role of calcium-dependent channels. Trends in Neurosci. **12,** 420-424.

31. Mawe G.M. and Gershon M.D. (1986) Functional heterogeneity in the myenteric plexus: demonstration using cytochrome oxidase as a verified cytochemical probe of the activity of individual enteric neurons. J. Comp. Neurol. **249,** 381-391.

32. Meech R.W. (1978) Calcium-dependent potassium activation in nervous tissues. Ann. Rev. Biophys. Bioenerg. **7,** 1-18.

33. Mithani S., Atmadja S., Baimbridge K.G. and Fibiger H.C. (1987) Neuroleptic-induced oral dyskinesias: effects of progabide and lack of correlation with regional changes in glutamic acid decarboxylase and choline acetyltransferase activities. Psychopharmacology **93,** 94-100.

34. Morgan J.I., Cohen D.R., Hempstead J.L. and Curran T. (1987) Mapping patterns of c-fos expression in the central nervous system after seizure. Science **237,** 192-197.

35. Robinson N.C. and Talbert L. (1986) Triton X-100 induced dissociation of beef heart cytochrome c oxidase into monomers. Biochemistry **25,** 2328-2335.

36. Sokoloff L. (1977) Relation between physiological function and energy metabolism in the central nervous system. J. Neurochem. **29,** 13-26.

37. Sokoloff L., Reivich M., Kennedy C., Des Rosiers M.H., Patlak C.S., Pettigrew K.D., Sakuroda O. and Shinohara U. (1977) The ^{14}C-deoxyglucose method for the measurement of local cerebral glucose utilization: theory, procedure, and normal values in the conscious and anesthetized rat. J. Neurochem. **28,** 897-916.

38. Sternberger L.A. and Joseph S.A. (1979) The unlabeled antibody method. Contrasting color staining of paired pituitary hormones without antibody removal. J. Histochem. Cytochem. **27,** 1424-1429.

39. Stichel C.C., Singer W. and Heizmann C.W. (1988) Light and electron microscopic immunocytochemical localization of parvalbumin in the dorsal lateral geniculate nucleus of the cat: evidence for coexistence with GABA. J. Comp. Neurol. **268,** 29-37.

40. Valnes K. and Brandtzaeg P. (1985) Retardation of immunofluorescence fading during microscopy. J. Histochem. Cytochem. **33,** 755-761.

41. Wielburski A., Kuzela S. and Nelson B.D. (1982) Studies on the assembly of cytochrome oxidase in isolated rat hepatocytes. Biochem. J. **204,** 239-245.

42. Wiener S.I. (1986) Laminar distribution and patchiness of cytochrome oxidase in mouse superior colliculus. J. Comp. Neurol. **244,** 137-148.

43. Wong-Riley M.T.T. (1976) Endogenous peroxidatic activity in brain stem neurons as demonstrated by their staining with diaminobenzidine in normal squirrel monkeys. Brain Res. **108,** 257-277.

44. Wong-Riley M.T.T., Merzenich M.M. and Leake P.A. (1978) Changes in endogenous enzymatic reactivity to DAB induced by neuronal inactivity. Brain Res. **141,** 185-192.

45. Wong-Riley M. (1979) Changes in the visual system of monocularly sutured or enucleated cats demonstrable with cytochrome oxidase histochemistry. Brain Res. **171,** 11-28.

46. Wong-Riley M.T.T., Walsh S.M., Leake-Jones P.A. and Merzenich M.M. (1981) Maintenance of neuronal activity by electrical stimulation of unilaterally deafened cats demonstrable with the cytochrome oxidase technique. Ann. Otol. Rhinol. Laryngol. **90(Suppl. 82),** 30-32.

47. Wong-Riley M. and Carroll E.W. (1984) The effect of impulse blockage on cytochrome oxidase activity in the monkey visual system. Nature **307,** 262- 264.

48. Wong-Riley M.T.T. and Kageyama G.H. (1986) Localization of cytochrome oxidase in the mammalian spinal cord and dorsal root ganglia, with quantitative analysis of ventral horn cells in monkey. J. Comp. Neurol. **245,** 41-61.

49. Wong-Riley M.T.T. (1989) Cytochrome oxidase: an endogenous metabolic marker for neuronal activity. Trends in Neurosci. **12,** 94-101.

FIGURE LEGENDS

Fig. 1. Relationship between immunohistochemical reaction product deposition and reaction time in sections of DRG and brain processed for CO immunohistochemistry by the PAP method. The points on each curve represent repeated optical density measurements in the same neuron and each curve represents an individual neuron in lumbar DRG (A), hippocampus (B) substantia nigra pars reticulata (C) and cerebellum (D).

Fig. 2. Photomicrographs of pairs of adjacent sections of lumbar DRG processed immunohistochemically (A,C,E) or histochemically (B,D,F) for CO. A is adjacent to B, C to D, and E to F. Low (A,B) and high (C,D) magnification showing correspondence of staining intensities in large cells. Corresponding lightly stained cells are indicated by arrowheads and densely stained cells by arrows in A,B and C,D. (E,F) Higher magnification showing correspondence of staining intensities in some small cells (arrows). Magnifications: A,B, X85; C-F, X205.

Fig. 3. Correlation between CO content and CO activity in neurons of adjacent DRG sections. Each point represents the optical density of a neuron stained histochemically for CO and the optical density of the same neurons stained immunohistochemically for CO in adjacent sections. The line through the data points was derived by linear regression analysis. (A) Data from all of the 89 neurons that were analyzed. (B) The same data as in A but with exclusion of 25% of corresponding neurons in adjacent sections exhibiting the greatest difference in area.

Fig. 4. Photomicrographs showing immunohistochemical localization of CO in neurons of hippocampus (A), substantia nigra pars reticulata (B), and cerebellum (C). (A,B) Immunolabelling is seen within processes of some densely stained hippocampal and nigral cells (arrows). (C) Immunoreactivity is seen largely within Purkinje cell bodies (arrows) and neurons located in the molecular layer (arrowheads). Abbreviations: SR, stratum radiatum; SP, stratum pyramidale; SO, stratum oriens; GCL, granule cell layer; PCL, Purkinje cell layer; ML, molecular layer. Magnifications: A,B,C X250.

Fig. 5. Photomicrographs showing CO- and PV-immunoreactivity in neurons of lumbar DRG. All sections except that in E were processed first for CO- immunohistochemistry by PAP and then for PV by immunofluorescence. (A,B) Low magnification of the same section showing CO-immunolabelling in neuronal cytoplasm (A) and PV-immunofluorescence in neuronal nuclei (B). Neurons densely stained for CO (arrowheads) exhibit PV-IR nuclei (arrows). (C,D,E) Photomicrographs of the same section (C,D) showing CO-immunolabelling (C) and PV-immunofluorescence (D) and an adjacent section (E) showing PV- immunofluorescence. Neurons with dense CO-immunostaining (arrows in C) exhibit PV-IR nuclei (arrows in D) and PV-IR cytoplasm (arrows in E). (F,G) Higher magnification showing CO-immunolabelling (F) and PV-immunofluorescence (G) in the same section. Note that faint cytoplasmic PV-immunofluorescence is evident in densely CO-immunostained cells (arrows) and that those cut through the nucleus exhibit PV-IR nuclei (arrowheads). Magnifications: A,B, X185; C,D,E, X150; F,G, X330.

Fig. 6. Pairs of photomicrographs of the same section showing PV-immunofluorescence (B,D,F,H) and CO-immunostaining (A,C,E,G) in cortex and various regions of the hippocampus. The sections were processed immunohistochemically for CO by PAP and then for PV by immunofluorescence. (A, B) Cingulate cortex. (C,D) Hippocampal CA3 region. (E,F) Higher magnification of the CA3 region. (G,H) Hippocampal CA1 region. Note that neurons densely stained for CO exhibit PV-immunoreactivity (arrows). Magnifications: A,B, X135; C,D, X70; E,F, X145; G,H, X175.

Fig. 7. Pairs of photomicrographs of the same section showing CO immunostaining density (A,C,E) in PV-IR neurons (B,D,F) in various structures of the basal ganglia. (A,B) Substantia nigra pars reticulata. (C,D) Globus pallidus. (E,F) Striatum. Note the relatively light CO-immunostaining in PV-IR striatal cells. Arrows indicate corresponding cells in each pair of photomicrographs. Magnifications: A,B, X205; C,D, X130; E,F, X125.

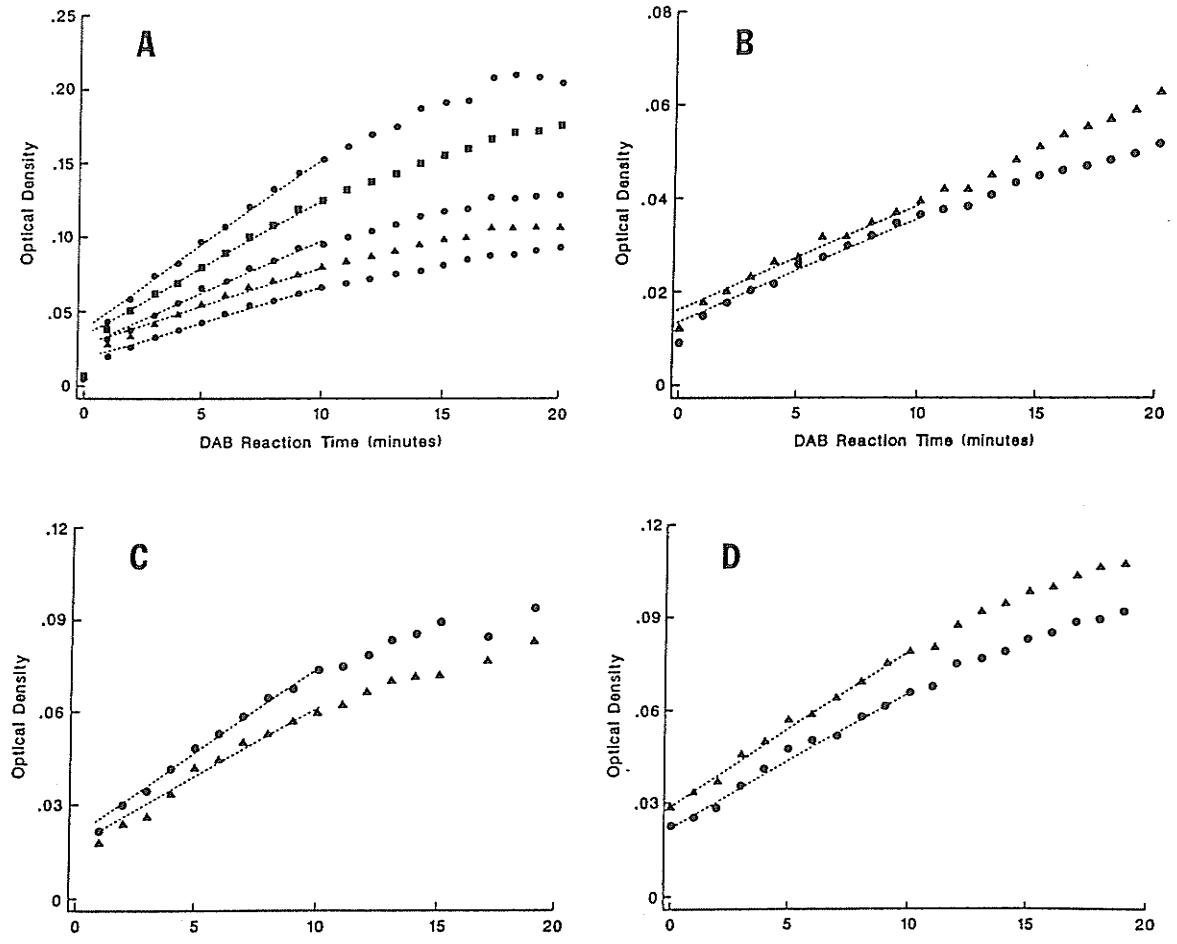
A
B
C
D
Optical Density
DAB Reaction Time (minutes)
.25
.20
.15
.10
.05
0
.08
.06
.04
.02
.12
.09
.03
5
10
15
20

Figure 1

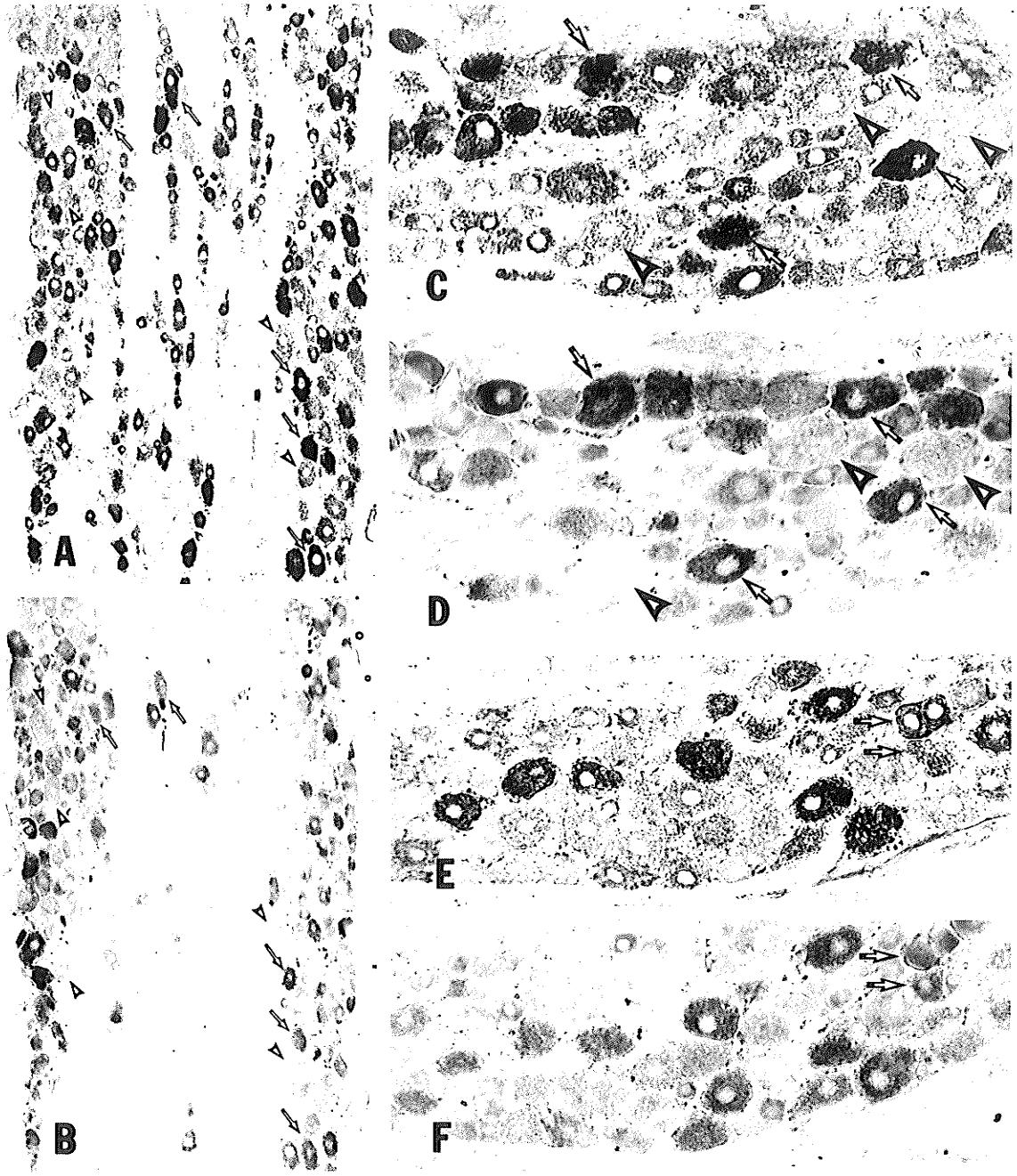

Fig. 2

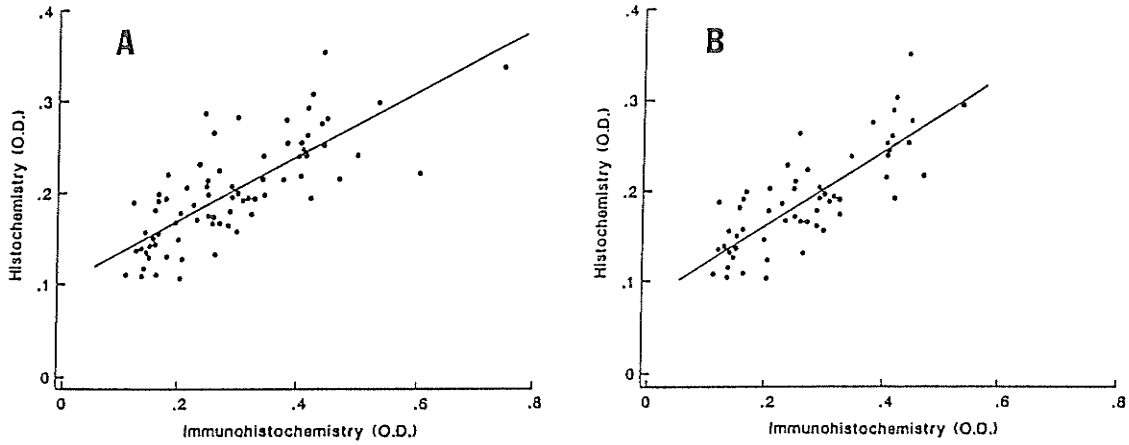

Figure 3

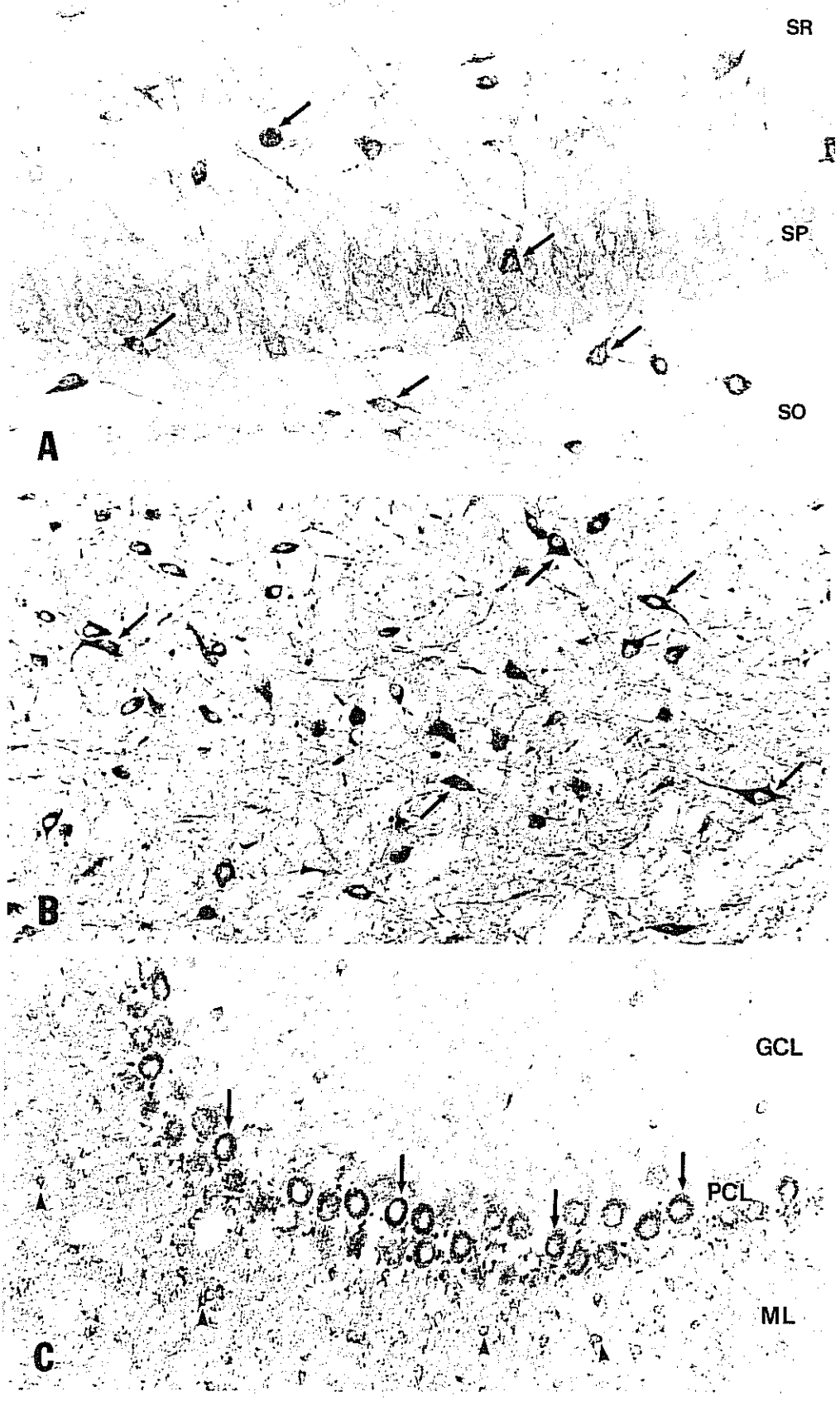

Fig. 4

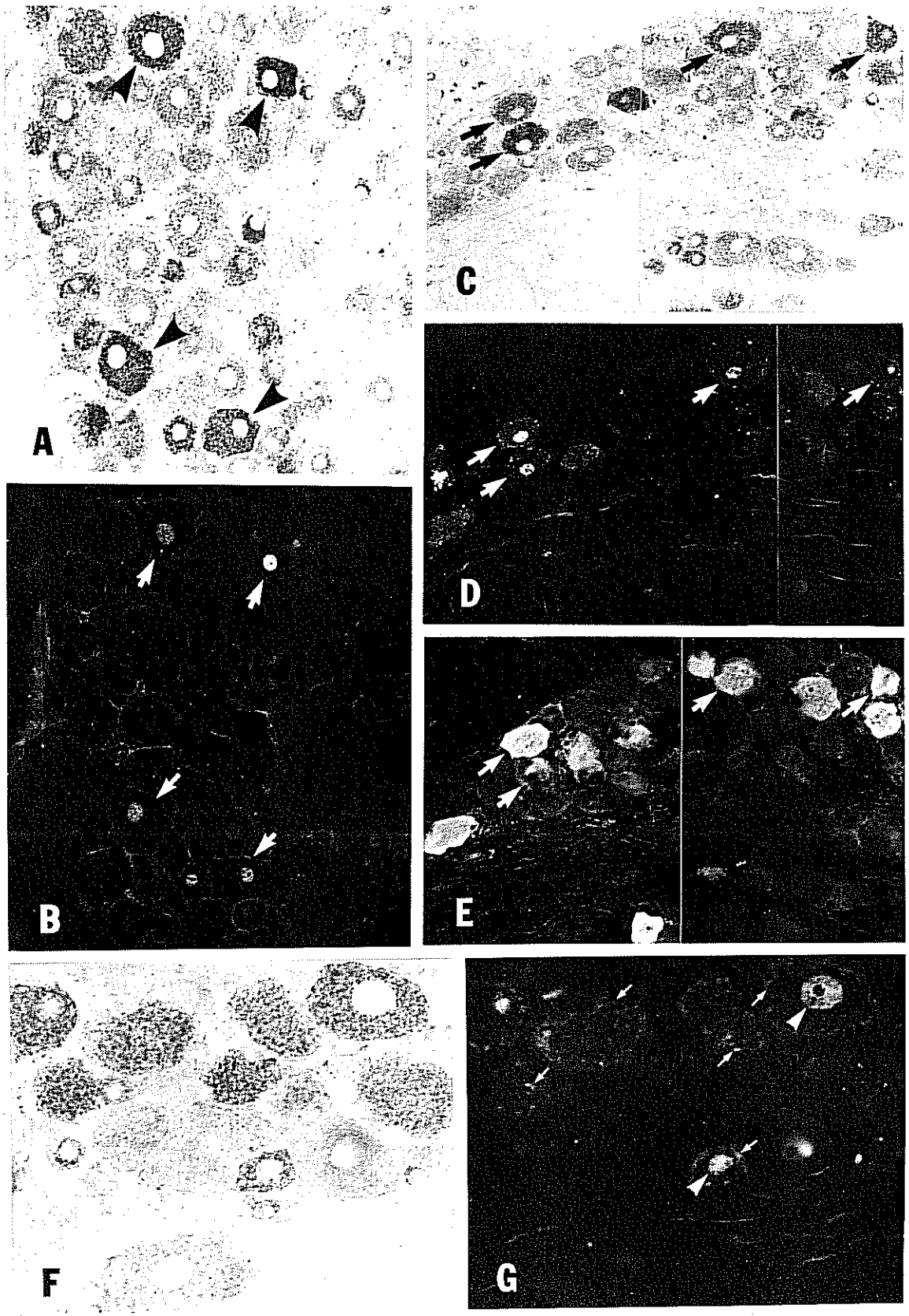

Fig. 5

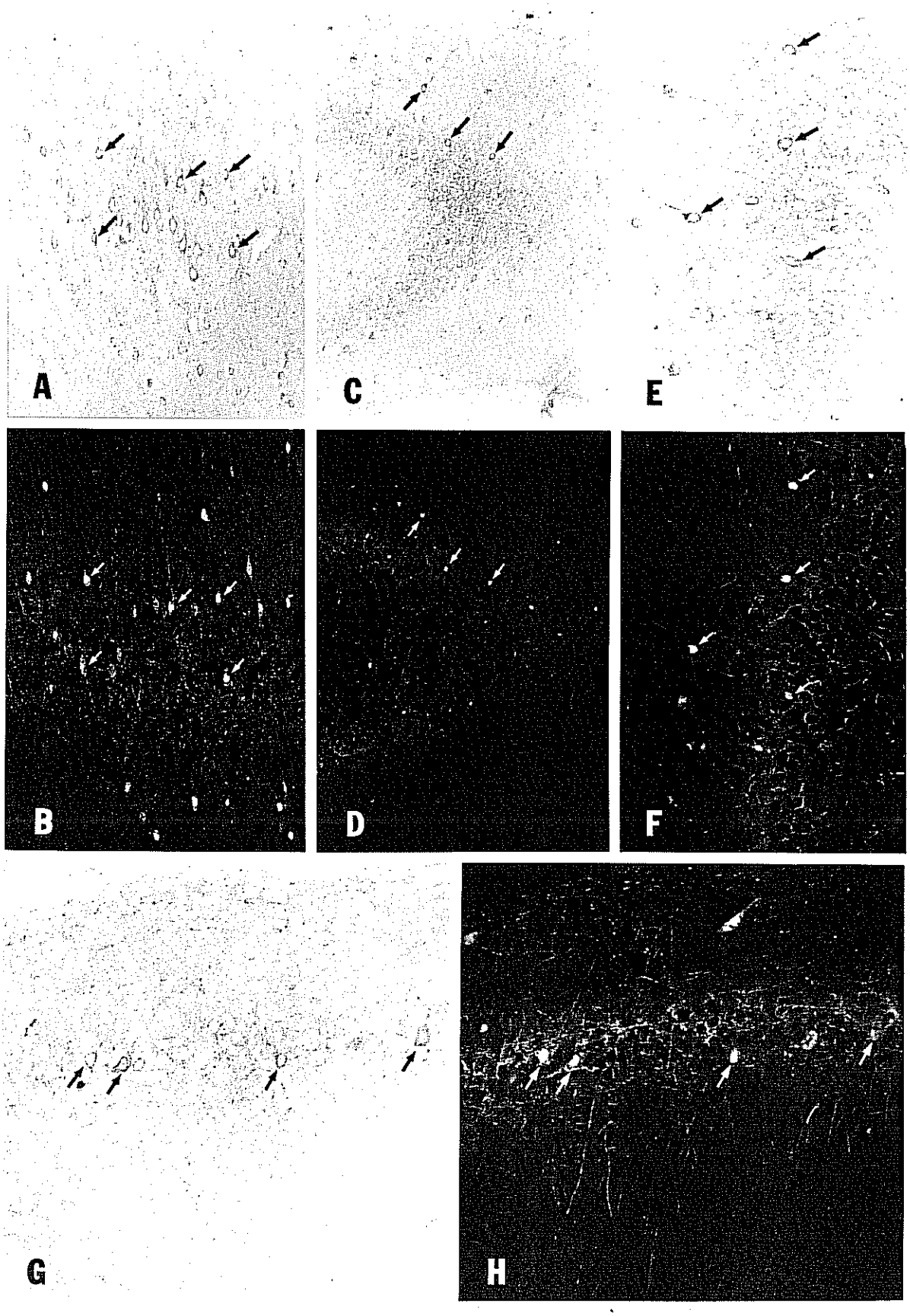

Fig. 6

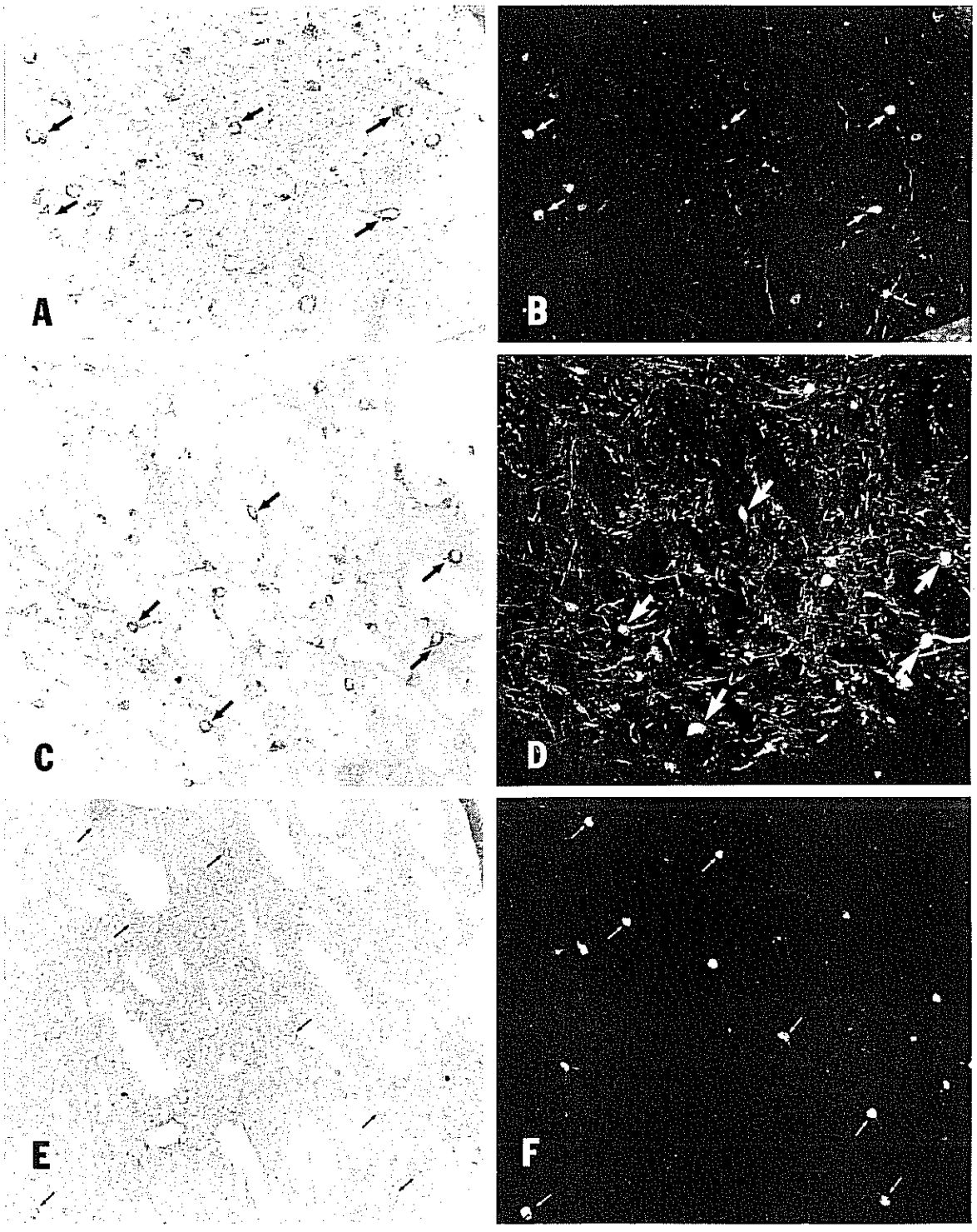

Fig. 7

Part VI

Cytochemical relationships and central terminations of a unique population of primary afferent neurons in rat

P.A. Carr, T. Yamamoto, G. Karmy, and J.I. Nagy

Brain Research Bulletin (1991) 26; 825-843

Abstract--Light and electron microscopic immunohistochemical techniques were used to investigate the central projections and colocalization relationships of a subpopulation of primary afferent neurons that were immunolabelled with an antibody (AB893) against rat liver gap junctions. In lumbar dorsal root ganglia AB893-immunoreactivity was seen in 14.5% of all cells and in both small and large size neurons. Colocalization analysis showed that 78% of all AB893-immunoreactive (AB893-IR) neurons contained calcitonin gene-related peptide, while only 7 to 10% contained the calcium binding proteins parvalbumin or calbindin D28k. Among small type B AB893-IR ganglion cells, it was calculated that over 90% contained fluoride-resistant acid phosphatase, while only 1 to 2% contained substance P or somatostatin. Cytochrome oxidase histochemistry revealed light staining in the vast majority of AB893-IR cells. In the dorsal horn of the spinal cord the antibody labelled fibers in the dorsal root, Lissauer's tract, lamina I and lamina II. Isolated immunoreactive fiber bundles were arranged in sheets spanning most of lamina II. Immunoreactive fibers were depleted from the dorsal horn after dorsal rhizotomy or neonatal capsaicin treatment. Ultrastructural examination showed that AB893-IR fibers were composed of closely associated clusters of 2 to 5 unmyelinated fibers each ranging from 0.1-0.4 μm in diameter. Immunoreactivity was distributed intermittently along the cytoplasmic membrane of axons and en passant sinusoid terminals located centrally within the fiber clusters, as well as along axonal membranes adjacent to the central axon or terminal. The results suggest that the immunoreactive fibers in lamina II of the dorsal horn originate from a subpopulation of AB893-IR neurons that contain FRAP and give rise to unmyelinated axons.

Ultrastructural, electrophysiological and dye-transfer studies conducted over the past two decades have provided a steady accumulation of evidence for the presence of gap junctions between neurons in many major structures of the mammalian central nervous system (CNS) (11). This evidence together with the establishment of gap junctions as the morphological correlate of electrotonic coupling between excitable cells, has led to a recent resurgence of interest in electrical synapses and electrotonic communication between central neurons in higher vertebrates. Attention in this area has been further aroused by the identification of the structural protein constituents of gap junctions, namely connexins, and by the availability of anti-connexin antibodies that allow immunohistochemical analysis of connexin expression and localization in neural tissues. In such studies of the CNS of several species, we have found that while antibodies against some of the known connexins (connexin32 and connexin43) clearly recognize gap junctions between a variety of cell types (27,36,40,42,43), a few antibodies against connexin32 also recognize cellular structures that are currently not thought to have morphological or functional features traditionally associated with gap junctions (27,28,36,40-42). Moreover, on Western blots some recognize potentially novel proteins the nature of which remain to be determined. In the course of a systematic immunohistochemical survey of the rat CNS, we found that a polyclonal antibody, designated AB893, against rat liver gap junctions labelled a subpopulation of neurons in dorsal root ganglia (DRG) as well as fibers in the dorsal horn of the spinal cord. Although the proteins recognized by this antibody have yet to be characterized, the appearance of AB893-immunoreactive (AB893-IR) fibers in the spinal cord was remarkable in that it resembled primary afferent arborization patterns previously revealed by classical anatomical methods and by studies of functionally identified single fibers, but did not correspond to any known cytochemically visualized primary afferent termination patterns in the dorsal horn.

In sensory ganglia the population of neurons labelled with the AB893 antibody may represent a novel class of afferents, or they may correspond to DRG neuronal subpopulations previously identified by histochemical or immunohistochemical localization of various endogenous markers. Such markers include the neuropeptides substance P (SP), somatostatin (SOM) and calcitonin gene-related peptide (CGRP) (10), the enzymes fluoride-resistant acid phosphatase (FRAP), cytochrome oxidase (CO) and carbonic anhydrase and the calcium binding proteins parvalbumin (PV) and calbindin D28k (CaBP) (3-5,9,24). Although several of these markers are colocalized within DRG neurons indicating considerable overlap of the various populations they individually define, those markers that are found to a considerable extent within separate sets of cells are of particular interest. Thus, SP, SOM and FRAP have been found largely, if not exclusively, in separate populations of small type B DRG cells (24). Among large type A cells, we have described a population that have high levels of CO and contain PV and CaBP, and a somewhat separate population that contains CGRP (3,4). One of the goals of studies designed to categorize DRG neurons according to their cytochemical profiles is to establish whether a relationship exists between certain characteristic profiles that cells display and the sensory modalities they transmit, ie. a relationship between cytochemical organization and function. The distinct pattern of AB893-IR fibers in the dorsal horn may provide an opportunity to deduce such relationships.

In order to determine which of the previously characterized DRG neuronal populations give rise to AB893-IR fibers in the dorsal horn and whether the anatomical arrangement of these fibers can be correlated with that of functionally-identified primary afferents, the aim of the present study was to identify the cytochemical markers contained in AB893-IR lumbar DRG neurons and to document the central distribution and morphology of AB893-IR primary afferent fibers. The results are considered primarily in relation to known organization patterns of primary afferents in the spinal

cord dorsal horn (12).

METHODS

Tissue Preparation

For light microscopy, a total of 50 male Sprague-Dawley rats (Charles River) weighing 220-320 g were anesthetized with chloral hydrate and perfused transcardially with 60 ml of cold (4°C) 0.9% saline containing 0.1% sodium nitrite and 60 units of heparin. This was followed by 400 ml of cold freshly prepared fixative consisting of either 4% paraformaldehyde or 4% paraformaldehyde and 0.16% picric acid in 0.1 M sodium phosphate buffer, pH 7.4 (44). The medulla and spinal cord along with sensory ganglia from the trigeminal, cervical, thoracic, lumbar and sacral levels were removed immediately after perfusion and post-fixed for 2 or 18 hr in cold fixative. Ganglia were then stored in cryoprotectant consisting of 15% sucrose and 0.001% sodium azide in 0.1 M sodium phosphate buffer (pH 7.4) and brain stem/spinal cord samples in 25% sucrose and 10% glycerol in 50 mM sodium phosphate buffer (pH 7.4) for at least two days. Sections of DRG were cut on a cryostat (Leitz) at a thickness of 7-10 μm and thaw-mounted onto gelatinized slides. Transverse, sagittal or horizontal sections of spinal cord and medulla were cut on a sliding microtome at a thickness of 20 μm and collected in cold 0.1 M sodium phosphate buffer, pH 7.4, containing 0.9% saline (PBS).

Experimental Manipulations

The contribution of unmyelinated primary afferent fibers to AB893-IR structures in the spinal cord was determined in animals treated with the sensory neurotoxin capsaicin. Tissue was obtained from three 10 to 12 week old rats that had been injected 48 hr after birth with a single subcutaneous dose of capsaicin (50 mg/kg) in 10% ethanol, 10% Tween-80 and 0.9% sterile saline. Three control littermates received equal volumes of vehicle (25,26). The effectiveness of the capsaicin treatment was confirmed by counts of

FRAP-positive neurons remaining in DRG of capsaicin injected rats compared with the numbers present in vehicle treated controls. The total primary afferent contribution of AB893-IR fibers in the dorsal horn was examined in 3 animals given unilateral dorsal rhizotomy of the 1st to 4th lumbar roots as previously described (13). In brief, three adult male rats were deeply anaesthetized with 2 ml/kg equithesin (4.2% chloral hydrate, 1% pentobarbital and 2.2% magnesium sulfate in 11.5% ethanol and 43% propylene glycol). A dorsal rostrocaudal incision medial to the iliac crest was then performed to permit partial laminectomy of the 3 lower lumbar vertebrae. The first to fourth lumbar roots caudal to their spinal cord dorsal root entry zone were then exposed on one side of the spinal cord, transected with fine surgical scissors and the wound closed. Animals were allowed to survive 12 to 15 days after surgery.

Immunohistochemistry

Sections were incubated with a polyclonal sheep antibody generated against isolated rat liver gap junctions. This antibody has been characterized as previously described (16-19,27,36,40). Immunohistochemical controls included sections processed with either preimmune serum or preadsorbed antibody at the same concentration as the primary antibody or omission of the first antibody (40). Spinal cord, brainstem and DRG sections processed by the biotin/streptavidin-peroxidase method were incubated for 40-68 hr at 4°C with primary antibody diluted 1:350 to 1:2000 in PBS containing 0.3% Triton X-100 (PBS-T), washed for 40 min in PBS-T, and incubated for 1.5 hr at room temperature with biotin-conjugated donkey anti-sheep antibody (1:100 in PBS-T). The tissue was then again washed for 40 min in PBS-T, incubated for 1.5 hr with horseradish peroxidase-conjugated streptavidin (1:150 in PBS-T) and washed for 20 min in PBS-T followed by 20 min in 50 mM Tris-HCl buffer (pH 7.4). Peroxidase activity was visualized by reaction of the tissue in 50 mM Tris-buffer (pH 7.4) containing 0.005% hydrogen peroxide and 0.02% diaminobenzidine tetrahydrochloride. Free floating spinal

cord sections were mounted on slides from gelatin-alcohol and dehydrated in alcohol, cleared in xylene and coverslipped with Lipshaw mounting medium. For DRG sections processed by immunofluorescence, sections were incubated with primary antibody as described above, washed and then incubated for 1.5 hr at room temperature with Texas Red-conjugated avidin diluted 1:50 in PBS-T. The tissue was then washed for 40 min in PBS-T and either taken directly for the next immunofluorescence procedure or coverslipped, photographed and washed again prior to the next histochemical procedure. Triton X-100 was excluded from the incubation media and all washes for tissue to be subsequently processed for CO.

Colocalization analyses in DRG

The relationship of AB893-IR DRG neurons to sensory neurons immunoreactive for CGRP, PV or CaBP as well as the CO histochemical staining density displayed by AB893-IR ganglion cells were examined in both adjacent and double-stained sections. Analysis of adjacent sections served, in part, as controls for the double labelling procedures which allow rapid examination of a large number of cells. Due to technical limitations in examining sufficient numbers of corresponding small cells in adjacent sections, all analyses of colocalization of AB893-immunoreactivity with the small cell cytochemical markers SP, SOM and FRAP were conducted using only double- labelled sections of DRG.

Adjacent Section Procedures. Adjacent cryostat sections were cut at a thickness of 7 or 8 μm and alternate sections were collected on separate slides. One set of an adjacent series of sections was processed by the biotin/streptavidin-peroxidase method for detection of AB893-IR cells as described above and the other was processed either by immunohistochemistry for CGRP, PV or CaBP or by histochemistry for CO as previously described (4). Following the immunohistochemical procedures, the sections

were dehydrated in alcohol, cleared in xylene and coverslipped with Lipshaw mounting medium. Histochemistry for CO on one set of adjacent sections was conducted as previously described (5). Both cytochrome oxidase reacted and their adjacent sections were dried and coverslipped with 3:1 glycerol-water. Corresponding areas in adjacent sections were then photographed to allow identification of the same cells in photomicrographs.

Double-labelling Procedures. All double immunofluorescence was conducted by sequential processing of sections rather than simultaneous incubation with primary antibodies. The sequential method gave a somewhat higher quality of staining. Sections were reacted initially to reveal AB893-IR neurons by immunofluorescence. Subsequent immunofluorescence localization of SP, SOM, CGRP, PV or CaBP was then undertaken using previously described (3,4,26) primary antisera to these in PBS-T at dilutions of 1:1000, 1:1000, 1:500-1:4000, 1:400-1:2000 and 1:400-1:2000, respectively. The tissue was incubated for 40-68 hr at 4°C, washed for 40 min in PBS-T and then incubated for 1.5 hr with fluorescein isothiocyanate (FITC)-conjugated donkey anti-rabbit IgG (Amersham) at 1:20 in PBS-T. Sections processed by double immunofluorescence were then washed for 40 min in PBS-T, coverslipped with anti-fade medium (38) and photographed. Sections taken for subsequent histochemical procedures for CO or FRAP were first coverslipped, photographed, and then the coverslips were removed. Sections to be reacted for CO were coverslipped with 3:1 glycerol-water and after photography, the coverslips were removed in 0.1 M sodium phosphate buffer, pH 7.4, (PB) and the sections washed for 40 min in PB prior to CO histochemistry (5). Following the CO reaction, the sections were coverslipped with 3:1 glycerol-water and rephotographed. Sections taken subsequently for FRAP histochemistry were coverslipped with 5% sucrose in 20 mM Tris-maleate buffer (pH 5.0) and after photography the coverslips were removed in the same medium without sucrose and the sections were washed

overnight in cold (4°C) Tris-maleate buffer. The tissue was then reacted for FRAP as previously described (6), coverslipped with 3:1 glycerol-water and rephotographed.

Data analysis

Although immunoreactive cells were observed at all levels, detailed analysis of the number and size distribution of AB893-IR neurons and the colocalization of immunoreactivity with other cytochemical markers was undertaken using sections of 4th or 5th lumbar DRG. Documentation of colocalization was conducted from inspection of photomicrographs of both adjacent and sequentially processed sections. Some peroxidase reacted spinal cord sections were counterstained with thionin or luxol fast blue/cresyl violet and examined by brightfield or darkfield illumination to allow assessment of the laminar localization of immunoreactivity. Analysis of the size distribution of AB893-IR of DRG cells was undertaken by image analysis (Amersham RAS-1000) of immunoperoxidase reacted sections that had been counterstained with toluidine blue to allow visualization of cellular nucleoli (5). Only cells with visible nucleoli were selected for areal quantification. Cells were categorized as very small ($\leq$500 μm^2), small (>500 to $\leq$1000 μm^2), intermediate (>1000 to $\leq$1800 μm^2) or large (>1800 μm^2) as previously described (5). Microscope counts of AB893-IR DRG cells were undertaken on fluorescent sections counterstained with ethidium bromide to allow selection of only those cells displaying nucleoli.

Electron microscopy

A total of six animals were perfused with saline wash as described above and then with 4% paraformaldehyde containing 0.2% picric acid, 0.2% glutaraldehyde and 0.1 M sodium phosphate buffer (pH 6.9). This was followed by postfixation of the spinal cord for 2 hr at 4°C in the same fixative without glutaraldehyde. Transverse or sagittal sections of the lumbar spinal cord were cut on a vibratome at a thickness of 20-30 μm

and washed overnight at 4°C in 0.1 M sodium phosphate buffer, pH 7.4. The sections were processed for immunohistochemistry by the biotin/streptavidin-peroxidase method as described above except that 0.15% Photo-Flo 200 (Kodak) instead of 0.3% Triton X-100 was used in all incubation and wash steps. Immunostained sections were then further fixed for 2 hr at room temperature in 2% osmium tetroxide diluted in 0.1 M sodium phosphate buffer, pH 7.4, dehydrated in ethanol, infiltrated with propylene oxide, and flat-embedded in resin (Jembed) between coated (Sigma-coat) glass slides. The desired areas of the dorsal horn were trimmed and glued onto resin blocks. Ultrathin sections were mounted on slit or mesh grids, counterstained with lead citrate for 0.5-1 min, and examined using a Philips-201 electron microscope.

RESULTS

General observations

All animals gave qualitatively reproducible AB893-IR patterns of staining at all medullary and spinal cord levels and in DRG sections processed by either peroxidase or fluorescence methods. In each of these areas, neuronal elements exhibited the most intense immunoreactivity. In no instances were immunoreactive neuronal cell bodies observed in the dorsal spinal cord, although lightly stained glial cell bodies and processes were seen dispersed in regions of white matter at some brain stem and spinal cord levels. On occasion, smooth homogeneous staining of the walls of blood vessels was seen in both spinal cord and DRG. This appeared to be an animal-specific phenomena as it was present in tissue of some animals, but was totally absent in others.

The results of tests for antibody specificity were similar to those we previously described in studies of AB893-IR structures in hippocampus (40); no staining was seen with preimmune serum or after omission of primary antibody; preadsorption of the antibody with purified rat liver gap junctions resulted in a substantial reduction of

immunostaining in both DRG (Fig. 2C,D) and spinal cord (not shown). Specificity tests by other methods have been previously discussed (27,36,40). In controls conducted for double immunofluorescence labelling, no cross-reactions were seen between the various primary antibodies used and inappropriate secondary antibodies.

AB893-IR DRG neurons

Two distinct forms of intracellular AB893-immunoreactivity were seen within neuronal cell bodies in trigeminal (Fig. 1A), cervical (Fig. 1B), thoracic (Fig. 1C), lumbar (Fig. 2A,B) and sacral (Fig. 1D) sensory ganglia. Granular immunoreactivity characterized by punctate or globular structures was seen in both large and small cells and was likely associated with the Golgi apparatus (Fig. 2A,B). Some small cells contained granular as well as dense, diffuse staining that filled much of the cytoplasm (Fig. 2B). Cellular nuclei were unstained. Occasionally, immunoreactive fibers arose from cells with either type of staining (Fig. 2A,B). From an examination of 4165 neurons in L4 and L5 DRG, the proportion found to be AB893-IR was 14.5%. Positive neurons ranged from 340 $\mu m^2$to 4577 μm^2 in area which encompassed the size distribution of the entire DRG cell population. However, a lower percentage of AB893-IR cells fell in the very small ($\leq$500 μm^2) size range than in the large (>1800 μm^2) and intermediate (>1000 $\mu m^2$and $\leq$1800 μm^2) size ranges (Table 1). Of 421 AB893-IR cells analyzed for size, 2.9% were very small, 32.3% were small, and 32.8% were found in each of the intermediate and large size categories. We are uncertain of the extent to which these quantitative results are representative of sensory ganglia at other levels.

<u>Colocalization with PV, CaBP, CGRP and CO</u>. Analyses of adjacent and double-labelled sections for the presence of PV or CaBP or for the levels of CO activity in AB893-IR DRG cells gave similar results and therefore all data obtained by the two procedures were combined. A small number (Table 2) of both large type A and small

type B AB893-IR neurons contained either PV (Fig. 3A,B) or CaBP (Fig. 3C,D). Neurons containing AB893-immunoreactivity consistently displayed what was considered to be the lightest CO staining seen in DRG neurons (Fig. 3E,F, Table 2). Comparison of the AB893-IR DRG cell population with CGRP-IR cells in adjacent immunoperoxidase reacted sections (Fig. 4A,B) and in double immunofluorescence labelled sections (Fig. 4C,D) showed that a large number of various sized AB893-IR cell bodies contained CGRP (Table 2). Conversely, 34.5% of the CGRP-IR cells were AB893-IR. Occasionally, doubled-labelled axons were also observed.

Colocalization with SP, SOM and FRAP. In comparisons of the AB893-IR small type B cell population with the markers SP (Fig. 5A,B), SOM (Fig. 5C,D) and FRAP (Fig. 5E,F), it was found that very few AB893-IR cells contained SP or SOM immunoreactivity, while nearly all such cells contained FRAP (Table 2). A much smaller percentage (22%) of FRAP-containing cells were AB893-IR; this was expected since the former far outnumber the latter.

Brainstem and spinal cord

In the medulla and spinal cord the AB893 antibody gave distinctive labelling of fibers in the nucleus of the solitary tract (Fig. 6A), in the spinal trigeminal subnucleus caudalis (Fig. 6B) and in the superficial regions of the cervical, thoracic and lumbar spinal cord. At brainstem (Fig. 6C) and at thoracic (Fig. 6D) and other spinal cord levels immunoreactive fibers were seen in isolation or in bundles. Fiber staining was characterized by robust immunoreactivity that resembled Golgi-impregnated preparations thereby revealing fine morphological details. Many fibers and their branches could be followed for long distances in a section with no apparent reduction in staining density along their length.

Fiber organization. Detailed analysis of the organization of AB893-IR fibers was undertaken at midlumbar levels in transverse, sagittal and horizontal sections. In each plane of section, AB893-IR fibers were seen in various superficial regions of the dorsal spinal cord including dorsal roots, Lissauer's tract, lamina I and lamina II. In dorsal roots located adjacent to the spinal cord, individual non-varicose AB893-IR fibers approximately 0.7-1 μm in diameter could be followed for considerable distances in sagittal sections (Fig. 7A,B) and, on occasion, could be seen coursing toward or into Lissauer's tract or lamina I (Fig. 7A). In Lissauer's tract AB893-IR smooth fibers of similar diameter were seen as rostrocaudally coursing axons in sagittal sections (Fig. 7A) and as short cross-cut segments in transverse sections (Fig. 7C). Some fibers emerged from Lissauer's tract and were spread across lamina I (not shown), while others penetrated ventrally into lamina II (Fig. 7C). In most instances, fibers in lamina I did not appear to give rise to ventrally directed processes. Solitary fibers oriented dorsoventrally were seen interspersed between lamina II fiber bundles (Fig. 7D,E) and these may have originated from either ventrally directed superficial fibers or dorsally directed ventral fibers (Fig. 7D).

In lamina II, AB893-IR fibers were arranged in discrete bundles or plexi. In transverse sections 1-15 bundles were observed on each side of the cord (Fig. 7F,G) with a more frequent occurrence in lateral than medial dorsal horn regions. The long axes of these plexi were arranged perpendicular to the curvature of the dorsal horn surface such that they had a dorsoventral orientation medially and a horizontal orientation laterally. Determination of the position of the fiber bundles in relation to the dorsal horn lamina in either thionin (Fig. 7F) or luxol fast blue/cresyl violet counterstained sections indicated that they reached the lamina II/III border and were situated largely within lamina II inner (IIi) and partially in lamina II outer (IIo). In the extreme lateral portion of the dorsal horn, bundles closely approaching the dorsal horn surface occupied a greater extent of

lamina IIo.

In sagittal and horizontal sections the radial bundles of lamina II fibers were seen to comprise aggregates of axons interwoven in complex longitudinally organized plexi (Fig. 8A,B). It was also apparent in horizontal sections (Fig. 8B) that longitudinally adjacent fiber plexi abutted each other and therefore were contained within discrete and much longer rostrocaudally organized sheets distributed across the mediolateral plane. Despite such abutments individual plexi were recognized by the mediolateral tapering of their extremities. From measurements in the three planes of section, individual plexi were situated 12-100 μm from the dorsal horn dorsal border with the lateral arbors more superficial and slightly smaller than those located medially. The bundles were composed of 20-35 fibers and spanned an average distance of 70 μm dorsoventrally (range 35-120 μm), 26 μm mediolaterally (range 12-50 μm) and 400 μm rostrocaudally (range 200-600 μm). They were mediolaterally separated by an average distance of 20-25 μm. Individual plexi were composed of fibers with diameters distributed over a continuum ranging from <0.5 μm up to about 1.0 μm and were characterized by a dorsal and ventral zone of more or less rostrocaudally oriented smooth fibers and a central zone of highly convoluted fibers with associated boutons that appeared to be concentrated within a narrow region in the middle of the plexus (Fig. 8A).

Fiber morphology. Varicosities and presumed terminal boutons were seen in association with fibers in lamina II in all three planes of section, but were most evident in sagittal or horizontal sections due to the rostrocaudal orientation of fiber plexi. Four common types of axonal enlargements were recognized. Least prevalent were axonal varicosities (Fig. 9A). These had average lengths of 2-4 μm and widths of 1-2 μm and were, in general, smaller than bouton endings. Round or oval enlargements were seen at the ends of long fibers (fiber boutons) and at the ends of short stalks arising from larger

fibers (stalk boutons) (Fig. 9B). Boutons at both locations had similar morphology and comprised two broad size classes; the average maximum and minimum diameters of small terminals was 1x1.5 μm and that of large terminals was 2 x 4 μm. On occasion, varicosities were seen at the origin of fiber stalks which themselves gave rise to stalk boutons (Fig. 9C). Multiple stalk- type boutons similar in morphology to solitary stalk elements were seen grouped in what was termed cluster boutons (Fig. 9D). Less commonly seen were large, amorphous boutons with dimensions of 2-3 μm and 7-8 μm along their short and long axis.

Many examples were found of large and medium diameter AB893-IR fibers that exhibited what appeared to be perforated expansions or bubble-shaped structures approximately 2-4 μm in diameter. The inner area of these elements were devoid of staining and their walls were usually smaller in diameter than the parent fiber from which they arose (Fig. 9E). The expansions were quite numerous in some plexi and occasionally several were seen along a single fiber. Also visible under high magnification were small, very lightly stained fibers less than 0.3 μm in diameter (Fig.9F). Although the light staining of these fibers precluded detailed analysis, their morphology appeared to be similar to the larger more densely immunoreactive fibers.

Capsaicin treatment and dorsal rhizotomy

In lumbar ganglia of capsaicin treated compared with littermate vehicle- injected animals there was a 67% reduction in the number of AB893-IR small cells ($\leq$1000 μm^2) and this coincided with a 56% reduction in the number of FRAP-containing cells. In spinal cord sections of animals that received neonatal capsaicin treatment, AB893-IR fibers were depleted at both thoracic (Fig. 10A) and lumbar (Fig. 10B) spinal cord levels. As shown in transverse (Fig. 10C) and sagittal sections (Fig. 10D), immunoreactive fibers were also eliminated in the upper lumbar dorsal horn of rhizotomized animals.

EM Observations

In vibratome sections of dorsal horn prepared for electron microscopy and viewed by LM, the configurations of AB893-IR fibers seen in lamina II were similar to those observed in LM preparations described above. In ultrathin transverse sections, AB893-IR fibers in laminae II were seen among sparsely distributed myelinated fibers. They were arranged in clusters composed of 2 to 5 cross-sectioned unmyelinated fibers ranging from 0.2-0.3 μm in diameter (Fig. 11A). A large axon terminal about 1.0 μm in diameter was often seen near the center of an immunoreactive cluster. These terminals contained a few mitochondria and large clear vesicles, and many spherical agranular synaptic vesicles 30-50 nm in diameter (Fig. 11A). They occasionally extended thin (0.1-0.2 μm) short processes that partially enveloped the more peripherally located fibers (Fig. 11C) or were interdigitated with these fibers (Fig. 11B). Various types of neuronal processes surrounding the central terminal included: 2-4 small, generally round fibers (0.1-0.2 μm) containing several microtubules; 1-3 comparatively large fibers 0.5-1.0 μm in diameter containing endoplasmic reticulum, microtubules and a few mitochondria; and axon terminals 0.4-0.6 μm in diameter containing sparsely distributed spherical synaptic vesicles 30-50 nm in diameter. Large fibers frequently indented central terminals at sites of typical asymmetric synaptic contacts (Fig. 11A). In addition to these components, dendritic spines were occasionally seen in apposition to the central and peripherally located terminals (Fig. 12A).

In sagittal sections the arrangement of immunolabelled unmyelinated fibers (Fig. 12A) was similar to that seen in transverse sections. Although individual longitudinally running fibers varied from 0.1-0.4 μm in diameter, they were clustered in bundles that had a roughly constant diameter of about 1.0 μm. Along their course within the bundles, single fibers frequently became enlarged to form en passant terminals at sites where

adjacent fibers narrowed in calibre to about 0.1 μm. AB893-immunoreactivity in these fiber bundles was distributed on very nearly the entire cytoplasmic membrane of the centrally located axon including sites where it formed en passant terminals. Peripherally located fibers were labelled only at regions where their cytoplasmic membranes were apposed to the centrally located fibers (Fig. 11D). Although immunoreaction product was deposited on both the inner and outer leaflets of the plasma membrane, the outer leaflet was more densely immunostained. Immunolabelling tended to be discontinuous along the membranes of elements within the fiber cluster. Occasionally, immunoreactive axons exhibited intermittent regions of close apposition where the extracellular space ranged from 4 to 6 nm and was sometimes filled with immunoreaction product. The close appositions varied from 30-200 nm in length and were separated from one another by distances of 60-100 nm (Fig. 12B). These sites of closely apposed membranes were densely labelled and axonal membranes that were more widely separated had an extracellular space of about 10 nm and exhibited weak or no immunoreactivity.

DISCUSSION

Dorsal root ganglia

It has been previously demonstrated that the antibody utilized here recognizes neuronal and glial gap junctions in rat hippocampus (27,36,40) and weakly electric fish brain (42). However, the appearance of labelled primary afferents is unlike labelling seen in other CNS regions and very probably represents a cross-reaction with a novel protein. In view of our uncertainty regarding the identity of this protein, the present results are discussed entirely in the context of primary afferent anatomical organization. However, we do not exclude the possibility that a connexin-related protein may exist in a certain population of primary afferent neurons and contribute to possible electrotonic coupling between these neurons.

The dual intracellular staining pattern seen in DRG, namely granular and diffuse cytoplasmic AB893-immunoreactivity, has also been observed in studies of peptides in DRG neurons (10), but its significance remains to be explained. Although only the initial axon segments of some large and small AB893-IR cells were stained, some of these axons may give rise to the immunoreactive fibers seen in dorsal roots. The cytochemical profile of AB893-IR DRG cells is consistent with previously determined colocalization relationships of other substances in sensory neurons. The extensive coexistence of AB893-immunoreactivity with CGRP and minimal coexistence with PV or CaBP is in accordance with our observations that the AB893-IR/CGRP population comprises both large and small cells and that the large CGRP-IR cell population is to a great extent separate from the PV-IR and CaBP-IR populations (3). The very light CO staining densities observed in AB893-IR neurons is also consistent with observations that most DRG cells containing PV or CaBP exhibit dense CO staining (4). Since high CO levels and the presence of PV and/or CaBP may be indicators of neurons with high electrical activity or those with fast-spiking capability (4,5,39), it would appear that the majority of AB893-IR large DRG cells, characterized by their lack of PV and CaBP and light CO staining density, have relatively low levels of electrical activity and do not require the proposed calcium buffering properties of PV or CaBP. The significance of the high level of coexistence between CGRP and AB893-immunoreactivity remains to be determined. Detailed analysis of PV, CaBP and CO in small AB893-IR cells was precluded by technical difficulties involving localization of these markers in cells that could be confidently identified as small DRG neurons. Where cells were clearly recognized as small type B neurons, the results were similar to those obtained for large cells.

The small cell AB893-IR population appears to be represented almost entirely by a subpopulation of type B neurons containing FRAP and overlaps to some as yet undetermined extent with type B cells containing CGRP. This concurs with our previous

observation of considerable coexistence between CGRP and FRAP in DRG neurons of rat (6). The negligible overlap of the AB893-IR and the SP- or SOM-positive cell populations is consistent with reports showing negligible or minimal FRAP coexistence with SP or SOM (9,24).

Origin and composition of AB893-IR dorsal horn fibers

It can be concluded that AB893-IR fibers in the dorsal horn are primary afferents based on: 1) the presence of AB893-IR neuronal cell bodies in DRG; 2) the presence of AB893-IR fibers in dorsal roots; 3) the presence of AB893- immunoreactivity in glomerular central terminals which are known to be of primary afferent origin (22); 4) the elimination of AB893-IR fibers in the dorsal horn after dorsal rhizotomy; and 5) the absence of AB893-IR neurons in the dorsal horn. That these fibers are unmyelinated C-fiber afferents is suggested by: 1) their confinement largely to lamina II which is a characteristic termination zone of C-afferents (37); 2) the presence of AB893-immunoreactivity in FRAP-positive DRG cell bodies which are thought to give rise to C-fibers (34); and 3) the absence of AB893-IR fibers in the dorsal horn of animals treated neonatally with capsaicin at a dose previously demonstrated to be relatively selective for depletion of C-fiber afferents (25). Fibers in the nucleus of the solitary tract may originate from the trigeminal ganglia or from sensory ganglion of the seventh, ninth and tenth nerves, all of which have inputs to this area (2). The latter three ganglia, however, were not examined for the presence of AB893-IR cells. The immunoreactive fibers in the trigeminal nucleus caudalis may also arise from the trigeminal ganglia.

It is difficult to imagine that what so clearly appeared to be individual immunostained fibers at the light microscopic level were, in fact, composed of several immunolabelled unmyelinated fibers arranged in a cluster. Yet, several observations consistent with this interpretation are as follows: 1) Single immunolabelled fibers were never encountered by

EM. Although very lightly labelled, thin (<0.5 μm) fibers were seen in LM preparations, these may represent pre-cluster or a separate class of axons that were rendered undetectable by the stronger fixation conditions used for EM. 2) The average diameter (1 μm) of immunolabelled clusters was similar to that of fibers seen by LM and the calibre of the individual axons within a cluster is consistent with that of unmyelinated fibers (7,14,15). 3) The immunolabelled configurations of central axon terminals and several peripherally located neuronal processes were similar to those found in one of three previously described types of glomerular complexes in lamina II (8,22,30,31,45). The AB893-IR central terminals probably correspond to the dense sinusoid type based on the size of their synaptic vesicles, their axoplasmic density and the presence of axo-axonic synapses. Most of these terminals are known to contain FRAP and all are thought to arise from unmyelinated primary afferents (20,21,23,34). Pertinent here is that immunoreactivity within a cluster was always most clearly associated with central terminals and their fine calibre axons rather than larger diameter axons as might have been expected from LM observations. The presence of label on processes adjacent to these central axons may represent diffusion of reaction product from its possible site of generation on central axons, but we believe not, based on the equal density of label seen on adjacent membranes. However, this point and the perplexing restriction of label to sites of peripheral processes in apposition to the central axons requires further investigation. And 4) A clustered arrangement of fibers may explain the occurrence of what we termed perforated expansions along fibers. Although these may represent an absence of staining within the central regions of single varicosities or a technical artifact of tissue processing procedures, they may alternatively represent regions of strand separations within a fiber cluster. Scalloped terminals with holes somewhat similar to these perforated expansions have been previously reported among fibers in lamina II (1).

At the LM level a possible correspondence between AB893-IR and a subpopulation

of FRAP-positive fibers in lamina II is not immediately obvious. Depending on fixation conditions, fluoride concentrations and incubation conditions, spinal cord sections processed for FRAP histochemistry can yield reaction product deposition that encompasses nearly all of lamina II (unpublished observations). Under more attenuated conditions, however, FRAP is restricted to a narrow region in the middle third of lamina II, i.e. straddling the border between lamina IIo and IIi (24,34). This latter distribution is more consistent with the EM localization of FRAP-containing terminals along the middle one third of lamina II and with observations that FRAP is more highly concentrated in these terminals than in preterminal axons (8,34). The broader dorsoventral distribution of FRAP staining sometimes observed may be due to detection of enzyme in axons as well as terminals and possibly to diffusion of reaction product away from its immediate site of production. In relation to this, the AB893-IR fiber plexi span most of lamina II, however their boutons within the central regions of these plexi correspond to the portion of the FRAP band that presumably represents the enzyme localized to terminals. Such a correspondence together with our other results suggest that the AB893 antibody labels a subpopulation of FRAP-containing fibers along their central course and therefore can be used as a tool to further examine the organization of FRAP-containing afferents in a way that has not previously been revealed by FRAP-histochemistry. The greater number of FRAP-positive compared with AB893-IR neurons in DRG may account for the apparently complete and uniform mediolateral distribution of FRAP across lamina II within the dorsal horn.

The above interpretations must remain tentative since our EM observations admittedly represent only a cursory inspection of AB893-IR fibers in lamina II. Definitive proof that the fibers seen by LM are indeed clusters of unmyelinated fibers and that these correspond to FRAP-containing afferents will require correlative LM-EM studies and double labelling for FRAP and AB893-immunoreactivity at the EM level.

Moreover, under the present immunohistochemical conditions, it appears that the central termination of the large presumably myelinated AB893-IR DRG neurons are not immunostained, despite occasional labelling of their initial axon segment in ganglia. The staining in these cell bodies may represent either a different localization of the same protein or cross-reaction with another protein. The possibility that a small portion of the AB893-IR fibers may be myelinated afferents must be considered in view of demonstrations that some myelinated fibers terminate in the ventral region of lamina II and in lamina I (12). Despite our observations on the effects of capsaicin, a loss in the expression of immunoreactivity in myelinated fibers after capsaicin-induced depletion of unmyelinated afferents cannot be excluded.

Organization of AB893-IR fibers in the dorsal horn

At the LM level, the AB893-IR primary afferent fibers in the dorsal horn were arranged in a pattern heretofore unseen in immunohistochemical or histochemical studies of endogenous substances contained in primary sensory neurons. However, they bear similarities to those previously seen by classical methods and in studies of functionally-identified single fibers. The arborizations of what were believed to be fine or superficial C-fibers appear to be contained almost exclusively in lamina II and were described as narrow sheets with widths of 16-25 μm that extend 340-930 μm rostrocaudally and up to 150 μm dorsoventrally. Other characteristics include their dorsal entrance to lamina II, their many en passant, terminal and cluster boutons ranging from 2-6 μm in diameter, and their terminal distributions which were directed towards the center of their arbors (1,29,32,33). The distribution and morphology of these fibers closely resemble those of the AB893-IR fibers in lamina II. In studies of single functionally-identified C-fibers labelled by PHA-L injection into DRG cell bodies of guinea pig (37), it was found that such fibers terminated in distinct lobuli in various portions of lamina I and II. These lobuli ranged in size from 50-300 μm dorsoventrally, 100-200 μm mediolaterally and

280-600 μm rostrocaudally. Among arbors classified as high-threshold mechanoreceptors, polymodal nociceptors, mechanical/cold nociceptors and low-threshold mechanoreceptors, those that most closely correspond to AB893-IR fiber plexi on the basis of position and dimensions, but bearing in mind possible species differences, are low-threshold mechanoreceptors with arbors concentrated in both lamina IIo and lamina IIi.

In various species studied by the Golgi technique (1,35), it has been well documented that large fibers, corresponding to functionally-identified hair follicle afferents, form flame-shaped arbors extending from lamina IV to the ventral portion of lamina IIi (12). In addition, fibers of unknown origin have been described (35) as capping plexi in lamina II that appear to be intermingled with the dorsal extremes of the flame-shaped arbors. Interestingly, the AB893-IR fibers were arranged in rostrocaudally oriented sheets similar to those of deep afferents. Although there is no a priori reason to consider that the flame-shaped arbors, capping plexi and AB893-IR fiber bundles are in register in the superficial dorsal horn, the possibility of such an arrangement would have implications for the organization of fibers in these two dorsal horn regions and for functional relationships between the substantia gelatinosa and deeper layers.

REFERENCES

1. Beal, J.A.; Fox, C.A. (1976) Afferent fibers in the substantia gelatinosa of the adult monkey (Macaco mulatta): A Golgi study. J. Comp. Neurol. **168,** 113-144.

2. Bystrzycka, E.K.; Nail, B.S. (1985) Brainstem nuclei associated with respiratory, cardiovascular and other autonomic functions. In: Paxinos, G., ed. The Rat Nervous System, Hindbrain and Spinal Cord, Vol. 2. Australia: Academic Press; 95-110.

3. Carr, P.A.; Yamamoto, T.; Karmy, G.; Baimbridge, K.G.; Nagy, J.I. (1989) Parvalbumin is highly colocalized with calbindin D28k and rarely with calcitonin gene-related peptide in dorsal root ganglia neurons of rat. Brain Res. **497,** 163-170.

4. Carr, P.A.; Yamamoto, T.; Karmy, G.; Baimbridge, K.G.; Nagy, J.I. (1989) Analysis of parvalbumin and calbindin D28k-immunoreactive neurons in dorsal root ganglia of rat in relation to their cytochrome oxidase and carbonic anhydrase content. Neuroscience **33,** 363-371.

5. Carr, P.A.; Yamamoto, T.; Staines, W.A.; Whittaker, M.E.; Nagy, J.I. (1989) Quantitative histochemical analysis of cytochrome oxidase in rat dorsal root ganglia and its colocalization with carbonic anhydrase. Neuroscience **33,** 351-362.

6. Carr, P.A.; Yamamoto, T.; Nagy, J.I. (1990) Calcitonin gene-related peptide in primary afferent neurons of rat: Coexistence with fluoride-resistant acid phosphatase and depletion by neonatal capsaicin. Neuroscience **36,** 751-760.

7. Chung, K.; Langford, L.A.; Applebaum, A.E.; Coggeshall, R.E. (1979) Primary

afferent fibers in the tract of Lissauer in the rat. J. Comp. Neurol. **184,** 587-598.

8. Coimbra, A.; Sodre-Borges, B.P.; Magalhaes, M.M. (1974) The substantia gelatinosa Rolandi of the rat. Fine structure, cytochemistry (acid phosphatase) and changes after dorsal root section. J. Neurocytol. **3,** 198-217.

9. Dalsgaard, C.-J.; Vincent, S.R.; Hokfelt, T.; Lundberg, J.M.; Dahlstrom, A.; Schultzberg, M.; Dockray, G.J.; Cuello, A.C. (1982) Coexistence of cholecystokinin- and substance P-like peptides in neurons of the dorsal root ganglia of the rat. Neurosci. Lett. **33,** 159-163.

10. Dalsgaard, C.-J. (1988) The sensory system. In: Bjorklund, A.; Hokfelt, T.; Owman, C., eds. Handbook of Chemical Neuroanatomy, The Peripheral Nervous System, Vol. 6. Amsterdam: Elsevier; 599-636.

11. Dudek, F.E.; Andrew, R.D.; MacVicar, B.A.; Snow, R.W.; Taylor, C.P. (1983) Recent evidence for and possible significance of gap junctions and electrotonic synapses in the mammalian brain. In: Jasper, H.H.; Van Gelder, N.M., eds. Basic Mechanisms of Neuronal Hyperexcitability. New York: Alan R. Liss, Inc.; 31-73.

12. Fyffe, R.E.W. (1984) Afferent fibers. In: Davidoff, R.A., ed. Handbook of the Spinal Cord, Anatomy and Physiology, Vols. 2 and 3. New York: Marcel Dekker; 79-136.

13. Geiger, J.D.; LaBella, F.S.; Nagy, J.I. (1984) Characterization and localization of adenosine receptors in rat spinal cord. J. Neurosci. **4,** 2303-2310.

14. Gobel, S.; Falls, W.M. (1979) Anatomical observations of horseradish peroxidase

filled terminal primary axonal arborizations in layer II of the substantia gelatinosa of Rolando. Brain Res. **175,** 335-340.

15. Gobel, S.; Falls, W.M.; Humphrey, E. (1981) Morphology and synaptic connections of ultrafine primary axons in lamina I of the spinal dorsal horn: Candidates for the terminal axonal arbors of primary neurons with unmyelinated (C) axons. J. Neurosci. **1,** 1163-1179.

16. Hertzberg, E.L. (1984) A detergent-independent procedure for the isolation of gap junctions from rat liver. J. Biol. Chem. **259,** 9936-9943.

17. Hertzberg, E.L.; Skibbens, R.V. (1984) A protein homologous to the 27,000 dalton liver gap junction protein is present in a wide variety of species and tissues. Cell **39,** 61-69.

18. Hertzberg, E.L. (1985) Antibody probes in the study of gap junctional communication. Ann. Rev. Physiol. **47,** 305-318.

19. Hertzberg, E.L.; Spray, D.C. (1985) Studies of gap junctions: biochemical analysis and use of antibody probes. In: Bennett, M.V.L.; Spray, D.C. eds. Gap Junctions. New York: Cold Spring Harbor; 57-65.

20. Knyihar, E.; Gerebtzoff, M.A. (1973) Extra-lysosomal localization of acid phosphatase in the spinal cord of the rat. Exp. Brain Res. **18,** 383-385.

21. Knyihar, E.; Laszlo, I.; Tornyos, S. (1974) Fine structure and fluoride-resistant acid phosphatase activity of electron dense sinusoid terminals in substantia gelatinosa

Rolandi of the rat after dorsal root transection. Exp. Brain Res. **19,** 529-544.

22. Knyihar-Csillik, E.; Csillik, B.; Rakic, P. (1982) Periterminal synaptology of dorsal root glomerular terminals in the substantia gelatinosa of the spinal cord in the rhesus monkey. J. Comp. Neurol. **210,** 376-399.

23. Knyihar-Csillik, E.; Krentzberg, G.W.; Csillik, B. (1989) Enzyme translocation in the course of regeneration of central primary afferent terminals in the substantia gelatinosa of the adult rodent spinal cord. J. Neurosci. Res. **22,** 74-82.

24. Nagy, J.I.; Hunt, S.P. (1982) Fluoride resistant acid phosphatase-containing neurons in dorsal root ganglia are separate from those containing substance P or somatostatin. Neuroscience **7,** 89-97.

25. Nagy, J.I.; Iversen, L.L.; Goedert, M.; Chapman, D.; Hunt, S.P. (1983) Dose-dependent effects of capsaicin on primary sensory neurons in the neonatal rat. J. Neurosci. **3,** 399-406.

26. Nagy, J.I.; Daddona, P.E. (1985) Anatomical and cytochemical relationships of adenosine deaminase-containing primary afferent neurons in the rat. Neuroscience **15,** 799-813.

27. Nagy, J.I.; Yamamoto, T.; Shiosaka, S.; Dewar, K.M.; Whittaker, M.E.; Hertzberg, E.L. (1988) Immunohistochemical localization of gap junction protein in rat CNS: A preliminary account. In: Hertzberg, E.L.; Johnson, R., eds. Gap Junctions. New York: Alan R. Liss, Inc.; 375-389.

28. Nagy, J.I.; Yamamoto, T.; Carr, P.A.; Hertzberg, E.L. (1989) Immunohistochemical localization of the 27kD and 43kD gap junction proteins in the central nervous system. Soc. Neurosci. Abstr., Vol. 15, Part 1, p. 680.

29. Prochansky, F.; Egger, M.D. (1977) Staining of the dorsal root projection to the cat's dorsal horn by anterograde movement of horseradish peroxidase. Neurosci. Lett. **5,** 103-110.

30. Ralston III, H.J. (1979) The fine structure of laminae I, II and III of the macaque spinal cord. J. Comp. Neurol. **184,** 619-642.

31. Rethelyi, M.; Szentagothai, J. (1969) The large synaptic complexes of the substantia gelatinosa. Exp. Brain Res. **7,** 258-274.

32. Rethelyi, M. (1977) Preterminal and terminal axon arborizations in the substantia gelatinosa of cat's spinal cord. J. Comp. Neurol. **172,** 511-528.

33. Rethelyi, M.; Capowski, J.J. (1977) The terminal arborization pattern of primary afferent fibers in the substantia gelatinosa of the spinal cord in the cat. J. Physiol. (Paris) **73** 269-277.

34. Ribeiro-Da-Silva, A.; Castro-Lopes, J.M.; Coimbra, A. (1986) Distribution of glomeruli with fluoride-resistant acid phosphatase (FRAP)-containing terminals in the substantia gelatinosa of the rat. Brain Res. **377,** 323-329.

35. Scheibel, M.E.; Scheibel, A.B. (1968) Terminal axonal patterns in cat spinal cord. II. The dorsal horn. Brain Res. **9,** 32-58.

36. Shiosaka, S.; Yamamoto, T.; Hertzberg, E.L.; Nagy, J.I. (1989) Gap junction protein in rat hippocampus: Correlative light and electron microscope immunohistochemical localization. J. Comp. Neurol. **281,** 282-297.

37. Sugiura, Y.; Lee, C.L.; Perl, E.R. (1986) Central projections of identified, unmyelinated (C) afferent fibers innervating mammalian skin. Science **234,** 358-361.

38. Valnes, K.; Brandtzaeg, P. (1985) Retardation of immunofluorescence fading during microscopy. J. Histochem. Cytochem. **33,** 755-761.

39. Wong-Riley, M.T.T. (1989) Cytochrome oxidase: an endogenous metabolic marker for neuronal activity. Trends in Neurosci. **12,** 94-101.

41. Yamamoto, T.; Shiosaka, S.; Whittaker, M.E.; Hertzberg, E.L.; Nagy, J.I. (1989) Gap junction protein in rat hippocampus: Light microscope immunohistochemical localization. J. Comp. Neurol. **281,** 269-281.

41. Yamamoto, T.; Hertzberg, E.L.; Nagy, J.I. (1989) Antibodies against rat liver connexin32 recognize subsurface cisterns in motoneurons: immunohistochemical evidence for similarities between gap junctional and subcisternal proteins. Soc. Neurosci. Abstr., Vol. 15, Part 1, p. 680.

42. Yamamoto, T.; Maler, L.; Hertzberg, E.L.; Nagy, J.I. (1989) Gap junction protein in Weakly electric fish (Gymnotide): Immunohistochemical localization with emphasis on structures of the electrosensory system. J. Comp. Neurol. **289,** 509-536.

43. Yamamoto, T.; Ochalski, A.; Hertzberg, E.L.; Nagy, J.I. (1991) LM and EM immunolocalization of the gap junctional protein connexin43 in rat brain. Brain Res. **527,** 135-139.

44. Zamboni, L.; De Martino, C. (1967) Buffered picric-acid formaldehyde: A new rapid fixative for electron microscopy. J. Cell Biol. **35,** 148A.

45. Zhu, C.G.; Sandri, C.; Akert, K. (1981) Morphological identification of axo-axonic and dendrodendritic synapses in the rat substantia gelatinosa. Brain Res. **230,** 25-40.

FIGURE LEGENDS

Fig. 1. Photomicrographs showing AB893-IR neurons in sections of trigeminal (A), cervical (B), thoracic (C) and sacral (D) sensory ganglia stained by immunoperoxidase. Magnifications: A,B,C X60; D, X70.

Fig. 2. (A,B) Photomicrographs showing AB893-IR axons (arrows) emerging from large immunofluorescence-labelled (A) and small immunoperoxidase-labelled (B) neurons in sections of lumbar DRG. (C,D) Immunoperoxidase reacted sections from the same DRG processed with AB893 antibody (C) or preadsorbed antibody (D). A large reduction in staining is seen with preadsorbed antibody. Magnifications: A, X200; B, X300; C, X80; D, X60.

Fig. 3. Photomicrographs showing AB893-IR neurons in lumbar DRG and their correspondence to neurons containing PV, CaBP and light CO staining. (A,B) Immunofluorescence micrographs of the same section showing the absence of PV (B) in AB893-IR (A) neurons (arrows). (C,D) Immunofluorescence micrographs of the same section showing AB893-IR (C) and CaBP-IR (D) neurons. Although some AB893-IR cells contain CaBP (arrows), most do not (arrowheads). (E,F) Adjacent sections showing AB893-IR neurons (E) and their histochemically detected level of CO activity (F). Note the light CO staining density in large AB893-IR neurons (arrows). Magnifications: A,B, X125; C,D, X175; E,F, X100.

Fig. 4. Photomicrographs of lumbar DRG sections showing AB893-IR (A,C) and CGRP-IR (B,D) neurons in adjacent sections processed by immunoperoxidase (A,B) and in the same section processed by immunofluorescence (C,D). As indicated by examples, many (arrows), but not all (arrowheads) AB893-IR cells display CGRP-immunoreactivity. Magnifications: A,B, X200; C,D, X125.

Fig. 5. Photomicrographs of lumbar DRG sections showing AB893-IR neurons and their relationships to neurons containing SP, SOM or FRAP. (A,B) The same section showing AB893-IR (A) and SP-IR (B) neurons. (C,D) The same section showing AB893-IR (C) and SOM-IR (D) neurons. Arrows indicate AB893-IR cells that lack SP or SOM. (E,F) The same section showing AB893-IR (E) and FRAP- positive (F) neurons. Nearly all small AB893-IR cells contain FRAP (arrows), but not all FRAP-positive cells are AB893-IR (arrowheads). Magnifications: A,B, X150; C,D, X125; E,F, X175.

Fig. 6. Photomicrographs of transverse sections showing AB893-IR fibers in the nucleus of the solitary tract (A, arrowhead), the spinal trigeminal nucleus caudalis at low (B) and higher magnification (C) and the thoracic dorsal horn (D). AB893-IR fibers are arranged in discrete bundles (arrows) in nucleus caudalis and at thoracic levels. Magnifications: A, X175; B, X75; C, X225; D, X125.

Fig. 7. Photomicrographs of sagittal (A,B) and transverse (C-G) sections showing AB893-IR fibers in the dorsal horn at midlumbar levels. (A) Low magnification of dorsal root (dr) and Lissauer's tract (Lt) and (B) higher magnification of AB893-IR fibers (arrowheads) in the dorsal root. AB893-IR fibers in the dorsal root are seen descending

into Lissauer's tract (arrows). (C-E) Sections showing dorsoventrally oriented AB893-IR fibers in the superficial dorsal horn. Some fibers extend from Lissauer's tract into lamina II (arrow in C), others course dorsally into lamina II apparently from below (arrows in D), and individual fibers are seen between immunoreactive fiber bundles in lamina II (arrows in E). (F) Thionin counterstained section showing the laminar location of AB893-IR fiber bundles (arrows). The dashed line indicates the ventral border of Lamina II. (G) Higher magnification of a non-counterstained section. Note the orientation of the long axis of the AB893-IR fiber bundles indicated by arrows. Magnifications: A,D,E, X325; B, X400; C, X250; F, X75; G, X200.

Fig. 8. Photomicrographs of sagittal (A) and horizontal (B) sections showing AB893-IR fibers in the superficial layers of the lumbar dorsal horn. (A) Photomontage showing a AB893-IR fiber plexus. Note the accumulation of immunoreactive boutons (arrows) along the central region of the plexus. (B) Micrograph showing fiber plexi (arrows) arranged in narrow parallel sheets composed of longitudinally running fibers. Magnifications: A, X425; B, X250.

Fig. 9. Photomicrographs of sagittal sections showing various types of AB893- IR fibers and their associated boutons in the lumbar dorsal horn. (A) Immunoreactive varicose fibers (arrows), (B) stalk boutons (arrows), (C) stalk bouton arising from an axon varicosity (arrow), and (D) clustered stalk boutons (open arrow). (E) AB893-IR fibers displaying perforated expansions (arrows). (F) Very fine lightly stained AB893-IR fibers (arrows) one of which gives rise to a stalk bouton (arrowhead). Magnifications: A-F, X1000.

Fig. 10. Photomicrographs showing depletions of AB893-IR fibers in transverse sections of lower thoracic (A) and midlumbar (B) dorsal horn after neonatal capsaicin treatment and in transverse (C) and sagittal (D) sections of the L2- 3 dorsal horn after dorsal rhizotomy. Magnifications: A,D X75; B, X100; C, X175.

Fig. 11. Electron micrographs showing AB893-IR neuronal elements in transverse sections through lamina II of the lumbar dorsal horn. (A) Low magnification micrograph showing several clusters of AB893-IR fibers (arrows) and a large immunoreactive terminal (arrowhead) associated with one of the clusters. (B) Micrograph showing a sinusoid axon terminal (sa) with deposition of immunoreaction product along its plasma membrane (arrowheads). (C,D) Higher magnification showing (C) an immunoreactive sinusoid terminal (sa) partially surrounding a dendrite (dr), and (D) an immunoreactive axonal process (ax) associated with adjacent fibers within a cluster. Note the immunolabelling of plasma membranes of the sinusoid terminals and adjacent structures (arrows). Magnifications: A, X20,600; B, X14,200; C,D, X65,000.

Fig. 12. Low (A) and high (B) magnification electron micrographs showing AB893-IR axons in sagittal sections through lamina II of the lumbar dorsal horn. (A) Micrograph showing a cluster of longitudinally running immunoreactive axons. Two axons (solid arrows) within the cluster are seen giving rise to en passant axon terminals (open arrows). Note lack of labelling of nearby unmyelinated fibers (large arrowhead) and the membrane labelling of one of these fibers (asterisk) at sites where it contacts the immunoreactive fiber cluster (small arrowhead). (B) Micrograph showing intermittent labelling of adjacent axonal plasma membranes (arrowheads). Magnifications: A, X15,600; B, X25,500.

TABLE 1. Size distribution of AB893-IR lumbar DRG neurons expressed as a percentage of the total number of all cells in each size category. The percentage of all DRG neurons in each size category is also indicated.

	Cross Sectional Area (μm^2)			
		Small*	Intermediate	Large
Neuronal Population	≤500	>500 to ≤1000	>1000 to ≤1800	>1800
All DRG neurons+	13.7	37.6	20.9	27.9
AB893-IR neurons	0.3	4.7	4.8	4.8

* Small cells are subdivided into two size categories

\+ As previously reported by Carr et al. (3)

TABLE 2. Cytochemical characteristics of AB893-IR lumbar DRG neurons expressed as percentage colocalization with the various markers listed.

Cytochemical Marker	Percent Colocalization
AB893-IR + parvalbumin	7 (1124)
AB893-IR + calbindin D28k	10 (588)
AB893-IR + calcitonin gene-related peptide	78 (1120)
AB893-IR + moderate/dark cytochrome oxidase	5 (375)
AB893-IR + substance P	2 (745)
AB893-IR + somatostatin	<1 (867)
AB893-IR + fluoride-resistant acid phosphatase	60 (582)
AB893-IR (small cells only) + fluoride-resistant acid phosphatase	90 (395)

Values in parenthesis indicate the number of AB893-IR neurons analyzed for each condition.
AB893-IR populations represent neurons of all size except where indicated.

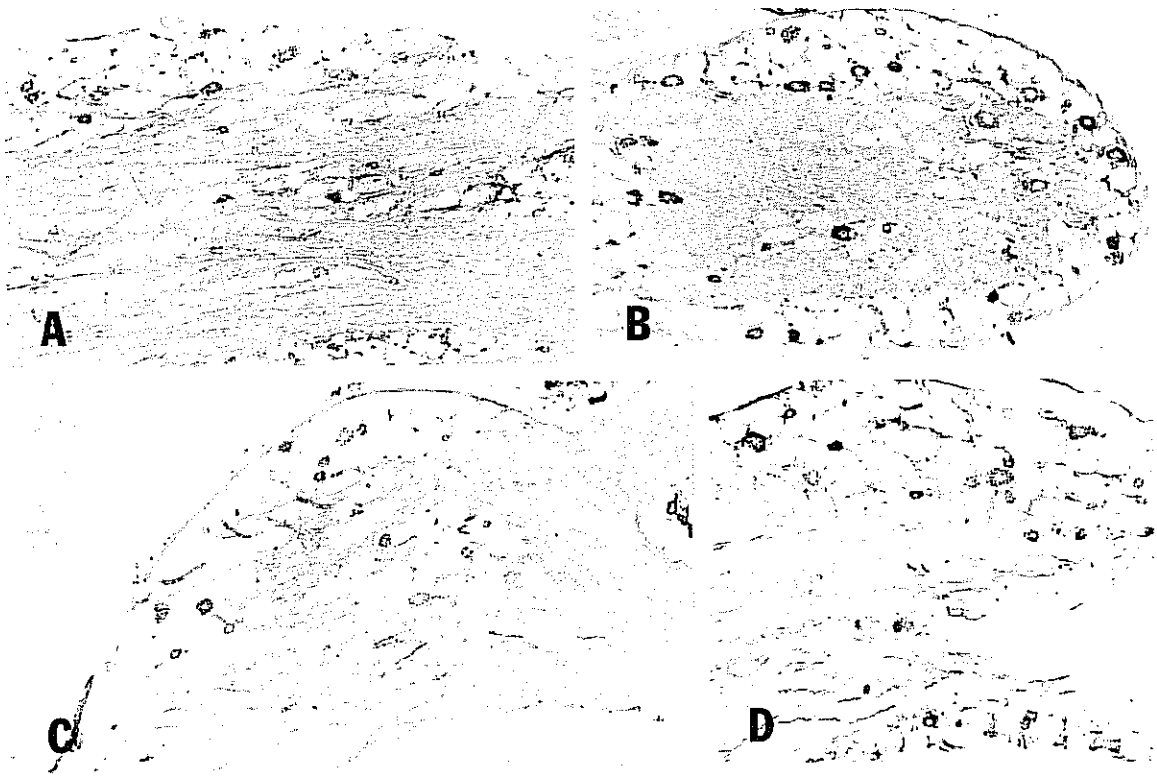

Fig. 1

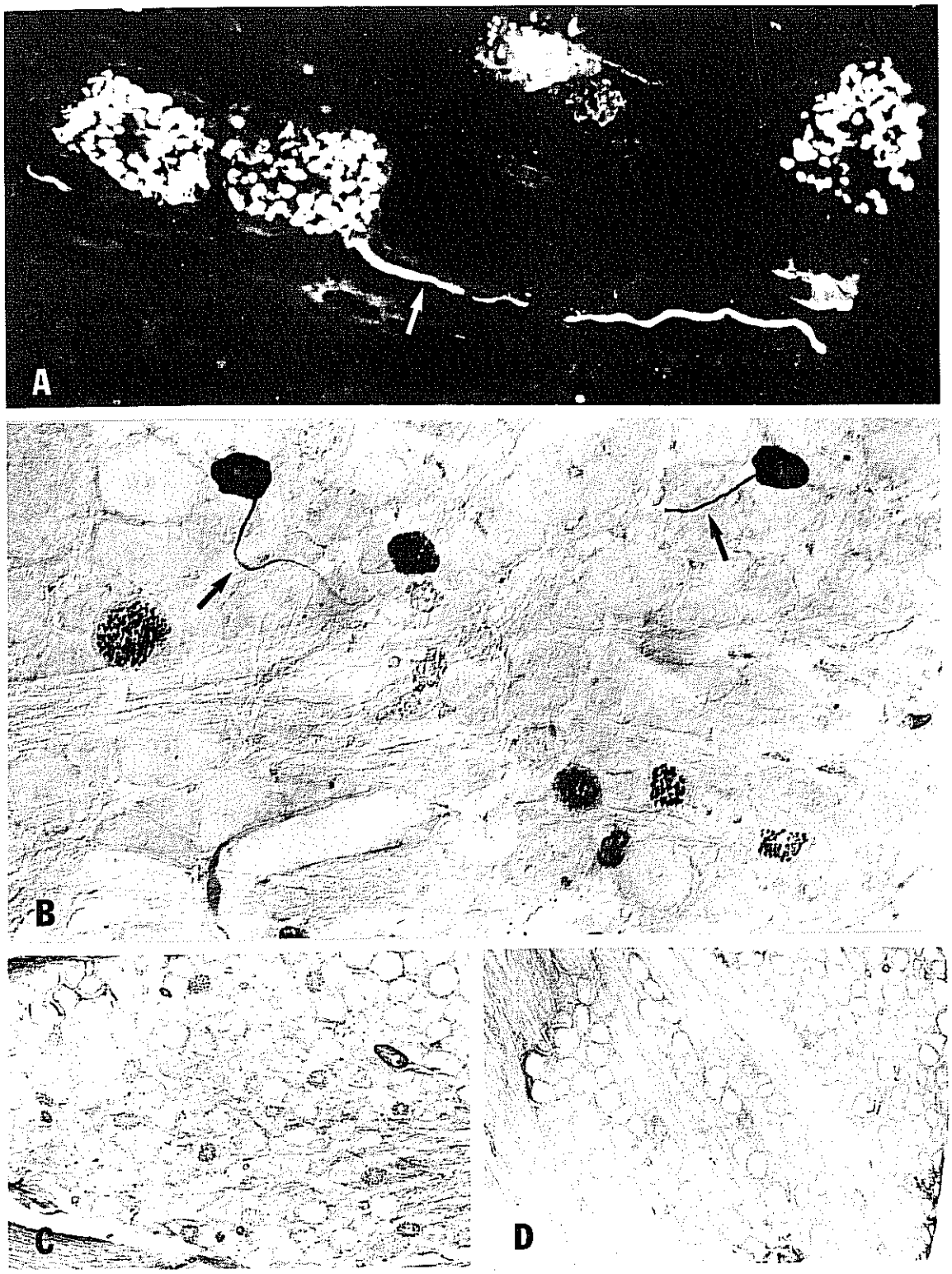

Fig. 2

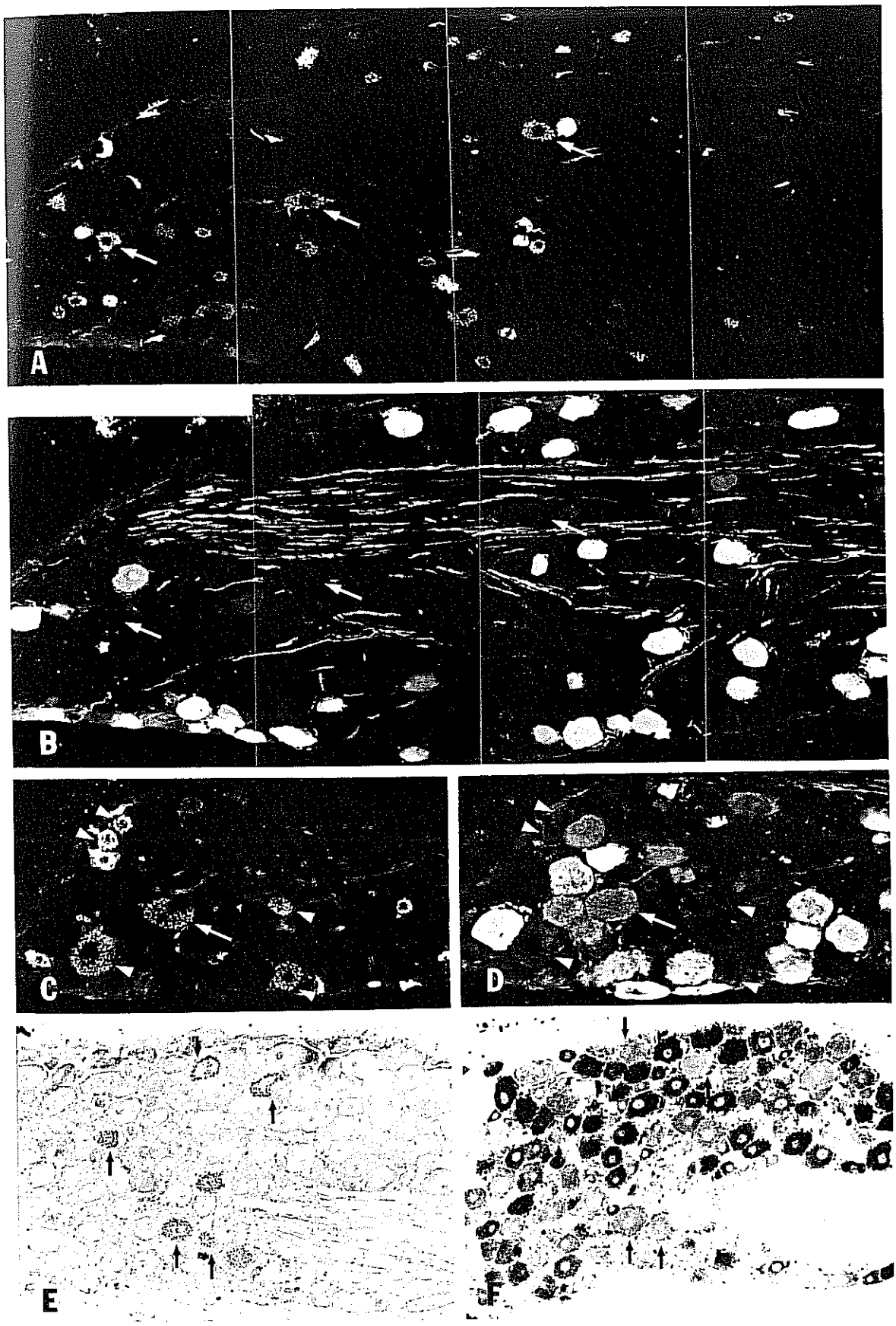

Fig. 3

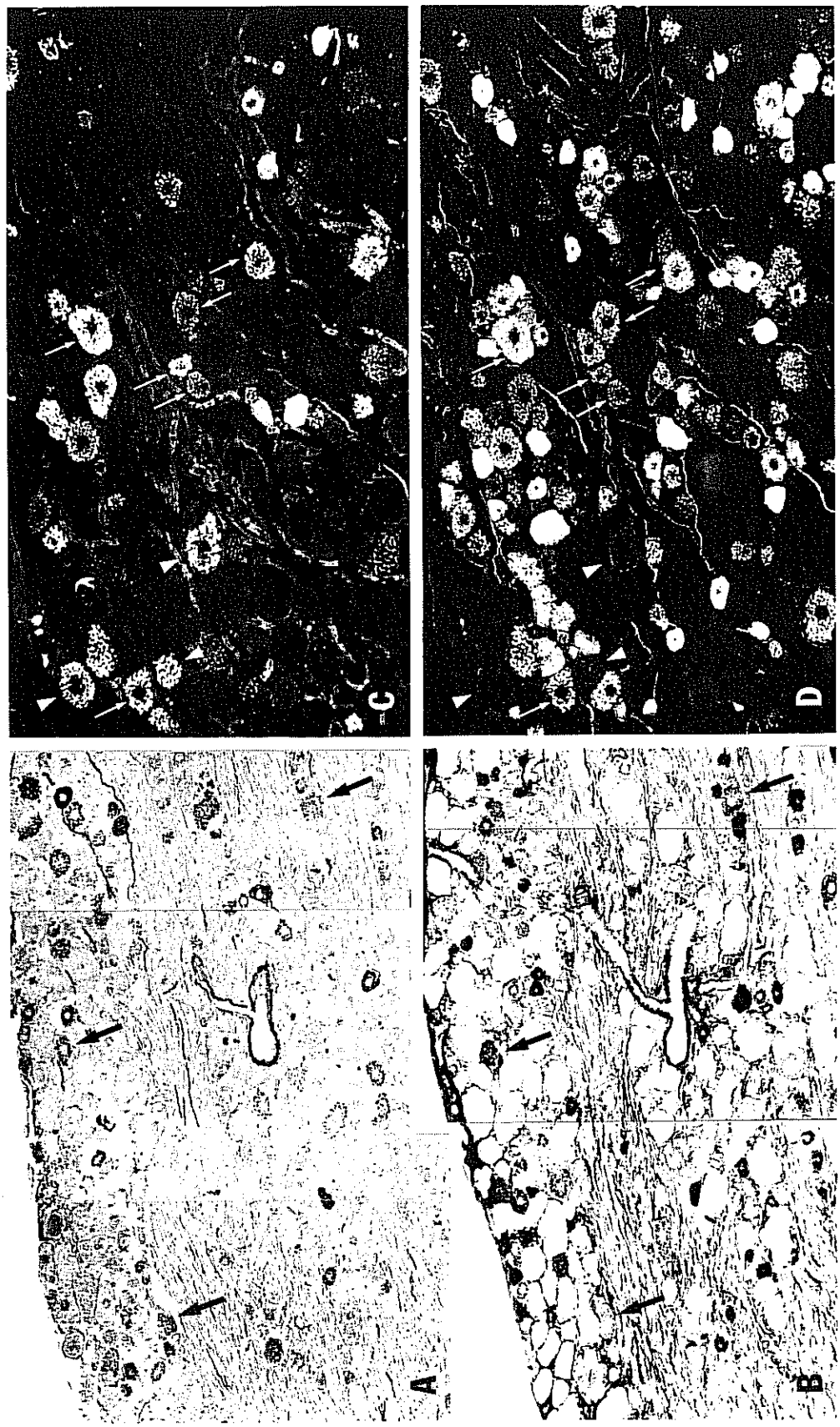

Fig. 4

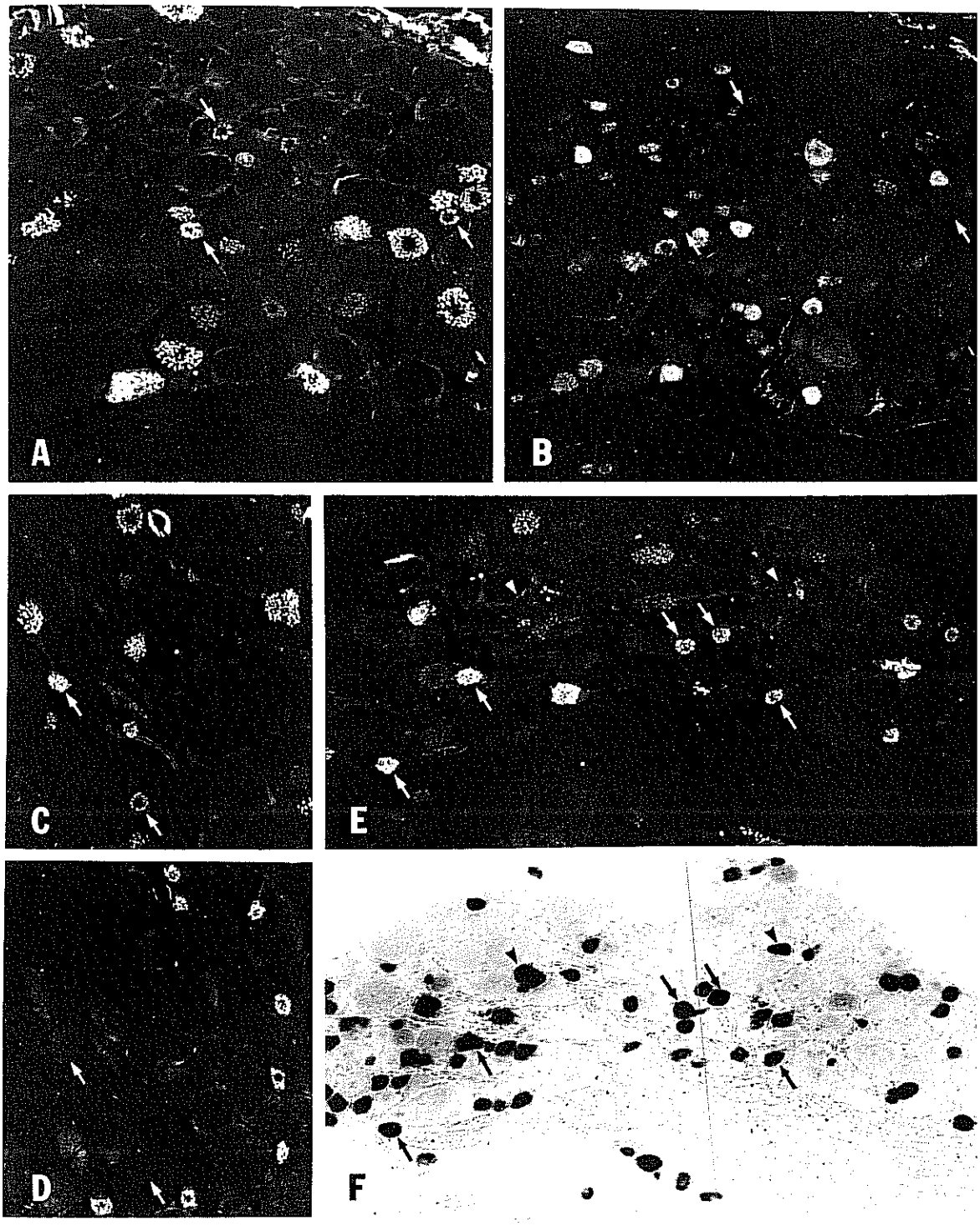

Fig. 5

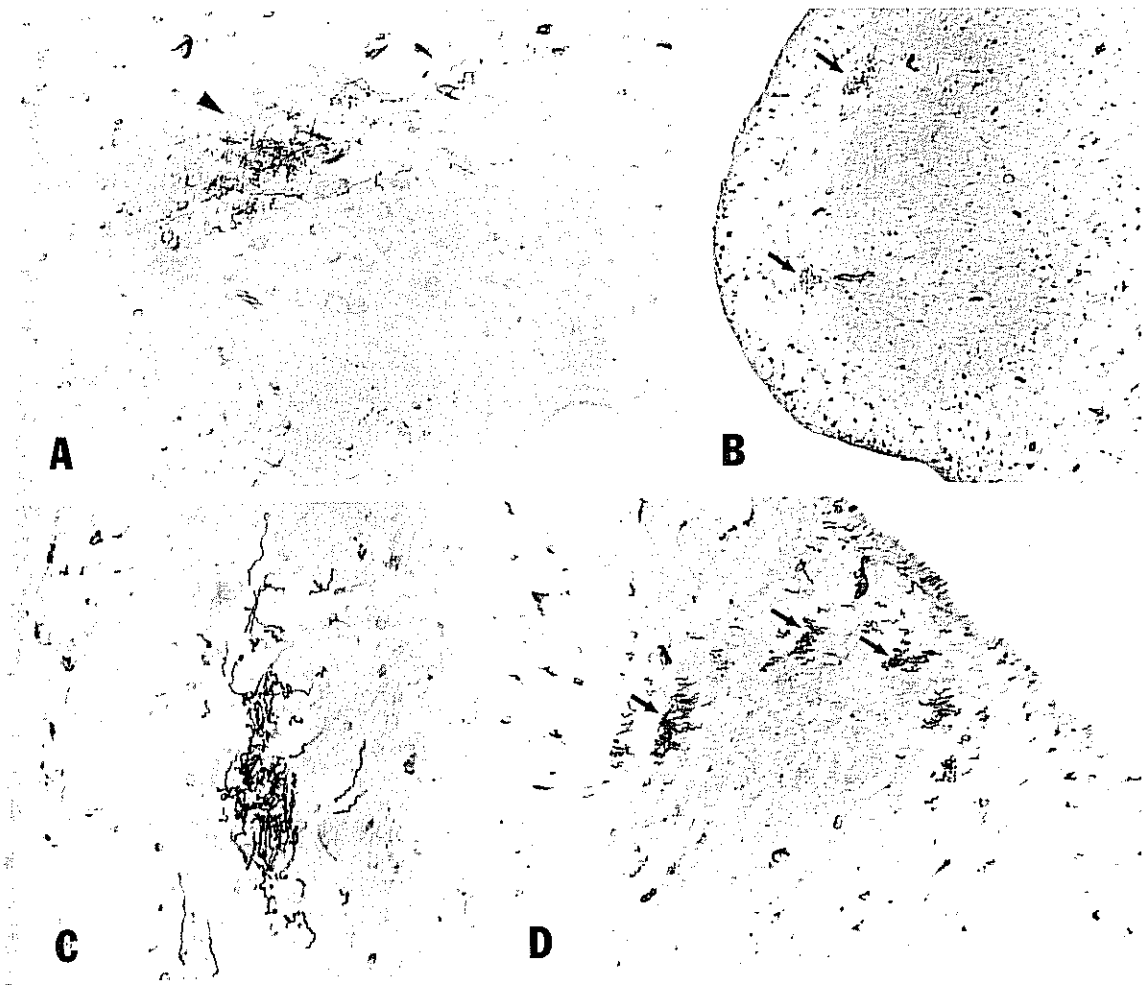

Fig. 6

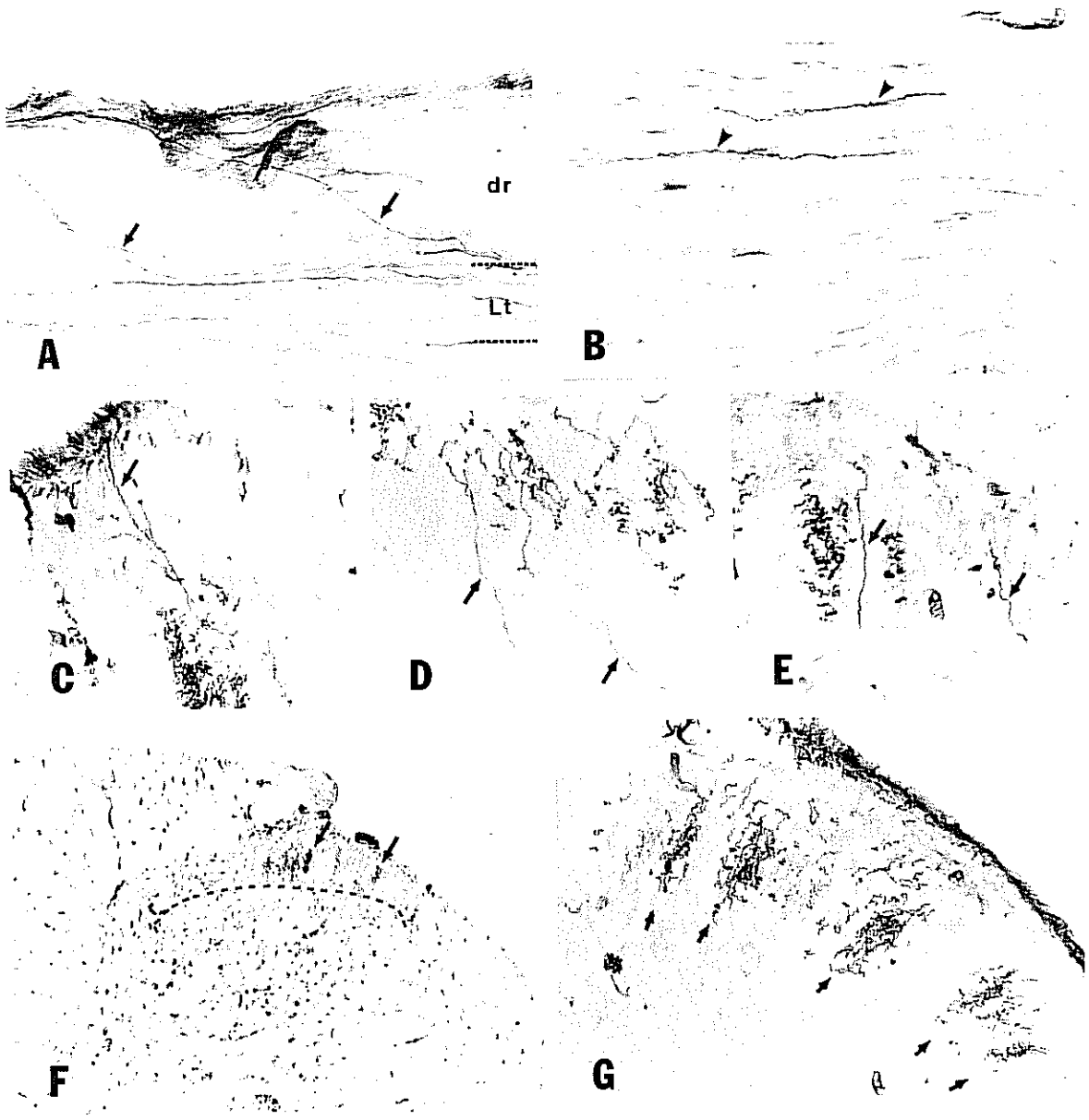

Fig. 7

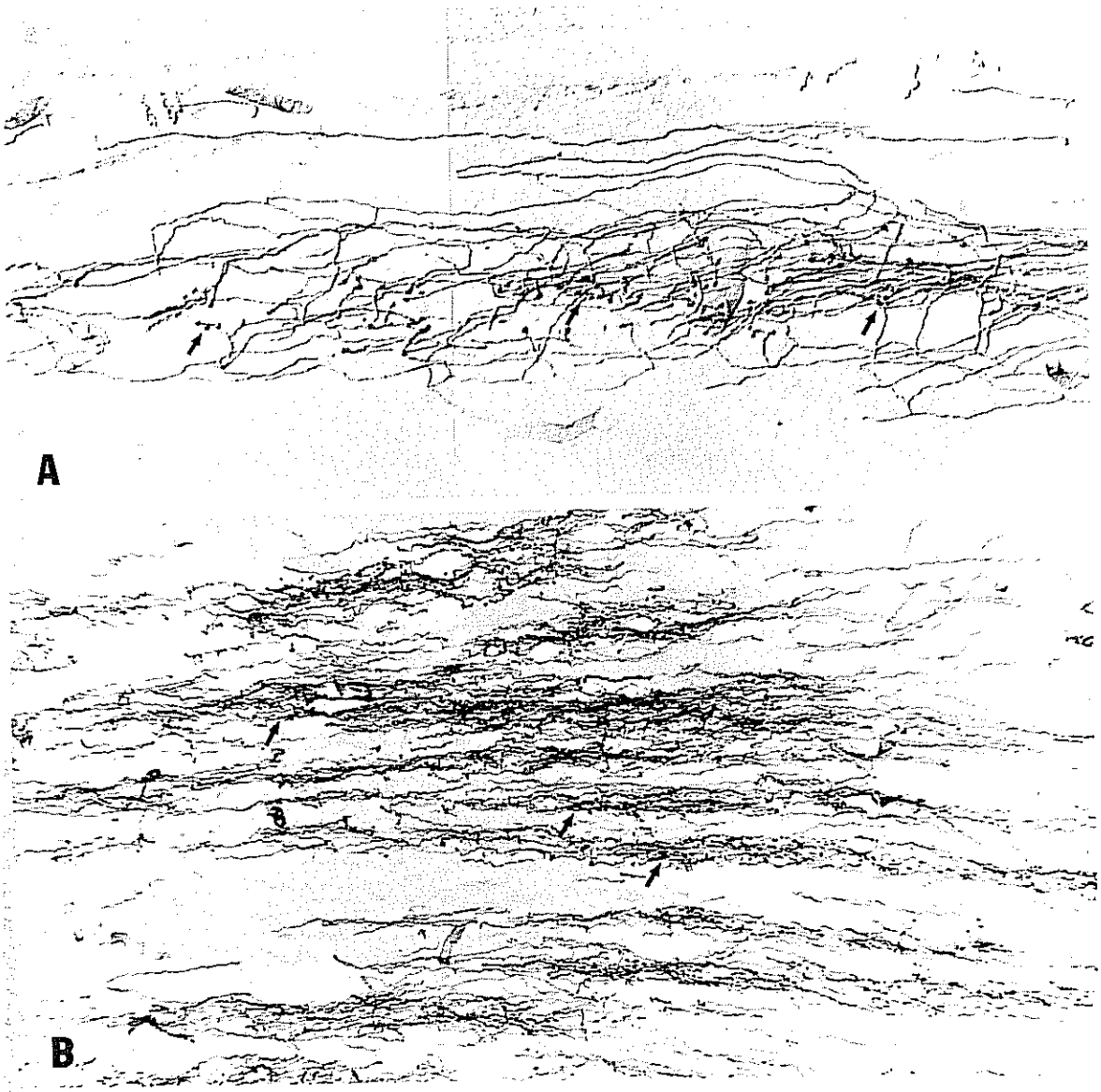

Fig. 8

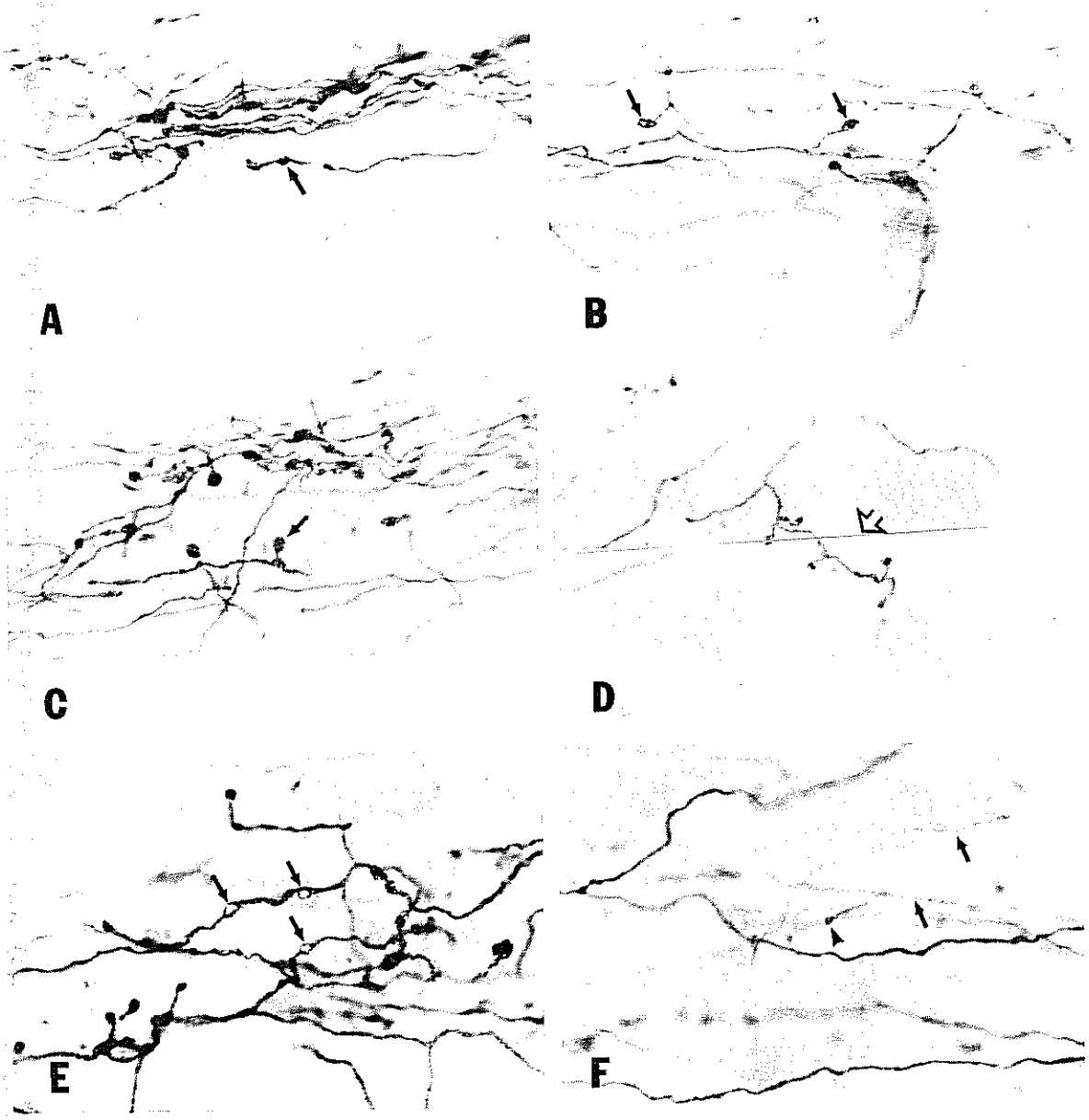

Fig. 9

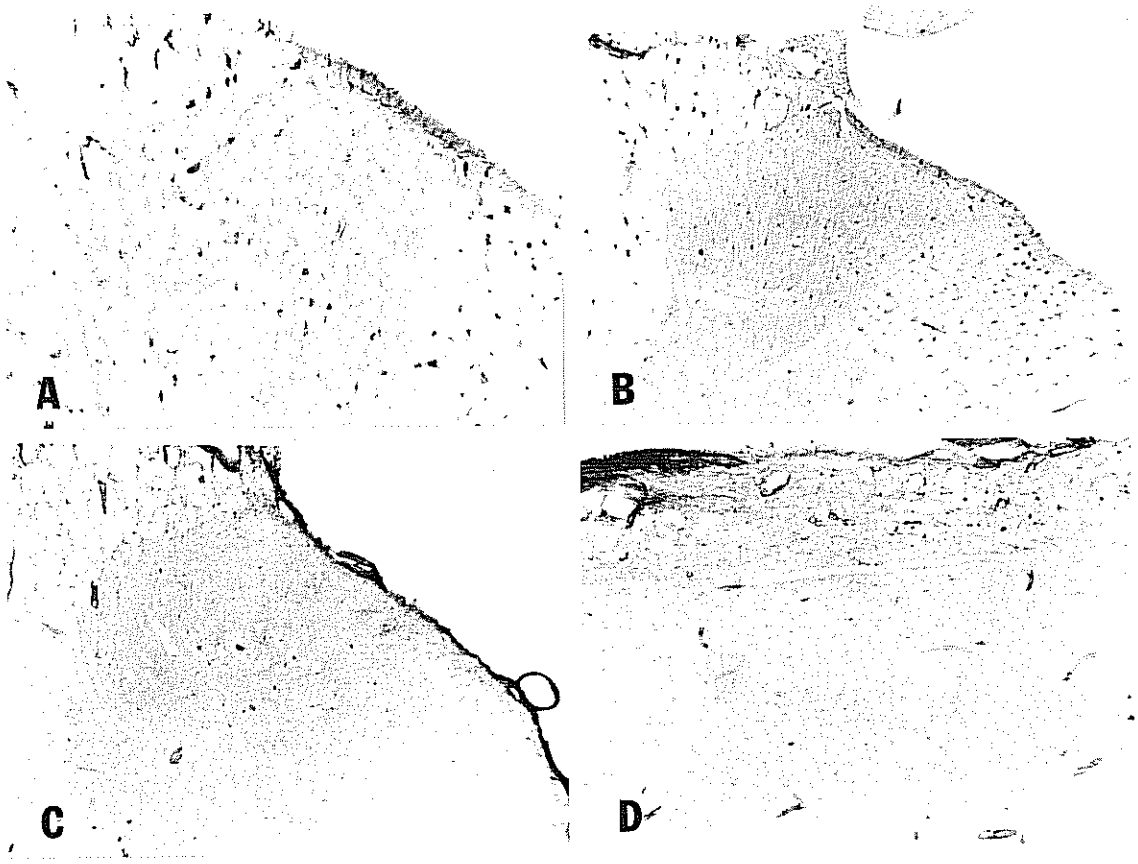

Fig. 10

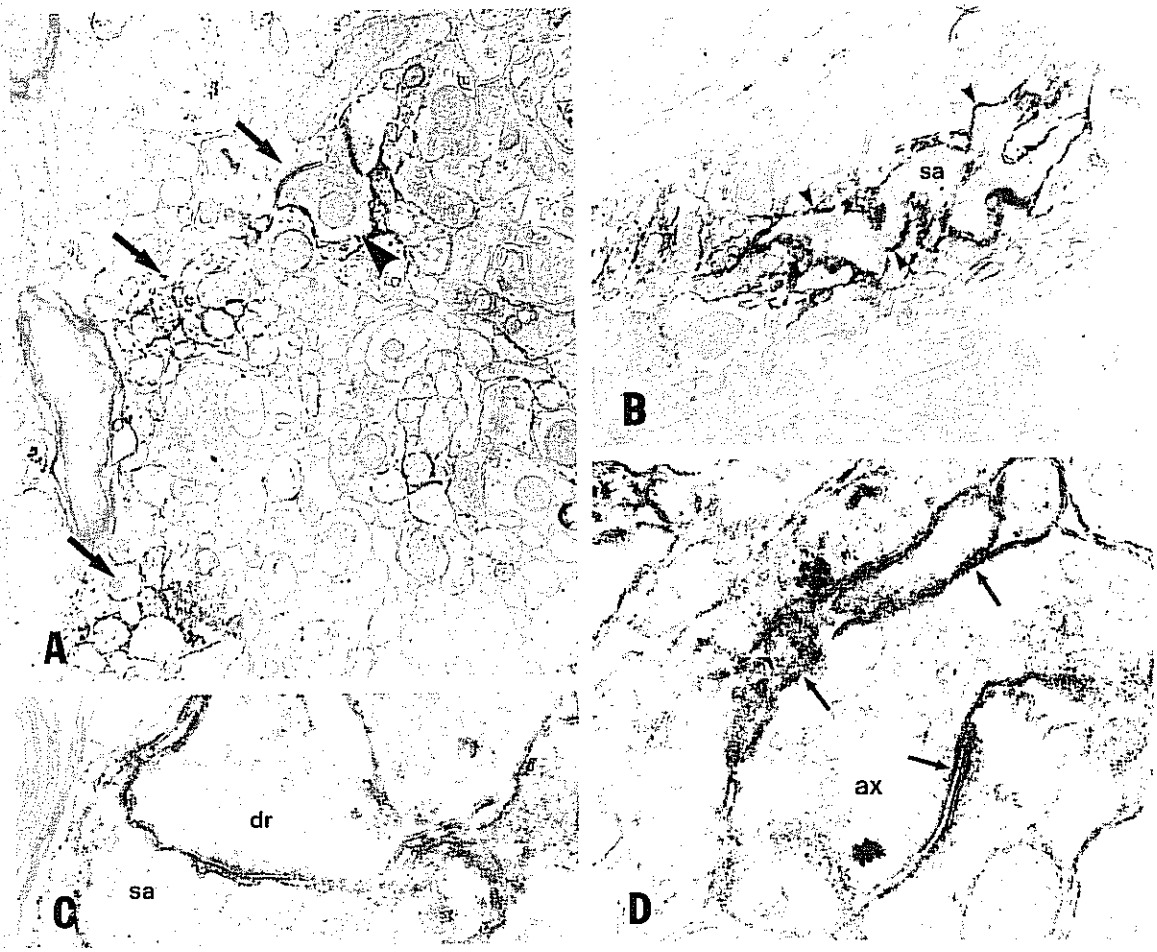

Fig. 11

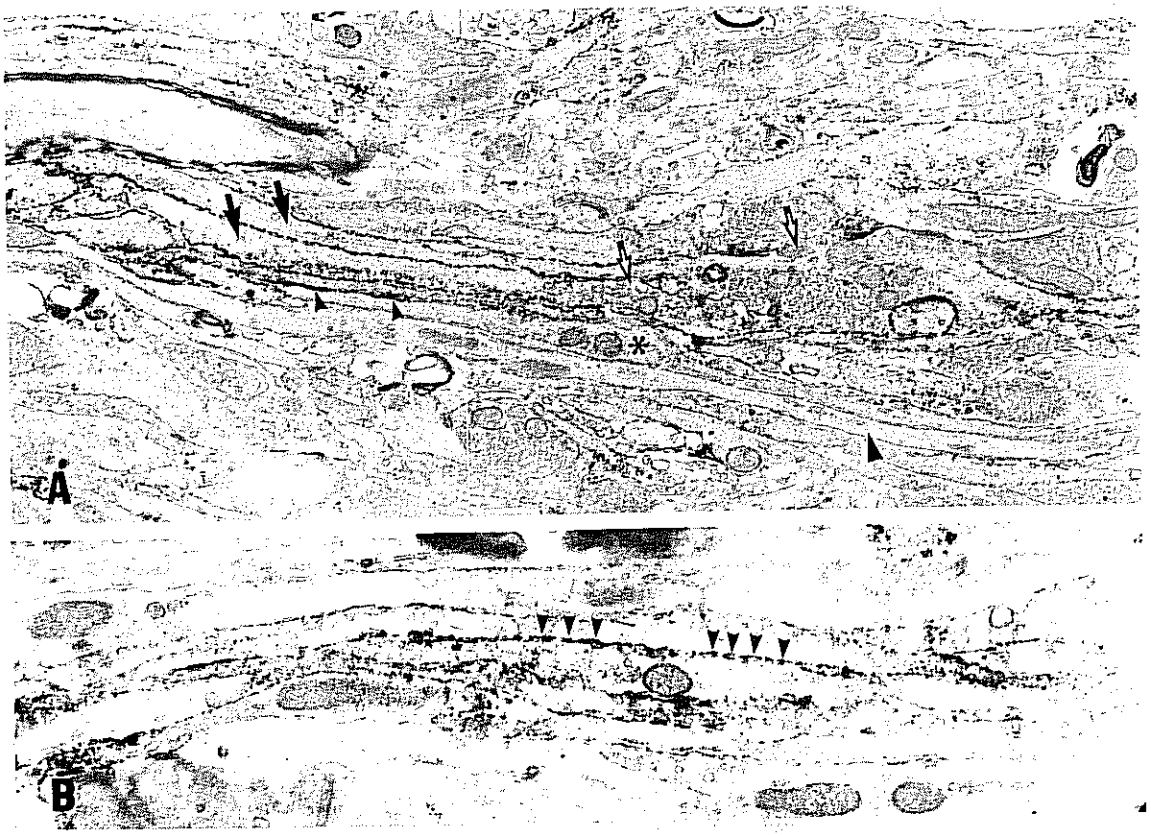

Fig. 12

General Conclusions

Analysis of various characteristics of CO-, CA-, CaBP-, PV-, CGRP-, FRAP-, and AB893-IR-containing primary sensory neurons has provided information regarding not only the individual substances themselves but also the neuronal populations in which they are localized. Specific details relating to this will be discussed below.

Cytochrome oxidase

With respect to CO, we have demonstrated a heterogeneity of staining among DRG sensory neurons by both histochemical and immunohistochemical methods. We have also shown a strong correlation between CO histochemical and immunohistochemical staining intensity in individual neurons thereby demonstrating that in DRG neurons CO activity closely parallels the amount of enzyme present. Our studies of CO levels in primary sensory neurons have revealed that different populations of cells containing PV, CaBP, AB893-IR or CA reaction product each display a characteristic level of CO, suggesting that certain basal levels of electrical activity may be a characteristic feature of some sensory neuron subpopulations. This basal level of activity may be determined by properties of the neuron itself, sensory receptors in the peripheral tissues innervated and/or the sensory modalities transmitted by these cells. It has been previously demonstrated that some cells, such as primary muscle spindle afferents, possess a tonic level of activity in contrast to high threshold afferents which have very low background activity (1,2,14). Our observations that a greater proportion of large size DRG neurons have a greater level of CO activity than smaller cells suggest that neurons containing dense CO may be low threshold afferents and those with light CO may be high threshold afferents.

In addition to indicating basal activity levels of DRG neurons, CO has the potential to

be used in future studies as a marker of neurons in which activity is altered by pharmacological or physiological means. Based on previous demonstrations of an increase in CO levels following specific manipulations (15,16,31,33), it may be feasible to evoke an upregulation of CO in a subpopulation of sensory afferents by application of specific sensory stimuli. In this manner, the cytochemical profile of modality specific DRG neurons, ie., those in which CO levels have increased, may then be investigated.

Carbonic anhydrase

Similarly, we have also explored the use of CA as a histochemical marker presumed to reflect activity of DRG neurons. Our results showed that all cells with dense CO contain CA, while most but not all CA-containing neurons are CO dense. If our CO results truly indicate basal levels of neuronal activity in DRG, then this suggests that there are two populations of CA containing cells, one with high and the other with low tonic activity. On the basis of observations of CA reaction product in muscle spindle afferent terminals, it has been suggested that a large portion of CA-containing neurons innervate muscle with only a minor contribution (4-6%) to cutaneous tissue (20-22,26,32). When the peripheral projections and CO levels of CA neurons are considered together, the CA neurons with dense CO staining may correspond to those cells projecting to the tonically active muscle afferents and the CA neurons with light or moderate CO staining may correspond to less active cutaneous afferents. If a large percentage of both CA and PV/CaBP containing sensory afferents innervate muscle spindles, then a high degree of coexistence of CA and PV/CaBP may be expected and this indeed was found. Regardless of function, the extensive colocalization of PV, CaBP and CA implies that these substances may be markers of a substantial population of DRG neurons with the same modality(ies).

Parvalbumin and calbindin D28k

This thesis describes the distribution and colocalization relationships of PV and CaBP in rat DRG. The localization of PV and CaBP to a subpopulation of DRG neurons has important implications for defining the cytochemical characteristics of a population of target-specific afferents (4). There is strong evidence supporting the specific localization of these calcium binding proteins to muscle afferents. In peripheral tissues, PV- or CaBP-IR nerve terminals were found in muscle spindles surrounding intrafusal muscle fibers. The CaBP-IR elements were described to be innervating chain and Bag 2 fibers while the PV-IR fibers were terminating on the polar region of Bag 1 and Bag 2 fiber endings. Few immunoreactive fibers were seen in the skin. These results, combined with previous studies demonstrating that muscle may be the peripheral target of CaBP-IR primary afferents in chick (23), suggests that PV-IR and CaBP-IR sensory neurons may indeed be muscle afferents. From our results, it may then be inferred that these PV- and CaBP-IR muscle afferents have high levels of electrical activity (as represented by dense CO and possibly CA) but do not contain CGRP. This suggests that CGRP, whatever its peripheral or CNS function, is not required in neurons containing these calcium binding proteins. In contrast to most regions of the CNS, but similar to cerebellar Purkinje cells (4), PV and CaBP coexist in many DRG neurons. This may suggest that these proteins have slightly different roles that are both required in certain sensory neurons. Our results also suggest that the role of PV and CaBP, be that in calcium regulation or buffering or some other unknown aspect of neuronal homeostasis, may be especially important in a subpopulation of tonically active (as indicated by coexistence with dense staining for CO) sensory neurons.

Fluoride-resistant acid phosphatase/ calcitonin gene-related peptide

The study described in Part IV demonstrating the colocalization of FRAP and CGRP has implications regarding fundamental principles of the colocalization of biochemical

markers in sensory neurons. Assuming that some correspondence exists between cytochemical markers in and sensory modalities transmitted by DRG neurons, then relationships between these markers may be used to deduce functional segregations among sensory neurons. For example, if two cytochemical markers never coexist in sensory neurons, then it is logically possible that those two markers represent neurons with distinct functions. However, if two markers coexist in a substantial percentage of DRG neurons, then they are less likely to be indicators of two populations of neurons each with distinct sensory functions. In this case, the two markers together would produce three populations of DRG neurons where one population contains the coexisting markers and each of the other two populations contain only one of the markers. This rationale directly applies to our demonstration of coexistence between FRAP and CGRP in primary sensory neurons. These two markers label one population containing CGRP alone, one population containing FRAP alone and one population in which CGRP and FRAP coexist. The coexistence of CGRP and FRAP has implications regarding the functional separation of sensory processing into cytochemically and anatomically separate parallel pathways for information conveyed by C-fibers and more specifically for pathways comprising nonpeptidergic (as represented by FRAP) and peptidergic afferents. As mentioned in the Introduction, Hunt and Rossi (7) proposed that "peptide and nonpeptide-containing afferents represent two distinct C-fiber pathways innervating similar peripheral structures and conveying similar information, but to different areas within the dorsal horn". However, based on our demonstration of CGRP and FRAP coexistence, it becomes apparent that peptide and nonpeptide afferents cannot represent two distinct C-fiber pathways. Moreover, our results showing overlap of peptide and non-peptide DRG subpopulations (ie., co-existence between FRAP and CGRP) may indicate that strict functional separation of primary afferent neurons cannot be made based on the dorsal horn distribution of a limited number of cytochemical markers.

We have also demonstrated that systemic neonatal capsaicin administration results in

a significant alteration in CGRP labelling in the dorsal horn of the spinal cord. This therefore suggests that a considerable proportion of the CGRP-IR DRG subpopulation are capsaicin-sensitive unmyelinated neurons. This conclusion would agree with previous results demonstrating that approximately 46% of identified C-fiber primary afferent neurons were CGRP-IR (17) and that in the periphery CGRP is often found in unmyelinated afferent terminals (8-10,13).

AB893-IR dorsal root ganglia neurons

Part VI of this thesis describes AB893-IR in a subpopulation of primary sensory neurons in DRG and the dorsal horn of the spinal cord. Although in theory, AB893 may label a population of DRG neurons capable of electrotonic coupling, there is no direct evidence to suggest the participation of AB893-IR primary afferents in electrical communication. Moreover, although this same antibody was found to recognize both neuronal and glial gap junctions in rat and fish CNS (18,28,35,36), it remains uncertain whether the material it recognizes in DRG is a gap junction protein (connexin). In the dorsal horn of the spinal cord, AB893-IR is localized to axonal plasma membranes in bundles of unmyelinated afferent fibers. Based on the localization of this staining, we speculate that this antibody may recognize a connexin32 related protein that may be involved in interneuronal communication or ion channel function. In any case, and as noted earlier, our uncertainty regarding the exact nature of the AB893 antigen in primary sensory neurons does not, at this juncture, allow us to employ this antibody as a marker of connexin32 in these cells. However, its unique localization in a subpopulation of DRG neurons and primary afferent fibers indicates that it may be an invaluable tool for the anatomical characterization of certain primary sensory neurons.

In rat L4 and L5 DRG, 14.5% of all neurons contain AB893-IR. We have shown that the vast majority of cells labelled by AB893 do not contain SP, SOM, PV or CaBP, while most (80%) are CGRP-IR. In addition, approximately 90% of AB893-IR small

cells contain FRAP. Conversely, however, only 22% of FRAP-containing and 34.5% of CGRP-IR cells were AB893-IR. This has implications for the possible division of cells containing FRAP or CGRP into subpopulations. Previous work has suggested that CGRP-containing primary sensory neurons consist of at least two subpopulations based on: 1. the demonstration that two distinct forms of CGRP mRNA are expressed in phenotypically distinct populations (19); 2. quantitative descriptions of both large and small size CGRP-containing neurons (10,11); 3. the variety of different markers that coexist with CGRP and the resultant cytochemically unique subsets of CGRP-containing cells (3,6,11); and 4. the two different immunohistochemical staining patterns observed in CGRP-IR DRG somata, namely, homogeneous cytoplasmic or puntate Golgi apparatus-like immunoreactivity (5,11). With respect to FRAP and CGRP, our data indicating the colocalization of 50% of FRAP-positive with CGRP-positive neurons (see Part IV) is consistent with other evidence that the FRAP-containing population of DRG neurons may consist of two subpopulations. It has been suggested that FRAP-reacted neurons display two different staining patterns, one diffuse and the other puntate (12). It is possible that AB893 may label one of these distinct subpopulations of FRAP-positive cells and that the entire CGRP or FRAP populations may not be functionally homogeneous. The results demonstrating that most small AB893-IR DRG neurons contain FRAP and that at least a portion of AB893-IR small cells are CGRP-IR led directly to our examination of FRAP-CGRP coexistence in DRG as described in Part IV.

AB893-IR fiber plexi

The AB893-IR fiber labelling in the dorsal horn is novel and important as it allows discrete individual unmyelinated fibers to be clearly visualized using an endogenous marker. Evidence also supports the likelihood that some of these fibers contain FRAP. Thus for the first time the organization of FRAP-containing fibers can be easily and clearly studied. The pattern of AB893-IR fiber plexi is very similar to an organizational

pattern previously suggested in this region of the dorsal horn (24,25,27). In addition, the mediolateral compartmentalization into longitudinal running slabs is very similar to that of flame-shaped hair follicle afferents, some of which extend dorsally to the ventral border of lamina II (29). Based on the similar organizational patterns of fiber columns in superficial and deep regions of the dorsal horn, the axonal bundles in these two regions may be in register with each other such that there is a congruence of input and synaptic processing among certain types of afferents terminating along the rostrocaudally oriented bands in superficial and deep layers. If the AB893-IR fibers in the superficial layers of the dorsal horn are in register with rostrocaudally oriented columns, which appear to be a regular arrangement of several types of hair afferents, and if the AB893-IR fibers are found to be low threshold mechanoreceptive afferents (at this point only speculation), then it may be proposed that there exists a commonality in the anatomical organization of myelinated and C-fiber low threshold afferents in deep and superficial dorsal horn zones, respectively. This would imply commonalities in the processing of information conveyed to these two areas by two separate classes of fibers.

Summary

In summary, this thesis describes a series of experiments which examine specific cytochemical properties of primary sensory neurons. This information was then used to speculate on both the role of the markers in these neurons and what their presence implies about other various neuronal characteristics. The long-term goal of this research is to develop cytochemical markers that label modality-specific populations of primary sensory neurons. Although we have yet to determine if any of these markers fulfill that role, we have made a significant contribution to the understanding of the biochemical characteristics of specific subpopulations of DRG neurons.

Finally, it is worth considering whether the sum of the work presented supports the hypothesis stated at the beginning of this thesis, namely, the proposal that a relationship

exists between cytochemistry and sensory modality in primary sensory neurons. Our results combined with the literature would support this contention. Parvalbumin, CaBP, CA and dense CO are contained in what we suggest are a subpopulation of muscle afferents. This proposal is based on: 1) the restricted peripheral projection of PV, CaBP and CA containing afferent fibers; 2) the characteristic high electrical activity of muscle afferents possibly reflected in the levels of CO and CA activity; and 3) reports of substantial calcium dependent spikes in muscle afferents suggesting a requirement for PV and CaBP. By exclusion it may be inferred that CGRP represents a population of primary afferents subserving a modality other than that mediated by PV-, CaBP-, CA- and dense CO-containing neurons. In addition, the morphology, distribution and laminar localization of AB893-IR/FRAP fibers in the dorsal horn suggests that they may be the central termination of a subpopulation of low threshold mechanoreceptors.

As mentioned earlier, it has been possible to visualize, in the CNS, a strong correlation between histochemically determined CO levels and neuronal activity (34). Our studies were designed to lay the groundwork for what we feel is the ultimate goal of the documentation of CO in DRG neurons. That is, to determine whether electrical, chronic experimental or physiological stimuli increase CO levels in DRG neurons and, if so, to utilize physiological stimuli to establish the modalities transmitted by specific subpopulations of cells. Although this goal has not been attained (due to a shortage of time rather than insurmountable methodological difficulties), our results, to date, indicate that CO histochemistry/immunohistochemistry may be a useful tool for the investigation of the relationship between modality and cytochemistry in DRG neurons.

REFERENCES

1. Bessou, P. and Perl, E.R. (1969) Response of cutaneous sensory units with unmyelinated fibers to noxious stimuli. J. Neurophysiol. **32**, 1025-1043.

2. Burgess, P.R. and Perl, E.R. (1967) Myelinated afferent fibres responding specifically to noxious stimulation of the skin. J. Physiol. **190**, 541-562.

3. Cameron, A.A.; Leah, J.D. and Snow, P.J. (1988) The coexistence of neuropeptides in feline sensory neurons. Neuroscience **27**, 969-979.

4. Celio, M.R. (1990) Calbindin D-28k and parvalbumin in the rat nervous system. Neuroscience **35**, 375-475.

5. Dalsgaard, C.-J. (1988) The sensory system. In: Bjorklund, A.; Hö kfelt, T.; Owman, C., eds. Handbook of chemical neuroanatomy, the peripheral nervous system, vol. 6. Amsterdam: Elsevier, 599-636.

6. Gibbins, I.L.; Furness, J.B. and Costa, M. (1987) Pathway-specific patterns of the co-existence of substance P, calcitonin gene-related peptide, cholecystokinin and dynorphin in neurons of the dorsal root ganglia of the guinea-pig. Cell Tissue Res. **248**, 417-437.

7. Hunt, S.P. and Rossi, J. (1985) Peptide- and non-peptide-containing unmyelinated primary afferents: the parallel processing of nociceptive information. Phil. Trans. R. Soc. Lond. **B308**, 283-289.

8. Ishida-Yamamoto, A. and Tohyama, M. (1989) Calcitonin gene-related peptide in the

nervous tissue. Prog. Neurobiol. **33**, 335-386.

9. Ishida-Yamamoto, A.; Senba, E. and Tohyama, M. (1989) Distribution and fine structure of calcitonin gene-related peptide-like immunoreactive nerve fibers in the rat skin. Brain Res. **491**, 93-101.

10. Ishida-Yamamoto, A. and Senba, E. (1990) Cell types and axonal sizes of calcitonin gene-related peptide-containing primary sensory neurons of the rat. Brain Res. Bull. **24**, 759-764.

11. Ju, G.; Hö kfelt, T.; Brodin, E.; Fahrenbrug, J.; Fischer, J.A.; Frey, P.; Elde, R. and Brown, J.C. (1987) Primary sensory neurons of the rat showing calcitonin gene-related peptide immunoreactivity and their relations to substance P-, somatostatin-, galanin-, vasoactive intestinal polypeptide- and cholecystokinin-immunoreactive ganglion cells. Cell Tissue Res. **247**, 417-431.

12. Knyihar-Csillik, E. and Csillik, B. (1981) FRAP: histochemistry of the primary sensory nociceptive neuron. Prog. Histochem. Cytochem. **14**, 1-137.

13. Kruger, L.; Silverman, J.D.; Mantyh, P.W.; Sternini, C. and Brecha, N.C. (1989) Peripheral patterns of calcitonin gene-related peptide general somatic innervation: cutaneous and deep terminations. J. Comp. Neurol. **280**, 291-302.

14. Loeb, G.E. and Duysens, J. (1979) Activity patterns in individual hindlimb primary and secondary muscle spindle afferents during normal movements in unrestrained cats. J. Neurophysiol. **42**, 420-440.

15. Mawe, G.M. and Gershon, M.D. (1986) Functional heterogeneity in the myenteric plexus: demonstration using cytochrome oxidase as a verified cytochemical probe of the activity of individual enteric neurons. J. Comp. Neurol. **249**, 381-391.

16. Mawe, G.M.; Gardette, R.; D'Agostaro, L. and Role, L.W. (1990) Development of synaptic transmission at autonomic synapses *in vitro* revealed by cytochrome oxidase histochemistry. J. Neurobiol. **21**, 578-591.

17. McCarthy, P.W. and Lawson, S.N. (1990) Cell type and conduction velocity of rat primary sensory neurons with calcitonin gene-related peptide-like immunoreactivity. Neuroscience **34**, 623-632.

18. Nagy, J.I.; Yamamoto, T.; Shiosaka, S.; Dewar, K.M.; Whittaker, M.E. and Hertzberg, E.L. (1988) Immunohistochemical localization of gap junction protein in rat CNS: a preliminary account. In: Hertzberg, E.L.; Johnson, R., eds. Gap junctions. New York: Alan R. Liss, Inc., 375-389.

19. Noguchi, K.; Senba, E.; Morita, Y.; Sato, M. and Tohyama, M. (1990) Co-expression of alpha-CGRP and beta-CGRP mRNAs in the rat dorsal root ganglion cells. Neurosci. Lett. **108**, 1-5.

20. Perry, M.J.; Lawson, S.N. and Wood, J. (1991) Immunocytochemical properties of rat dorsal root ganglion (DRG) neurones innervating muscle, skin or viscera. Soc. Neurosci. Abstr. **17**, 105.

21. Peyronnard, J.M.; Charron, L.; Messier, J.P. and Lavoie, J. (1988) Differential

effects of distal and proximal nerve lesions on carbonic anhydrase activity in rat primary sensory neurons, ventral and dorsal root axons. Exp. Brain Res. **70,** 550-560.

22. Peyronnard, J.M.; Charron, L.; Lavoie, J.; Messier, J.P. and Dubreuil, M. (1988) Carbonic anhydrase and horseradish peroxidase: double labelling of rat dorsal root ganglion neurons innervating motor and sensory peripheral nerves. Anat. Embryol. **177,** 353-359.

23. Philippe, E.; Garosi, M. and Droz, B. (1988) Influence of peripheral and central targets on subpopulations of sensory neurons expressing calbindin immunoreactivity in the dorsal root ganglion of the chick embryo. Neuroscience **26,** 225-232.

24. Rethelyi, M. and Capowski, J.J. (1977) The terminal arborization pattern of primary afferent fibers in the substantia gelatinosa of the spinal cord in the cat. J. Physiol. (Paris) **73,** 269-277.

25. Rethelyi, M.; Light, A.R. and Perl, E.R. (1989) Synaptic ultrastructure of functionally and morphologically characterized neurons of the superficial spinal dorsal horn of cat. J. Neurosci. **9,** 1846-1863.

26. Riley, D.A.; Sanger, J.R.; Matloub, H.S.; Yousif, N.J.; Bain, J.L.W. and Moore, G.H. (1988) Identifying motor and sensory myelinated axons in rabbit peripheral nerves by histochemical staining for carbonic anhydrase and cholinesterase activities. Brain Res. **453,** 79-88.

27. Scheibel, M.E. and Scheibel, A.B. (1968) Terminal axonal patterns in cat spinal cord. II The dorsal horn. Brain Res. **9**, 32-58.

28. Shiosaka, S.; Yamamoto, T.; Hertzberg, E.L. and Nagy, J.I. (1989) Gap junction protein in rat hippocampus: Correlative light and electron microscope immunohistochemical localization. J. Comp. Neurol. **281**, 282-297.

29. Shortland, P.; Woolf, C.J. and Fitzgerald, M. (1989) Morphology and somatotopic organization of the central terminals of hindlimb hair follicle afferents in the rat lumbar spinal cord. J. Comp. Neurol. **289**, 416-433.

30. Sugiura, Y.; Lee, C.L. and Perl, E.R. (1986) Central projections of identified, unmyelinated (C) afferent fibers innervating mammalian skin. Science **234**, 358-361.

31. Vaughn, T.; Behbehani, M.M.; Zemlan, F.P. and Shipley, M. (1984) Increased cytochrome oxidase staining in rat spinal cord subsequent to peripheral noxious stimulation. Soc. Neurosci. Abstr. **14**, 119.

32. Wong, V.; Barrett, C.P.; Donati, E.J. and Guth, L. (1987) Distribution of carbonic anhydrase activity in neurons of the rat. J. Comp. Neurol. **257**, 122-129.

33. Wong-Riley, M.T.T.; Walsh, S.M.; Leake-Jones, P.A. and Merzenich, M.M. (1981) Maintenance of neuronal activity by electrical stimulation of unilaterally deafened cats demonstrable with cytochrome oxidase technique. Ann. Otol. Rhinol. Lar. **90 (Suppl. 82)**, 30-32.

34. Wong-Riley, M.T.T. (1989) Cytochrome oxidase: an endogenous metabolic marker for neuronal activity. Trends Neurosci. **12**, 94-101.

35. Yamamoto, T.; Shiosaka, S.; Whittaker, M.E.; Hertzberg, E.L. and Nagy, J.I. (1989) Gap junction protein in rat hippocampus: Light microscope immunohistochemical localization. J. Comp. Neurol. **281**, 269-281.

36. Yamamoto, T.; Maler, L.; Hertzberg, E.L. and Nagy, J.I. (1989) Gap junction protein in weakly electric fish (Gymnotide): Immunohistochemical localization with emphasis on structures of the electrosensory system. J. Comp. Neurol. **289**, 509-536.